'THE KINETIC REGULATION OF THE COMPLEMENT PROTEASE MASP-2'

Nicole Catherine Drentin

B. Biomed Sci (Hons) (Monash)

Department of Biochemistry and Molecular Biology

Monash University

A thesis submitted for the degree of Doctor of Philosophy

June 2015

<u>CONTENTS</u>

Chapter 3
'Investigation into the role of the MASP-2 CCP domain binding exosite in the kinetic mechanism of interaction between MASP-2 and its substrate C4'.

Chapter 4
'**Investigation into the role of the disease-linked MASP-2 CCP domain mutation D371Y in the kinetic mechanism of interaction between MASP-2 and its substrate C4'.**

Chapter 5

'Investigation into the role of the MASP-2 SP domain binding exosite in the kinetic mechanism of interaction between MASP-2 and its substrate C4.'

Chapter 6
'**Investigations into the regulation of MASP-2 activity by polyphosphate**'

Chapter 7

GENERAL DECLARATION

In accordance with Monash University Doctorate Regulation 17.2 Doctor of Philosophy and Research Master's regulations the following declarations are made:

I hereby declare that this thesis contains no material which has been accepted for the award of any other degree or diploma at any university or equivalent institution and that, to the best of my knowledge and belief, this thesis contains no material previously published or written by another person, except where due reference is made in the text of the thesis.

This thesis includes 1 original paper published in a peer reviewed journal and no unpublished publications. The core theme of the thesis is the kinetic regulation of the complement protease MASP-2. The ideas, development and writing up of all the papers in the thesis were the principal responsibility of myself, the candidate, working within the Department of Biochemistry and Molecular Biology, under the supervision of Prof. Robert Pike and Dr. Lakshmi Wijeyewickrema.

The inclusion of co-authors reflects the fact that the work came from active collaboration between researchers and acknowledges input into team-based research.

In the case of Appendix A.2, my contribution to the work involved the following:

Thesis chapter	Publication title	Publication status*	Nature and extent of candidate's contribution
Appendix A.2	Investigation of the mechanism of interaction between Mannose-binding lectin-associated serine protease-2 and complement C4	In press	The candidate contributed to the generation of ideas for the experiments carried out in the paper, carried out the majority of the experimental work, and assisted in writing up the paper. Dr. Paul Conroy and Dr. Menachem Gunzberg provided assistance in the generation of the protocol used to collect SPR data, and in carrying out the SPR experiments.

I have not renumbered sections of submitted or published papers in order to generate a consistent presentation within the thesis.

Signature of candidate:

Date:

ACKNOWLEDGEMENTS

ABSTRACT

Complement is an ancient component of immunity, playing a primary role in defending against pathogens as part of the innate immune system. Mannose-binding lectin-associated serine protease-2 (MASP-2) is a critical component of the lectin complement pathway and cleavage of its substrates C2 and C4 contributes to the formation of a key complement component, the C3 convertase. MASP-2 has been implicated in a number of inflammatory diseases, thus the development of inhibitors of MASP-2 presents a potential route for prevention and/or treatment of these diseases.

The structure of MASP-2 in complex with C4 confirmed the location of an accessory binding site (exosite) on the complement control protein (CCP) domains and revealed a potential exosite on the serine protease (SP) domain. This study sought to quantitate the contribution of these MASP-2 exosites to the kinetic mechanism of interaction between the enzyme and C4. This was done by mutating selected residues from the CCP and SP domain exosites and measuring the effects on C4 binding and cleavage efficacy using a variety of methods. The role of the CCP domain exosite in high affinity binding and efficient cleavage of C4 was confirmed and it was shown to play a major role in the initial interaction with C4. A naturally occurring mutation in the CCP2 domain that has been linked to a number of chronic infectious diseases, D371Y, did not impair efficient cleavage of C2 and C4, nor was the activation by MASP-1 or MASP-2 affected. The effect of the mutation in the context of the disease linkages is thus unknown. The potential SP domain exosite was shown to be a functional exosite, with residues R578 and R583 shown to be necessary for efficient C4 binding and cleavage. The SP domain exosite was also shown to play the major role in a secondary conformational change between MASP-2 and C4 required to form a high affinity complex.

The serine protease inhibitor (serpin), C1 inhibitor (C1-INH) is known to be the main endogenous inhibitor of MASP-2. C1-INH activity can be enhanced through the binding of polyanionic molecules, such as the naturally occurring glycosaminoglycan, heparin. The polyanionic molecule, polyphosphate (polyP), has recently been found to reduce complement activity and may represent a more potent enhancer than heparin of C1-INH activity. Heparin and long chain polyP (>1000 units) were both shown to bind to MASP-2, with the SP domain exosite shown to play a key role in this process. Platelet-

length polyP (70-120 units) was found to have no effect on C1-INH activity against MASP-2 at physiological concentrations and had an inhibitory effect on C1-INH activity at higher concentrations. Heparin had an inhibitory effect on C1-INH activity, even at lower concentrations. Further study into the effects of polyP size on C1-INH activity is required to determine if polyP represents a more potent enhancer of C1-INH activity against MASP-2 than heparin.

The results from this study provide information on the regulation of MASP-2 activity that may be used to design potential therapeutics to regulate the enzyme in inflammatory diseases.

COPYRIGHT NOTICES

LIST OF FIGURES

LIST OF TABLES

VIII

ABBREVIATIONS

Abz	Ortho-aminobenzoic acid
Abs	Absorbance
A_{280}	Absorbance at the wavelength 280 nm
APC	Antigen-presenting cell
BSA	Bovine serum albumin
CCP	Complement control protein module
CD	Circular dichroism
CRD	Carbohydrate recognition domain
CUB	Complement C1r/C1s, Uegf, Bmp1
C1-INH	C1 inhibitor
DMF	N.N-dimethylformamide
DSC	Differential scanning calorimetry
DTT	Dithiothreitol
EC_{50}	Half maximal effective concentration
EDC	1-ethyl-3-(3-dimethylaminopropyl) carbodiimide hydrochloride
EDTA	Ethylenediaminetetra-acetic acid
EGF	Epidermal Growth Factor
EMSA	Electromobility shift assay
GAG	Glycosaminoglycan
H	Hill-coefficient
HAE	Hereditary Angioedema
HBSS	Hank's buffered saline solution
HEPES	4-(2-hydroxyethyl)-1-piperazineethanesulfonic acid
HTLV-1	Human T-lymphocytic virus 1
IPTG	Isopropyl-1-thio-β-D-galactopyranoside
k_a	Association rate constant
K_1	Rate constant for the initial binding step
K_2	Rate constant for the second binding step
k_{cat}	First-order rate constant/ catalytic constant

k_d	Dissociation rate constant
K_d	Equilibrium dissociation constant
kDa	Kilodalton
$K_{0.5}$	Substrae concentration corresponding to half-maximal velocity
LB	Luria Bertani
LGR	N-t-Boc-leucine-glycine-arginine-7-amido-4-methyl-courmain
LPS	Lipopolysaccharide
MAC	Membrane Attack Complex
MASP	Mannan-binding lectin-associated serine protease
MAp19/ MAp44	MBL Associated Protein 19/44
MBL	Mannan-binding Lectin
MHC	Major Histocompatibility Class
MIDAS	Metal-ion dependent adhesion site
MilliQ	Ultra purified water
NHS	N-Hydroxysuccinimide
OD	Optical density
PBST	Phosphate buffered saline with Tween 20
PCR	Polymerase chain reaction
PDEA	2-(2-pyridinyldithio) ethaneamine hydrochloride
PEG	Polyethylene glycol
polyP	Polyphosphate
RCL	Reactive centre loop
RFU	Relative fluorescence units
RF	Rheumatic fever
RHD	Rheumatic heart disease
SDS-PAGE	Sodium dodecyl sulfate polyacrylamide gel electrophoresis
SP	Serine protease
SPR	Surface Plasmon Resonance

TAE	Tris, acetate, EDTA
TBE	Tris, Borate, EDTA
TBS	Tris-buffered saline
T_h1	T helper 1 cell
T_h2	T helper 2 cell
V_{max}	Maximal velocity
vWFA	von Willebrand Factor Type A
WT	Wild-type
2YT	2x yeast tryptone
3MC	3- Carnevale, Mingarelli, Malpuech, and Michels

Chapter 1

'Introduction'

1.1 The Complement System

Complement is an ancient and essential component of immunity, and plays one of the first roles of defence against pathogen entry as part of the innate immune system. First discovered in the late 19th century in human serum, complement can work in an antibody-independent manner to immediately lyse invading pathogens (Fujita et al., 2004, Liszewski and Atkinson, 2015). The complement system consists of over 35 proteins, and there are three different initial proteolytic cascades that can be activated depending on the molecular trigger detected. These pathways are named the classical, lectin and alternative pathways. As seen in Figure 1.1, although the initial stages of each pathway are distinct, each pathway generates a proteolytic cascade that eventually converges and leads to the formation of a C3 convertase complex, consisting of the cleavage products C4b and C2a, or C3b and Bb (Duncan et al., 2008).
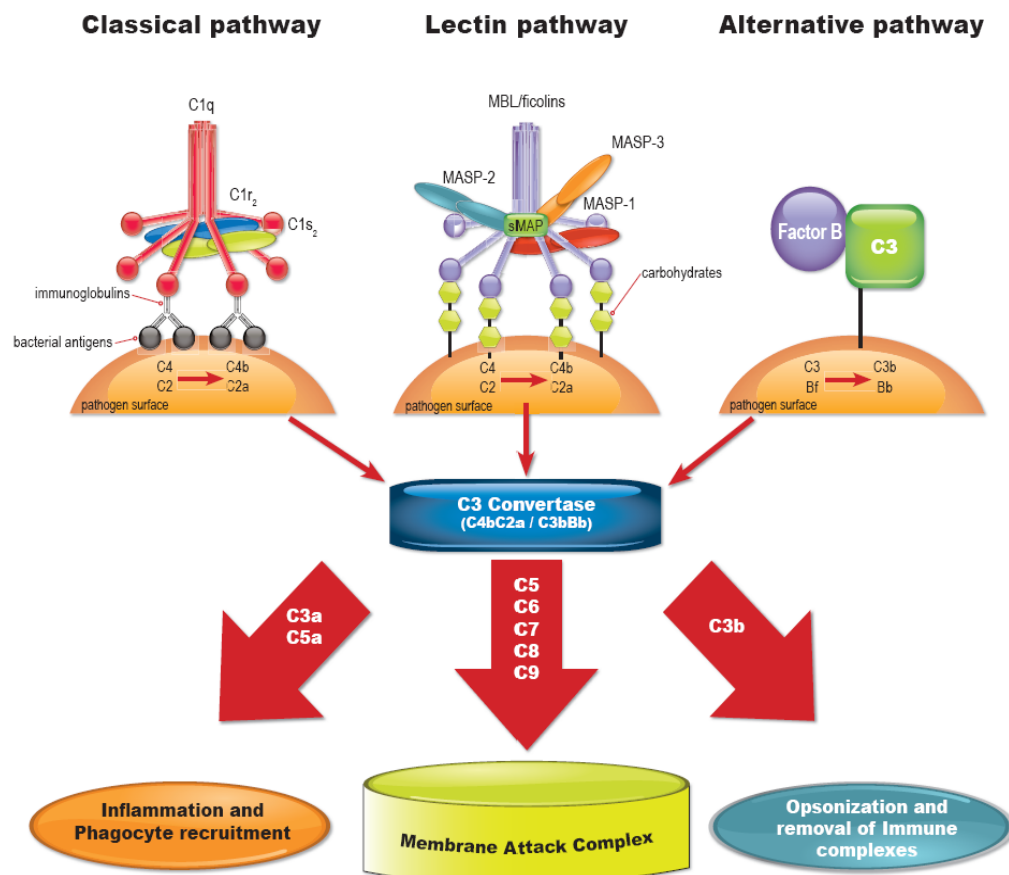
Figure 1.1: The three pathways of complement- despite beginning in different manners, all 3 pathways converge upon the formation of the C3 convertase, which leads to inflammation and pathogen opsonisation, lysis and removal. Taken from Duncan et al., 2008.

The formation of the C3 convertase allows the final section of the complement proteolytic cascade to begin. The final section of the cascade produces three main end results: disruption of the pathogen surface through pore formation via assembly of the Membrane Attack Complex (MAC), pathogen (and immune complex) opsonisation and the promotion of inflammation (Duncan et al., 2008).

Although classified as part of the innate immune system, complement also plays a role in the regulation of adaptive immune system activity. For example, complement has been shown to play a role in B-cell differentiation and also in T-cell responses (Carroll, 2004, Kolev et al., 2014). The role of complement in non-immune related functions is also coming to light, such as lectin pathway proteases having roles in the coagulation cascade (Hajela et al., 2002, Krarup et al., 2007, Krarup et al., 2008). In particular, there are an increasing number of studies that show that there is complement involvement in development pathways and tissue homeostasis (Kolev et al., 2014). An example is that the molecule C1q has been identified to play a role in neuronal maturation through pruning of excitatory synapses, as well as increased levels of it leading to a loss of synaptic plasticity, cognitive function and tissue homeostasis during aging (Naito et al., 2012, Stephan et al., 2013, Schafer et al., 2012).

1.2 The Complement Pathways

1.2.1 The Classical Pathway

The classical pathway has been an object of study for many decades. The pathway begins with the recognition molecule C1q. C1q comprises of six heterotrimeric collagen-like triple helices, which assemble through their N-terminal moieties to form a central stalk region. From this stalk region, six individual branches emerge, and end in a C-terminal globular recognition domain (Kishore and Reid, 2000). C1q can bind to a number of different molecules, both self (C-reactive protein, apoptotic cells, Fc region of antibodies) and non-self-molecules presented by pathogens, such as LPS (Gal et al., 2009). C1q binds zymogenic C1r and C1s, which form a calcium-dependent heterotetramer, and this forms the 790 kDa C1 complex (Figure 1.2) (Rossi et al., 1998, Arlaud et al., 2001).
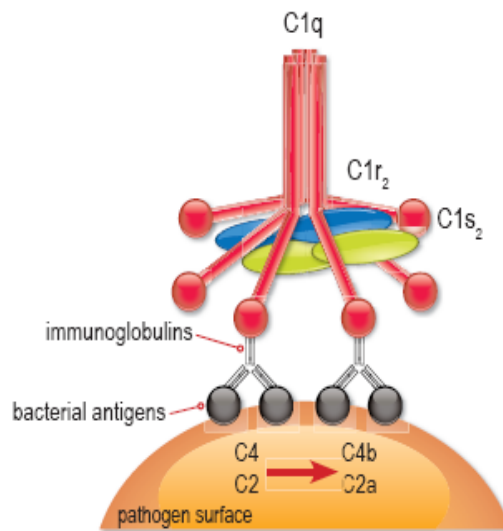
Figure 1.2: The classical complement pathway, where bacterial antigens and immunglobulins trigger conformational changes in the recognition molecule C1q, which lead to the activation of the pathway. Taken from Duncan et al., 2008.

C1r and C1s each comprise of two Complement C1r/C1s, Uegf, Bmp1-like domains (CUB1 and CUB2), an Epidermal Growth Factor-like domain (EGF), two complement control protein domains (CCP1 and CCP2) and a serine protease domain (SP). In the tetramer, C1r is proposed to form a dimer through interactions with the serine protease (SP) domain of one C1s molecule and another's CCP1 domain (Budayova-Spano et al., 2002). In the presence of calcium, each C1r chain binds a C1s polypeptide through its CUB1 and EGF domains (Wallis et al., 2010). The binding of the globular heads of C1q to pathogenic surfaces and molecules allows autoactivation of C1r (Duncan et al., 2008). C1r then activates C1s by cleaving it at the Arg422-Ile423 cleavage point in the SP domain (Gaboriaud et al., 2004). Now activated, C1s is able to cleave its substrates, C2 and C4 (Sim and Tsiftsoglou, 2004). Firstly, C4 is cleaved into C4a and C4b molecules. C4b binds to the pathogenic surface covalently through its exposed reactive groups liberated from a thioester bond found within its structure, and attracts C2 (Law and Dodds, 1997, Wallis et al., 2007). This allows C2 to then be cleaved by C1s into C2a and C2b (Muller-Eberhard, 1988). The cleaved components C4b and C2a then form the C3 convertase (C4bC2a) (Muller-Eberhard, 1988). As discussed, the major ultimate outcome of C3 convertase activity is the formation of the Membrane Attack Complex (MAC) on the surface of the pathogen, which leads to pathogen lysis. The activity of both C1r and

C1s has been found to be regulated by the serine protease inhibitor, C1 inhibitor [C1-INH] (Arlaud et al., 1979).

1.2.2 The Lectin Pathway

The lectin pathway was discovered more recently than the classical pathway, and shares many intriguing similarities with the classical pathway, despite being defined as a separate complement pathway. Activation of the lectin pathway begins with recognition molecules, such as Mannose-Binding Lectin (MBL) and the ficolins, recognizing carbohydrate moieties, e.g. N-acetylglucosamine, on pathogen surfaces (Figure 1.3) (Matsushita, 1996).
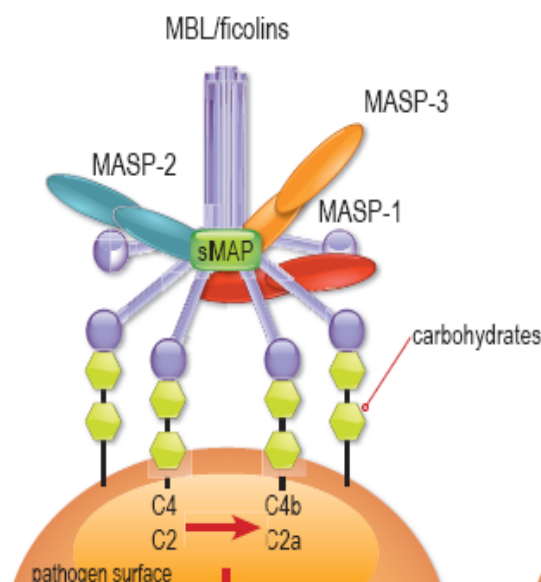
Figure 1.3: The Lectin Pathway. Unlike the classical pathway, the lectin pathway is activated by conformational changes upon MBL/ficolin binding to bacterial carbohydrates. However, just as in the classical pathway, the C3 convertase is formed using the C4b and C2a molecules produced by cleavage of C2 and C4 by MASP-1 and MASP-2. Taken from Duncan et al., 2008.

MBL shares a similar structure to C1q, with an N-terminal cysteine-rich region, a collagen-like region, and a C-terminal carbohydrate recognition domain (CRD) that recognises the pyranose ring of many carbohydrates (Weis et al., 1992, Matsushita, 1996). In serum, MBL has been found in a number of forms, but the two major forms consist of a trimer (named MBL I) and a tetramer (MBL II) (Teillet et al., 2005). As seen in Figure 1.3, MBL and ficolins bind to MBL-Associated Serine Proteases (MASPs), of which there

are three kinds (MASPs 1, 2 and 3) and two alternative MASP variations (MAp19 and MAp44). MASPs have a homologous structure to C1r and C1s, again being composed of CUB1, EGF, CUB2, CCP1, CCP2 and SP domains (Bork and Beckmann, 1993, Gregory et al., 2004). Alternative splicing of the primary RNA transcript means only two genes are required to produce the different MASP variants, with MASP-1, MASP-3 and MAp44 encoded by one gene, and MASP-2 and MAp19 encoded by another (Sorensen et al., 2005). MBL I has been found to associate with MASP-1 and MAp19, whereas MASP-2 and MASP-3 associate with MBL II (Dahl et al., 2001, Teillet et al., 2005, Tateishi et al., 2011). However, the recent finding that MASP-1 activates MASP-2 suggests that further research is required to confirm this (Degn et al., 2012, Heja et al., 2012b, Megyeri et al., 2013).

Of all the MASPs, MASP-2 has the best defined role in the lectin pathway at this point in time. Like C1s, MASP-2 must be cleaved at the Arg/Ile activation cleavage site (R444/I445) to form the active enzyme. MASP-2 is capable of autoactivation, even without MBL/ficolins, and so activated MASP-2 has been said to represent the minimal requirement for lectin pathway activation (Vorup-Jensen et al., 2000). However, research in the past few years has shown that MASP-2 activation is more complex, with MASP-1 shown to be the primary activator of MASP-2, as opposed to MASP-2 autoactivation (Degn et al., 2012, Heja et al., 2012b, Megyeri et al., 2013). It is thought that MASP-1 and MASP-2 can form heterodimers, somewhat like C1r can do with C1s, although there is not yet any evidence that this occurs *in vivo* (Degn et al., 2013, Parej et al., 2013). In addition to sharing a domain layout with C1s, MASP-2 also cleaves the same substrates, as it is able to cleave C2 and C4 to produce the C4b and C2a molecules that form the C3 convertase (Matsushita et al., 2000, Wallis et al., 2007). The activity of MASP-2 has been found to be regulated by the C1-INH, and, more recently, the serpin, antithrombin, has also been found to be able to inhibit MASP-2 activity in the presence of heparin (Matsushita et al., 2000, Parej et al., 2013).

The activities of MASP-1 and MASP-3 are still under much study, with some surprising findings over the last few years leading to a better understanding of their roles in not only complement, but in other non-immune related systems as well. Initially, it was thought that MASP-1 enhanced complement activation triggered by MASP-2, as it was shown to be unable to trigger lectin pathway activation itself. However, Heja *et al*. (2012a

and 2012b) recently created monospecific inhibitors for both MASP-1 and MASP-2 (Heja et al., 2012a, Heja et al., 2012b). It was thought that use of the MASP-1 inhibitor would lead to only partial lectin pathway blockage because MASP-1 is viewed as an auxiliary component in the pathway. However, use of the MASP-1 inhibitor led to complete arrest of the lectin pathway, suggesting that MASP-1 may play a more central role in the lectin pathway than previously thought (Heja et al., 2012a, Heja et al., 2012b). MASP-1 has also been associated with activation of MASP-3 (Iwaki et al., 2011, Degn et al., 2012). Further work suggests that MASP-1 is responsible for MASP-2 activation in normal human serum, and the study also found that MASP-1 is responsible for producing approximately 60% of the C2a required for formation of the C3 convertase complex, while MASP-2 was responsible for approximately 40% (Heja et al., 2012b). It was hypothesised that although MASP-1 is less efficient at C2 cleavage than MASP-2, its concentration in the blood far exceeds that of MASP-2 (11 µg/mL vs 0.5 µg/mL), which appears to compensate for the reduced efficiency (Heja et al., 2012b). Like MASP-2, MASP-1 is inhibited by C1 Inhibitor, and, in the presence of heparin, antithrombin (Matsushita et al., 2000, Parej et al., 2013). In addition to its role in MASP-2 activation and C2 cleavage, it also appears that MASP-1 cleaves C3, although there is some debate about this (Duncan et al, 2008). MASP-1 may also activate complement Factor D from the alternative pathway (Takahashi et al., 2010). Outside of the complement system, MASP-1 has been shown to cleave fibrinogen and factor XIII from the blood-clotting cascade in a manner quite similar to thrombin (Kraup et al., 2008, Gulla et al., 2010).

MASP-3 is the most recently discovered of the MASPs, and the least understood. With a median concentration of 5.0 µg/mL in plasma, MASP-3 has only shown activity against some synthetic peptide substrates, as well as insulin-like growth factor binding protein-5 (Cortesio and Jiang, 2006, Degn et al., 2010, Yongqing et al., 2013). Its role in complement, and the immune system, is not yet understood. Unlike MASP-1 and MASP-2, MASP-3 is not inhibited by C1 inhibitor (Gal et al., 2007). One theory is that MASP-3 plays a role in complement through the downregulation of C4 and C2 cleavage by MASP-2 (Dahl et al., 2001). However, MASP-3 has recently been found to play a role outside of the immune system, where certain MASP-3 mutations have been associated with the developmental disorder, Carnevale, Mingarelli, Malpuech, and Michels (3MC) syndrome (Sirmaci et al., 2010, Rooryck et al., 2011). One mutation, the G666E mutation, has been characterized and is found to cause a loss of activity in MASP-3, as it leads to a

disturbance of the catalytic serine residue (Yongqing et al., 2013). The characterisation of MASP-3 and the determination of the role/s it plays in both immunity and in other biological processes is still a work in progress.

MBL Associated Protein 19 (MAp19), also known as sMAP, is a truncated 19 kDa product of alternative splicing and polyadenylation of the primary RNA transcript of the MASP-2 gene (Stover et al., 1999b, Takahashi et al., 1999). It contains the same CUB1 and EGF domains as MASP-2, but has an extra four unique amino acids at the C-terminal end of the protein (Gregory et al., 2004). Like MASP-2, it forms homodimers via the CUB1 and EGF domains, and associates with MBL and L-ficolin in a calcium-dependent manner (Gregory et al., 2004). It has also been shown to be able to bind to complexes of MASP-2, as well as MASP-1/MASP-3/MAp44 complexes in a ficolin/MBL-dependent manner (Degn et al., 2013). The function of MAp19 is not yet fully understood, but it is speculated that because of its ability to bind to MBL and ficolins, it competes with the MASPs to prevent the activation of the lectin pathway (Iwaki et al., 2006). For this to be effective, however, the concentrations of the MASPs and MAp19 would have to be greater than the total number of binding sites on MBL and ficolin in the blood (Gal et al., 2009). Currently, this is believed to be unlikely, as it is thought that MBL and ficolins are present in excess amounts within the circulation (Mayilyan et al., 2006). More work is required on MAp19 to discern its role in the complement system.

MAp44 is a 44 kDa product of alternative splicing of the MASP-1/3 gene. It is non-catalytic, and contains the first four domains (CUB1-EGF-CUB2-CCP1) of MASP-1 and MASP-3, but has an additional unique sequence of 17 amino acids at the C-terminus. Gathered data indicates that MAp44 inhibits lectin pathway activity by competitively inhibiting MASP-2 binding of MBL, and also by displacing MASP-2 from co-complexes of MASP-1 and MASP-2 (Degn et al., 2009, Skjoedt et al., 2010, Degn et al., 2013). *In vivo* studies in mice have shown that MAp44 displaces MASP-1, 2 and 3 from the MBL complex, and is able to reduce damage during myocardial ischemia/reperfusion injury (Pavlov et al., 2012). Therefore, it appears that the function of MAp44 in the complement system is that of an inhibitor.

1.2.3   The Alternative Pathway

The alternative pathway, originally called the properdin pathway, is the oldest of the pathways, with a number of creatures, such as corals, sea urchins and sponges, having an alternative pathway almost identical to that in humans (Zhu et al., 2005, Ariki et al., 2008). It may be perceived as the older and less complex complement pathway due to the smaller number of components involved, but is more complex than it was first given credit for. It shares some similarities with the classical and lectin pathways, but its activation is dependent on a tightly controlled balance of spontaneous, low-level cleavage of C3 and various inhibitors that regulate this cleavage activity (Dodds, 2002). In the 'fluid phase', C3, due to the instability of its thioester bond, is transiently activated continuously at a slow rate (Holers and Thurman, 2004). However, the C3b generated through this activation is normally hydrolysed quickly by inhibitors such as Factors H and I. If a molecule of C3b is able to bind to a surface and form a covalent bond, two outcomes can occur. If C3b binds to a host cell, Factors H, I and other surface controllers such as Decay Accelerating Factor (DAF) break this C3b down to prevent further alternative pathway activation occurring. However, if C3b binds to pathogen surfaces, which lack the regulators found on host cells, it is protected from this inhibition, and alternative pathway activation is allowed to occur (Dodds, 2002). An amplification loop occurs, as more C3 binds to the pathogen surface and becomes activated (Harboe et al., 2009). The inhibitors that are so critical to prevent inappropriate alternative pathway activation are a genetically, structurally and functionally related multigene family, the regulators of complement activation (RCA) gene/protein cluster (Zipfel and Skerka, 2009). In addition to C3b formation, Factor B binds and is cleaved by Factor D into the fragments Ba and Bb. The C3 convertase is then formed upon the pathogen surface when the Bb fragment binds to the C3b fragment (Holers and Thurman, 2004)(Figure 1.4).
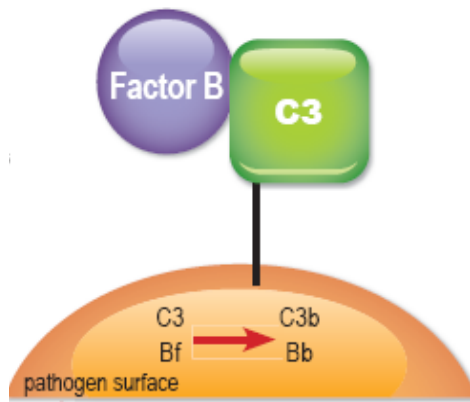
Figure 1.4: The Alternative Pathway. Although considered the older and less complex of the 3 pathways, it is quite complex and quite different from the other complement pathways. The cleavage of C3 and Factor B leads to the formation of the C3b and Bb molecules, which make up the C3 convertase. Taken from Duncan et al., 2008.

Unregulated alternative pathway activity is increasingly been associated with disease. In particular, atypical haemolytic uraemic syndrome (aHUS), and age-related macular degeneration (AMD), a leading cause of blindness worldwide, have been linked to alternative pathway dysfunction due to loss of function mutations in regulators such as Factor H, Factor I and Membrane Cofactor Protein (CD46) (Liszewski et al., 1991, Liszewski and Atkinson, 2015).

1.3 Important serine proteases of the Classical and Lectin Pathways: MASP-2 and C1s

1.3.1 MASP-2, a key serine protease of the Lectin Pathway

1.3.1.1 The Structural Chemistry of MASP-2

The MASP-2 serine protease is comprised of three N-terminal non-catalytic domains (CUB1-EGF-CUB2) and three catalytic domains (CCP1-CCP2-SP) (Figure 1.5). MASP-2 is activated by MASP-1, which cleaves at the activation cleavage point R444/I445, but it is also capable of autoactivation (Gal et al., 2005, Degn et al., 2012, Heja et al., 2012b, Megyeri et al., 2013). MASP-2 normally circulates in the blood in its zymogen

form, bound to MBL and ficolins through the CUB and EGF domains found on the protease (Wallis and Dodd, 2000).
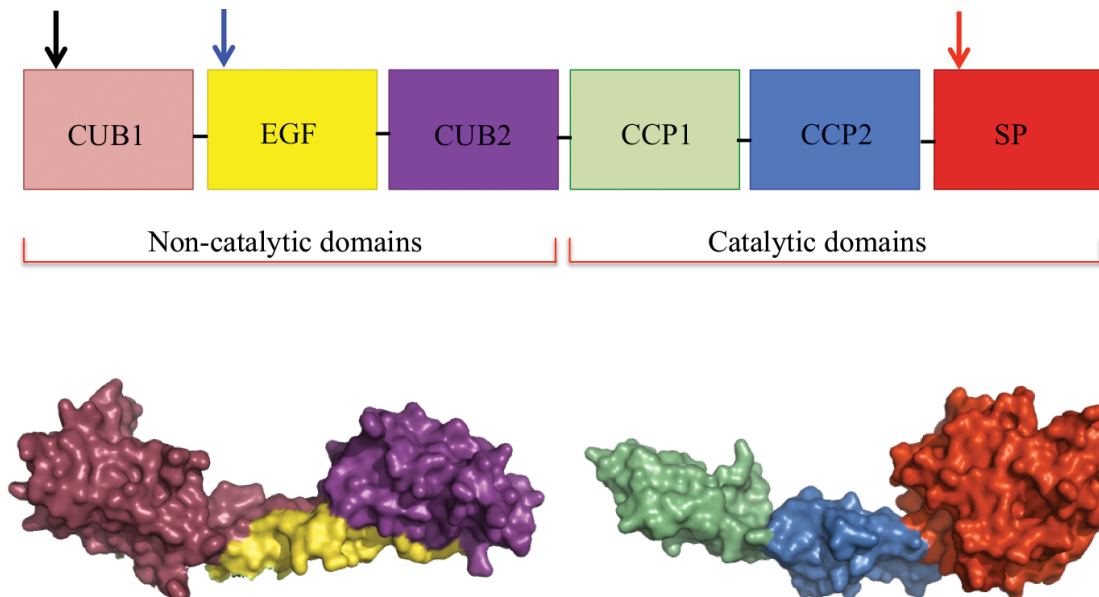
Figure 1.5: The domain layout of MASP-2. A schematic depiction of the layout of MASP-2 is seen on top, with the black arrow indicating the potential Ca^{2+} binding site on the CUB1 domain, and the blue arrow indicating the confirmed Ca^{2+} binding site on the EGF domain. The red arrow indicates the point of cleavage where MASP-2 is cleaved in order for it to become an active enzyme. At the bottom of the image, a structural depiction of the non-catalytic domains (PDB file 1NT0, DOI: 10.2210/pdb1nt0/pdb) and the catalytic domains (PDB file 1ZJK, DOI: 10.2210/pdb1zjk/pdb) of MASP-2 is shown.

1.3.1.2 The non-catalytic domains of MASP-2

The non-catalytic domains are important in allowing MASP-2 to perform two functions. One is that these domains allow MASP-2 to form homodimers. It appears that only the first two domains (CUB1 and EGF) are required for this to occur (Thielens et al., 2001), and that the dimerization process is calcium-independent (Wallis and Dodd, 2000). The second is that these domains allow the MASP-2 homodimer to bind to MBL in a calcium-dependent manner through its CUB1 and EGF domains (Wallis and Dodd, 2000). A calcium-binding site has been found at the N-terminus of the EGF domain, and it is thought that this is required for direct interaction between MASP-2 and MBL (Feinberg et al., 2003). This binding of calcium ions has been shown to help to protect against proteolysis and to stabilize the orientation of these domains (Wallis and Dodd, 2000). The CUB1 domain is also thought to house a Ca^{2+} binding site since the MASP-2 splice variant, MAp19 (discussed in more detail earlier on), which shares the CUB1-EGF and CUB2 domain of MASP-2, has been shown to contain a Ca^{2+} binding site

on the distal end of the CUB1 domain (Gregory et al., 2004). This site was shown to be important for MAp19 binding to MBL (Gregory et al., 2004). The CUB regions may help to increase the EGF domain's affinity for calcium, as it has been shown that calcium binding EGF-like domains experience an increase in affinity for calcium ions by up to three orders of magnitude in the presence of an adjacent protein domain (Stenflo et al., 2000). The structure of the non-catalytic region was elucidated in 2003, and displayed an elongated 'letter C' shape (Feinberg et al., 2003).

1.3.1.3 The catalytic domains of MASP-2

The CCP1 and CCP2 domains associate with the serine protease domain and help to stabilize it. The CCP domain contains four invariant cysteine residues, and highly conserved proline, glycine and hydrophobic residues (Kirkitadze and Barlow, 2001). The CCP1 domain is comprised of six β-strands, and contains a large hydrophobic patch, comprised of residues 299-307 and 357-363 of unknown function (Gal et al., 2005). A linker between the two CCP domains, comprising of a β-strand made up of residues 360-366, is also seen. It forms a number of contacts, such as hydrogen bonds, with the two CCP domains (Gal et al., 2005). The CCP2 domain also shares the traditional features of CCP domain molecules, consisting of six β-strands (Harmat et al., 2004). It has been shown that the conformation of the CCP2 domain remains similar between zymogen and active MASP-2, with it being suggested that the CCP2 domain is necessary to stabilize the SP domain (Gal et al., 2005). Recently, a structure showing the catalytic domains of MASP-2 in complex with C4 was produced (Kidmose et al., 2012). In the structure, a C4 binding exosite was found upon the CCP domains and the linker between them, consisting principally of residues E333, P340, D365 and P368 (Figure 1.6) (Kidmose et al., 2012). As discussed in further detail later on, mutation of these residues, both singly and in combination, led to severely reduced C4 cleavage, with the double mutant MASP-2 E333R D365R essentially unable to cleave C4 (Kidmose et al., 2012).
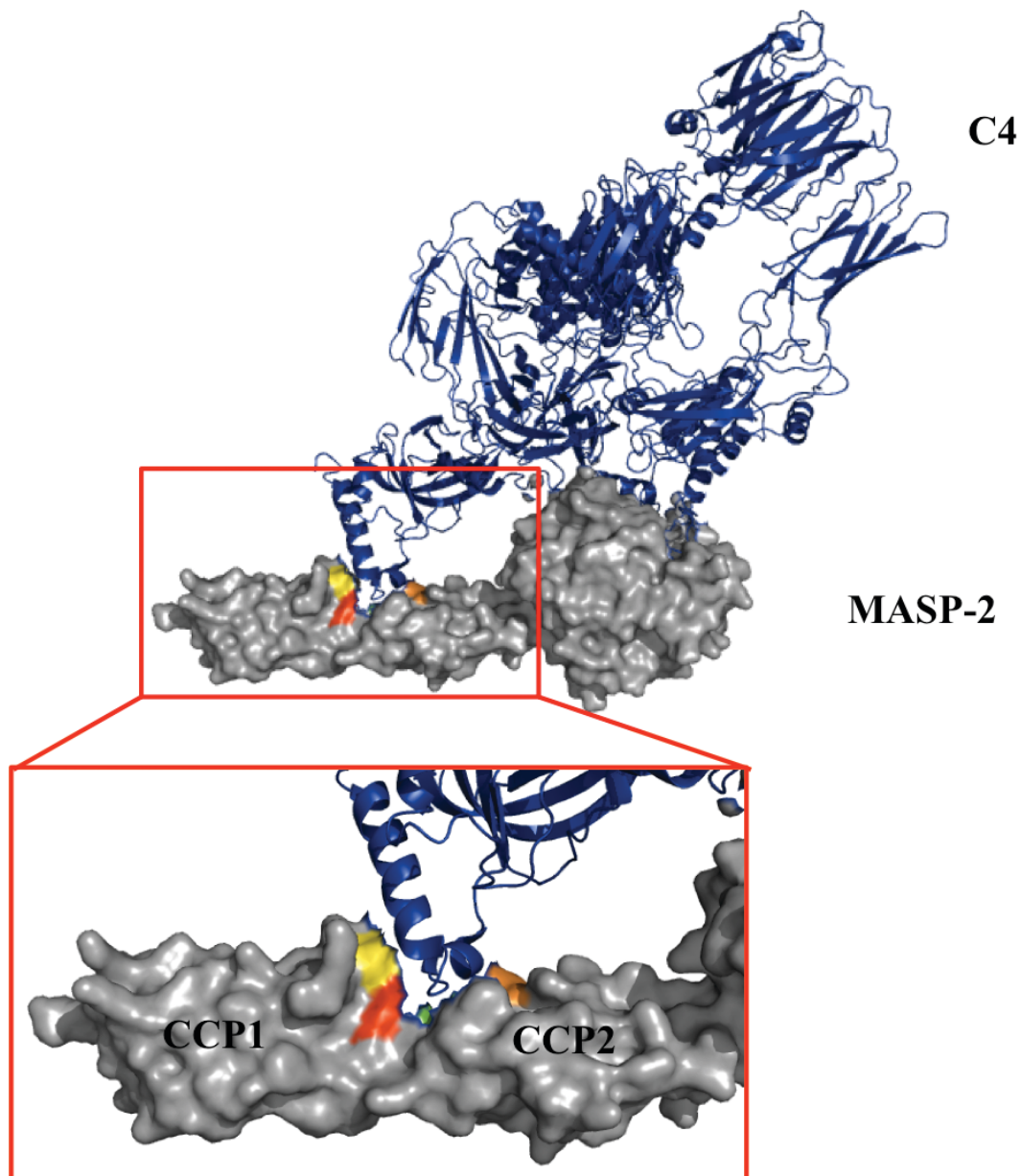
Figure 1.6: The CCP domain exosite of MASP-2. In the image, MASP-2 (grey) is bound to its substrate C4 (blue). Four residues have been shown to play a role in this exosite-E333 (red), P340 (yellow), D365 (green) and P368 (orange). Generated from PDB file 4FXG (DOI: 10.2210/pdb4fxg/pdb).

This correlates with earlier studies, which have shown that for efficient C4 cleavage, the CCP domains are necessary (Ambrus et al., 2003). This recognition appears to be a part of the MASP-2 CCP units, as when C1s had its CCP1 and CCP2 domains replaced with MASP-2 CCP1 and CCP2 domains, it experienced a strong increase in C4 cleavage (Rossi et al., 2005). Truncated forms of MASP-2 have demonstrated that the absence of one or both of these domains does not affect the rate of C2 cleavage, and so it appears that they do not assist cleavage of C2 (Ambrus et al., 2003, Duncan et al., 2012a).

The serine protease (SP) domain displays a typical chymotrypsin fold, with two six-stranded β-barrel domains packed against one another (Harmat et al., 2004, Gal et al., 2005). At the junction of these barrels are the catalytic triad of S633, H483 and D532 (S195, H57, D102 in chymotrypsin numbering) (Harmat et al., 2004). The SP domain also contains the R444 / I445 activation cleavage point, which must be cleaved to allow activation of MASP-2 from the zymogen state. It contains eight loops that help to determine substrate specificity.
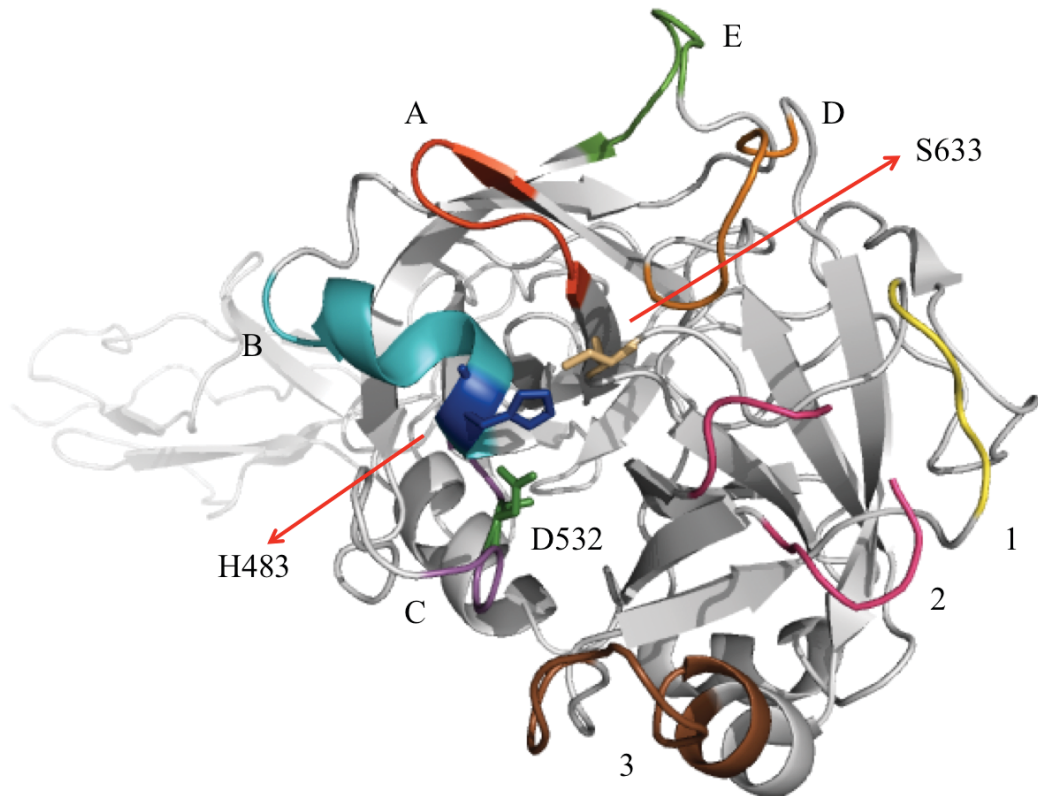
Figure 1.7: The SP domain of MASP-2. The SP domain contains the catalytic triad of residues required for MASP-2 catalytic functioning- H483 (dark blue), D532 (dark green) and S633 (light orange). It contains eight loops that play a role in determining substrate specificity- Loop A (red), Loop B (teal), Loop C (magenta), Loop D (orange), Loop E (green), Loop 1 (yellow), Loop 2 (hot pink) and Loop 3 (brown). Determination of loops using protocol outlined by Perona and Craik, 1997. Image generated using PDB file 1ZJK (DOI: 10.2210/pdb1zjk/pdb).

The specificity of the S1 pocket and other substrate binding sites are determined by eight surface loops (Figure 1.7) (Harmat et al., 2004). Despite sharing characteristics with other complement proteases, such as the same substrates with C1s, many of these loops differ in length, amino acid composition and conformation (Harmat et al., 2004). In fact, some of the loops are quite similar to those of thrombin or trypsin (Harmat et al.,

2004). Given the narrow substrate specificity of MASP-2, it is believed that the conformation of these loops helps to ensure this by restricting access to substrate-binding sites (Gal et al., 2009). It is thought that loops 1, 2 and D, along with the activation peptide, show a high degree of flexibility and form the 'activation domain' (Bode and Huber, 1978, Gal et al., 2005).

Both an active form and a zymogen mutant (R444Q) form of MASP-2's catalytic domains have been crystallized (Harmat et al., 2004, Gal et al., 2005). Crystal structures have shown that the β-barrel domains in both active and zymogen forms are very similar, and that the catalytic triad is in its active confirmation in both forms (Gal et al., 2005). However, some major structural differences between active and zymogen form are seen in the loops (Gal et al., 2005). A number of these loops (Loops A, B, C and 3) are normally unchanged in chymotrypsin-like enzymes upon activation, but in the active structure of MASP-2 structure they were significantly altered compared to the zymogen form, indicating their flexibility (Gal et al., 2005). Another autoactivating enzyme, C1r, also undergoes major conformational changes in these loops upon activation (Budayova-Spano et al., 2002, Gal et al., 2005). Gal et al. (2005) hypothesize that this may be a feature of autoactivating enzymes, and that this flexibility permits the conformational changes required of the loops to form an active enzyme (Gal et al., 2005). The authors suggest that these loops, along with the activation domain, form an 'autoactivation domain' (Gal et al., 2005).

Crystallization of the active form of MASP-2 has revealed two different orientations for the CCP2-SP domain interface (Harmat et al., 2004). Both conformations share new patterns of interactions in this CCP2-SP interface that differ from the usual hydrogen bonds and van der Waal's contacts at the same interface seen in structures of C1r and C1s (Harmat et al., 2004). The interactions between the CCP-2 and SP domains are quite strong and differential scanning calorimetry (DSC) performed by Harmat et al. (2004) has shown that CCP2 helps to increase the stability of the SP domain (Harmat et al., 2004). Despite this strong interaction, when compared to the rigid CCP2-SP interface of C1s, the interface is quite flexible. This may be due to a lower number of proline residues in the interface region (two for MASP-2, as opposed to four for C1s and five for C1r), as well as the reduced number of disulfide bonds (only two compared to the usual four to six bonds in human trypsin-like enzymes) (Kenesi et al., 2003, Harmat et al.,

2004). A recently solved structure of MASP-2 complexed with C4 demonstrates the flexibility of this interface, as upon C4 binding, the CCP domains of MASP-2 do not move, but the SP domain rotates by 24-29° (Kidmose et al., 2012). It is thought that this flexibility allows MASP-2 to move its serine protease domains into the correct position during activation and C2 and C4 cleavage, while also helping to contribute towards MASP-2's substrate specificity (Harmat et al., 2004, Gal et al., 2005).

The SP domain may also contain a potential C4 binding exosite. The recently released structure of MASP-2 complexed with C4 shows a run of sulfated tyrosine residues located between residues 1412 to 1432 on C4 coming into contact with, or in close proximity to, a number of residues upon the SP domain of MASP-2 (K450, K503, R578 and R583) (Figure 1.8) (Kidmose et al., 2012). The importance of this binding site is not yet known.
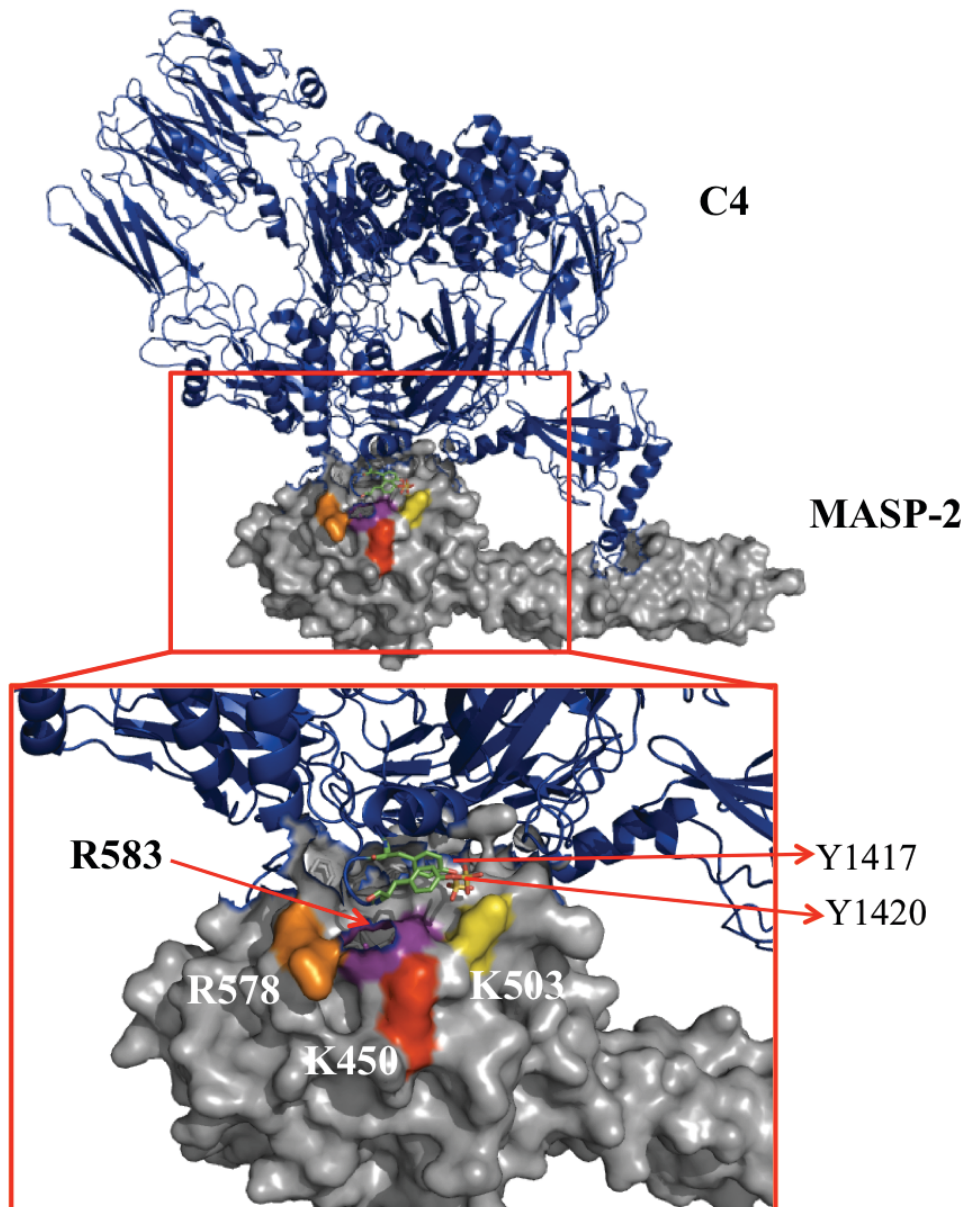
Figure 1.8: The SP domain exosite of MASP-2. In this image, MASP-2 (grey) is bound to its substrate C4 (blue). Four residues have been highlighted as potentially playing a role in this exosite- K450 (red), K503 (yellow), R578 (orange) and R583 (purple). The structure shows the sulfated tyrosines of C4 in close proximity to the highlighted exosite residues. Generated from PDB file 4FXG (DOI: 10.2210/pdb4fxg/pdb).

1.3.2 C1s, a key serine protease of the Classical Pathway

1.3.2.1 The Structural Chemistry of C1s

C1s, like MASP-2, is a serine protease comprised of three N-terminal non-catalytic domains (CUB1-EGF-CUB2) and three catalytic domains (CCP1-CCP2-SP) (Figure 1.9). It shares identical domain organisation to the MASPs and C1r, and similar overall domain

structure. C1s circulates as a zymogen until it is activated by C1r, which cleaves at the activation cleavage point R422-I423 (Rossi et al., 1998, Gregory et al., 2003).
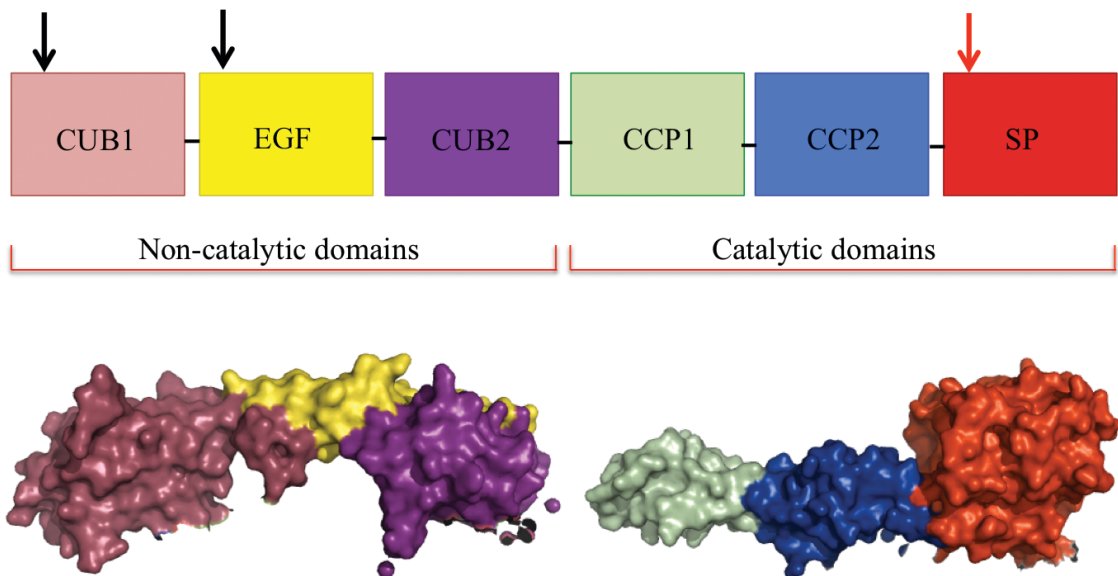
Figure 1.9: The domain layout of C1s. A schematic depiction of the domain layout of C1s is shown on top. The red arrow indicates the point of cleavage where C1s is cleaved by C1r in order to become an active enzyme. The black arrows indicate calcium binding sites (Site I and Site II), which are important in the stability and binding abilities of the non-catalytic domains of C1s. At the bottom of the image, structural depictions of the non-catalytic domains (PDB file 4LMF [DOI: 10.2210/pdb4lmf/pdb]) and the catalytic domains (PDB file 4J1Y [DOI: 10.2210/pdb4j1y/pdb]) of C1s are shown.

1.3.2.2 The non-catalytic domains of C1s

The non-catalytic domains of C1s play a critical role in the formation of Ca^{2+}-dependent interactions between C1s and components of the C1 complex, such as C1r and C1q (Villiers et al., 1985, Busby and Ingham, 1990). One calcium ion is bound within the EGF domain and another is bound to the distal end of the CUB1 domain (Figure 1.10). This CUB1 calcium-binding site (called Site II) mediates a large number of interactions (such as hydrogen bonds and oxygen bonds) that are very important in helping to stabilise the distal end of the CUB1 domain (Gregory et al., 2003). The calcium ion found in the EGF domain (called Site I) is coordinated by seven oxygen ligands, and plays a key role in the intra and inter-molecular CUB1-EGF interfaces (Gregory et al., 2003). The CUB1 and EGF domains can form calcium-dependent homodimers in the absence of C1r (Gregory et al., 2003). The solved structure of the CUB1 and EGF domains showed a head-to-tail assembly mode, where the CUB1 domain of one C1s molecule interacts with

the EGF domain of another C1s molecule (Figure 1.10) (Feinberg et al., 2003, Gregory et al., 2003).
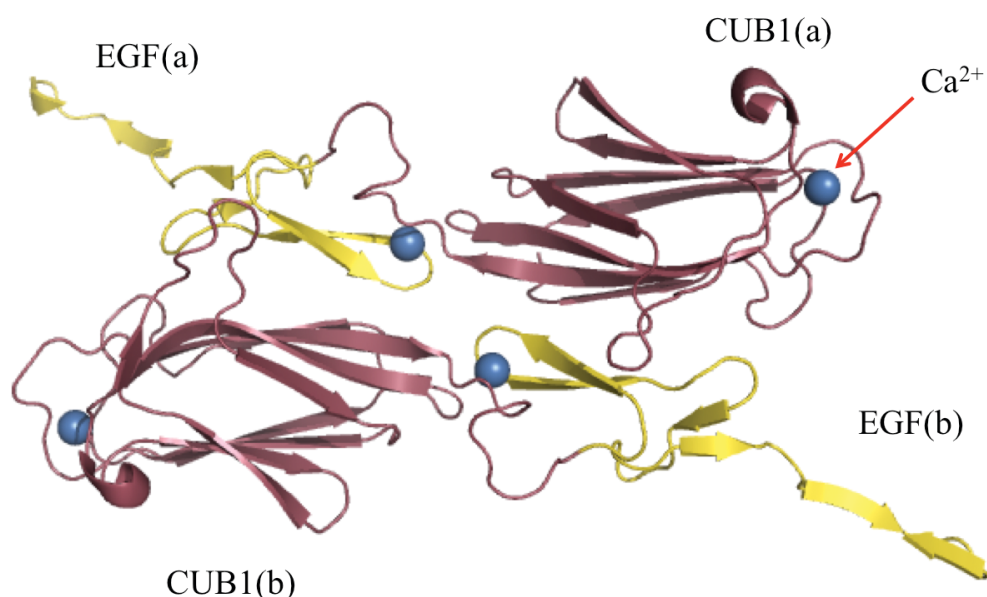
Figure 1.10: The 'head-to-toe' binding mechanism of the C1s CUB and EGF domains. The CUB1 domains are shown in pink, while the EGF domains are shown in yellow. The two C1s molecules are referred to as either a or b. Calcium ions are shown as blue balls. Generated using PDB file 4LMF (DOI: 10.2210/pdb4lmf/pdb).

1.3.2.3 The catalytic domains of C1s

The catalytic domains of C1s play an important role in the enzymatic functions of this protease. Structural work has shown that the CCP1 domain of C1s may contain a CCP binding exosite for C4, as is seen in MASP-2 (Figure 1.11). The CCP1 domain contains a β hairpin loop, comprised of residues 327-334, and is structurally equivalent to a loop on MASP-2 containing residues 333-340 (Perry et al., 2013). As discussed earlier, of these residues, residues 333 and 340 in MASP-2 have been shown to contribute to a CCP domain exosite (Kidmose et al., 2012). In addition to this, residue R331 of C1s has been predicted to form a salt bridge with residue D1732 of C4 in a model of C1s and C4 binding (Perry et al., 2013).
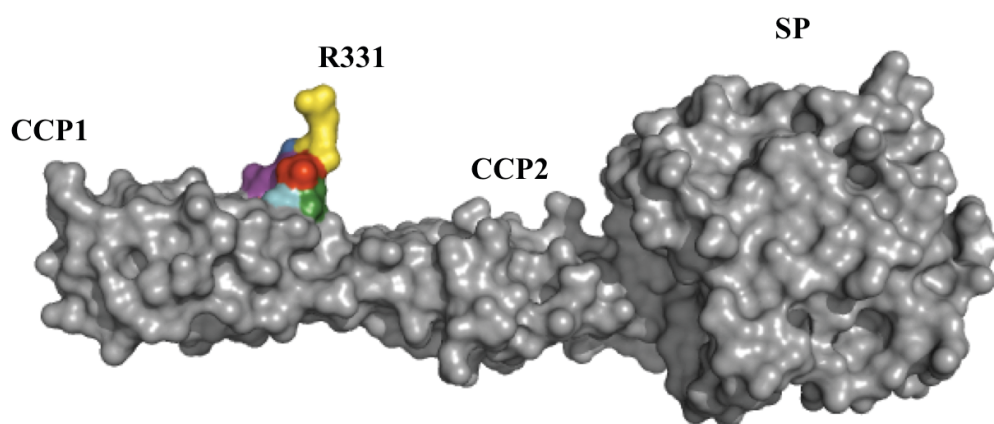
Figure 1.11: The potential C1s CCP domain exosite for C4 binding. Residues E329 (purple), R331 (yellow), V332 (red), G333 (dark green) and A334 (cyan) are clearly visible, while residues V327 (orange), V328 (blue) and G330 (light blue) are obscured. Generated using PDB 4J1Y (DOI: 10.2210/pdb4j1y/pdb).

The CCP2 domain has been shown to possess a compact hydrophobic core enveloped by six β-strands (Gaboriaud et al., 2000). The CCP2 domain is linked to the SP domain on the opposite side of the active site. The interface between the CCP2 and SP domains, as briefly mentioned above, is quite rigid (Gaboriaud et al., 2000). It is thought that the high number of hydrophobic tyrosine and proline residues in this interface help to enhance this rigidity (Gaboriaud et al., 2000). Certain segments that have this high percentage of hydrophobic residues, such as residues 407-410 (an intermediary segment), have also been noted to be "clamped" by hydrophobic residues in other areas (Gaboriaud et al., 2000). For instance, residues 407-410 are "clamped" on one side by a run of tyrosine residues (375-77) on the CCP2 domain, and on the other side by residues 532 to 534 of the SP domain (Gaboriaud et al., 2000). The "clamping" provided is strengthened by direct interactions between the CCP2 and SP domains as well (Gaboriaud et al., 2000). In models of C1s' interactions within the C1 complex, it is proposed that the SP domain of C1s is buried within the C1 complex prior to activation (Weiss et al., 1986, Arlaud and Colomb, 1987). When the R426-I427 bond is cleaved by C1r, it is thought that the region

connecting the CCP1 and CCP2 acts in a hinge-like manner and allows the SP domain to be exposed outside the C1 complex in order to cleave its substrates, C2 and C4 (Gaboriaud et al., 2000).

The SP domain is responsible for the cleavage of C2 and C4, and interacting with C1 inhibitor. The catalytic triad residues are S632 (S195), H475 (H57) and D529 (D102) (chymotrypsin numbering in brackets), and again, like MASP-2, these residues are located in between two six-stranded β-barrels connected by three trans segments, several surface loops and a C-terminal α helix (Gaboriaud et al., 2000). The SP domain of C1s has seven surface loops, with loops 3 and C inserted in one side of the active site, while the loops 1, 2 and A, which have been identified as having deletions, are located on the other side (Figure 1.12) (Gaboriaud et al., 2000). The loops (1-3 and loops A-E) have been shown to play an important role in determining fine substrate specificity (Perona and Craik, 1997). Upon activation of C1s, loops A, D, 1 and 2 have been shown to undergo significant structural rearrangement (Perry et al., 2013). Loop D in particular shows significant alterations in orientation upon activation, with residues seen to shift up to 11Å (Perry et al., 2013).
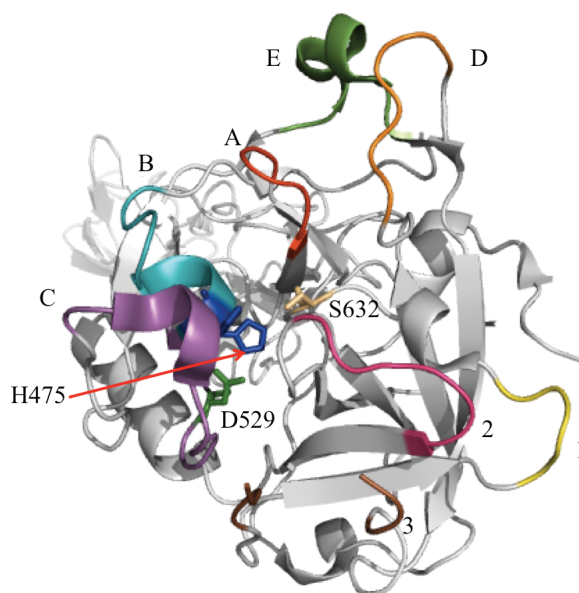
Figure 1.12: The SP domain of C1s. The SP domain contains the catalytic triad of residues required for C1s catalytic functioning- H475 (dark blue), D529 (dark green) and S632 (light orange). It also contains seven loops that play a role in determining substrate specificity- Loop A (red), Loop B (teal), Loop C (magenta), Loop D (orange), Loop E (green), Loop 1 (yellow), Loop 2 (hot pink) and Loop 3 (brown). Determination of loops using protocol outlined by Perona and Craik, 1997. Image generated using PDB 4J1Y(DOI: 10.2210/pdb4j1y/pdb).

Recently, a C4 binding exosite was discovered upon the SP domain of C1s. It was comprised of the charged residues K575, K576, R581 and R583 (Figure 1.13) (Duncan et al., 2012b, Perry et al., 2013). These residues are part of Loop D, which showed significant structural changes upon C1s activation (Duncan et al., 2012b). Discussed in further detail in Section 1.4.1.5, mutation of all four residues simultaneously to alanine was found to severely reduce C4 cleavage efficiency, and Surface Plasmon Resonance (SPR) showed a lack of binding between this C1s mutant and C4 (Perry et al., 2013). This exosite also forms a sulfate-binding site, as antibodies against the sulfated tyrosines of C4 were unable to bind in the presence of C1s. In a model of C1s and C4 docking developed, two of the three sulfated tyrosines of C4 (residues 1420 and 1422) were seen to interact with these identified C1s residues (Duncan et al., 2012b).
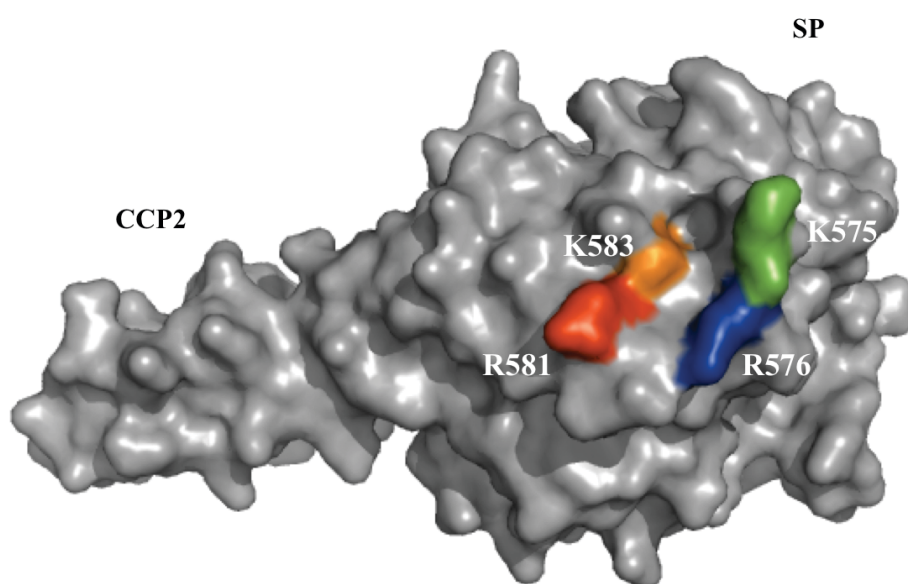
Figure 1.13: The SP domain exosite of C1s. Consisting of four residues, this exosite has been shown to play a critical role in efficient C4 binding and cleavage by C1s. Residues K575, R576, R581 and K583 are shown in green, blue, red and orange respectively. The CCP2 and SP domains of C1s are depicted in grey. Generated using PDB file 1ELV (DOI: 10.2210/pdb1elv/pdb).

1.4 Substrates of MASP-2 and C1s- C2 and C4

1.4.1 The substrate C4

1.4.1.1 The structure and layout of C4

C4 genes in humans are located in the Major Histocompatibility Class III (MHC III) region of Chromosome 6 (Blanchong et al., 2001). It is classified as a member of the α macroglobulin protein family, along with other complement family members, such as C3 (Sottrup-Jensen et al., 1985). This ~200 kDa protein is synthesised as an inert single chain precursor, until it is processed into a disulphide-bonded 3 chain structure (α, β and γ chains) that is glycosylated and sulfated prior to secretion (Figure 1.14)(Blanchong et al., 2001). C4 shares a structure very close to its paralogues, C3 and C5 (Fredslund et al., 2006, Fredslund et al., 2008). C4 is comprised of six N-terminal MG domains, and these domains form what is called the β-ring. The C4 α chain is comprised of the MG8 and CUB domains, along with the thioester domain. This has been referred to as the α chain superdomain (Kidmose et al., 2012). The C4a domain is located between the β-ring and the α chain superdomain, and the MG7 and C345C domains are found on the periphery of the α chain superdomain (Kidmose et al., 2012). Initially, only the C4d segment of the C4 α chain was crystallised, but in recent years, the entire C4 molecule has been structurally characterised, both alone and in complex with MASP-2 (van den Elsen et al., 2002, Kidmose et al., 2012).

When the α-chain of C4 is cleaved by either C1s or MASP-2, two molecules are produced: C4a and C4b. C4a is an anaphylatoxin that promotes inflammatory effects at the site of infection, while the C4b generated binds to the pathogen's cell surface through an exposed thioester created during cleavage, and plays a role in the formation of the C3 convertase (Law and Dodds, 1997). The C4b molecule has also been found to contribute to immune clearance through interaction with the CR1 receptor (Krych-Goldberg and Atkinson, 2001).
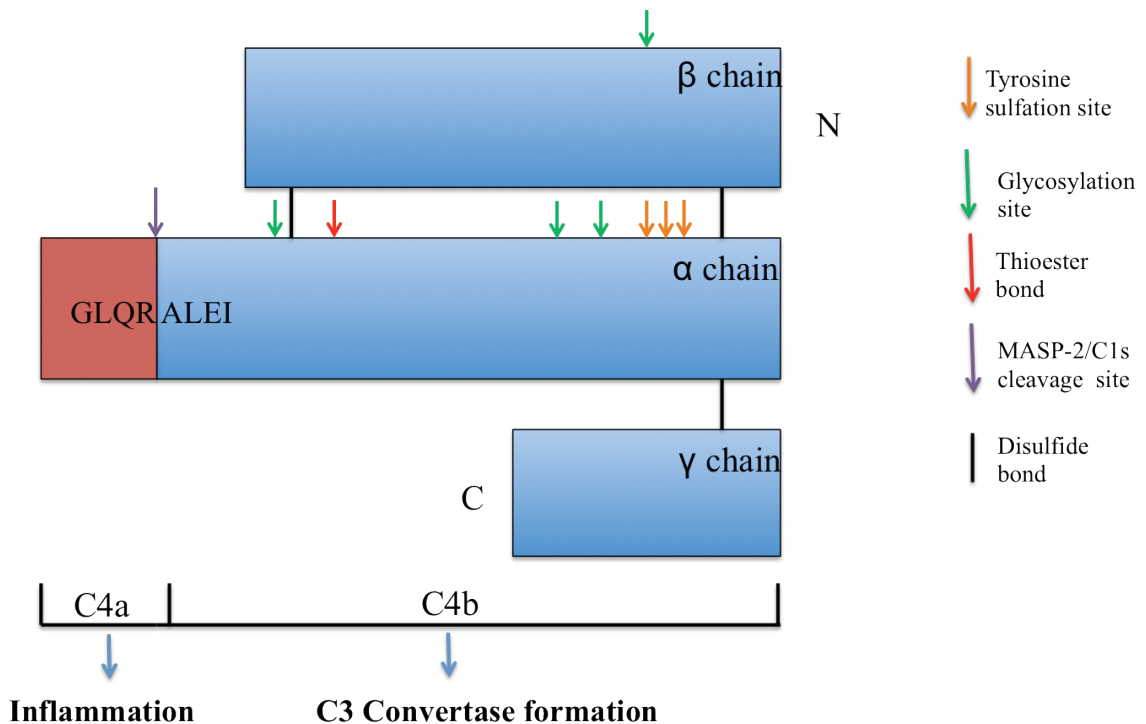
Figure 1.14: The structure of C4. A large and complex substrate, C4, upon cleavage by MASP-2 and C1s, becomes a 3-chain molecule. As can be seen, it has a number of important features, such as the thioester bond (depicted by the red arrow), the site for MASP-2 and C1s cleavage (depicted by the purple arrow), and the sulfated tyrosine residues (depicted by the three orange arrows).

About 90% of C4b remains in the 'fluid phase', as it does not bind to a target, and so becomes inactivated (Law and Dodds, 1997). Cleavage of C4 by C1s or MASP-2 leads to breaking of a thioester bond. The thioester bond, formed between residues C1010 and Q1013, is buried between the MG8 domain and the thioester domain (Kidmose et al., 2012). The thioester bond is not only required for allowing C4 to bind to biological surfaces, but is also required for maintaining the native conformation of the protein (Issac et al., 1998). If the thioester bond is rendered non-functional, for example through selective mutagenesis in the thioester bond region, C1s and MASP-2 are unable to cleave C4 (Issac et al., 1998).

1.4.1.2 The isotypes of C4

C4 exists as two isotypes, C4A and C4B (Belt, et al., 1985). There are separate C4A and C4B genes, but there is great variation in the number and combination of genes within populations. Approximately 55% of Caucasians possess both genes, with 13.3% possessing two C4A genes, and 0.67% possessing two C4B genes (Blanchong et al.,

2001). Of Caucasian populations, 31% of people possess not two, but one or three of these genes in varying combinations (Blanchong et al., 2001). The two isotypes share a 99% sequence identity, but have different serological and haematological activities (Blanchong et al., 2001). Discounting polymorphic variation, C4A and C4B differ by only four amino acids between residues 1101-1106 (Figure 1.15) (Dodds et al., 1996). Thus, these four residues have been referred to as 'isotypic determining residues' (Reilly, 2006).
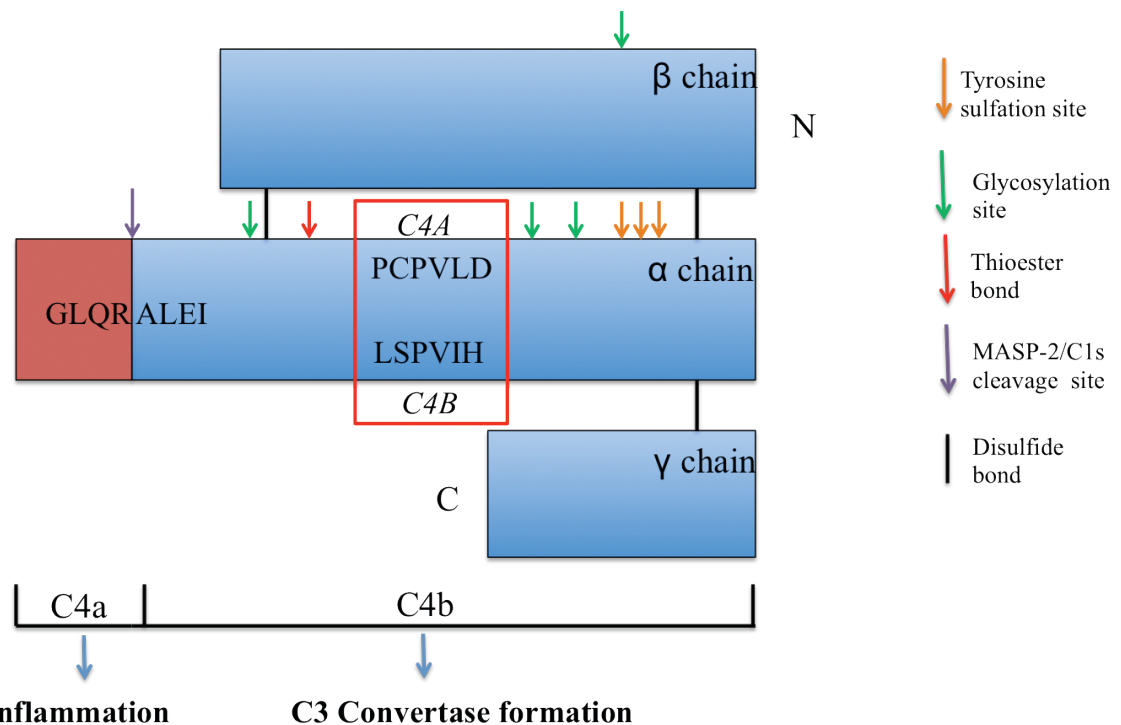
Figure 1.15: Isotypes of C4. The isotypic residues, which are classed as residues 1101-1106, are boxed in red. These residues have been shown to play a key role in determining the serological activity of C4.

The meta-stable C4B tends to form a covalent ester bond with hydroxyl groups after activation, while C4A prefers forming amine bonds with amino groups (Law et al., 1984). Each isotype can bind to both groups, but they are much more efficient when binding to their preferred group. For instance, C4A binds to immune complexes approximately 30% better than C4B (Law et al., 1984). These differences are believed to impact upon the role each isotype plays, with C4A helping to solubilise antibody-antigen aggregates and prevent immune precipitation, while C4B is thought to be more involved in the formation of the MAC (Campbell et al., 1980). Interestingly, Sepp *et al.* (1993) performed site-directed mutagenesis on residues 1101-1106 of C4B and found that

mutating residue 1106 to aspartate, alanine or asparagine caused the C4B molecule to become C4A-like and to bind more efficiently to glycerin, whereas histidine was required to confer C4B-like activity at this position (Sepp et al., 1993). It is thought that the histidine residue in this position may play a catalytic role in the reaction of the activated thioester with hydroxyl groups (Sepp et al., 1993).

1.4.1.3 The interaction between MASP-2 and the substrate C4

In the interaction of MASP-2 with C4, it has been found that the catalytic domains (CCP domains and the SP domain) all have the ability to bind C4 (Duncan et al., 2012a). It was postulated for many years that the CCP domains of MASP-2 housed a binding exosite for C4, as the CCP domains were shown to be important for efficient C4 binding and cleavage. Duncan *et al.* (2012a) showed that the amount of MASP-2 required to achieve 50% C4 cleavage increased from nanomolar quantities when the entire catalytic region of MASP-2 was examined (2.63 nM for the CCP12SP fragment) to micromolar quantities (1.13 µM) for the SP domain alone (Duncan et al., 2012a). It was thought that there was no binding exosite for C4 on the SP domain of MASP-2, as use of the synthetic peptide inhibitor EGRck, which blocks the active site of MASP-2, appeared to prevent binding between the MASP-2 SP domain construct and C4 (Duncan et al., 2012a).

In 2012, the structure of MASP-2 in complex with C4 was published, and the location of the CCP domain binding exosite was found to span the N-terminal end of the CCP1 domain, the linker region, and the C-terminal end of the CCP2 domain (Kidmose et al., 2012). This exosite was seen to be interacting with the C345C domain of C4, and four MASP-2 residues were identified as primary contributors to the exosite- E333, P340, D365 and P368 (Kidmose et al., 2012). This exosite provides a negatively charged binding patch with which the stretch of C4 residues 1716-1725 interacts. This stretch of residues, which contains four arginine residues, is located immediately prior to the large C-terminal helix of the C354C domain (Kidmose et al., 2012). The E333 residue interacts with the R1724 residue, and the D365 residue was shown to interact with the T1721 residue of C4 (Kidmose et al., 2012). Mutation of these residues to arginine lead to a decrease in C4 cleavage in deposition assays, with the P340R and P368R mutations recording C4 cleavage rates of ~ 60%, while the E333R and D365R mutants showed even further reduced rates of C4 cleavage (Kidmose et al., 2012). The double mutants P340R P368R

and E333R and D365R were even more affected than the single mutants, with the E333R D365R mutant showing no C4 cleavage (Kidmose et al., 2012).

The SP domain of MASP-2 unsurprisingly also interacts with C4, given that it is the location of the MASP-2 active site. The structure of MASP-2 in complex with C4 revealed that the SP domain of MASP-2 interacted with a loop containing residues 748-760 of C4 (Kidmose et al., 2012). This run of residues contains the scissile bond region of C4 (P2-P1-P1'-P2' [Q755-R756-A757-L758]). The SP domain surface loops A, B, D, E, 2 and 3 were found to interact with C4 (Kidmose et al., 2012). The SP domain was also shown to form some contacts with the anchor region connecting the MG8 and C345C domains of C4 (Kidmose et al., 2012). However, what was a surprise find in the structure was that MASP-2 appeared to house an SP domain binding exosite, with residues K450, K503, R578 and R583 located very close to the sulfated tyrosines of C4, with the K503 residue being shown to interact with the sulfated tyrosine residue 1417 (Kidmose et al., 2012). The K450, R578 and R583 residues were shown to interact with the C4 residue, D1419.

1.4.1.4 The C4 bypass model of Lectin Pathway activation

Interestingly, a C4 bypass model of lectin pathway activation has been observed in studies, and appears to be dependent on both MASP-2 and C2 (Schwaeble et al., 2011, Asgari et al., 2014). The normal lectin pathway activity requires C4 to be cleaved by MASP-2 to produce C4b, with C4b then recruiting C2 for cleavage by MASP-1 or MASP-2 (Wallis et al., 2007). In this C4 bypass pathway, C4 has been found to not be required for C3 cleavage activity. Why such a pathway has developed is not known, but it may have developed during the evolution of the complement system, or as a 'backup pathway' in case of C4 deficiency (Atkinson and Frank, 2006). The idea of a C4 bypass pathway has been floated for some time, with MBL being implicated in playing a role in it, but recent work has discerned the events of the pathway in greater detail (Atkinson and Frank, 2006, Selander et al., 2006, Clark et al., 2008). Schwaeble *et al.* (2011) showed that even in C4 deficient guinea pig serum, C3 cleavage activity could be seen when the lectin pathway was activated (Schwaeble et al., 2011). MASP-2 appears to be required for this pathway, as MASP-2 deficient plasma did not have this C3 cleavage activity. C2 was identified as playing a role in this C4 bypass pathway, as lectin pathway cleavage of C3

was restored to C2 and Factor B depleted plasma with the addition of recombinant C2 (Schwaeble et al., 2011). MASP-1 was also found to play a role in this pathway, most likely due to its ability to activate MASP-2, and to cleave C2 (Schwaeble et al., 2011). This C4 bypass model of C3 activation appears to be specific to the lectin complement pathway, as no cleavage of C3 was seen in C4-deficient plasma after activation of the classical complement pathway (Schwaeble et al., 2011). Asgari *et al.* (2014) examined the role of this C4 bypass pathway in renal ischemia reperfusion injury in mice that underwent kidney transplantations (Asgari et al., 2014). They found that MASP-2 deficient mice showed better kidney function, less C3 deposition and reduced ischemia reperfusion injury when a kidney from a wild-type mouse was grafted, whereas wild-type mice that received a kidney graft from another wild-type mouse suffered acute renal failure (Asgari et al., 2014). A deficiency in C4 caused no difference in the phenotype seen when grafting a wild-type kidney to a wild-type recipient, and, in addition, mice deficient in both MASP-2 and C4 were shown to be no more protected from injury than mice who were only MASP-2 deficient (Asgari et al., 2014). This strongly suggests that there is indeed a C4 bypass pathway of lectin complement activity, and that MASP-2 plays a key role in it. This C4 bypass pathway has also been seen in humans. A human donor with an inherited deficiency in both C4 genes was found to be completely deficient in C4 (Yang et al., 2004). A monoclonal antibody that inhibits MASP-2 functional activity was used on human C4 deficient serum, and it inhibited C3b deposition in both C4 deficient plasma and C4 sufficient plasma in a similar manner (Schwaeble et al., 2011).

1.4.1.5 The interaction between C1s and the substrate C4

The binding of C1s to C4 shares many similarities to the binding between MASP-2 and C4. Like MASP-2, the three catalytic domains (CCP1, CCP2 and SP domains) are required for efficient C4 binding and cleavage. The catalytic portions of C1s are positioned such that, after activation, the SP domain is able to be exposed from the C1 complex in order to complete the function of activating its substrates, such as C4 (Wallis et al., 2010). Both CCP domains appear to be involved in the binding of C4, and it is thought that C1s also houses a C4 binding exosite within the CCP domains. From current literature, the CCP1 domain appears to be the most likely of the two CCP domains to house the exosite, as removal of the CCP1 domain reduces C4 cleavage by C1s by ~70 fold (Rossi et al., 1998). Perry *et al.* (2013) have postulated that residues 327-334 form

part of this exosite, as they structurally correlate to residues 333-340 of MASP-2, which have been found to form part of the MASP-2 CCP domain binding exosite (Perry et al., 2013). In addition, the linker region between the CCP domains and SP domains (consisting of residues Gln340-Val-Pro-Asp343) appears to be very important for C1s cleavage of C4. Bally *et al.* (2005) created numerous single and double mutations of these residues, and found that most of the mutations created lead to reduced C4 cleavage, with a notable exception being the double mutant Q340E/N391Q, which showed optimal activity against C4 (Bally et al., 2005). The authors postulate that the mutation would cause repulsion between the carboxyl groups with such a mutation, thus leading to a modification of the positioning of the CCP domains and allowing the linker region greater flexibility for optimal C4 cleavage (Bally et al., 2005). Kidmose *et al.* (2012) have shown that C1s is also capable of interacting with the C345C domain of C4, with mutation of the C4 residues T1721 and R1724 leading to a reduced K_D value in SPR experiments (Kidmose et al., 2012). It is hypothesised that the CCP domain exosite of C1s is interacting with this domain, such as occurs with MASP-2. However, this has not been confirmed.

Recently, a C4 binding exosite was discovered upon the SP domain of C1s, comprised of the charged residues K575, K576, R581 and R583 (Duncan et al., 2012b, Perry et al., 2013). When individual residues were mutated to glutamine, the residues K576, R581 and R583 were found to have considerably slower C4 cleavage rates than wild-type C1s (~ 40% C4 cleavage in 120 minutes), while the K575 residue achieved ~ 80% cleavage of C4 over the same time frame (Duncan et al., 2012b). When all four residues were mutated simultaneously to alanine or glutamine (forming a cluster of either alanine or glutamine mutations), C4 cleavage was severely reduced, with the alanine cluster achieving only a 5% C4 cleavage rate even after 16 h (Duncan et al., 2012b). When binding was examined between the C1s alanine cluster mutant and C4 using Surface Plasmon Resonance (SPR), C1s was found to be unable to bind C4 (Perry et al., 2013). Therefore, this SP domain binding exosite is crucial to binding and cleavage of C4 by C1s.

This exosite was also found to form a sulfate-binding site, binding to the three sulfated tyrosines of C4. Anti-sulfotyrosine antibodies were found to be unable to bind to C4 in the presence of C1s. A sulfated C4-derived peptide, containing the stretch of C4 that

houses the three sulfated tyrosines, was created, and in time courses was found to reduce C4 cleavage by C1s by roughly 50% (Duncan et al., 2012b). The same peptide made with phosphorylated tyrosines instead of sulfated tyrosines was found to result in only a small reduction in C4 cleavage, while the same peptide made with no modifications to the tyrosine residues showed no reduction in C4 cleavage by C1s (Duncan et al., 2012b). Intriguingly, the C1s SP domain fragment was shown to have the greatest reduction in C4 cleavage in the presence of the sulfated peptide. Using a column lined with the sulfated peptide, affinity chromatography showed that the while wild-type C1s was able to bind the column, the single mutants of the SP domain exosite, as well as the alanine and glutamine cluster mutants, were unable to do so, and were eluted in the wash (Duncan et al., 2012b). This suggested that the SP domain exosite was involved in the binding of C1s to the sulfated tyrosines of C4. A model of C1s binding to C4 showed that two of these sulfated tyrosines (residues 1420 and 1422) interact with the residues of the exosite (Duncan et al., 2012b). Interestingly, the residue K575, which was the least affected of the four single mutants, is the farthest away from these sulfated tyrosine residues, which may account for why mutation of this residue displayed less severe effects upon C4 cleavage (Duncan et al., 2012b).

1.4.2 The substrate C2

1.4.2.1 The structure and layout of C2

C2 is produced as a heavily glycosylated 100 kDa protein consisting of 3 CCP domains, a von Willebrand Factor Type A (vWFA) domain and an SP domain (Figure 1.16)(Bentley, 1986). At pH 7.4, C2 is found in zymogen form (Halili et al., 2009). C2 firstly interacts with C4b in a magnesium-dependent manner, as sedimentation analytical ultracentrifugation analysis indicates that C4 and C2 do not interact before C4 is activated (Wallis et al., 2007). This indicates that C2 is recruited by C4b, and not unactivated C4 (Wallis et al., 2007). It is thought that the open metal-ion dependent adhesion site (MIDAS), found on the vWFA domain, helps to promote affinity for C4b (Milder et al., 2006). After being recruited by C4b, C2 is then cleaved at the residues Arg223 and Lys224 into the molecules C2a (70 kDa) and C2b (30 kDa) by C1s in the classical pathway, or MASP-1 and MASP-2 in the lectin pathway (Milder et al., 2006). The C2b fragment consists of the three CCP domains, while the C2a fragment consists of the vWFA and SP domains (Figure 16). At this point in time, zymogen C2 has not been

crystallised, but the cleavage products C2a and C2b have been crystallised and structurally characterised (Milder et al., 2006, Krishnan et al., 2009).
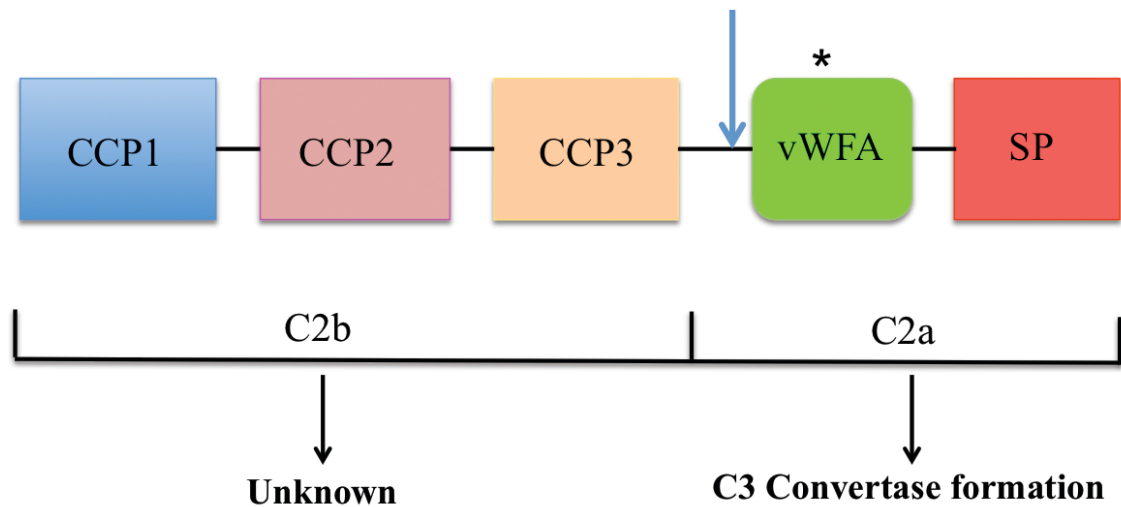
Figure 1.16: The domain layout of C2. The blue arrow indicates the R223/K224 site of cleavage by MASP-2 and C1s. The location of the MIDAS is indicated by *.

The role of C2b after cleavage is not known, although it has been suggested that it causes edema by enhancing vascular permeability in humans and guinea pigs (Strang et al., 1988). The C2a fragment contributes to the formation of the C3 convertase (Kerr, 1980, Rossi et al., 2001). However, there has been some evidence that C2 can be cleaved by C1s without binding to C4b, although at a much slower rate (Thielens et al., 1984). Initially, it was thought that MASP-1 was able to cleave C2, but in a less efficient manner than MASP-2 (Rossi et al., 2001, Ambrus et al., 2003, Tateishi and Mastsushita, 2011). However, recent work indicates that MASP-1 is responsible for most of the C2 cleavage produced by lectin pathway activation- upwards of 60% of the C2a produced by C2 cleavage is done by MASP-1, with the remaining 40% produced by MASP-2 (Heja et al., 2012b). Therefore, it appears that MASP-2 is not the dominant MASP involved in the cleavage of C2.

1.4.2.2 The interaction of MASP-2 and C1s with the substrate C2

Much is unknown about the interaction between C2 and the complement enzymes that cleave it - C1s, MASP-1 and MASP-2. It has been found that C2 cleavage by both C1s and MASP-2 requires only the SP domain, as removal of the CCP domains does not affect the ability of either protease to cleave C2 (Rossi et al., 1998, Ambrus et al., 2003,

Duncan et al., 2012a). In addition, for C1s, the linker region between the CCP2 and SP domains, which is important to C4 cleavage, has been shown not to affect C2 recognition and cleavage, with all mutants created showing similar recognition and cleavage of C2 as wild-type C1s (Bally et al., 2005). Therefore, it appears that the structural motifs required for efficient binding and cleavage of C2 by C1s and MASP-2 are all located in the SP domain.

As discussed above in more detail, C2 appears to play a role in a C4 bypass pathway of lectin complement activation, with the addition of recombinant C2 restoring C3 cleavage activity to the plasma of C2 deficient mice (Schwaeble et al., 2011). However, others have found that C3 cleavage occurs even in C2 deficient serum, raising the idea of a C2 bypass pathway (Selander et al., 2006). It is believed to be MBL-dependent, as the presence of MBL appeared to support C3 deposition even in the absence of C2 (Selander et al., 2006). More research is needed to discern further details of this C2 bypass pathway, as well as the role of C2 in the C4 bypass pathway.

1.5 The major inhibitor of the Classical and Lectin Pathways, C1 inhibitor

1.5.1 The multiple roles of C1 inhibitor in the body

C1 inhibitor (C1-INH), also known as SERPING1, is considered the primary regulator of classical and lectin pathway activity. C1 inhibitor belongs to the family of serine protease inhibitors (serpins). C1-INH has been found to inhibit the activity of C1s and C1r of the classical pathway, and MASP-1 and MASP-2 of the lectin pathway (Pensky et al., 1961, Sim et al., 1979, Matsushita et al., 2000, Ambrus et al., 2003). However, C1-INH is not only active in the complement system: it also is responsible for inhibiting enzymes in other systems, such as factor XIa of the extrinsic coagulation pathway, and factor XIIa and kallikrein of the contact pathway of coagulation (Schapira et al., 1982, Pixley et al., 1985, Wuillemin et al., 1995). A lack of C1-INH has been linked to the disease Hereditary Angioedema (HAE), in which patients suffering heterozygous C1-INH deficiency suffer from recurrent tissue swelling, which can be fatal if it occurs in the upper airways (Landermann et al., 1962, Donaldson and Evans, 1963).

1.5.2 The structure and mechanism of inhibition by C1 inhibitor

As a 478 amino acid serpin, C1-INH shares sequence homology with other members of this family in its serpin domain, located at the C-terminal of the molecule. It also contains a large, non-conserved N-terminal extension of ~100 amino acids. This N-terminal extension is quite heavily glycosylated, with 13-17 of the potential 20 N and O-linked glycosylation sites of C1-INH being located within this region (Bock et al., 1986). In particular, glycosylation of the N330 residue appears to be important for proper folding of the serpin domain, as mutagenesis of this residue led to a sharp decrease in expression yield (Rossi et al., 2010). The glycosylation of this region does not appear to affect proteinase activity, but the N-glycosylation sites have been shown to affect affinity for endotoxins and selectins (Coutinho et al., 1994, Bos et al., 2003). The function of the N-terminal extension is not yet fully understood, but does not appear to be involved in protease inhibition (Bos et al., 2003, Rossi et al., 2010). However, it has been shown to bind to bacterial lipopolysaccharide (LPS) in mice and so helps to prevent endotoxic shock (Liu et al., 2003, Liu et al., 2005). The serpin domain of C1-INH, following the classical serpin domain structure, consists of three β-sheets and nine α helices. Of the β sheets, Sheet A, which consists of five strands and a protein recognition region, acts as the dominant feature. The β Sheet A of C1 inhibitor is the largest found of the serpins, containing seven β strands (Beinrohr et al., 2007). The protein recognition region, which consists of a flexible peptide loop, is also known as the Reactive Centre Loop (RCL). This loop presents specific peptide sequences at the P1-P1' residues of the loop to attract its target protease by acting as a potential substrate. In C1-INH, this sequence consists of R444-T445. In the crystal structure of the serpin domain of latent C1-INH, the RCL was found to be integrated into a seven-stranded anti-parallel β-sheet (Figure 1.17) (Beinrohr et al., 2007).
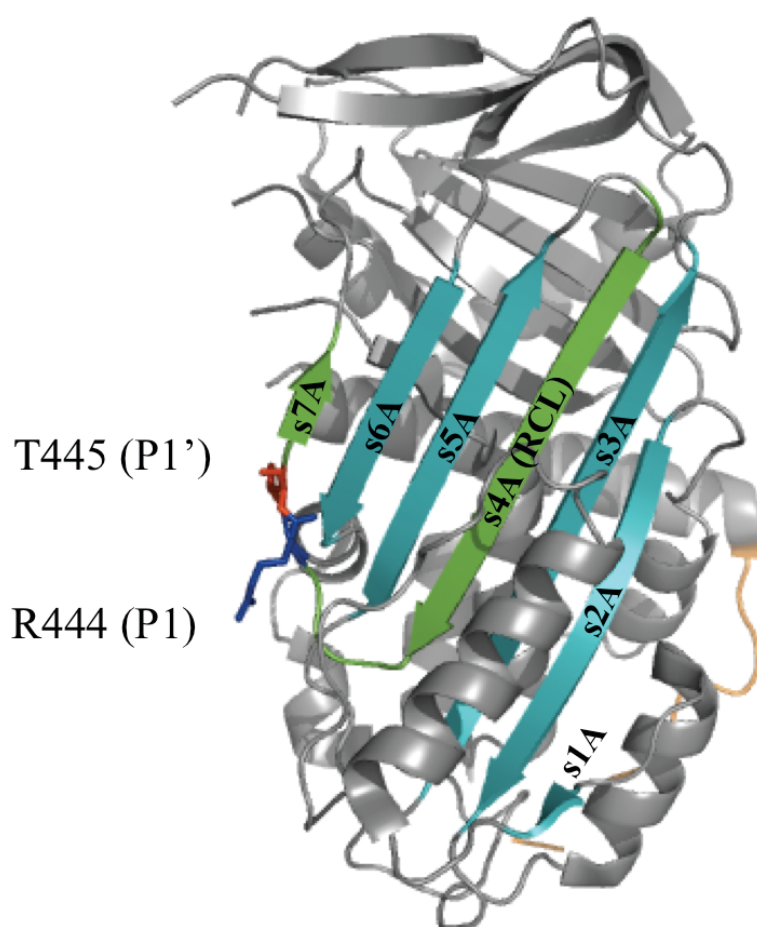
Figure 1.17: The structure of latent C1-INH. In the structure, the crucial P1 and P1' residues of the RCL (shown in green) can be seen, with R444 in dark blue and T445 in red. The rest of the β Sheet A is depicted in cyan. The small amount of the N-terminal extension shown in the structure is shown in orange. Imaged generated using PDB file 2OAY (DOI: 10.2210/pdb2oay/pdb).

When the target protease attempts to cleave the RCL, the RCL integrates itself into the β sheet A. This halts enzyme activity, as the catalytic triad becomes distorted and prevents de-acylation by water. This leaves the enzyme at the acyl-intermediate stage of catalysis, and at this point, the reaction can have one of two outcomes. One is that of successful inhibition of the protease by the serpin (the inhibitory pathway), where the cleaved end of the RCL is swung from one end of the serpin molecule to the other, and further distorts the catalytic triad of the enzyme. After this, the enzyme and serpin remain tightly bound in a stable but inactive complex. The second outcome is that of unsuccessful protease inhibition (the serpin proteolysis and substrate pathway), where the RCL of the serpin is cleaved by the protease, but the protease is not inhibited. The method in which

serpins inhibit their targets is often referred to as the 'suicide mechanism', as at the end of mechanism, both the serpin and protease are inactivated.

The balance between these two outcomes is seen in the stoichiometry of inhibition (S.I.). A typical inhibitory serpin (such as C1-INH) displays an S.I. close to 1 when interacting with its protease target, which indicates that the inhibitory pathway proceeds faster than the serpin proteolysis and substrate pathway. They also display a rate of protease inhibition (k_a) of $\geq 10^5$ M^{-1} sec^{-1} (Horvath et al., 2011).

1.5.3 The effects of polyanions on C1 inhibitor activity

The activity of C1-INH towards its target proteases has been shown to be enhanced by highly charged polyanionic molecules, such as the naturally occurring glycosaminoglycan (GAG), heparin. It has been shown that C1-INH binds heparin through its serpin domain, with the C1-INH still able to bind heparin in SPR studies, even with the removal of the N-terminal extension (Rossi et al., 2010). Heparin has been shown to enhance C1-INH activity against C1s, as well as MASP-2 (Nilsson and Wiman, 1983, Murray-Rust et al., 2009, Parej et al., 2013). The level of enhancement of C1-INH activity provided by heparin varies between proteases. Heparin appears to enhance C1-INH activity against factor XIa the most strongly, with a 60-115-fold potentiation (Wuillemin et al., 1996, Mauron et al., 1998). The enhancement of C1-INH activity against C1s by heparin is more moderate (~15-60-fold), and is more minor against kallikrein and C1r, with 2 and 5-fold increases (Sim et al., 1980, Wuillemin et al., 1997, Gozzo et al., 2003). For factor XIIa, heparin reduces the inhibitory activity of C1-INH against it 2-4-fold (Wuillemin et al., 1996). The level of inhibitory enhancement produced by heparin against the target proteases can even rely upon other factors than the target protease. For instance, in the MBL-dependent lectin pathway, the enhancement of C1-INH inhibition of C3 and C4 deposition in the presence of heparin is much less pronounced than seen in the H-Ficolin dependent lectin pathway (Parej et al., 2013). It is thought that polyanions like heparin bind to the highly-positively charged region under the RCL. In doing so, they neutralise the positive charge and instead create a negative charge in the area. Given that many proteases have positively charged contact zones around their active sites, it is thought that the negative charges provided by the polyanions attracts the proteases to C1-INH (Beinrohr et al., 2007).

1.6 Project Objectives

The main objectives of this study were to investigate the contribution of the CCP and SP exosites of MASP-2 to the binding and cleavage of the substrate C4, and to investigate the effects of the polyanions heparin and polyphosphate on C1-INH activity against MASP-2. This was achieved via the following aims:

1. Further characterise the MASP-2 CCP domain exosite in a quantitative manner in order to determine the contribution of the exosite to the kinetic mechanism of interaction between MASP-2 and the substrate C4 (Chapter 3).

2. Characterisation of the MASP-2 disease-associated mutation D371Y at a kinetic level to discern a functional explanation for the linkage between the mutation and a number of chronic infectious diseases (Chapter 4).

3. Characterise the potential MASP-2 SP domain exosite to determine if it is indeed a relevant binding exosite, and to investigate its contribution to the kinetic mechanism of interaction between MASP-2 and the substrate C4 (Chapter 5).

4. Investigate the effects of the polyanions heparin and polyphosphate upon the regulation of MASP-2 activity by C1-INH (Chapter 6).

Chapter 2

'General Materials and Methods'

2.1 Materials

The following reagents were purchased from Sigma Aldrich (St. Louis, MO, USA): glacial acetic acid, Bromophenol blue, HCl, chloramphenicol, ampicillin, PEG 8000, DMF, Coomassie blue R-250, toluidine blue-O, Heparin sodium salt derived from porcine intestinal mucosa Grade I-A, Bovine Serum Albumin (BSA), secondary anti-chicken antibody, ovalbumin, β mecaptoethanol, methanol, acrylamide and bis-acrylamide. From Amresco (Ohio, USA), the following reagents were purchased: glycerol, glycine, boric acid, agarose, Triton-X, NaCl, Tris, HEPES, L-arginine, glutathione (oxidised and reduced), EDTA, Tween 20, SDS, APS and sodium acetate. Dpn1, Pfu DNA polymerase, Plasmid Mini-Prep System and pET17b were purchased from Promega (Madison, WI, USA). Tryptone, yeast extract, agar, sodium phosphate were purchased from Merck (Darmstadt, Germany). IPTG and DTT were purchased from Astral Scientific (Gymea, NSW, Australia). All primers were purchased from Geneworks (Hindmarsh, SA, Australia). Superdex 75 16/60, Hi-Trap Heparin HP 1 mL column, Hi-Trap Q-Sepharose Fast Flow column, Hi-Trap NHS column, TEMED, Thiol Coupling Kit, CM5 Biacore chips, BIAevaluation and IQTL ImageQuant^{TM} software, Biacore X100 and T100 instruments were purchased from GE Healthcare (Uppsala, Sweden). Hank's Buffered Saline Solution (1x) was purchased from Gibco (Life Technologies, Mulgrave, Victoria, Australia). The 96-well assays plates used in peptide substrate assays were purchased from Corning (Corning, NY, USA). Sypro Ruby was purchased from Molecular Probes (Life Technologies, Mulgrave, Victoria, Australia). C2, C4 and C1 inhibitor were purchased from Complement Technologies (Tyler, Texas, USA). Fluorescence quenched substrates and coumarin substrates were synthesised by GL Biochem (Shanghai, China). BMG FLUOstar Optima fluorescent plate reader from BMG LabTech (Offenberg, Germany). ECL Western Blotting Detection Kit from Amersham (GE Healthcare, Uppsala, Sweden). Fuji Medical X-Ray film (Super Rx) from Fujifilm (Tokyo, Japan). 6 x DNA loading dye from New England BioLabs (Ipswich, MA, USA). SDS-PAGE Mini-PROTEAN electrophoresis equipment and Mini Trans-Blot Western transfer equipment from Bio-Rad (Hercules, CA, USA). GraphPad Prism Version 6.0 software from GraphPad Software, (San Diego, USA). Long chain and platelet length polyphosphate molecules were kindly synthesised and donated by Dr. Stephanie Smith of the University of Illinois.

2.2 Protein production and purification

2.2.1 Plasmids for MASP-2 expression and site-directed mutagenesis

For recombinant constructs, pET17b vectors were used. Preceding the MASP-2 sequence, the forward primers contained the codons for 4 amino acids (MASM) of the T7-Tag sequence, which is used to increase efficiency of expression for recombinant proteins. Primers for each mutant were designed with a length of approximately 5 amino acids on either side of the mutation location, as seen in Appendix A.1 (Geneworks, Hindmarsh, S.A, Australia), and PCR carried out, with Pfu DNA Polymerase (Promega, Madison, WI, USA), with a denaturing temperature of 95°C, an annealing temperature 3-5°C below the melting temperature of the primer (T_M), and an elongation temperature of 75°C. After PCR, 2 µL of sample was added to 4 µL of 6 x DNA loading dye (New England Biolabs, Ipswich, MA, USA), centrifuged for 1 min at 13,000 x g, and then electrophoresed at 100 V for 40 min on a 1.5% agarose gel containing ethidium bromide. The running buffer consisted of 1x Tris-acetate-EDTA (TAE) buffer (40 mM Tris, 20 mM acetic acid, 1 mM EDTA). After finishing electrophoresis, the gel was placed under UV light to examine if amplification had occurred. If so, the restriction enzyme Dpn1 (Promega, Madison, WI, USA) was added to the PCR reaction and left to incubate for 2 h at 37°C in order to remove template DNA left in the reaction. After this, 5 µL of the PCR reaction was transformed into the DH5α strain of *E. coli*. This was then plated onto Luria-Bertani (LB) plates containing ampicillin (100 µg/mL), and left at 37°C overnight. Upon obtaining colonies, 3 mL cultures were grown overnight, shaking at 225 rpm at 37°C, and the plasmids extracted from the culture the next morning using the PureYield™ Plasmid Miniprep System kit (Promega, Madison, WI, USA). The DNA plasmids were sent for sequencing to ensure the plasmids were complete with the correct mutation inserted.

2.2.2 Expression, refolding and purification of recombinant MASP-2 proteins

After DNA sequencing confirmation, the plasmids carrying the mutation were transformed into an *E. coli* strain suitable for recombinant protein expression (BL21*DE3pLysS). Successfully transformed plasmids were selected for on LB plates containing ampicillin (100 µg/mL) and chloramphenicol (34 µg/mL). Prior to large-scale expression, small-scale expression of a number of colonies was examined. Here, a 3 mL overnight culture was grown in 2YT media (1.6% [w/v] tryptone, 1.0% [w/v] yeast extract, 0.5% [w/v] NaCl) with ampicillin (100 µg/mL) and chloramphenicol (34 µg/mL)

at 37°C while shaking at 225 rpm. The next morning, 50 µL of the overnight culture was added to 950 µL of fresh 2YT and left to shake at 225 rpm at 37°C for 2 h, with the remaining overnight culture being stored at 4°C. After 2 h, 1 mM isopropyl-D-Thiogalactoside (IPTG) was added to the culture to induce protein expression, and the culture was left to shake for 4 h at 225 rpm at 37°C. Protein expression for each clone was examined by adding 35 µL of reducing SDS-PAGE loading buffer to 100 µL of non-induced and induced culture. These samples were incubated at 95°C for 5 min, centrifuged at 13,000 x g for 1 min, and then 35 µL loaded onto 12.5% SDS-PAGE gels and electrophoresed. After electrophoresis, gels were stained with 0.2 µm filtered Coomassie blue R-250 for 1 h, and then destained using a solution containing 40% (v/v) methanol and 10% (v/v) acetic acid, to allow for analysis of protein expression. Following analysis, LB plates containing ampicillin (100 µg/mL) and chloramphenicol (34 µg/mL) were streaked with the clone expressing the most recombinant protein and left at 37°C overnight.

From these plates, clones were picked for large-scale expression. The clones were grown in 50 mL of 2TY with ampicillin (100 µg/mL) and chloramphenicol (34 µg/mL) overnight at 37°C, while shaking at 225 rpm. The next day, the 50 mL of overnight culture was added to 950 mL of 2TY with ampicillin (100 µg/mL) and chloramphenicol (34 µg/mL) to create a total volume of 1 L. This 1 L of culture was incubated at 37°C, with shaking at 225 rpm, for 2 hours or until an OD_{600} reading of 0.6 was obtained, whichever occurred first. At this point, 1 mM isopropyl-D-Thiogalactoside (IPTG) was added to induce protein expression, and the culture left to shake for 4 h at 225 rpm. After this period of time, the cultures were centrifuged at 5000 rpm for 20 min at 4°C, collected in 30 mL resuspension buffer (50 mM Tris, 20 mM EDTA pH 7.4) and stored at -80°C. Again, protein expression for each culture was examined through SDS-PAGE analysis.

When ready to extract the protein, the pellets were thawed and then sonicated on ice for 6 x 30 sec, with 30 sec breaks in between rounds. After sonication, the inclusion bodies were collected by centrifugation (27,000 x g, 4°C for 20 min). They were then washed 3 times, each time using 25 mL of a different buffer. The buffer for the first wash was 50 mM Tris, 20 mM EDTA, 0.05% (v/v) Triton X, 100 mM DTT pH 7.4, the second wash was 50 mM Tris, 20 mM EDTA, 1M NaCl pH 7.4, and the third wash was 50 mM Tris, 20 mM EDTA pH 7.4. Prior to each wash, the pellet was centrifuged (27,000 x g, 4°C for 15 min), and then frozen at -80°C for 10 min, after which the wash was added. At

each step, the supernatant from the washes was discarded, with the pellet formed being kept. After the three washes, 10 mL of denaturing buffer (8M Urea, 50 mM Tris pH 8.3, 100 mM DTT) was added and left to incubate and break down the inclusion bodies for 3 h at room temperature. After 3 h, the solution was centrifuged for 20 min (22,000 x g, 4°C), and the supernatant (~10 mL) was kept. This supernatant was added to 40 mL of pre-refold buffer (50 mM Tris, 500 mM arginine, 300 nM NaCl, 5 mM EDTA, 3 mM reduced glutathione, 1 mM oxidised glutathione, pH 9). This mixture of supernatant and pre-refold buffer was dripped into 5 L of refold buffer (50mM Tris, 500 mM Arginine, 300 nM NaCl, 5mM EDTA, 3 mM reduced glutathione, 1 mM oxidised glutathione, pH 9) overnight at room temperature. The next day, the 5 L of refolded protein mixture was concentrated down to 200 mL and dialysed against 10 L of 20 mM Tris, pH 9 overnight at room temperature. The next day, the refolded proteins were flowed over a 5ml Q-Sepharose Fast Flow Column (GE Healthcare, Uppsala, Sweden) equilibrated with 6 column volumes of 20 mM Tris, pH 9. The protein was eluted from the column using a 0-400mM NaCl gradient at 1mL/min. Samples of relevant fractions were taken and reducing SDS loading buffer added, followed by incubation at 95°C for 5 min and centrifugation at 13,000 x g for 1 min. After this, samples were loaded onto 12.5% SDS-PAGE gels and electrophoresed. After electrophoresis, gels were stained with 0.2 μm filtered Coomassie blue R-250 for 1 h, and then destained using a solution containing 40% (v/v) methanol and 10% (v/v) acetic acid to allow analysis of the sample. After analysis, the appropriate fractions were selected and purified further using a Superdex 75 16/60 column (GE Healthcare, Uppsala, Sweden) in gel filtration buffer (20 mM Tris, 145 mM NaCl, pH 7.4). Relevant fractions obtained from the Superdex column had samples taken, and reducing SDS loading buffer added. The samples were then incubated at 95°C for 5 min, centrifuged at 13,000 x g for 1 min and then loaded onto 12.5% SDS-PAGE gels and electrophoresed. After electrophoresis, gels were stained with 0.2 μm filtered Coomassie blue R-250 for 1 h, and then destained using a solution containing 40% (v/v) methanol and 10% (v/v) acetic acid to allow for gel analysis. After analysis, the appropriate fractions were selected, aliquoted and frozen at -80°C until required. Prior to experimental use, each MASP-2 mutant created was confirmed through western blotting using an antibody targeted to the SP domain of MASP-2.

The concentration of recombinant proteins was determined from OD_{280} values using the calculated absorption co-efficient ($\varepsilon_{1\%, 1 cm}$) of 18.7 for the MASP-2 CCP12SP construct.

2.2.3 Activation of MASP-2 for use in SPR

The MASP-2 mutants used in SPR experiments required activation, as these mutants all contained a mutation to the active site serine of MASP-2, and so were unable to autoactivate. NHS columns (GE Healthcare, Uppsala, Sweden) were prepared to contain active wild-type MASP-2. After the column had been washed with 5 column volumes of gel filtration buffer (20mM Tris, 145 mM NaCl, pH 7.4), one column volume of the selected MASP-2 mutant was then added and left to incubate at 26°C overnight. The next day, the activated MASP-2 mutant was eluted in 5 column volumes of gel filtration buffer at pH 6 instead of pH 7.4. The 5 column volumes were eluted in 1 mL fractions. The column was then washed using 5 column volumes of gel filtration buffer at pH 7.4. Following elution of the activated protein, samples were taken from each eluted fraction, mixed with reducing SDS-PAGE loading buffer, and incubated at 95°C for 5 min and centrifuged at 13,000 x g for 1 min. The samples were then loaded onto 12.5% SDS-PAGE gels and electrophoresed. After electrophoresis, gels were stained with 0.2 μm filtered Coomassie blue R-250 for 1 h, and then destained using a solution containing 40% (v/v) methanol and 10% (v/v) acetic acid, to allow for analysis of the fractions to ensure full activation had occurred.

2.2.4 Sodium dodecyl sulfate polyacrylamide gel electrophoresis (SDS-PAGE) analysis

Stock solutions

Acrylamide/bis-acrylamide 30% (w/v) mix ratio 29:1

4 x Running gel buffer- 1.5 M Tris-HCl, pH 8.8

4 x Stacking gel buffer- 0.5 M Tris-HCl

10% (w/v) SDS

20% (w/v) APS

Reducing SDS loading buffer- 0.125 M Tris-HCl, 4% (w/v) SDS, 20% (v/v) glycerol, 4% (v/v) β-mecaptoethanol, 0.02% (w/v) bromophenol blue, pH 8.3

Tank buffer- 0.25 M Tris-HCl, 0.192 M glycine, 0.1% (w/v) SDS, pH 8.3

Coomassie blue stain solution- 40% (v/v) methanol, 7% (v/v) glacial acetic acid, 0.025% (w/v) Coomassie R-250 Brilliant Blue

Coomassie blue destain solution- 40% (v/v) methanol, 10% (v/v) glacial acetic acid

Sypro Ruby stain- purchased from Molecular Probes (Invitrogen), used undiluted

Sypro Ruby fixing buffer- 50% (v/v) methanol, 5% (v/v) glacial acetic acid

Sypro Ruby destain- 10% (v/v) methanol, 5% (v/v) glacial acetic acid

Method

      SDS-PAGE gels were prepared and electrophoresed using a Biorad Minigel system. The 10% and 12.5% running gels, and a 4% stacking gel were prepared, as per Table 2.1. After the addition of 10 μl of reducing SDS loading buffer, samples were boiled for 5 min at 95°C, centrifuged at 13,000 x *g* for 1 min, and then loaded into the wells and electrophoresed in tank buffer at a constant 100 V for 1 gel, or 120 V for 2 gels. When the dye front reached the bottom of the gel, gels were stained using either Coomassie blue stain or Sypro Ruby stain (Molecular Probes, Life Technologies, Mulgrave, Victoria, Australia). If using Coomassie blue stain, the gels were immersed for 1 h with rocking, and then destained in Coomassie destain solution with rocking until the background stain had faded sufficiently so as to see the protein bands clearly. If staining using Sypro Ruby, gels were immersed for 1 h prior to staining using Sypro Ruby fixing buffer with rocking. The fixing buffer was changed every half hour. Following this, the gels were then stained overnight with rocking in 30 mL of Sypro Ruby stain in a light-tight container. An hour prior to densitometric analysis, the gels were destained in light-tight containers using the Sypro Ruby destain solution with rocking.

Table 2.1: Preparation of SDS-PAGE gels

	Running gel 10% (2 gels)	Running gel 12.5% (2 gels)	Stacking gel (2 gels)
Acrylamide (mL)	3.3	4.1	0.44
4 x Running gel buffer (mL)	2.5	2.5	
4 x Stacking gel buffer (mL)			0.83
10% SDS (μL)	100	100	33
20% APS (μL)	60	60	20
TEMED (μL)	8	8	3
MilliQ (mL)	4	3.2	2

2.2.5 Western blot analysis

Solutions

Transfer buffer- 25 mM Tris, 190 mM glycine, 20% (v/v) methanol (kept at 4°C)

Tris-buffered saline (TBS)- 20 mM Tris, 150 mM NaCl

Blocking solution- 3% (w/v) skim milk in TBS

Stripping solution- 3% (w/v) skim milk and 0.1% (v/v) Tween 20 in TBS

Method

Samples were prepared and electrophoresed upon SDS-PAGE gels as outlined in Section 2.1.4. Once electrophoresis had finished, the gel and transfer sandwich components (2 x sponges, 1 x nitrocellulose membrane) were immersed in transfer buffer for 2 min. The transfer sandwich components were then assembled in the Biorad Trans-Blot® cell western blot cassette, with the membrane facing the cathode and the gel facing the anode. Care was taken to ensure that all components of the transfer sandwich were kept moist, and that no air bubbles were formed between the membrane and the gel. The cassette was placed into the tank, and an ice block added before the tank was filled with transfer buffer. The blot was run at 100 V for 1 h, with the transfer buffer being stirred slowly to maintain a cool temperature throughout the tank. After the hour, the membrane was covered in blocking solution, and left to rock at room temperature for 1 h. Following this, the blocking solution was removed, and replaced with fresh blocking solution containing the primary antibody, which was a peptide antibody directed to the SP domain of MASP-2. The membrane was left in the solution overnight, while being rocked at 4°C. The following day, the membrane was washed three times using stripping solution, where it was rocked for 10 min at room temperature each wash. The membrane was then immersed in a blocking solution containing an anti-chicken secondary antibody, and left rocking at room temperature for 2 h. The membrane was then washed three times using TBS solution, where it was rocked for 10 min at room temperature for each wash. Following this, the membrane was then completely covered in ECL Western Blotting Detection (Amersham, GE Healthcare, Uppsala, Sweden) and left for 3 min. The detection solution was removed from the membrane, and the membrane patted dry gently prior to imaging using Fuji Medical X-Ray film (Super Rx) (Fujifilm, Tokyo, Japan).

2.3 Peptide substrate activity assays

2.3.1 Peptide substrate activity assays using the synthetic peptide substrate C4 P4-P4'

Assays were carried out in fluorescence assay buffer (50 mM Tris, 150 mM NaCl, 0.2% [w/v] PEG 8000, pH 7.4) at 37°C. The fluorescence quenched substrate C4 P4-P4'

[2Abz-GLQRALEI-Lys(Dnp)-NH$_2$] (GL Biochem, Shanghai, China) was solubilised in 10% (v/v) N,N-dimethylformamide (DMF). A BMG Technologies FLUOstar Optima fluorescent plate reader (BMG LabTech, Offenberg, Germany) was used with an excitation wavelength of 320 nm and an emission wavelength of 420 nm. The instrument was set to read for 150 cycles, with a gain of 1700. MASP-2 used at a final concentration of 10 nM, with the substrate concentration range extending from 0-100 μM. All measurements were done in duplicate. To determine steady-state reaction constants, the data was analysed using non-linear regression in GraphPad Prism Version 6.0 software using the equation [Y=(Vmax*X^h)/(K$_{0.5}^h$ + X^h)] for allosteric sigmoidal binding. This equation allows the determination of the steady-state reaction constants V$_{max}$ (maximal velocity), $K_{0.5}$ (half-saturation constant) and h (Hill coefficient). Using these constants, k_{cat} and $k_{cat}/K_{0.5}$ values were calculated as described previously (O'Brien et al., 2003).

2.4 Cleavage efficacy assays

2.4.1 Investigation into the cleavage efficacy of MASP-2 for the substrate C4 through the determination of EC$_{50}$ values

Depending on their cleavage efficacy (revealed through range-finding assays), MASP-2 mutants were diluted to a concentration range of 0-1500 nM in EC$_{50}$ assay buffer (20 mM sodium phosphate, 150 mM NaCl, 5mM EDTA, pH 7.4). C4, purchased from Complement Technology Inc. (Complement Technology Inc., Tyler, Texas, USA), was also diluted in the EC$_{50}$ assay buffer to a final concentration of either 100 or 25 nM. The protease and substrate were incubated for 5 min at 37°C separately before being added together in a 1:1 ratio to allow the cleavage reaction to begin. For reactions containing 100 nM C4, the reaction proceeded for 30 min before being ended by adding reducing SDS loading buffer to the reaction. For reactions containing 25 nM C4, the reaction was allowed to proceed for 10 min before being ended with the addition of reducing SDS loading buffer to the sample. Samples were then incubated at 95°C for 5 min, centrifuged at 13,000 x *g* for 1 min and then loaded onto 10% SDS-PAGE gels and electrophoresed.

Gels were then stained using one of two methods. The first method, used to stain gels where samples containing 100 nM C4 were electrophoresed, stained the gels using 0.2 μm filtered Coomassie blue R-250 for 1 h, following which they were destained using a solution containing 40% (v/v) methanol and 10% (v/v) acetic acid to allow for

densitometric analysis. The second method, used to stain gels where 25 nM C4 samples had been electrophoresed, utilised the Sypro Ruby stain (Molecular Probes, Life Technologies, Mulgrave, Victoria, Australia) due to its higher staining sensitivity. After electrophoresis, the gels required fixing for 1 h prior to staining using a solution of 50% (v/v) methanol and 7% (v/v) acetic acid, with the solution being changed every half hour. Following this, the gels were stained overnight in Sypro Ruby stain in a light-tight container. An hour prior to densitometric analysis, the gels were destained for 1 h in light-tight containers using a solution of 10% (v/v) methanol and 5% (v/v) acetic acid, which was changed every half hour.

A Typhoon Trio (containing Argon Blue 488nm, SYAG Green 532 nm and HeNe Red 633nm lasers) was used for densitometry analysis of the gels, and the scanned gels were analysed using IQTL ImageQuant^{TM} software's 1D Gel analysis option (GE Healthcare, Uppsala, Sweden). The cleavage of the C4 α band was analysed, and the C4 γ band was used as a loading control. The data generated from the 1D gel analysis was then entered into GraphPad Prism Version 6.0 software (GraphPad Software, San Diego, USA) and the EC_{50} value was obtained using the non-linear regression equation: log (inhibitor) vs. response - variable slope equation [$Y=Ymin + (Ymax- Ymin)/(1+10^{((LogEC50-X)*h)})$], where Ymin is the minimum Y value, Y max the maximum Y value and h is the Hill Slope.

2.4.2 Investigation into the cleavage efficacy of MASP-2 for the substrate C4 through cleavage time courses

Using EC_{50} assay buffer, MASP-2 mutants were diluted to a final concentration of 1 nM, and C4 was diluted to a final concentration of 100 nM or 25 nM. The substrate and protease were incubated separately for 5 min at 37°C before being added together in a 1:1 ratio to begin the cleavage reaction, which was conducted at 37°C. Time points where the reaction was to be ended were selected (0, 1, 2, 5, 15, 30, 60 and 120 min), and the reactions were ended by adding reducing SDS loading buffer to the sample. The samples were incubated at 95°C for 5 min, centrifuged at 13,000 x g for 1 min, and then loaded onto 10% SDS-PAGE gels and electrophoresed. Gels were stained as described in Section 2.3.1.

A Typhoon Trio (containing Argon Blue 488nm, SYAG Green 532 nm and HeNe Red 633nm lasers) was used for densitometry analysis of the gels, and the scanned gels analysed using IQTL ImageQuant^{TM} software's 1D Gel analysis option. The cleavage of the C4 α band was analysed, and the C4 γ band was used as a loading control. The data generated from the 1D gel analysis was then entered into GraphPad Prism Version 6.0 software to create a time course graph depicting the cleavage of C4 by each MASP-2 mutant.

2.4.3 Investigation into the cleavage efficacy of MASP-2 for the substrate C2 through the determination of EC_{50} values

Wild-type and mutant MASP-2 enzymes were diluted to a concentration range 0-2.5 nM in EC_{50} assay buffer. C2, purchased from Complement Technology Inc., (Complement Technology Inc., Tyler, Texas, USA), was also diluted in the EC_{50} assay buffer to a final concentration of 1 μM. The protease and substrate were incubated for 5 min at 37°C separately before being added together in a 1:1 ratio to allow the cleavage reaction to begin. The reaction proceeded for 1 h before being ended by adding reducing SDS loading buffer to the reaction. After this step, 2 μL of 0.5 mg/mL ovalbumin was added to each reaction to act as a loading control for analysis in later stages. Samples were then incubated at 95°C for 5 min, centrifuged at 13,000 x g for 1 min, and then loaded onto 10% SDS-PAGE gels and electrophoresed. After electrophoresis, the gels were stained using 0.2 μm filtered Coomassie blue R-250 for 1 h, and then destained in a solution containing 40% (v/v) methanol and 10% (v/v) acetic acid.

A Typhoon Trio (containing Argon Blue 488nm, SYAG Green 532 nm and HeNe Red 633nm lasers) was used for densitometry analysis of the gels, and the scanned gels analysed using IQTL ImageQuant^{TM} software's 1D Gel analysis option. The disappearance of the zymogen C2 band was analysed, with ovalbumin used as a loading control. The data generated from the 1D gel analysis was then entered into GraphPad Prism Version 6.0 software, and an EC_{50} value obtained using the non-linear regression equation: log (inhibitor) vs. response- variable slope equation [$Y=Ymin + (Ymax-Ymin)/(1+10^{((LogEC50-X)*h)})$], where Ymin is the minimum Y value, Y max the maximum Y value and h is the Hill Slope.

2.4.4 Investigation into the cleavage efficacy of MASP-2 for the substrate C2 through cleavage time courses

Wild-type and mutant MASP-2 enzymes were diluted to a final concentration of 5 nM in EC_{50} assay buffer. C2 was diluted to a final concentration of 1 μM in EC_{50} assay buffer. The substrate and protease were incubated separately for 5 min at 37°C before being added together in a 1:1 ratio to begin the cleavage reaction, which was conducted at 37°C. Time points where the reaction was to be ended were selected (0, 1, 2, 5, 15, 30, 60 and 120 min), and the reactions were ended by adding reducing SDS loading buffer to the sample. After this step, 2 μL of 0.5 mg/mL of ovalbumin was added to each reaction to act as a loading control for analysis in later stages. The samples were then incubated at 95°C for 5 min, centrifuged at 13,000 x *g* for 1 min, and then loaded onto 10% SDS-PAGE gels and electrophoresed. After electrophoresis, the gels were stained using 0.2 μm filtered Coomassie blue R-250 for 1 h, and then destained in a solution containing 40% (v/v) methanol and 10% (v/v) acetic acid.

A Typhoon Trio (containing Argon Blue 488nm, SYAG Green 532 nm and HeNe Red 633nm lasers) was used for densitometry analysis of the gels, and the scanned gels analysed using IQTL ImageQuant[TM] software's 1D Gel analysis option. The disappearance of the zymogen C2 band was analysed, with ovalbumin used as a loading control. The data generated from the 1D gel analysis was then entered into GraphPad Prism Version 6.0 software to create a time course graph depicting the cleavage of C2 by the MASP-2.

2.4.5 Investigation into the efficacy of MASP-1 and MASP-2 activation of zymogen MASP-2

A cleavage time course to examine the activation of zymogen MASP-2 by MASP-1 and MASP-2 was utilised. Wild-type MASP-1 and MASP-2 constructs were diluted to a final concentration of 200 nM in EC_{50} assay buffer, with 1 μg of zymogen MASP-2 CCP12SP Cys D371Y S618A and MASP-2 CCP12SP Cys S618A used in each reaction. Each component was incubated separately for 5 min at 37°C, before being added together to begin the cleavage reaction, which was conducted at 37°C. Time points where the reaction was to be ended were selected (0, 2, 5, 15, 30, 60, 120 and 240 min), and the reactions were ended by adding reducing SDS loading buffer to the sample. After this step, 2 μg Bovine Serum Albumin (BSA) was added to each reaction to act as a loading

control for analysis in later stages. The samples were incubated at 95°C for 5 min, centrifuged at 13,000 x *g* for 1 min, and then loaded onto 12.5% SDS-PAGE gels and electrophoresed. Gels were then stained using 0.2 μm filtered Coomassie blue R-250 for 1 h, and then destained in a solution of 40% (v/v) methanol and 10% (v/v) acetic acid.

A Typhoon Trio (containing Argon Blue 488nm, SYAG Green 532 nm and HeNe Red 633nm lasers) was used for densitometry analysis of the gels, and the scanned gels analysed using IQTL ImageQuant™ software's 1D Gel analysis option. The cleavage of the zymogen MASP-2 band was analysed, with the BSA band used as a loading control. The data generated from the 1D gel analysis was then entered into GraphPad Prism Version 6.0 software to create a time course graph depicting the cleavage of zymogen MASP-2 by MASP-1 and MASP-2.

2.5 Binding analysis

2.5.1 Analysis of MASP-2 binding of C4 using Surface Plasmon Resonance (SPR) Studies

Surface Plasmon Resonance Studies were carried out using Biacore T100 and X100 instruments (GE Healthcare, Uppsala, Sweden). Selected activated MASP-2 mutants were immobilised upon the flow cells of a Biacore Series S CM5 sensor chip for use in the Biacore T100, or a CM5 sensor chip for use in the Biacore X100 (GE Healthcare, Uppsala, Sweden). All MASP-2 variants were diluted to a concentration of 20 μg/mL in a 10 mM sodium acetate, pH 5 solution prior to immobilisation, and each protein was given a contact time of 1000 seconds during the immobilisation protocol. Immobilisation was achieved using the ligand thiol coupling method outlined by the manufacturer in their Thiol Coupling Kit (GE Healthcare, Uppsala, Sweden). Briefly, NHS (N-hydroxysuccinimide) and EDC [1-ethyl-3-(3-dimethylaminopropyl) carbodiimide hydrochloride] were used to activate the chip surface to allow the attachment of PDEA [2-(2-pyridinyldithio) ethaneamine hydrochloride] . The PDEA that attached to the chip was used to capture the free cysteine of MASP-2, and so allowed the immobilisation of the protein on the chip. Any active PDEA on the chip surface that had not attached any MASP-2 was inactivated using L-cysteine.

On the Biacore T100 instrument, triplicate analyses with 0 - 1 μM C4 were performed, with the protein being injected at 30 μl/min for 2 min, with a 5 min

dissociation. On the Biacore X100 instrument, each analysis was performed individually three times in a row, with sample ranges of C4 from 0 to 500 nM or 1μM, depending upon the MASP-2 variant being examined. The running buffer consisted of 1 x phosphate buffered saline solution with Tween 20 (1 x PBST [137 mM NaCl, 2.7 mM KCl, 10 mM Na_2HPO_4, 1.8 mM KH_2PO_4, 0.05% (v/v) Tween 20, pH 8]). The data obtained was then examined using the BIAevaluation software (GE Healthcare, Uppsala, Sweden) in two ways. Firstly, the affinity of the interaction was examined using the steady-state affinity model, using the equation $R_{eq}= KACR_{max}/KAC+1$, where R_{eq} is the equilibrium response level, C is the concentration of analyte, and KA is the equilibrium association constant calculated by fitting a plot of R_{eq} to analyte concentration. The K_D is obtained by calculating the inverse of KA (1/KA). The maximal response units for each concentration obtained at equilibrium were then plotted against the corresponding concentration of C4 and fitted using non-linear regression to a one-site binding model in GraphPad Prism Version 6.0 (GraphPad Software, San Diego, USA), described by the following equation: Y = Bmax*X/(Kd + X), where Bmax represents the maximal specific binding and Kd is the equilibrium binding constant.

Secondly, a two-state binding model was examined, using the equation [M2 + C4 →(M2:C4)→(M2*C4)], where the initial complex (M2:C4) is converted to a higher affinity complex (M2*C4) due to conformational change. The data obtained was then used to determine the rate constants for the first ($K_1= Ka_1/ Kd_1$) and second steps ($K_2= Ka_2/Kd_2$) of the interaction. Calculation of the K_1 and K_2 constants allowed the determination of the overall association rate constant ($K_a= K_1 (1+K_2)$) of the interaction, as well as determination of the equilibrium dissociation constant ($K_d= 1/K_a$) of the interaction.

2.5.2 Investigation of polyphosphate binding to MASP-2 through Electromobility Shift Assays (EMSA)

Binding of the polyphosphate (>1000 units) molecule to MASP-2 was examined using electrophoresis on TBE (Tris, Borate and EDTA) gels. Polyphosphate was diluted in MilliQ water to a range of final concentrations from 0-200 μM, while wild-type MASP-2 and the CCP and SP domain exosite mutants being examined were diluted to a concentration of 2.27 μM in 20 mM HEPES, pH 7.4. Polyphosphate and MASP-2 were incubated together at room temperature for 10 min before 6 x DNA loading dye (New

England BioLabs, Ipswich, MA, USA) was added. The samples were centrifuged at room temperature for 1 min at 13,000 x g, before being loaded onto 10% TBE gels. Samples were electrophoresed at 12 mA for 5 h, with cold 1 x TBE as a running buffer (89 mM Tris, 89 mM boric acid, 20 mM EDTA, pH 8.0) and then stained using either 0.2 μm filtered Coomassie blue R-250 for 1 h to stain for protein or 0.2 μm filtered toluidine blue-O stain (0.05% (w/v) toluidine blue-O, 25% (v/v) methanol, 5% (v/v) glycerol) for 10 min, which visualises highly negatively charged molecules, such as polyphosphate. Gels stained in Coomassie blue R-250 were destained using a solution of 40% (v/v) methanol and 10% (v/v) acetic acid, while gels stained in toluidine blue O were destained in a solution of 25% (v/v) methanol and 5% (v/v) glycerol.

2.5.3 Analytical heparin-Sepharose chromatography

Wild-type MASP-2 and the CCP and SP domain exosite mutants being examined were subjected to gel filtration chromatography in 20 mM Tris, 70 mM NaCl, pH 7.4 using a Superdex 75 16/60 column (GE Healthcare, Uppsala, Sweden), and the fractions analysed using a 12.5% SDS-PAGE gel. The relevant fractions were then concentrated down to 1 mL. A Hi-Trap Heparin HP 1 mL column (GE Healthcare, Uppsala, Sweden) was equilibrated in 6 column volumes of Buffer A (20 mM Tris, 70 mM NaCl, pH 7.4) and the protein was injected onto the column. Bound protein was eluted from the column using a linear NaCl gradient using Buffer B (20 mM Tris, 1 M NaCl, pH 7.4) over 17 mL at 1 mL/ min. The A_{280} (AU) and conductivity (mS/cm) were plotted using GraphPad Prism Version 6.0.

2.6 Analysis of inhibition assays

2.6.1 Analysis of the active site concentration of MASP-2 by assessing the stoichiometry of inhibition (S.I.) with C1-INH

After purification, the active concentration of MASP-2 protein was determined by examining the stoichiometry of inhibition between MASP-2 and its cognate serpin, C1-INH (Complement Technology Inc., Tyler, Texas, USA). This was carried out using SDS-PAGE analysis and by examining residual activity using a fluorescence plate reader.

For SDS-PAGE analysis, MASP-2 was diluted in fluorescence assay buffer [50 mM Tris, 150 mM NaCl, 0.2% (w/v) PEG, pH 7.4] to a final concentration of 1 μM,

and C1-INH was likewise diluted in fluorescence assay buffer to achieve ratios of 0.2:1, 0.4:1, 0.6:1, 0.8:1, 1:1, 1.5:1 and 2:1 relative to the MASP-2 concentration. MASP-2 and C1-INH were mixed together, the reaction was incubated for 1 h at 37°C and ended by adding reducing SDS loading buffer. Samples were incubated at 95°C for 5 min, centrifuged at 13,000 x g for 1 min, loaded onto 10% SDS-PAGE gels and electrophoresed. After electrophoresis, gels were stained with 0.2 µm filtered Coomassie blue R-250 for 1 h and destained using a solution containing 40% (v/v) methanol and 10% (v/v) acetic acid, to allow for analysis. The reduction of free MASP-2 and C1 inhibitor, and increase in MASP-2/C1-INH complex was examined to determine the active concentration of the MASP-2 form of interest.

For plate reader analysis, MASP-2 was diluted in fluorescence assay buffer to a final concentration of 100 nM, and C1-INH was diluted in fluorescence assay buffer to achieve ratios of 0.2:1, 0.4:1, 0.6:1, 0.8:1, 1:1, 1.5:1 and 2:1 relative to the MASP-2 concentration. MASP-2 and C1-INH were mixed together and the reaction was incubated for 1 h at 37°C. After the incubation, a final concentration of 50 µM LGR substrate (Z-LGR-AMC) (GL Biochem, Shanghai, China) was added to the reaction, and the activity of the reaction was measured in duplicate on a BMG FLUOstar Optima fluorescent plate reader (BMG LabTech, Offenberg, Germany), using an excitation wavelength of 360 nm, an emission wavelength of 460 nm and a gain of 700. The raw data was analysed using linear regression in GraphPad Prism Version 6.0 (GraphPad Software, San Diego, USA) to determine the active concentration of the MASP-2 protein of interest.

2.6.2 Effect of polyphosphate on the interaction between C1-INH and MASP-2

Polyphosphate (70-120 units) was diluted in MilliQ water to produce a range of concentrations that would allow final concentrations of 0-100 µM during the experiment. A 2 µM stock of wild-type MASP-2 and the CCP and SP domain exosite mutants being examined were made in 1 x Hank's Buffered Saline Solution (HBSS) (Life Technologies, Mulgrave, Victoria, Australia), to allow for a final concentration of 500 nM during the experiment. C1-INH was also diluted in 1x HBSS to make a 2 µM stock to allow a final concentration of 500 nM, ensuring a 1:1 ratio between MASP-2 and C1-INH.

Each component of the experiment was added in a sequential order. At room temperature, polyphosphate and C1-INH were added first and second, with MASP-2 being added last. After the addition of MASP-2, the reaction was incubated for 1 h at 37°C, after which

reducing SDS loading buffer was added to end the reaction. Samples were then incubated at 95°C for 5 min, centrifuged at 13,000 x g for 1 min and then loaded onto 10% SDS-PAGE gels and electrophoresed. After electrophoresis, gels were stained with 0.2 µm filtered Coomassie blue R-250 for 1 h and destained.

Activity levels were also examined through activity assays using the substrate Z-LGR-AMC [LGR] (GL Biochem, Shanghai, China). As in the SDS-PAGE protocol, polyphosphate (70-120 units) was diluted in MilliQ water to produce a range of concentrations that would allow final concentrations of 0-100 µM during the experiment. A 200 nM stock of each MASP-2 variant was made in 1 x HBSS to allow for a final concentration of 50 nM during the experiment. C1-INH was also diluted in 1x HBSS to make a 200 nM stock to allow a final concentration of 50 nM, ensuring a 1:1 ratio between MASP-2 and C1-INH.

Each component of the experiment was added in a sequential order. At room temperature, polyphosphate and C1-INH were added first and second, with MASP-2 being added last. After the addition of MASP-2, the reaction was incubated for 1 hour at 37°C. After the incubation, a final concentration of 50 µM LGR substrate was added to the reaction and the activity of the reaction was measured in duplicate on a BMG FLUOstar Omega fluorescent plate reader (BMG LabTech, Offenburg, Germany), using an excitation wavelength of 360 nm, an emission wavelength of 460 nm and a gain of 700. The raw data was then visualized using GraphPad Prism Version 6.0.

2.6.3 Effect of heparin on the interaction between C1-INH and MASP-2

Heterogenous heparin (Heparin sodium salt derived from porcine intestinal mucosa Grade I-A [Sigma-Aldrich, St. Louis, MO, USA]) was diluted in MilliQ water to produce a range of concentrations that would allow final concentrations of 0-50 µg/mL during the experiment. A 2 µM stock of wild-type MASP-2 and the CCP and SP domain exosite mutants being examined were made in 1 x HBSS to allow for a final concentration of 500 nM during the experiment. C1-INH was also diluted in 1x HBSS to make a 2 µM stock to allow a final concentration of 500 nM, ensuring a 1:1 ratio between MASP-2 and C1-INH.

Each component of the experiment was added in a sequential order. At room temperature, heparin and C1-INH were added first and second, with MASP-2 being added

last. After the addition of MASP-2, the reaction was incubated for 1 hour at 37°C, after which reducing SDS loading buffer was added to end the reaction. Samples were then incubated at 95°C for 5 min, centrifuged at 13,000 x g for 1 min and then loaded onto 10% SDS-PAGE gels and electrophoresed. After electrophoresis, gels were stained with 0.2 μm filtered Coomassie blue R-250 for 1 h and then destained.

Activity levels were also examined through activity assays using the LGR substrate. As in the SDS-PAGE protocol, heparin was diluted in MilliQ water to produce a range of concentrations that would allow final concentrations of 0-50 μg/mL during the experiment. A 200 nM stock of wild-type MASP-2 and the CCP and SP domain exosite mutants being examined were made in 1 x HBSS to allow for a final concentration of 50 nM during the experiment. C1-INH was also diluted in 1x HBSS to make a 200 nM stock to allow a final concentration of 50 nM, ensuring a 1:1 ratio between MASP-2 and C1-INH.

Each component of the experiment was added in a sequential order. At room temperature, heparin and C1-INH were added first and second, with MASP-2 being added last. After the addition of MASP-2, the reaction was incubated for 1 h at 37°C. After the incubation, a final concentration of 50 μM LGR substrate was added to the reaction, and the activity of the reaction was measured in duplicate on a BMG FLUOstar Omega fluorescent plate reader (BMG LabTech, Offenburg, Germany), using an excitation wavelength of 360 nm, an emission wavelength of 460 nm and a gain of 700. The raw data was then visualized using GraphPad Prism Version 6.0.

Chapter 3

'Investigation into the role of the MASP-2 CCP domain binding exosite in the kinetic mechanism of interaction between MASP-2 and its substrate C4'

3.1 Introduction

MASP-2 is an integral part of the lectin pathway of complement. Its activation leads to the cleavage of the substrates C4 and C2. The enzyme is able to bind to a number of pattern recognition molecules, such as Mannose Binding Lectin (MBL), L-ficolin, M-ficolin and H-ficolin (Thiel et al., 2009). MASP-2 is an autoactivating enzyme, and so is able to activate itself, unlike C1s, which has led to it being said that it represents the minimal requirement for lectin pathway activation (Vorup-Jensen et al., 2000, Gal et al., 2005). However, new evidence suggests that MASP-1 is primarily responsible for activation of MASP-2, as well as playing a large role in C2 cleavage (Degn et al., 2012, Heja et al., 2012b). Once C4 and C2 are cleaved, the resultant C4b and C2a cleavage products go on to form the C3 convertase complex, which leads to Membrane Attack Complex (MAC) formation.

It has been suggested for some time that there is a binding exosite located on MASP-2 that is necessary for optimal cleavage of C4. This exosite is in addition to the active site of the enzyme, located on the SP domain. In particular, it was thought that this exosite would be located on the CCP domains, as their removal appeared to impair C4, but not C2 cleavage (Ambrus et al., 2003, Harmat et al., 2004, Rossi et al., 2001, Rossi et al., 2005). In 2005, Rossi *et al.* (2005) conducted an experiment where they switched the CCP domains of C1s and MASP-2, to create constructs where the C1s SP domain was linked to the CCP1 and CCP2 domains of MASP-2 [C1s (MASP-2 CCP1/CCP2)], and the SP domain of MASP-2 was linked to the CCP1 and CCP2 domains of C1s [MASP-2 (C1s CCP1/CCP2)] (Rossi et al., 2005). When C1s had its CCP domains substituted for those of MASP-2, it experienced a $\sim$ 34-fold decrease in the K_M value for C4 cleavage. In contrast, the construct in which MASP-2 had its CCP domains substituted for those of C1s showed K_M values similar to that of wild-type C1s. These results indicate that the CCP domains of MASP-2 have a stronger affinity for C4 than those of C1s (Rossi et al., 2005). Work in the host laboratory supported this theory, as removal of both CCP domains had a severe affect upon the ability of MASP-2 to cleave C4 in an efficient manner (Duncan et al., 2012a). In contrast, removal of the CCP domains does not appear to affect C2 cleavage efficacy, and so it is thought that only the SP domain is required for efficient cleavage of C2 (Rossi et al., 2005). In 2012, Kidmose *et al.* (2012) published the structure of the catalytically inactive MASP-2 CCP12SP S195A construct in complex with C4 and

discovered the location of the CCP binding exosite (Kidmose et al., 2012). The site was found to span across the C-terminal region of the CCP1 domain, the linker region between the CCP domains, and across to the N-terminal of the CCP2 domain, with residues E333, P340, D365 and P368 contributing the key points of contact with the binding site on C4 (Figure 3.1).
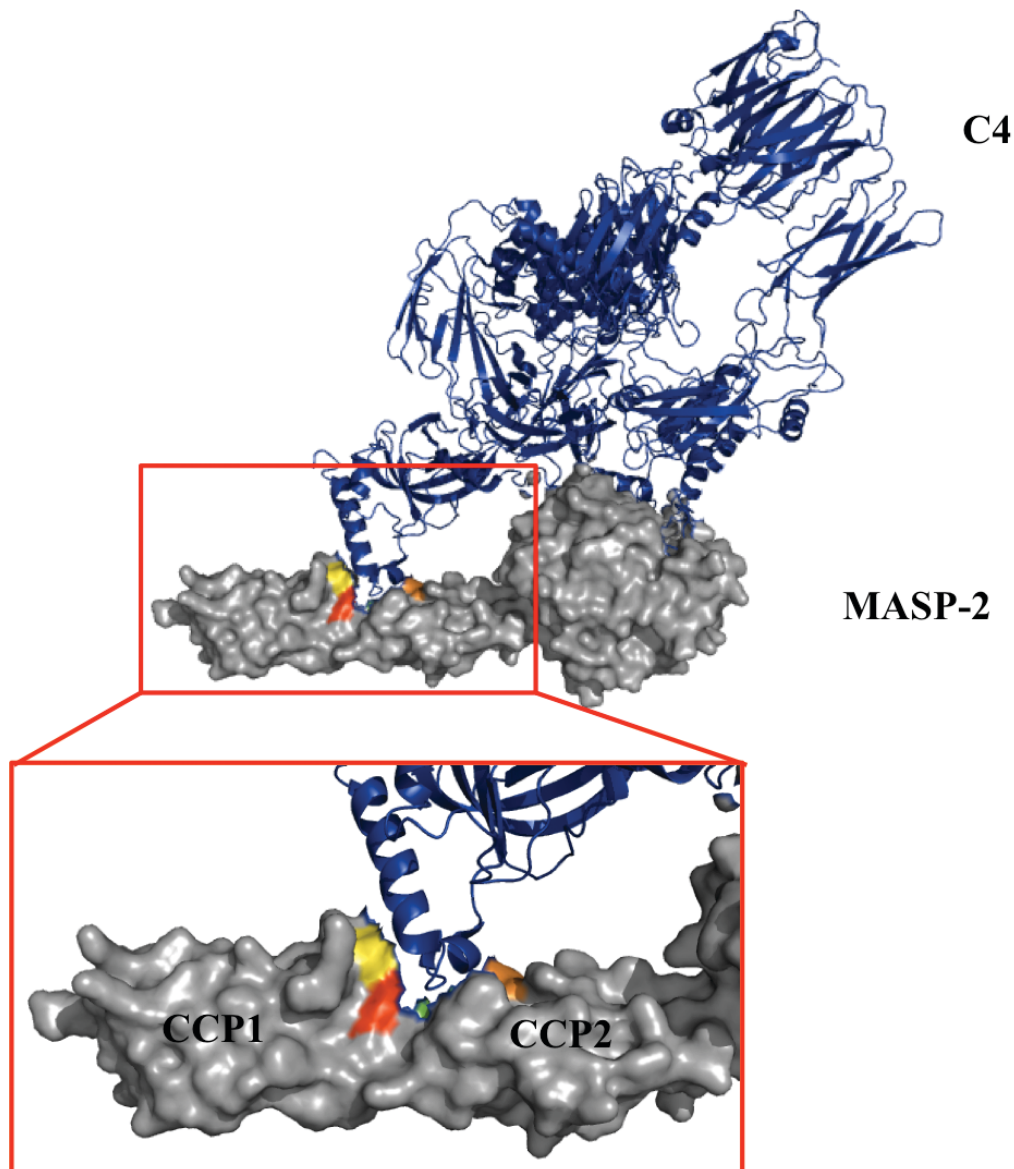
Figure 3.1: The CCP domain binding exosite of MASP-2. The exosite consists of the CCP1 domain residues E333 (red), P340 (yellow), the CCP1-CCP2 domain linker residue D365 (green) and CCP2 domain residue P368 (orange). MASP-2 is depicted in grey, while C4 is in blue. Image generated using PDB file 4FXG (DOI: 10.2210/pdb4fxg/pdb).

Mutation of these residues to arginine severely reduced C4 cleavage, with the least impacted mutants (P368R and P340R) only achieving ~60% C4 cleavage activity in a C4b deposition assay (Kidmose et al., 2012). The most impacted mutant (the double mutant MASP-2 CCP12SP E333R D365R) was unable to mediate cleavage of C4 in the assay conducted.

Kidmose *et al.* (2012) provided valuable information on the CCP domain binding exosite, with the structure of MASP-2 in complex with C4 contributing a great deal of knowledge upon the subject. However, the paper did not delve deeply into the kinetics of the interaction. A reduction in the deposition of C4b by the E333R, P340R, D365R and P368R mutants of MASP-2 was demonstrated in the paper, but no quantitative measures on kinetic activity, such as the effects of these mutations on the efficiency and rate of cleavage of C4, were presented.

Therefore, the aim of this study was to further explore the kinetic mechanism of the interaction between various MASP-2 CCP domain exosite mutants and the substrate C4. This will establish the kinetic role of the identified CCP domain exosite of MASP-2. In order to do this, a number of MASP-2 CCP domain mutants were produced. These mutants were selected from the Kidmose *et al.* (2012) paper, as well as from our own predictions. The mutants subjected to a series of kinetic tests to measure any effect the mutation had upon the binding and cleavage of C4 by MASP-2. Following this, selected mutants were examined for their ability to bind C4 using Surface Plasmon Resonance (SPR) studies.

3.2 Materials and Methods

Please refer to Chapter 2 for the protocols relevant to the experiments carried out in this chapter.

3.3 Selection of MASP-2 CCP domain exosite mutations

3.3.1 Addition of a cysteine residue on the N-terminus of MASP-2

Prior to the creation of the MASP-2 mutants, a cysteine residue was inserted at the N-terminal end of the wild-type MASP-2 CCP12SP protein, between the T7 promoter region and the beginning of the protein sequence (Figure 3.2).

A)

B)
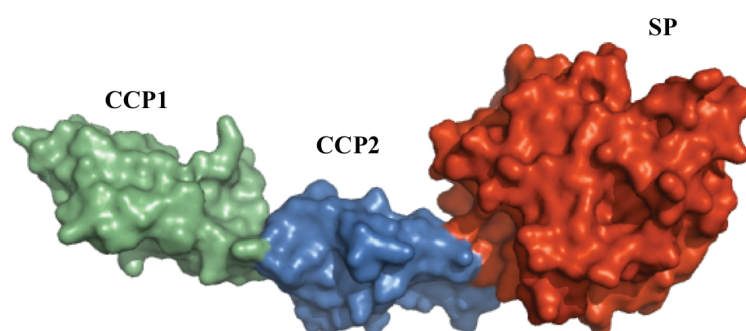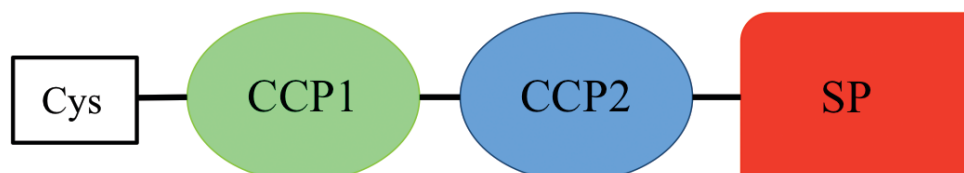
Figure 3.2: The domain layout of the MASP-2 experimental construct. A) The structure of the catalytic domains of MASP-2 (CCP1-CCP2-SP), imaged using PDB file 1ZJK (DOI: 10.2210/pdb1zjk/pdb). B) A diagrammatic depiction of the domain layout of the MASP-2 construct used experimentally without i) and with ii) an additional cysteine added to the N-terminus of the protein.

This free cysteine residue allows for the protein to be biotinylated, which is necessary for the Surface Plasmon Resonance (SPR) experiments completed in this study. Previous work in the laboratory has indicated that coupling MASP-2 and C1s directly to the Biacore chip through amine interactions is ineffective in allowing binding between these proteases and C4 to be observed. It is theorised that this amine coupling method allows MASP-2 and C1s to attach to the chip in various conformations, some of which may interfere with active site and exosite access for the substrate. The free cysteine

residue allows the protease of interest to be biotinylated and then attached to the chip in a uniform manner that allows for maximum active site and exosite access for the substrate. To date, this method has been successfully used with C1s in investigating its interactions with C4 (Perry et al., 2013). Confirmation of the presence of the cysteine residue was done using DNA sequencing. However, this approach proved problematic for MASP-2, as the biotinylation process was inefficient, and we were unable to get sufficient biotinylated protein to bind to the chip. Instead, a new approach was utilised. The free cysteine was instead coupled to the surface of a CM5 chip directly through thiol coupling. The wild-type MASP2 construct with the added cysteine was then used as a template for all mutations required for the investigation.

3.3.2 Selection of MASP-2 CCP domain exosite mutations

As discussed above, the CCP domains of MASP-2 appear to play an important role in the binding and cleavage of C4 (Ambrus et al., 2003, Rossi et al., 2005 and Duncan et al., 2012a). At the time that initial predictions were being made in the host laboratory (prior to the publication of Kidmose et al., 2012), it appeared that the CCP domain exosite would be housed upon the CCP2 domain of MASP-2, as initial studies indicated that the CCP1 domain played a more minor role relative to the CCP2 domain in the binding and cleavage of C4 by MASP-2 (Ambrus et al., 2003, Harmat et al., 2004, Duncan et al., 2012a). Therefore, a number of residues from the CCP2 domain were selected to undergo alanine-scanning mutagenesis in order to locate the CCP binding exosite. To select these residues, the sequences of MASP-1, MASP-2, C1s and C1r were aligned and the residues of the CCP domains studied. Selection of residues for study were chosen through the following criteria:

1) Some residues were selected because the residue present in MASP-2 at this position was unique compared to those present in MASP-1, C1s and C1r at the same position.

2) Some residues were selected because MASP-2 and C1s shared similar residues at this position, while MASP-1 and C1r did not.

3) The residues had been identified as being of potential importance in a previously proposed theoretical model of interaction between MASP-2 and C4 (Harmat et al., 2004).

In addition, the MASP-2 sequences from another 4 different species (*Homo sapiens, Rattus norvegicus, Mus musculus, Xenopus laevis*) were also aligned. After alignment, the residues highlighted earlier as being of interest were studied to see if the

residue was conserved in different species. Residues were selected for further study if the residue was conserved across MASP-2 from different species, but not shared by MASP-1, C1s or C1r.

From the sequence alignments described above, a number of residues were selected. However, the release of the MASP-2/C4 complex structure by Kidmose *et al.* (2012) rendered the investigation of many of the residues selected unnecessary, as the residues were shown to be located too far away from the CCP domain exosite to contribute to it. Of the residues initially selected, it was decided to investigate residue D370 further, as it is located near the CCP domain exosite (Table 3.1). Residue D370 was chosen as MASP-2 and C1s have similarly charged residues at this position (aspartic acid for MASP-2 and glutamate for C1s), while C1r has an arginine and MASP-1 a glycine at this position.

From Kidmose *et al.* (2012), residues E333 and D365 were selected for mutation, both as single mutants and also as a double mutant to allow further kinetic study of the CCP domain exosite to be completed (Figure 3.3). Each single mutant underwent charge reversal mutagenesis, as well as charge neutralisation mutagenesis (Table 3.1). The double mutant underwent charge neutralisation mutagenesis, but charge reversal mutagenesis was unsuccessful due to poor protein expression and subsequent low levels of refolded protein being produced.

In addition to the residues above, residue D371 was also selected for mutation. In recent years, this residue has been implicated in an increased susceptibility to a number of diseases. These include chronic hepatitis C infection (Tulio et al., 2011), Human T-Lymphocytic Virus (HTLV-1) infection (Coelho et al., 2013), and an increased risk of clinically significant bacterial infection after orthotopic liver transplantation (de Rooij et al., 2010). Mutation of this residue has also been linked to an increased susceptibility to rheumatic heart disease and the development of cardiomyopathy in chronic Chagas Disease (Boldt et al., 2011, Catarino et al., 2014). It was therefore decided to include this residue in our analyses to deduce if mutation of this residue led to an impaired ability to bind and cleave C4.

Table 3.1: Table of MASP-2 CCP domain exosite mutants to be examined.

CCP domain exosite mutant	CCP domain location
E333Q	CCP1
D365N	CCP2
E333Q D365N	CCP1/CCP2
E333R	CCP1
D365R	CCP2
D370A	CCP2
D371A	CCP2
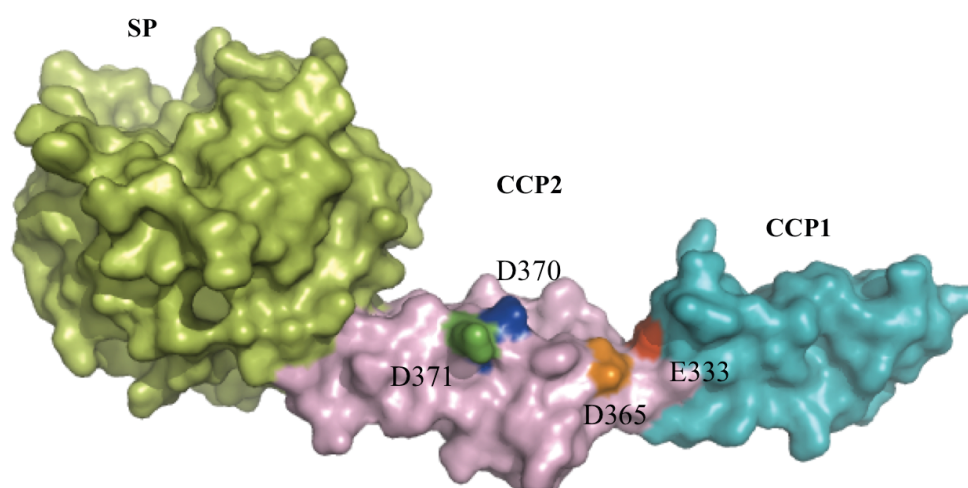
Figure 3.3: MASP-2 CCP domain exosite mutant locations. Residue E333 is in red, D365 in orange, D370 in dark blue and D371 in green. The CCP1 domain is in teal, the CCP2 domain in pink and the SP domain in yellow. Image generated using PDB file 1ZJK (DOI: 10.2210/pdb1zjk/pdb).

In addition, any CCP domain exosite mutants selected for use in SPR required an additional mutation. This mutation involved mutating the active site serine of MASP-2 to an alanine (S618A, or S195A in chymotrypsin numbering) (Figure 3.4). By replacing this catalytic serine, which is one of a triad of residues required for serine protease activity, with an alanine residue, it renders MASP-2, and indeed other serine proteases,

catalytically inactive. This additional mutagenesis was required, as earlier SPR work uncovered a complication where, upon cleavage of C4 by C1s, the exposed thioester bond of the resulting C4b product bound to the SPR chip, and could not be removed. By using the catalytically inactive S195A form of MASP-2, it allows the binding between MASP-2 and C4 to be observed, while avoiding the complications that arise through the cleavage of C4.
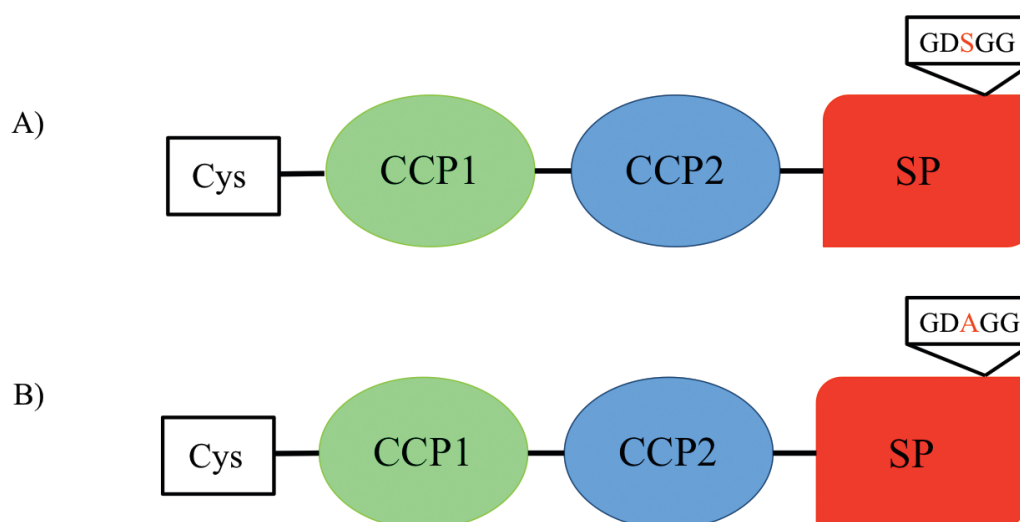
Figure 3.4: Mutation of the catalytic serine of MASP-2 (S618A). A) denotes the basic layout of the MASP-2 construct used for CCP domain mutagenesis. The text box shows the location of the catalytic serine, shown in red. For any mutants used in SPR studies, an additional mutation (S618A) was required to produced a catalytically inactive MASP-2 construct, as shown in B). The text box shows the location of the catalytic serine, now mutated to alanine, shown in red.

3.4 Production and characterisation of the MASP-2 CCP domain exosite mutants

Site-directed mutagenesis (see Section 2.2.1) and protein expression and purification (see Section 2.2.2) were carried out as described earlier. The amount of enzyme recovered for the various mutants ranged from 0.1-0.5 mg/ml per litre of *E. coli* culture. Each of the mutants purified in a similar manner to the wild type MASP-2 CCP12SP construct (Fig. 3.5), being eluted in the same peaks when purified with an anion-exchange Q-Sepharose column and a Superdex 75 16:60 gel filtration column (GE Healthcare, Uppsala, Sweden).

SDS-PAGE analysis confirmed that all the mutants purified to homogeneity. All of the active mutants were able to autoactivate during purification upon the Q-Sepharose

column, which was confirmed upon SDS-PAGE gel analysis. Under reducing conditions, activated MASP-2 runs as two fragments- the SP domain at ~ 28 kDa and the CCP domains at ~ 17 kDa. This indicates that cleavage of the Arg-Ile bond of the protease was complete. Zymogen MASP-2 runs as a single ~ 44 kDa fragment in reducing conditions. Each mutant was incubated with a molar excess of the serpin, C1-INH, to confirm the active concentration of each mutant, and all mutants reacted with C1-INH at a 1:1 ratio of protease: serpin, confirming that the proteases were fully active.
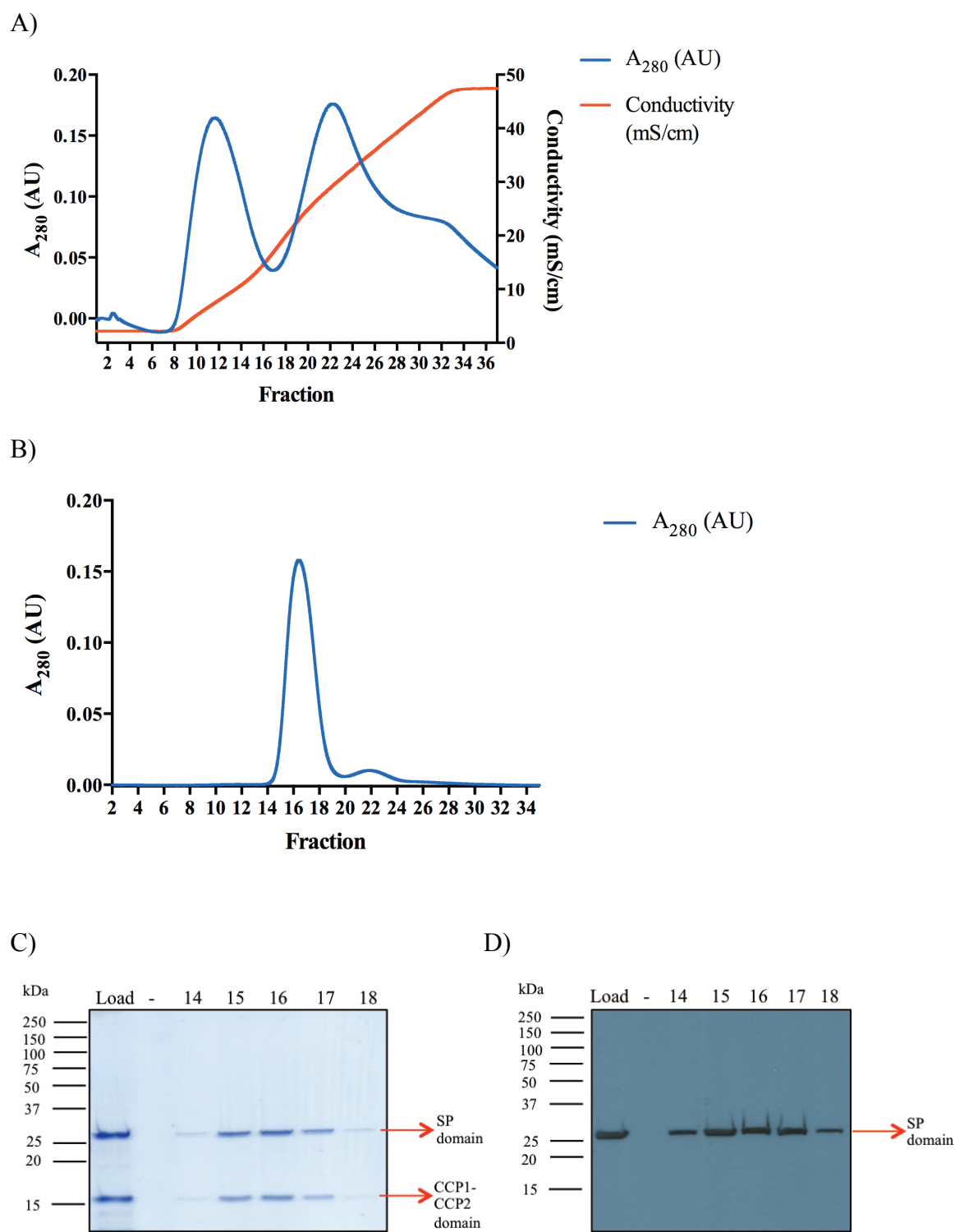
Figure 3.5: Purification of MASP-2 CCP12SP Cys WT. A) The purification profile of MASP-2 CCP12SP Cys WT using a QFF-Sepharose column to perform anion-exchange chromatography. MASP-2 was eluted in the second peak. B) The gel filtration chromatography profile of MASP-2 CCP12SP Cys WT. C) SDS-PAGE analysis of MASP-2 CCP12SP Cys WT after gel filtration chromatography, with a corresponding Western blot using a peptide antibody directed against the SP domain of MASP-2 (D). Samples were reduced prior to SDS-PAGE analysis.

3.5 Effects of the addition of the cysteine residue to the N-terminus of MASP-2

As discussed earlier, in order for SPR to be completed, it was necessary to add a cysteine residue to MASP-2 in order to facilitate binding to a CM5 chip through thiol coupling in a uniform manner. In order to be assured that the addition of the cysteine residue did not affect the functionality of MASP-2, the MASP-2 CCP12SP Cys WT construct was tested against the C4 peptide substrate and compared to the MASP-2 CCP12SP WT construct, which lacked the free cysteine, to investigate the active site integrity and cleavage efficacy of each construct.

Active site integrity was examined using the fluorescent peptide substrate C4 P4-P4' [2Abz-GLQRALEI-Lys(Dnp)-NH$_2$]. This peptide is a mimic of the physiological cleavage sequence of C4 that MASP-2 cleaves in order to create the C4 cleavage products, C4b and C4a. Testing revealed little significant difference between the non-cysteine and cysteine constructs, with both constructs recording similar $K_{0.5}$ and k_{cat} values, and consequently similar $k_{cat} / K_{0.5}$ values (Figure 3.6 and Table 3.2). This indicates that the addition of the cysteine residue does not disrupt protein folding, and so does not impact the integrity of the active site of MASP-2.

Table 3.2: Cleavage of the C4 peptide by MASP-2 constructs with or without the additional N-terminal cysteine residue.

M2 form	$K_{0.5}$ (μM)	k_{cat} (s^{-1})	$k_{cat}/ K_{0.5}$ (M^{-1} s^{-1})
MASP-2 CCP12SP WT	15.76 ± 0.96	0.46	2.9×10^4
MASP-2 CCP12SP Cys WT	10.39 ± 0.56	0.40	3.8×10^4
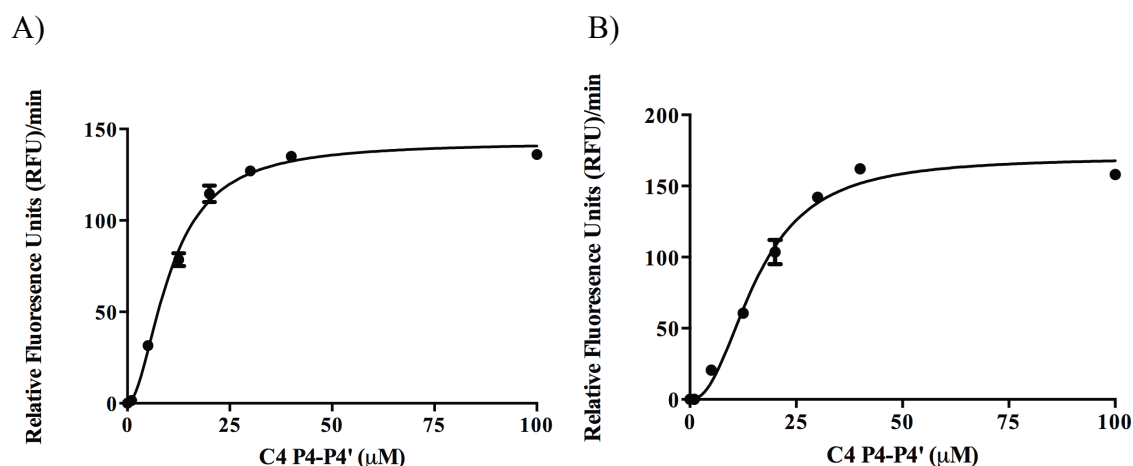
Figure 3.6: Cleavage of the C4 peptide by MASP-2 constructs with a) or without b) the additional cysteine residue. The peptide substrate was used over a concentration range of 0-100 μM, while MASP-2 was used at a concentration of 10 nM.

The effect of the addition of a cysteine residue on MASP-2 cleavage efficiency was also examined through examination of EC_{50} values. To determine this value, the amount of wild-type MASP-2 enzyme required to cleave 50% of a set amount of C4 was examined. With the assay carried out once, both constructs recorded EC_{50} values that were not significantly different to one another, suggesting that the additional cysteine residue does not impact the cleavage efficiency of MASP-2 (Figure 3.7 and Table 3.3).

Table 3.3: Cleavage of C4 by wild-type MASP-2 constructs with or without the additional N-terminal cysteine residue

M2 form	C4 EC_{50} value (nM)
MASP-2 CCP12SP WT	0.29
MASP-2 CCP12SP Cys WT	0.34
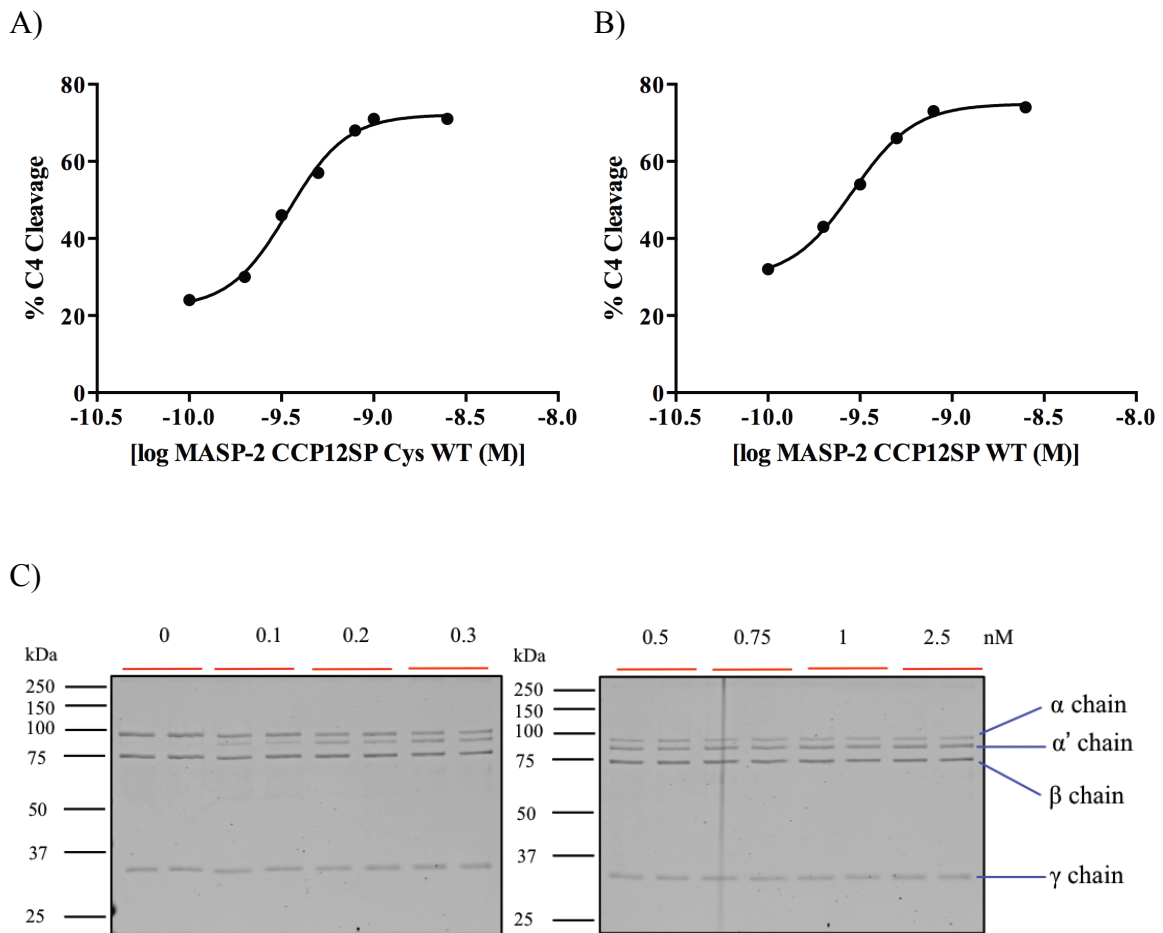
Figure 3.7: Determination of EC_{50} values for cleavage of C4 by wild-type MASP-2 with or without the additional cysteine residue. A) EC_{50} response curve of MASP-2 CCP12SP Cys WT. B) EC_{50} response curve of MASP-2 CCP12SP WT. C) SDS-PAGE analysis depicting C4 cleavage by both MASP-2 CCP12SP Cys WT (Lanes 1, 3, 5, 7, 9, 11, 13 and 15) and MASP-2 CCP12SP WT (Lanes 2, 4, 6, 8, 10, 12, 14 and 16). Both proteases were used in a concentration range of 0-2.5 nM, with reactions ended at 10 min by adding reducing SDS-PAGE loading buffer.

3.6 Testing the active site integrity of MASP-2 CCP domain exosite mutants

Mutagenesis studies of residues on the CCP domains of MASP-2 have the potential to lead to impacted protein folding, which in turn may cause destabilisation of the active site. A reduction in active site integrity would lead to a reduced cleavage ability for protein substrates that is not directly due to the mutation itself affecting the binding of substrates by MASP-2 at the exosites. To ensure that any results generated were due to the mutations created, and not due to instability of the active site caused by improper folding, each MASP-2 mutant was analysed using an assay for the cleavage of the fluorescent C4

peptide substrate C4 P4-P4' [2Abz-GLQRALEI-Lys(Dnp)-NH$_2$]. As discussed earlier, this peptide mimics the cleavage site on C4 for MASP-2. For the assays, a final concentration of 10 nM of each MASP-2 mutant was used against varying concentrations of C4 P4-P4' peptide, ranging from 0-100 µM. From the results, it appears that the mutations do not impact the active site of MASP-2 in a negative manner, as the $K_{0.5}$ and k_{cat} values of the mutants were similar to that obtained for the wild type MASP-2 enzyme (Table 3.4). This also led to the mutants obtaining similar k_{cat} / $K_{0.5}$ values to wild-type MASP-2 (Table 3.4). Interestingly, the D365R mutation appeared to increase the activity of MASP-2, displaying a higher k_{cat} value, and a lower $K_{0.5}$ value (Table 3.4). This lead to the D365R mutant obtaining a $k_{cat}/K_{0.5}$ value a magnitude of order higher than that achieved by wild-type MASP-2 (Table 3.4). Since no mutation had a pronounced negative effect on peptide substrate cleavage, it therefore appears that any changes in the EC$_{50}$ values and cleavage of C4 time course results achieved by each mutant reflect the effect of the mutation upon C4 binding via an exosite, and are not caused by reduced active site integrity.

Table 3.4: Comparison of the kinetics of cleavage of the synthetic peptide C4 P4-P4' by CCP domain exosite mutants

M2 form	$K_{0.5}$ (µM)	k_{cat} (s^{-1})	k_{cat}/ $K_{0.5}$ (M^{-1} s^{-1})
WT	9.08 ± 0.73	0.35	3.8 x 10^4
E333Q	15.6 ± 2.27	0.47	3.0 x 10^4
D365N	11.6 ± 0.46	0.39	3.4 x 10^4
E333Q D365N	11.9 ± 0.75	0.64	5.3 x 10^4
E333R	11.1 ± 0.84	0.37	3.3 x 10^4
D365R	3.5 ± 0.14	1.45	4.1 x 10^5
D370A	14.35 ± 1.32	0.38	2.6 x 10^4
D371A	15.83 ± 1.91	0.38	2.4 x 10^4

3.7 Investigation into the C4 cleavage efficiency of the MASP-2 CCP domain exosite mutants

The C4 cleavage efficiency of each mutant produced was investigated through the determination of EC_{50} values. Initially, standard laboratory protocol was followed, with 1 μM of C4 being used (Duncan et al., 2012a, Duncan et al., 2012b). However, when the initial assays were done on mutants from the SP domain, no significant differences between the SP domain mutants and wild-type MASP-2 were detected, which gave rise to some concerns. Given that the K_M value of MASP-2 for C4 is ~ 58 nM, with 1 μM of C4, the assay would be working at a 17-fold higher concentration of C4 than the K_M of MASP-2 for C4 (Duncan et al., 2012a). This high amount of substrate could lead the assay to be examining zero-order kinetics in the Michaelis-Menten model for enzymatic reactions. In zero-order kinetics, the active sites of all the enzyme molecules present are saturated with substrate. This causes the rate and observed kinetics of the enzymatic reaction to no longer be dependent on the concentration of substrate. In these circumstances, it would mean that only mutations causing the most severe reductions in C4 cleavage efficacy would show altered EC_{50} values, with many of the more moderate effects on C4 cleavage efficacy being masked. Ideally, the amount of substrate used in the assay would be at a level equal to or below the K_M value of the enzyme for the substrate. This would allow the examination of first-order kinetics, where the rate and observed kinetics of a reaction do depend on substrate concentration. This in turn would allow us to detect a wider range of effects upon C4 cleavage efficacy in the determination of EC_{50} values, not only the most severe. This had not been an issue for C1s in determining EC_{50} values, as C1s has a K_M of ~ 5 μM for C4 (Rossi et al., 1998, Bally et al., 2005), so the use of C4 at 1 μM (Duncan et al., 2012b) was ideal for examining first-order kinetics.

Therefore, in an effort to come as close to the K_M of MASP-2 for C4 as possible, and also considering the limits of Coomassie blue staining sensitivity, a standard concentration of 100 nM of C4 was used in the assay. This allowed us to come to a value that was slightly less than 2-fold greater than the K_M value of MASP-2 for C4. With this reduction in C4 concentration, the effects each mutation on C4 cleavage efficacy were better visualised.

A varying concentration range of 0-2.5 nM was used for wild-type MASP-2, and adjusted as required for each mutant examined. Each concentration was incubated with 100 nM C4 for 30 min, after which the reaction was ended using reducing SDS loading buffer. Each reaction was then analysed on 10% SDS-PAGE, with the cleavage-induced reduction in intensity of the C4 α chain analysed through densitometry, and the γ chain used as a loading control. Statistical significance was assessed through the comparison of 95% confidence intervals between wild-type and mutant MASP-2.

.

Table 3.5: MASP-2 CCP domain exosite mutant EC_{50} values for cleavage of C4

M2 form	Mutant assay 1 (nM)	WT assay 1 (nM)	Mutant assay 2 (nM)	WT assay 2 (nM)
D370A	0.33	0.22	0.23	0.24
D371A	0.17	0.37	0.16	0.47
E333Q	*0.64*	*0.25*	*0.70*	*0.22*
D365N	*0.85*	*0.25*	*0.64*	*0.21*
E333Q D365N	*3.2*	*0.54*	*3.29*	*0.2*
E333R	*2.8*	*0.44*	*2.98*	*0.38*
D365R	*1.27*	*0.24*	*1.02*	*0.31*

Mutants with significant alterations in EC_{50} value are bolded and italicised.

Of the 7 mutants, 5 were found to have decreased the efficiency of MASP-2 in cleaving C4 (Table 3.5). The D370A mutation showed no significant difference in EC_{50} value compared to wild-type MASP-2, indicating that this mutation was not affecting the binding and cleavage of C4 by MASP-2 (Table 3.5). The D371A mutation appeared to have an increased efficiency of C4 cleavage, with EC_{50} values ~ 2-3 fold lower than that of wild-type MASP-2 (Table 3.5). However, these results were found to not be statistically significant. As found by Kidmose *et al.* (2012), mutation of the E333 and D365 residues impacted the ability of MASP-2 to cleave C4 (Kidmose et al., 2012). Neutralising the charge of the 333 and 365 residues caused a ~ 2.5-3.5 fold increase in the EC_{50} value obtained (Table 3.5). Even more pronounced was the increase in EC_{50} with these residues when they underwent charge reversal mutations, with a 6-8 fold and 3.4-5.4 fold increase

in EC_{50} value seen for the E333R and D365R residue mutants, respectively (Table 3.5). When both residues were mutated to form the MASP-2 CCP12SP Cys E333Q D365N mutant, the increase in EC_{50} value was much higher, with a ~ 6-17 fold increase in EC_{50} value seen (Figure 3.8 and Table 3.5).
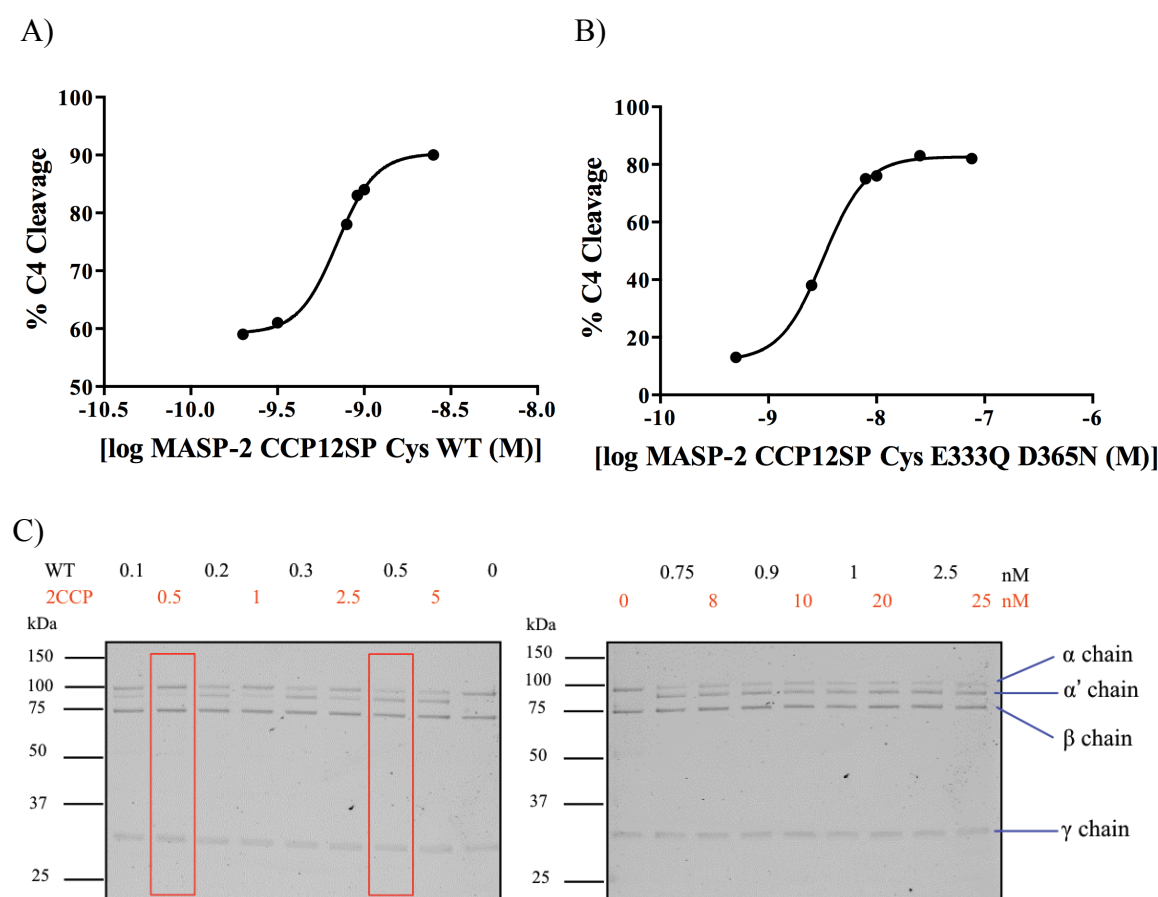
Figure 3.8: Determination of EC_{50} values for cleavage of C4 by the MASP-2 CCP domain exosite mutant MASP-2 CCP12SP Cys E333Q D365N. A) EC_{50} response curve of MASP-2 CCP12SP Cys WT. B) EC_{50} reponse curve of MASP-2 CCP12SP E333Q D365N. C) SDS-PAGE analysis depicting C4 cleavage by both MASP-2 CCP12SP Cys WT and MASP-2 CCP12SP Cys E333Q D365N. C4 was used at 100 nM, with wild-type MASP-2 concentrations from 0-2.5 nM (in black), and the double CCP domain exosite mutant MASP-2 E333Q D365N using a concentration range of 0-25 nM (in red). The reaction was ended at 30 min with reducing SDS-PAGE loading buffer. As a comparison measure, red boxes are placed around the concentration 0.5 nM, which was a common concentration used for both MASP-2 variants. In the gel, it can clearly be seen that the double CCP domain exosite mutant E333Q D365N is cleaving C4 less efficiently than wild-type MASP-2.

3.8 Investigations into the time course of C4 cleavage by affected MASP-2 CCP domain exosite mutants

The mutants that showed impacted C4 EC_{50} values were further investigated to evaluate how the mutations affected the ability of MASP-2 to cleave C4 over a period of time using a fixed concentration of 1 nM of the enzymes.
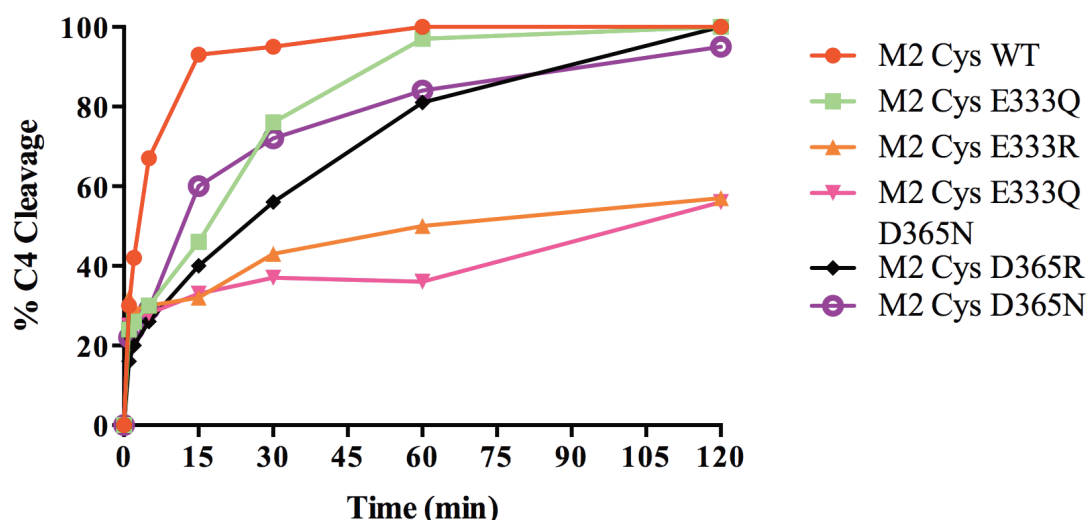
Figure 3.9: C4 cleavage time course for MASP-2 CCP domain exosite mutants. Time points of 0, 1, 2, 5, 15, 30, 60 and 120 min were selected. The α chain of C4 was analysed using densitometry, with the C4 γ chain used as a loading control.

Upon examination of the time courses, the E333Q, D365N and D365R mutants all showed a reduced rate of C4 cleavage compared to wild-type MASP-2 (Figure 3.9). At one hour, only the E333Q mutation shows a similar level of cleavage to wild-type MASP-2 (Figure 3.9). By 2 h, the D365N and D365R mutants also show similar levels of cleavage to wild-type MASP-2 (Figure 3.9). The E333R and E333Q D365N mutants showed severely reduced cleavage rates, and only managed to reach a ~ 50% cleavage rate in 2 h (Figure 3.10).

These cleavage time courses correlate with the C4 EC_{50} results obtained, as the E333R and E333Q D365N mutants displayed the most impacted EC_{50} values, indicating that these mutations suffered the most severe reductions in C4 cleavage efficacy (Figure 3.9 and Table 3.5). The E333Q, D365N and D365R mutants, which recorded smaller increases in EC_{50} values, recorded time courses that, while displaying a slower rate of

cleavage than the wild-type, where much less affected that the E333R and E333Q D365N mutants, as they all reached over 90% C4 cleavage by the end of the second hour (Figure 3.9 and Table 3.5).
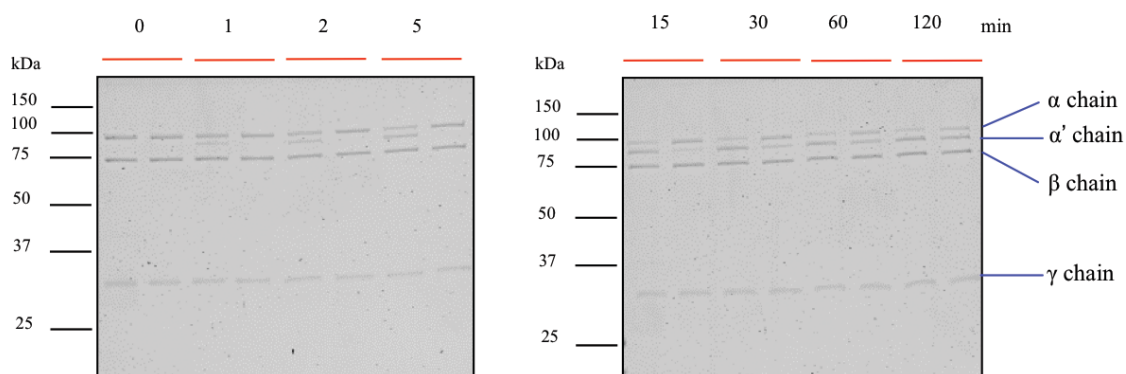
Figure 3.10: Time course for C4 cleavage by the MASP-2 double mutant E333Q D365N. Time points of 0, 1, 2, 5, 15, 30, 60 and 120 min were selected, with each reaction ended using reducing SDS loading buffer. The α chain of C4 was analysed using densitometry, with the C4 γ chain used as a loading control.

3.9 Analysis of the contribution of the MASP-2 CCP domain exosite to C4 binding using Surface Plasmon Resonance (SPR)

3.9.1 Selection of MASP-2 mutants to undergo SPR and their activation

Based upon the results obtained from the EC_{50} values and time course work, the most affected mutant, the double mutant E333Q D365N, was selected to be examined using SPR to investigate how the mutations affected the ability of the mutant to bind to C4. Previous SPR work in the laboratory has shown that when active wild-type C1s is placed upon a chip, its cleavage of C4 causes one of the products of C4 cleavage, C4b, to become free and bind to the chip through the activated elements of its thioester bond in an irreversible manner, damaging the chip. Therefore, to avoid this problem, C1s was mutated to the catalytically inactive S632A mutant (S195A in chymotrypsin numbering nomenclature) where the crucial serine residue of the active site is mutated to an alanine. By mutating this residue, C1s was able to bind C4 (Perry et al., 2013), but could not cleave it, thus preventing the production of C4b. Therefore, a similar approach was used for observing MASP-2 binding to C4. As MASP-2 cannot autoactivate with the S195A mutation present, both wild-type MASP-2 and the double mutant MASP-2 E333Q D365N

required manual activation. Each variant was placed onto a column lined with active wild-type MASP-2 CCP12SP and incubated at 26°C overnight in a buffer at pH 7.0. They were then eluted the next day with the same buffer, but at pH 6.0. When analysed using SDS-PAGE under reducing conditions, the activated MASP-2 migrated in two bands under reducing conditions. The SP domain migrates as a band at ~ 28 kDa, while the CCP1-CCP2 domains form another band at ~ 17 kDa (Figure 3.11). This indicated that cleavage at the Arg/Ile bond of the protease had occurred. Zymogen MASP-2 exhibits a single ~44 kDa band under reducing conditions (Figure 3.11).
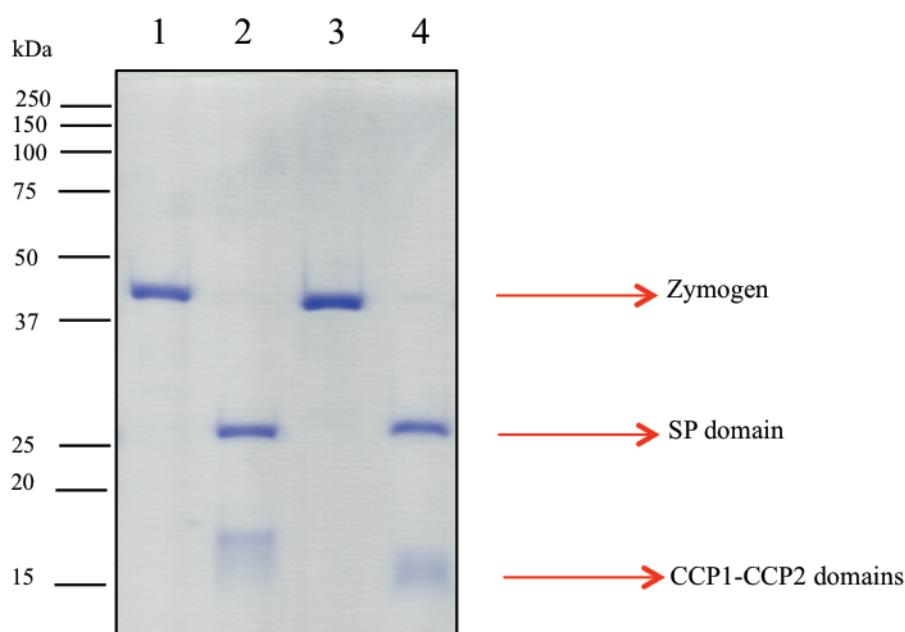
Figure 3.11: The activation of the MASP-2 variants used in SPR. Lane 1 shows the zymogen form of the MASP-2 CCP12SP Cys S618A enzyme, while Lane 2 shows the activated form of the enzyme. Lane 3 shows the zymogen form of MASP-2 CCP12SP Cys E333Q D365N S618A, while Lane 4 shows its activated form. All samples were reduced prior to electrophoresis.

3.9.2 Immobilisation of MASP-2 via Thiol Coupling

Coupling MASP-2 to a chip for the Biacore instrument through biotinylation proved problematic, so a new tactic utilising the free cysteine on the N-terminus of MASP-2 was required. It was decided to attempt using the free cysteine on the N-terminus of MASP-2 to directly bind MASP-2 to a CM5 chip through thiol coupling. This allowed the protein to still be able to bind to the surface of the chip in the uniform manner desired. However, this process required some refinement due to the different surface chemistry of

CM5 Biacore chips compared to that of Streptavidin SA Biacore chips. Initial binding experiments showed that very little MASP-2 bound to the CM5 chip, and upon examination, it was deduced that the buffer the protein was in (50 mM Tris, 150 mM NaCl pH 7.0), while appropriate for use in binding biotinylated protein to Streptavidin SA chips, was not appropriate for binding MASP-2 to CM5 chips. This is because the surface of CM5 chips utilises a carboxymethyl dextran matrix to bind molecules, unlike Streptavidin SA chips, which utilise streptavidin to bind biotinylated molecules. The carboxymethyl dextran matrix is highly positively charged, and so the high pH and salt content of the buffer may have caused electrostatic interference, thus preventing MASP-2 from binding to the chip.

To deduce the buffer pH and salt content required for optimal MASP-2 binding, the scouting function of the Biacore X100 was utilised. Scouting allows testing of numerous buffers to find optimal immobilisation conditions without the need to irreversibly utilise the flow cells upon the chip. Initial scouting with gel filtration buffer (50 mM Tris, 145 mM NaCl) of different pH values indicated that lower pH values (pH 4-4.5) allowed somewhat better binding by MASP-2 to the chip surface than pH values between 5 and 6. However, the improvement was not large. It was theorised that the salt content of the gel filtration buffer was still causing electrostatic repulsion between the protein and the chip. To investigate this issue further, MASP-2 was placed in three buffers, all of which contained 10 mM NaOAc, but had different pH values (pH range of 5-6). Although the pH values of 4 and 4.5 had proved the most successful for MASP-2 immobilisation with gel filtration buffer in previous scouting, there was concern that such low pH values would be detrimental to the protein, potentially destabilising it. It could also lead to precipitation, which would cause many issues in data collection, as well as damaging the microfluidics of the Biacore system. Therefore, some compromise was required, and so a pH range of 5-6 was examined.

Of all the buffers examined, 10 mM NaOAc pH 5 was the most successful at promoting MASP-2 binding to the CM5 chip. Therefore, this buffer was selected as the best compromise between reducing salt concentration and pH to promote protein immobilisation, while still maintaining the integrity of the protein, and so was used to dilute MASP-2 during the thiol coupling procedure.

3.9.3 Effects of pH upon MASP-2 active site stability

The activity of MASP-2 after incubation at pH 5 was tested to ensure that the reduction in pH from 7 to 5 did not have a negative impact upon the stability of the active site. This was done utilising the fluorescent peptide substrate C4 P4-P4' [2Abz-GLQRALEI-Lys(Dnp)-NH$_2$]. MASP-2 was incubated in fluorescence assay buffer at either pH 7.4 (normal conditions) or pH 5, with the remainder of the assay carried out in fluorescence assay buffer at pH 7.4. Testing revealed no significant difference between MASP-2 CCP12SP Cys WT at pH 7.4 and at pH 5, with both constructs recording similar $K_{0.5}$ and k_{cat} values (Figure 3.12 and Table 3.6). As a result, they also obtained similar $k_{cat}/K_{0.5}$ values (Table 3.6). This indicates that the alteration of pH value does not disrupt the integrity of the active site of MASP-2, and so its ability to cleave substrates is unaffected.

Table 3.6: The cleavage of the C4 P4-P4' peptide by wild-type MASP-2 to test the effects of pH upon MASP-2 cleavage ability.

pH	$K_{0.5}$ (μM)	k_{cat} (s^{-1})	$k_{cat}/K_{0.5}$ (M^{-1} s^{-1})
7.4	11.46 ± 0.66	0.42	3.7×10^4
5	14.39 ± 1.61	0.35	2.4×10^4

A)   B)
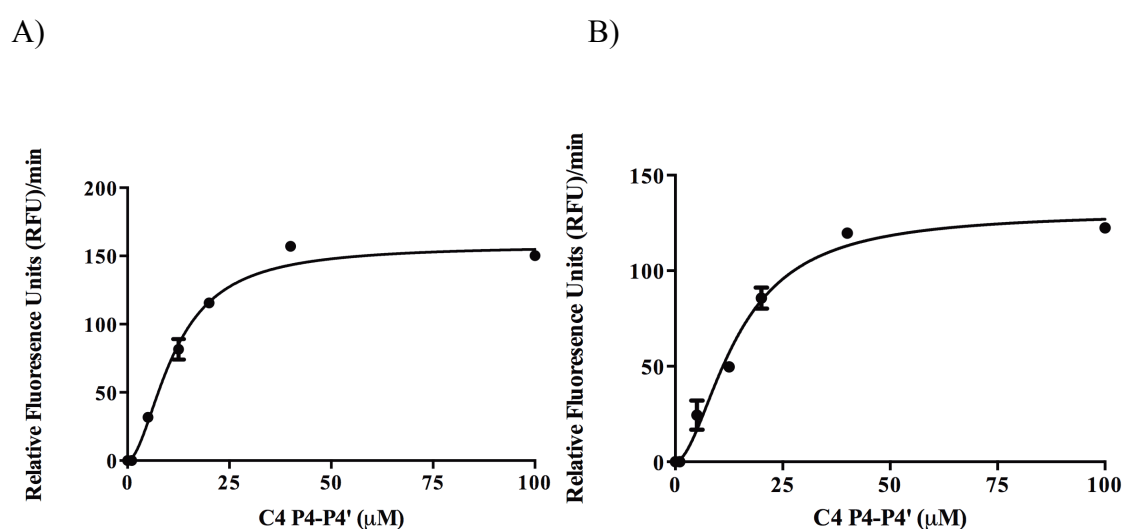
Figure 3.12: Cleavage of the C4 P4-P4' peptide by MASP-2 constructs after incubation at A) pH 7.4 and B) pH 5.0.

3.9.4 Analysis of the ability of selected MASP-2 CCP domain exosite mutants to bind to C4 using Surface Plasmon Resonance (SPR)

Under the newly deduced conditions just described, immobilisation of each MASP-2 mutant using thiol coupling was successful, with an acceptable level of each MASP-2 mutant immobilising to the chip as evidenced by the subsequent binding analysis.

After immobilisation was completed, serial dilutions of C4 were performed from 0-500 nM (on the Biacore X100) or 0-1 μM for MASP-2 CCP12SP Cys S618A (on the Biacore T100), or 0-1 μM for MASP-2 CCP12SP Cys E333Q D365N S618A on both instruments. Each mutant was analysed in triplicate using the Biacore T100, or in single runs completed three times consecutively upon the Biacore X100.

3.9.4.1 Steady-state affinity and its application to the binding interaction between MASP-2 and C4

From the data obtained, the affinity of the interaction was examined using the steady-state affinity model, using the equation $R_{eq} = K_A C R_{max}/K_A C + 1$, where R_{eq} is the equilibrium response level, C is the concentration of analyte, and K_A is the equilibrium association constant calculated by fitting a plot of R_{eq} against analyte concentration (Table 3.7 and Figure 3.13). This allowed us to obtain the dissociation constant value (K_D) for the binding of each MASP-2 variant to C4.

Activated wild-type MASP-2 yielded a K_D value of 82.6 nM (Table 3.7). The CCP exosite double mutant was severely affected, with a K_D of 608 nM, showing a ~ 7-fold increase in K_D value over that of the wild-type (Table 3.7). These results indicate that the CCP domain exosite of MASP-2 is crucial in promoting high affinity binding to C4.

Table 3.7: Steady-state K_D values for MASP-2 S618A and MASP-2 E333Q D365N S618A

M2 form	K_D (nM)
S618A n = 9	82.6 ± 6.5
CCP exosite n = 7	608 ± 63

A)

B)
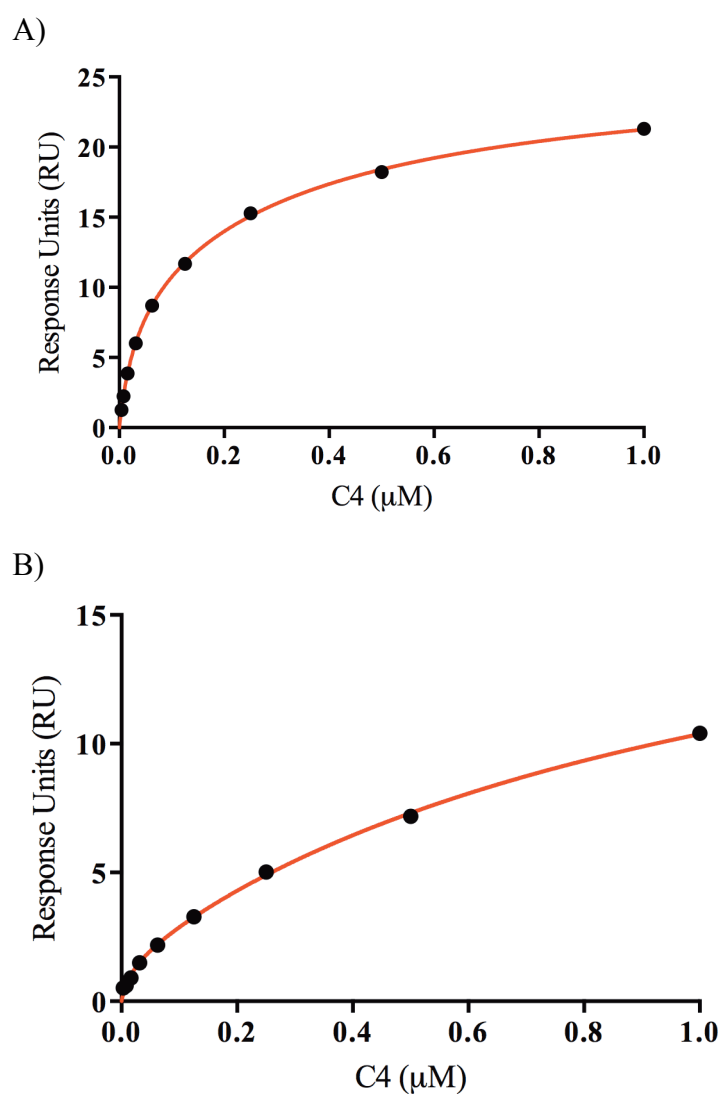
Figure 3.13: Analysis of binding of A) MASP-2 CCP12SP Cys S618A and B) MASP-2 CCP12SP Cys E333Q D365N S618A to C4, using fitting to a steady-state equation. The binding of both mutants to C4 was examined over a concentration range of 0-1 µM C4.

3.9.4.2 A two-site binding model and its application to the binding interaction between MASP-2 and C4

A two-state binding model was then used to fit the data in order to obtain the kinetic constants for C4 binding by MASP-2 (Figure 3.14 and Table 3.8). The data was also fitted to a one-state binding model, but this gave a very poor fit. Mutations to the CCP domain exosite decreased the initial association rate constant (K_1) 10-fold (Table 3.8), and also decreased the overall association rate constant for the entire reaction (K_a) by approximately 6-fold (Table 3.8), indicating that this exosite plays an important role in the first association event between enzyme and substrate. Conversely, mutations to the CCP domain exosite appeared to actually increase the conformational change constant (K_2) four-fold (Table 3.8).

Table 3.8: Two-state binding model and associated kinetic data for the binding of C4 by MASP-2.

M2 form	k_{a1} (M^{-1}.s^{-1})	k_{d_1} (s^{-1})	K_1 (M^{-1}.s^{-1})	k_{a_2} (s^{-1})	k_{d_2} (s^{-1})	K_2 (s^{-1})	K_a (M^{-1}.s^{-1})
S618A n = 9	1.2 x 10^6 ±1.8 x 10^5	0.2 ± 0.032	6.0 x 10^6	5.4 x 10^{-3} ± 0.001	3.2 x 10^{-2} ± 0.010	0.17	6.9 x 10^6
CCP exosite n = 7	2.7 x 10^5 ± 4.8 x10^4	0.45 ± 0.113	6.0 x 10^5	1.4 x 10^{-3} ± 6.8 x10^{-4}	1.9 x 10^{-3} ± 0.001	0.756	1.1 x 10^6

Figure 3.14: Binding of C4 to immobilised MASP-2 constructs. SPR curves for 0–1 μM C4 flowed over A) the immobilised activated form of MASP-2 CCP12SP Cys S618A without fit lines, as compared to B) which includes lines of fit for each concentration. SPR curves for 0–1 μM C4 flowed over C) the immobilised activated form of MASP-2 CCP12SP Cys E333Q D365N without fit lines, and D) which includes lines of fit for each concentration. The obtained responses were fitted to a two-state binding equation within the program BIAevaluation.

3.10 Discussion

It has been speculated for some time that there was a binding exosite upon the CCP domains of MASP-2 (Rossi et al., 2001, Ambrus et al., 2003, Harmat et al., 2004, Rossi et al., 2005). This was highlighted clearly by Duncan *et al.* in 2012, where removal of the CCP domains of MASP-2 to create a MASP-2 SP construct, resulted in a sharp increase in EC_{50} value, indicating that the cleavage efficacy of MASP-2 had been severely reduced by the removal of the CCP domains (Duncan et al., 2012a). However, the exact location of the exosite upon the CCP domains of this exosite was unknown until 2012,

when Kidmose *et al.* (2012) published a structure of the catalytically inactive MASP-2 CCP12SP S618A construct in complex with C4 (Kidmose et al., 2012). The structure clearly showed C4 making contact with MASP-2 at the most C-terminal end of the CCP1 domain up to the most N-terminal end of the CCP2 domain. However, little kinetic analysis was done upon the CCP domain binding exosite to determine its kinetic contribution to the interaction between MASP-2 and C4. Therefore, the aim here was to further explore the kinetic contribution of this exosite to the interaction between MASP-2 and C4.

An important aim in this study was to investigate binding between MASP-2 and C4 by use of SPR, and how mutations in the CCP domain exosite affected this binding interaction. In order to perform SPR, a cysteine residue was added to the N-terminus of the MASP-2 CCP12SP construct. It was firstly designed to allow biotinylation, but was later used in thiol coupling. This cysteine residue was shown to have no deleterious effect upon the functionality of MASP-2, with the EC_{50} values obtained from assays and from cleavage of the synthetic peptide C4 P4-P4' indicating that the addition of the cysteine residue did not impact the active site of MASP-2, nor did it impair C4 cleavage efficiency.

With mutagenesis studies comes the potential to impact the integrity of the protein under examination by destabilising its structure. If this occurs, it can complicate mutagenesis studies, as any effects seen in the functionality of the protein cannot be attributed directly to the mutation under investigation. In the case of MASP-2, if the active site of MASP-2 were to be destabilised by a mutation, it would have serious effects upon the ability of MASP-2 to bind and cleave C4. In turn, this could lead to confounding of data gathered from the experiments. To ensure that the results we were observing were due to the mutations made, and not due to the mutations leading to impacted protein folding, and so causing destabilization of the active site of MASP-2, all mutants were tested using the synthetic peptide substrate C4 P4-P4'. This peptide substrate is a mimic of the physiological cleavage sequence on C4 for MASP-2. From the results obtained, it appears that none of the mutations led to active site instability, as the majority of the mutants displayed similar $K_{0.5}$ and k_{cat} values to that of the wild-type MASP-2. Interestingly, the D365R mutation appeared to improve cleavage of the peptide substrate, displaying a $k_{cat}/K_{0.5}$ value an order of magnitude higher than wild-type MASP-2. An explanation may lie in the nature of the interface between the CCP1 and CCP2 domains.

Gal *et al.* (2005) have hypothesised a model where the junction between the CCP1 and CCP2 domains displays a quasi-rigid nature (Gal et al., 2005). Replacement of aspartate with arginine at this position could potentially increase this stability between the CCP1 and CCP2 domains by the introduction of new bonds being formed. Arginine is a larger residue than aspartate, and could potentially form stronger interactions with surrounding residues such as Gly 367, Thr 386 and Thr 387 than the naturally occurring aspartate residue at this position could. The increased stability of the CCP1-CCP2 domain junction could promote further flexibility of the junction between the CCP2 and SP domains, leading to an orientation of the SP domain that promotes improved cleavage of the C4 peptide substrate. However, the mutation would not confer an advantage in the binding and cleavage of a full C4 molecule, as mutation of this residue would abolish the interaction between it and the C4 residue Thr 1721 (Kidmose et al., 2012). The loss of this interaction would promote weakened binding between MASP-2 and C4, leading to reduced C4 cleavage efficacy.

The determination of EC_{50} values allows changes to cleavage efficacy created by mutations of interest to be examined, and has shown a good level of sensitivity in detecting these changes in prior work in the laboratory (Duncan et al., 2012a, Duncan et al., 2012b). However, work with MASP-2 has demonstrated the importance of observing the K_M of the enzyme of interest for its substrate in being able to see such effects. Previously, 1 µM of C4 was the standard amount of C4 used in the assay to determine EC_{50} values. However, after questioning why many of the mutants appeared to have no effect upon C4 cleavage efficacy, upon examination, it was found that this amount of C4 was much higher than the K_M value of MASP-2 for C4 [~ 58 nM, with K_M being a measure of the affinity of an enzyme for a substrate (Duncan et al., 2012a)]. This would mean that in the case of using 1 µM of C4, the assay would be working at a 16-fold higher concentration of C4 than the K_M of MASP-2 for C4. This would lead us to be examining zero-order kinetics, where the active sites of all the enzyme molecules present are saturated with substrate. This causes the rate and observed kinetics of the enzymatic reaction to no longer be dependent on the concentration of substrate. If this is what is being examined, it would mean that only the most severe reductions in C4 cleavage efficacy would be seen in the assays, with many of the more moderate effects on C4 cleavage efficacy being masked. Ideally, the amount of substrate used in the assay would be at a level equal to or below the K_M value of the enzyme for the substrate. This would

allow the examination of first-order kinetics, where the rate and observed kinetics of a reaction do depend on substrate concentration. In turn, this would lead to the detection of a wider range of effects upon C4 cleavage efficacy in the assay, not only the most severe. To reach first-order kinetics, we therefore reduced the amount of C4 in the assay to the minimal amount able to be detected by Coomassie blue staining (100 nM of C4). This allowed us to come to a value that was slightly less than 2-fold greater than the K_M value of MASP-2 for C4. With this reduction in C4 concentration, we were better able see the effects each mutation had upon C4 cleavage efficacy.

Investigations into the efficacy of C4 cleavage by the CCP domain exosite mutants through determination of EC_{50} values revealed some interesting results. The CCP domain exosite mutants selected by our laboratory (D370A and D371A) were shown to have no effect upon C4 cleavage efficacy, with these mutants obtaining EC_{50} values that were not significantly different from those obtained by wild-type MASP-2. This is not entirely unsurprising, given the location of these residues within the CCP domain exosite. When the structure of the MASP-2/C4 complex is studied, D370 and D371 are shown to be located on the outer periphery of the CCP domain exosite, and so would be less likely to impact C4 binding and cleavage if mutated.

Mutagenesis of the other CCP domain exosite residues studied tells a different story. Residues E333 and D365 are located in the centre of the CCP domain exosite. Single mutants of these residues displayed reduced C4 cleavage efficacy, both with the charge reversal mutants and the charge neutralised mutants. However, the largest impact came from mutating both residues simultaneously to create a double mutant (MASP-2 CCP12SP Cys E333Q D365N). This double mutant caused increases in EC_{50} value of over 20-fold over that seen in the wild-type. From the data, it appears that the effects of mutagenesis on this CCP domain exosite are cumulative, with each additional mutation further decreasing the ability of MASP-2 to cleave C4 efficiently. The work done by Kidmose *et al.* (2012) also supports this, as while both the E333R and D365R single mutants displayed reduced C4 cleavage, the MASP-2 E333R D365R mutant was unable to mediate C4 cleavage in C4b deposition assays (Kidmose et al., 2012).

The results of the time courses examining C4 cleavage, performed on the mutants that displayed altered EC_{50} values, correlate with the C4 EC_{50} values obtained. The two mutants showing the biggest reduction in C4 EC_{50} value, the E333R single mutant and the

E333Q D365N double mutant, showed the most impacted cleavage time courses, reaching only ~ 55% C4 cleavage even after 2 h. The other mutants (E333Q, D365N and D365R), which showed less of a reduction in C4 EC_{50} values, displayed a slower rate of C4 cleavage over the length of the time course, compared to wild-type MASP-2. This was especially noticeable over the first hour of the time course. However, by the end of the second hour, all had reached over 90% cleavage.

The C4 EC_{50} values and cleavage time course assays results obtained displayed the importance of the CCP domain exosite in ensuring efficient cleavage of C4 by MASP-2. In order to investigate the contribution of CCP domain exosite to the binding of C4 by MASP-2, SPR was utilised. The data obtained revealed the double CCP domain exosite mutant E333Q D365N exhibited an impacted steady-state affinity, with a 7-fold increase in K_D value over that of wild-type MASP-2. This increase in K_D value demonstrates the importance of the CCP domain exosite in promoting a high affinity interaction between MASP-2 and C4.

Previous work on C1s and C4 binding (Perry et al., 2013) was able to successfully fit a two-state binding model to the data obtained, allowing the kinetic constants of the interaction to be calculated. According to the two-state binding model, the enzyme forms an initial lower affinity complex with the substrate, following which a conformational change occurs that locks the enzyme and substrate into a higher affinity complex. The data obtained for the binding of MASP-2 to C4 could also be fitted to a two-state binding model. Mutations to the CCP domain exosite decreased the overall association rate constant (K_1) 10-fold, and also decreased the overall association rate constant for the entire reaction (K_a) by approximately 6-fold. These figures indicate that the CCP domain exosite plays an important role in the first association event between enzyme and substrate. Conversely, in the second part of the reaction, mutations to the CCP domain exosite appeared to actually increase the conformational change constant (K_2) four-fold, which suggests that the CCP domain exosite plays a less important role in the formation of a high affinity complex between MASP-2 and C4 than the SP domain exosite, which is discussed further in Chapter 5. The use of catalytically inactive forms of MASP-2 in SPR potentially raises some questions as to the relevance of the data obtained for the second part of the reaction. There is almost no doubt that the initial interaction between MASP-2 and C4 would occur in a similar manner with either catalytically active or inactive version

in the enzyme in order to achieve cleavage, thus requiring a catalytically active form of MASP-2, though this is not certain. The active enzyme would cleave C4 to yield C4b, which, based upon the large conformational changes seen between C3 and C3b (Janssen et al. 2005, Janssen et al., 2006), is likely to undergo a major conformational change upon the formation of the C4b product. This makes it likely that C4b would also undergo conformational change after cleavage. Thus, as we are using catalytically inactive MASP-2, the data obtained for the second phase of the reaction with inactive C4 is potentially of more questionable relevance. Technically, this is a difficult issue to overcome. The cleavage of C4 causes the production of C4b, which is able to bind to the Biacore chip through its thioester bond. Any mutation of MASP-2 or C4 that prevents this cleavage reaction from occurring, such as the mutation of the MASP-2 catalytic serine seen here, or the mutation of the MASP-2 residue R444, which Gal *et al.* showed prevents MASP-2 autoactivation (Gal et al., 2005), will have an impact on the potential structural changes MASP-2 and C4 undergo during the reaction. A potential solution to this issue is the use of stronger reagents to remove the C4b bound to the Biacore chip. Currently, a solution containing 100 mM NaOH is used. However, there is a real risk that the Biacore chips could be damaged irreparably if stronger cleaning reagents or higher levels of NaOH are used, and so this is not an ideal solution.

If MASP-2 was to undergo conformational change in order to cleave C4, structural knowledge suggests that the major rearrangements that occur would be in regard to the SP domain exosite of the enzyme. The structure of MASP-2 in complex with C4 (Kidmose et al., 2012) revealed that the major conformational change in MASP-2 that occurred when the molecules complexed was a large rotation of the SP domain relative to the CCP2 domain. Therefore, it appears that the CCP domain exosite plays a more minor role in this relative conformational rearrangement of the domains. The data obtained appears to reflect this, with the kinetic constants for the second phase of the reaction indicating that the SP domain exosite plays the major role (this will be discussed in Chapter 5 in further detail).

In conclusion, the results indicate that the CCP domain exosite of MASP-2 is crucial in allowing efficient binding to C4, and that removal of it severely impairs the ability of MASP-2 to bind and subsequently cleave C4

Chapter 4

'Investigation into the role of the disease-linked MASP-2 CCP domain mutation D371Y in the kinetic mechanism of interaction between MASP-2 and its substrate C4'

4.1 Introduction

The MASP-2 gene is found on chromosome 1p36.23-31. It contains 12 exons over 20 kb that encode both the MASP-2 protein, as well as the MAp19 (also known as sMAP) protein, which is derived through alternative splicing and inclusion of exon 5 in the mature mRNA (Stover et al., 1999a, Stover et al., 1999b).

Studies have found that there are a number of naturally occurring single nucleotide polymorphisms (SNPs) in the MASP-2 gene (Figure 4.1 and Table 4.1). Some are located in the promoter region, and other in introns. The impact of these mutations is not well understood, with only a few, such as the g.1945560C>A (rs7548659) mutation in the promoter region, being shown to lead to altered MASP-2 levels or functionality thus far (Boldt et al., 2011). A number of other SNPs occur in the 12 exons that make up the MASP-2 gene, and have been shown to lead to missense mutations. Thus far, eight missense mutations have been reported- R99Q, R118C, D210G and P126L in the CUB1 domain, H155R in the EGF domain, D371Y and V377A in the CCP2 domain and R439H in the SP domain (Figure 4.1 and Table 4.1)(Thiel et al., 2007). A 12 base pair duplication mutation, which results in residues 156-159 of the EGF domain being duplicated (referred to as CHNHdup), has also been found (Figure 4.1 and Table 4.1)(Thiel et al., 2007). These polymorphisms occur at different frequencies in different ethnic populations (Thiel et al., 2007). For example, the D120G polymorphism has presently been found to occur only in Caucasian and Inuit West Greenland populations, while the CHNHdup mutation has been found to occur only in people of Chinese descent thus far (Thiel et al., 2007). Polymorphisms appear to occur predominantly in the non-catalytic CUB1-EGF-CUB2 segment of the MASP-2 protein, with only three polymorphisms occurring outside these domains found so far (D371Y, V377A and R439H).
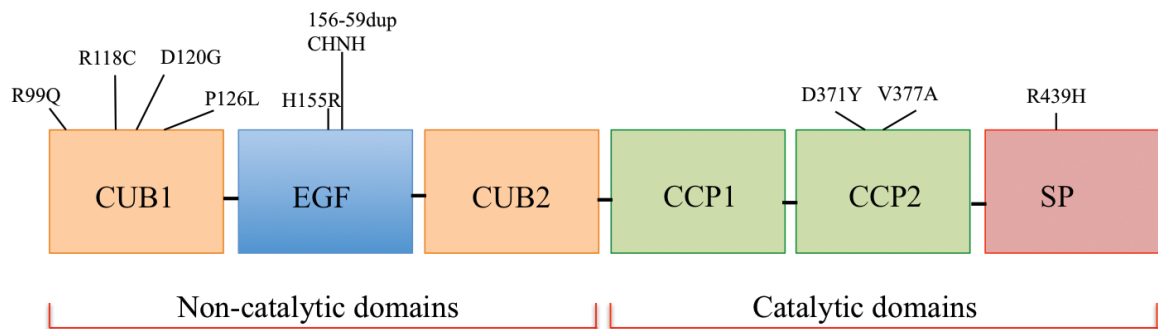
Figure 4.1: Pictorial layout of MASP-2 domains and the currently known MASP-2 polymorphisms. Five of the eight known polymorphisms (R99Q, R118C, D120G, P126L, H155R and the CHNH duplication in the EGF domain) occur in the non-catalytic domains of MASP-2, while the other three (D371Y, V377A and R439H) occur in the catalytic domains of MASP-2.

MASP-2 polymorphisms that lead to reduced MASP-2 levels and/or cause impairment to MASP-2 function have been associated with increased risk of developing a number of diseases. Reduced levels of MASP-2, associated with the D120G, P126L and R439H polymorphisms have been associated with greater risk of developing rheumatoid arthritis (Goeldner et al., 2014). Reduced levels of MASP-2 have also been associated with increased susceptibility to leprosy (Boldt et al., 2013). In particular, homozygosity for the D120G mutation has been linked to the development of chronic inflammatory disease and a higher rate of infection in certain individuals (Stengaard-Pedersen et al., 2003). A small number of individuals with the mutation have been found to suffer from Cystic Fibrosis or recurrent respiratory infections (Cedzynski et al., 2005, Olesen et al., 2006). The D120G polymorphism is found with an approximate frequency of 4% in European populations, yet this does not appear to match the presentation of disease with this mutation (Stengaard- Pedersen et al., 2003, Thiel et al., 2007). This suggests that in these instances the MASP-2 mutation contributes to the development of disease, but is not the only factor involved.

Table 4.1: MASP-2 polymorphisms and their location

Mutation	Domain Location	Effect on MASP-2 functionality	Effect upon serum levels	Reference
R99Q	CUB1	Normal	Increased	1, 2
R118C	CUB1	Unknown	Unknown	1
D120G	CUB1	Reduced- Prevents MASP-2 from binding MBL	Reduced	1, 2, 3
P126L	CUB1	Reduced- reason unknown	Reduced	1, 2
H155R	EGF	Normal	Unknown	1, 2
156-159CHNHdup	EGF	Reduced- Prevents MASP-2 from binding MBL	Reduced	1, 2
D371Y	CCP2	Unknown	Varied	1
V377A	CCP2	Normal	Reduced	1, 2
R439H	SP	Reduced- Prevents activation of MASP-2	Reduced	1, 2

References: 1) Thiel et al., 2007. 2) Thiel et al., 2009. 3) Stengaard-Petersen et al., 2003. 4) Boldt, A et al., 2011.

One MASP-2 polymorphism that has been linked with increased susceptibility to a number of diseases is that of D371Y. This mutation occurs in exon 10 of the MASP-2 gene, with the residue being located in the CCP2 domain of the MASP-2 protein, and in this mutation a G to T substitution at base pair 1111 in the cDNA position (counting from the methionine starting codon), leads to the original aspartic acid residue being altered to a tyrosine (Figure 4.2).
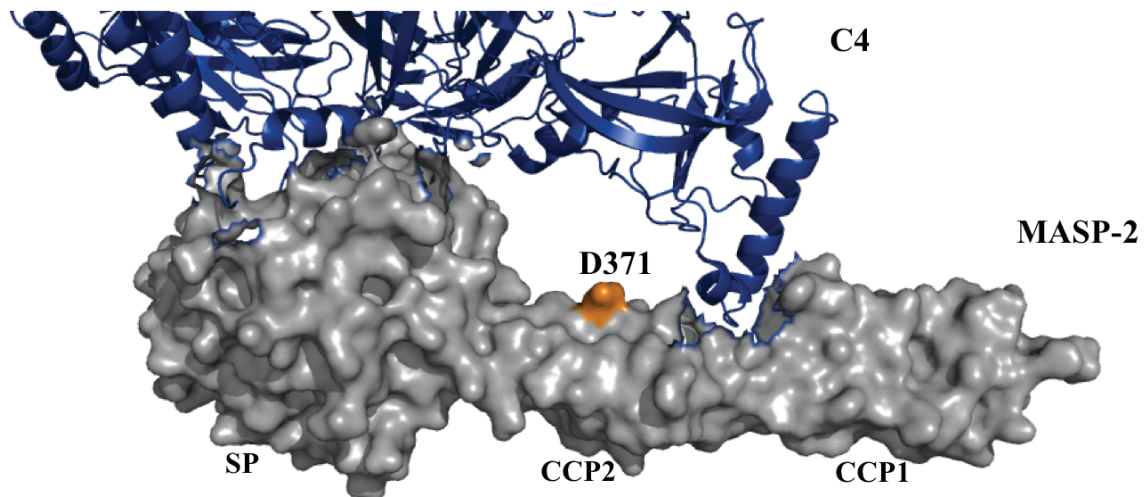
Figure 4.2: The location of MASP-2 residue D371. The D371 residue is shown in orange. MASP-2 is depicted in grey, while C4 is depicted in blue. Image generated using PDB file 4FXG (DOI: 10.2210/pdb4fxg/pdb).

A number of studies have associated this polymorphism with susceptibility to chronic infectious disease caused by a number of different microbial pathogens. The D371Y polymorphism has been associated with increased susceptibility to certain viral infections. Coelho *et al.* (2013) identified a link between the polymorphism and increased susceptibility to Human T-Lymphotropic Virus (HTLV-1) infection, as this polymorphism occurred at higher rates in infected individuals than in healthy controls (Coelho et al., 2013). It was found that having this mutation in either homozygous or heterozygous form led to a 2-fold increase in risk for HTLV-1 infection compared to those homozygous for the wild-type form (Coelho et al., 2013). In addition, Tulio *et al.* (2011) found that the D371Y mutation was associated with susceptibility to developing chronic HCV within a Euro-Brazillian population with moderate and chronic HCV (Tulio et al., 2011). The polymorphism has not been linked to an increased susceptibility to all viral infections however, with the D371Y polymorphism having been found to lack an association with an increased susceptibility to SARS coronavirus infection (Wang et al., 2009).

The D371Y polymorphism has also been associated with increased susceptibility to certain bacterial infections. De Rooij *et al.* (2010) found that homozygosity for the D371Y polymorphism lead to an increased risk of bacterial infection after orthotopic liver transplantation, with 45% of homozygotes for the polymorphism developing clinically significant bacterial infections, as opposed to 22% for those who were not homozygous (de Rooij et al., 2010). Catarino *et al.* (2014) discovered an association between the D371Y polymorphism and an increased risk in the development of rheumatic heart disease

(RHD), a complication stemming from infection with rheumatic fever (RF), which is caused by infection with the bacteria, *Streptococcus pyogenes*. In the study, the mutation was found to be associated with a five-fold increased risk in the development of the disease, although it was not associated with an increased susceptibility to RF (Catarino et al., 2014). As seen with viral infections, the D371Y polymorphism does not lead to an increased risk of infection to all bacteria, with the polymorphism having been shown to lack association with the development of leprosy (Boldt et al., 2013).

In addition to an increased susceptibility to certain viral and bacterial infections, Boldt *et al*. (2011) discovered an association between the D371Y polymorphism and the development of cardiomyopathy in chronic Chagas disease, which is caused by the flagellated protozoan *Trypanosoma cruzi*. This mutation occurred at a higher frequency amongst symptomatic patients (Boldt et al., 2011).

At this point in time, the studies completed upon this mutation have been epidemiologically based, and so have been unable to discern functional reasons as to why this mutation may be linked to the increased susceptibility to the diseases being studied. Tulio *et al.* postulated that the mutation could potentially create modifications to the substrate specificity of MASP-2 (Tulio et al., 2011). However, now that the structure of MASP-2 in complex with C4 has been solved, this would be surprising, as the residue shows no contacts with C4 in the MASP-2/C4 complex structure, and while it is located near the CCP domain C4 binding exosite, it is on the outer perimeter of it, and so is unlikely to play a role in the actions of this exosite (Figure 4.2) (Kidmose et al., 2012).

Therefore, one of the aims of this study was to investigate this mutation at a kinetic level, and to discern a functional reason that could explain why this mutation appears to be linked to a number of chronic infectious diseases.

4.2 Materials and Methods

4.2.1 Investigation into the cleavage efficacy of MASP-2 for the substrate C2 through the determination of EC_{50} values

Wild-type MASP-2 and MASP-2 mutants were diluted to a concentration range 0-2.5 nM in EC_{50} assay buffer. C2, purchased from Complement Technology Inc., (Complement Technology Inc., Tyler, Texas, USA), was also diluted in the EC_{50} assay buffer to a final concentration of 1 μM. The protease and substrate were incubated for 5 min at 37°C separately before being added together in a 1:1 ratio to allow the cleavage reaction to begin. The reaction proceeded for 1 h before being ended by adding reducing SDS loading buffer to the reaction. After this step, 2 μL of 0.5 mg/mL ovalbumin was added to each reaction to act as a loading control for analysis in later stages. Samples were then incubated at 95°C for 5 min, centrifuged at 13,000 x g for 1 min, and then loaded onto 10% SDS-PAGE gels and electrophoresed. After electrophoresis, the gels were stained using 0.2 μm filtered Coomassie blue R-250 for 1 h, and then destained in a solution containing 40% (v/v) methanol and 10% (v/v) acetic acid.

A Typhoon Trio (containing Argon Blue 488nm, SYAG Green 532 nm and HeNe Red 633nm lasers) was used for densitometry analysis of the gels, and the scanned gels were analysed using IQTL ImageQuant^{TM} software's 1D Gel analysis option. The disappearance of the zymogen C2 band was analysed, with ovalbumin used as a loading control. The data generated from the 1D gel analysis was then entered into GraphPad Prism Version 6.0 software, and an EC_{50} value obtained using the non-linear regression equation: log (inhibitor) vs. response- variable slope equation [$Y=Ymin + (Ymax-Ymin)/(1+10^{((LogEC50-X)*h)})$], where Ymin is the minimum Y value, Y max the maximum Y value and h is the Hill Slope.

4.2.2 Investigation into the cleavage efficacy of MASP-2 for the substrate C2 through cleavage time courses

Wild-type MASP-2 and MASP-2 mutants were diluted to a final concentration of 5 nM in EC_{50} assay buffer. C2 (Complement Technology Inc., Tyler, Texas, USA) was diluted to a final concentration of 1 μM in EC_{50} assay buffer. The substrate and protease were incubated separately for 5 min at 37°C before being added together in a 1:1 ratio to begin the cleavage reaction, which was conducted at 37°C. Time points where the reaction was to be ended were selected (0, 1, 2, 5, 15, 30, 60 and 120 min), and the reactions were ended by adding reducing SDS loading buffer to the sample. After this step, 2 μL of 0.5 mg/mL of ovalbumin was added to each reaction to act as a loading control for analysis in later stages. The samples were then incubated at 95°C for 5 min, centrifuged at 13,000 x *g* for 1 min, and then loaded onto 10% SDS-PAGE gels and electrophoresed. After electrophoresis, the gels were stained using 0.2 μm filtered Coomassie blue R-250 for 1 h, and then destained in a solution containing 40% (v/v) methanol and 10% (v/v) acetic acid.

A Typhoon Trio (containing Argon Blue 488nm, SYAG Green 532 nm and HeNe Red 633nm lasers) was used for densitometry analysis of the gels, and the scanned gels were analysed using IQTL ImageQuant^{TM} software's 1D Gel analysis option. The disappearance of the zymogen C2 band was analysed, with ovalbumin used as a loading control. The data generated from the 1D gel analysis was then entered into GraphPad Prism Version 6.0 software to create a time course graph depicting the cleavage of C2 by the MASP-2.

4.2.3 Investigation into the efficacy of MASP-1 and MASP-2 activation of zymogen MASP-2

A cleavage time course to examine the activation of zymogen MASP-2 by MASP-1 and MASP-2 was utilised. Wild-type MASP-1 and MASP-2 constructs were diluted to a final concentration of 200 nM in EC_{50} assay buffer, with 1 μg of zymogen MASP-2 CCP12SP Cys D371Y S618A used in each reaction. Each component was incubated separately for 5 min at 37°C, before being added together to begin the cleavage reaction, which was conducted at 37°C. Time points where the reaction was to be ended were selected (0, 2, 5, 15, 30, 60, 120 and 240 min), and the reactions were ended by adding

reducing SDS loading buffer to the sample. After this step, 2 μg Bovine Serum Albumin (BSA) was added to each reaction to act as a loading control for analysis in later stages. The samples were then incubated at 95°C for 5 min, centrifuged at 13,000 x g for 1 min, and then loaded onto 12.5 % SDS-PAGE gels and electrophoresed. Gels were then stained using 0.2 μm filtered Coomassie blue R-250 for 1 h, and then destained in a solution of 40% (v/v) methanol and 10% (v/v) acetic acid.

A Typhoon Trio (containing Argon Blue 488nm, SYAG Green 532 nm and HeNe Red 633nm lasers) was used for densitometry analysis of the gels, and the scanned gels were analysed using IQTL ImageQuant^{TM} software's 1D Gel analysis option. The cleavage of the zymogen MASP-2 band was analysed, with the BSA band used as a loading control. The data generated from the 1D gel analysis was then entered into GraphPad Prism Version 6.0 software to create a time course graph depicting the cleavage of zymogen MASP-2 by MASP-1 and MASP-2.

4.3 Production and characterisation of the MASP-2 CCP12SP Cys D371Y mutant

As was done in Chapter 3, the MASP-2 D371Y mutant was created on a MASP-2 construct featuring an additional free cysteine residue on the N-terminus of the protein (MASP-2 CCP12SP Cys D371Y). A construct was also produced for use in SPR, which contained an additional mutation, where the catalytic serine (S618, or S195 in chymotrypsin numbering) was mutated to an alanine (MASP-2 CCP12SP Cys D371Y S618A). The MASP-2 CCP12SP Cys D371Y and MASP-2 CCP12SP Cys D371Y S618A constructs were produced using the mutagenesis and purification protocols outlined in Chapter 3. The amount of enzyme recovered for this mutation was ~ 0.3 mg/ml per litre of *E. coli* culture. Both D371Y constructs purified in a similar manner to the wild type MASP-2 CCP12SP construct, being eluted in the same peaks when purified with an anion-exchange Q-Sepharose column and a Superdex 75 16:60 gel filtration column. SDS-PAGE analysis confirmed that both D371Y constructs purified to homogeneity. The cataytically active MASP-2 D371Y construct was able to autoactivate during purification upon the Q-Sepharose column, which was confirmed upon SDS-PAGE gel analysis (Figure 4.3). Under reducing conditions, activated MASP-2 runs as two fragments- the SP domain at ~ 28 kDa and the CCP domains at ~ 17 kDa (Figure 4.3). This indicates that

cleavage of the Arg-Ile bond of the protease was complete. The catalytically inactive MASP-2 D371Y S618A construct, which was unable to autoactivate due to mutation of the catalytic serine, ran as a single fragment in reducing conditions at ~44 kDa. The D371Y mutant was incubated with a molar excess of the serpin, C1-INH, to confirm the active concentration of mutant. It reacted with C1-INH at a 1:1 ratio of protease: serpin, confirming that the protease was fully active.
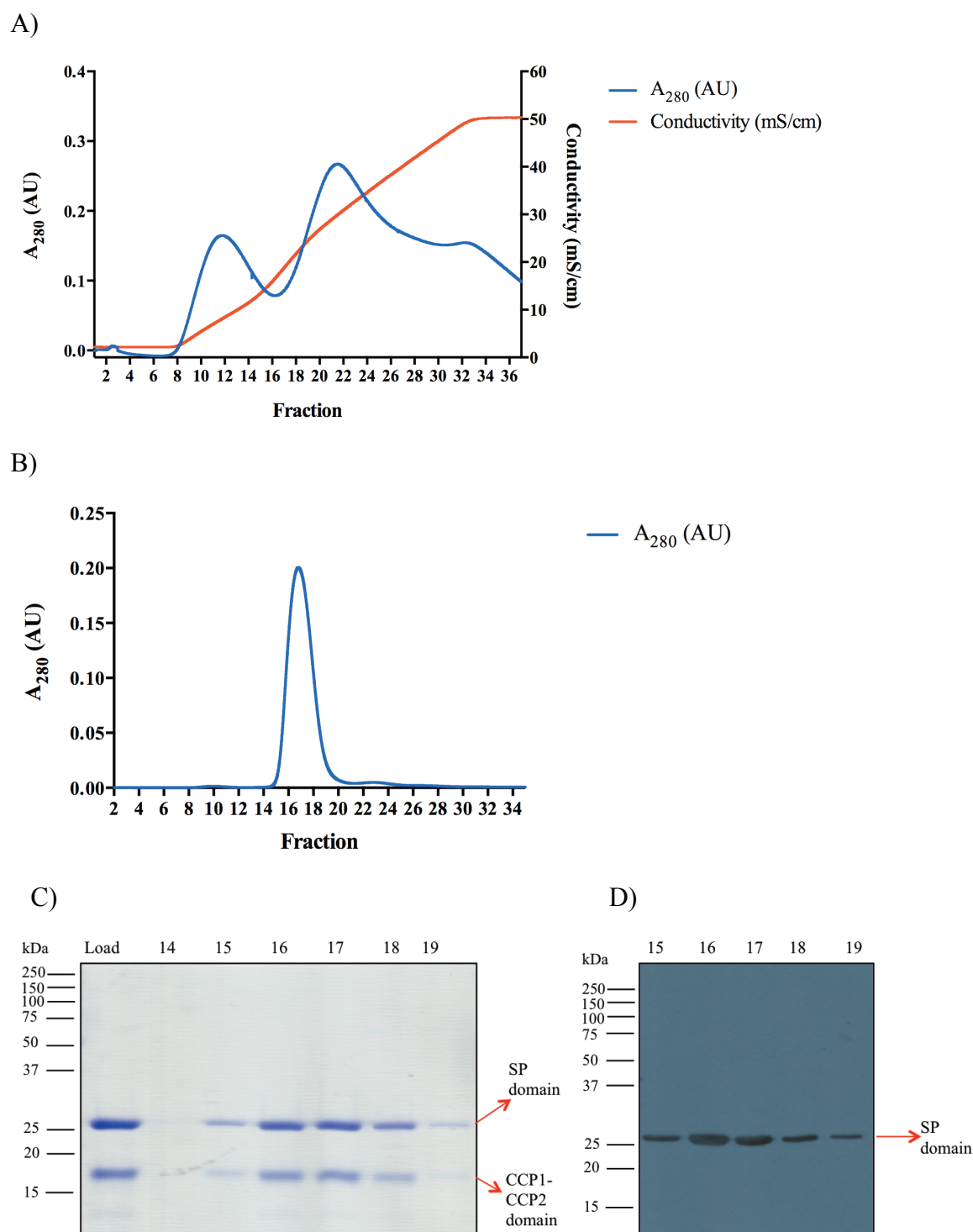
Figure 4.3: Purification of MASP-2 CCP12SP Cys D371Y. A) The purification profile of the MASP-2 mutant D371Y from anion-exchange chromatography on QFF-Sepharose:. MASP-2 eluted in the second peak. B) The gel filtration chromatography profile of the MASP-2 D371Y mutant. C) SDS-PAGE analysis of the MASP-2 D371Y mutant after gel filtration chromatography, with a corresponding Western blot using a peptide antibody directed against the SP domain of MASP-2 (D). Samples were reduced prior to SDS-PAGE analysis.

4.4 Testing the active site integrity of the MASP-2 D371Y mutant

When mutating residues in the CCP domains of MASP-2, there is always the potential risk of the mutation impeding the proper folding of the enzyme, which would lead to destabilization of the active site of the enzyme. This would then affect the ability of MASP-2 to cleave its substrates. To ensure that any results generated were due to the D371Y mutation created, and not due to potential improper folding and consequent active site destabilization caused by the mutation, this MASP-2 mutant was assayed for cleavage of the C4 peptide substrate C4 P4-P4' [2Abz-GLQRALEI-Lys(Dnp)-NH$_2$]. This peptide mimics the cleavage site on C4 for MASP-2. From the results, it appears that the D371Y mutation does not have a deleterious effect upon the folding of the MASP-2 enzyme, as the $K_{0.5}$ value for the mutant was similar to that obtained for the wild type MASP-2 enzyme (Figure 4.4 and Table 4.2). In addition, the k_{cat} and k_{cat} / $K_{0.5}$ values did not show a large amount of difference between the mutant and wild-type MASP-2 (Table 4.2). It therefore appears that any changes in C2 and C4 cleavage will reflect the effect of the mutation upon C4 binding and cleavage, and are not caused by improper folding of the enzyme due to the mutation.

Table 4.2: Comparison of the kinetics of cleavage of the synthetic peptide C4 P4-P4' by wild-type MASP-2 and the MASP-2 D371Y mutant

M2 form	$K_{0.5}$ (µM)	k_{cat} (s^{-1})	$k_{cat}/K_{0.5}$ (M^{-1} s^{-1})
WT	17.12 ± 0.82	0.49	2.8 x 10^4
D371Y	14.85 ± 1.08	0.42	2.8 x 10^4

Figure 4.4: Cleavage of the C4 P4-P4' peptide by A) wild-type MASP-2 and B) the MASP-2 mutant D371Y.

4.5 Investigation into the C2 and C4 cleavage efficiency of the MASP-2 D371Y mutant

4.5.1 C4 cleavage efficacy of the MASP-2 D371Y mutant

To assess the impact of the D371Y mutation on MASP-2 cleavage of C4, EC_{50} values were determined. A final concentration of 25 nM of C4 was used when examining the D371Y mutation and the enzymes were used in a range from 0-2.5 nM. The EC_{50} values determined indicate that there is no significant difference in C4 cleavage efficacy between the wild-type MASP-2 and the D371Y mutant, with the D371Y mutant achieving an EC_{50} very similar to that of wild-type MASP-2 (Figure 4.5 and Table 4.3). This indicates that the mutation is having no effect upon the ability of MASP-2 to cleave C4 in an efficient manner.

Table 4.3: MASP-2 D371Y mutant C4 EC_{50} values

M2 form	Analysis 1 (nM)	Analysis 2 (nM)
M2 WT	0.14	0.39
M2 D371Y	0.22	0.46
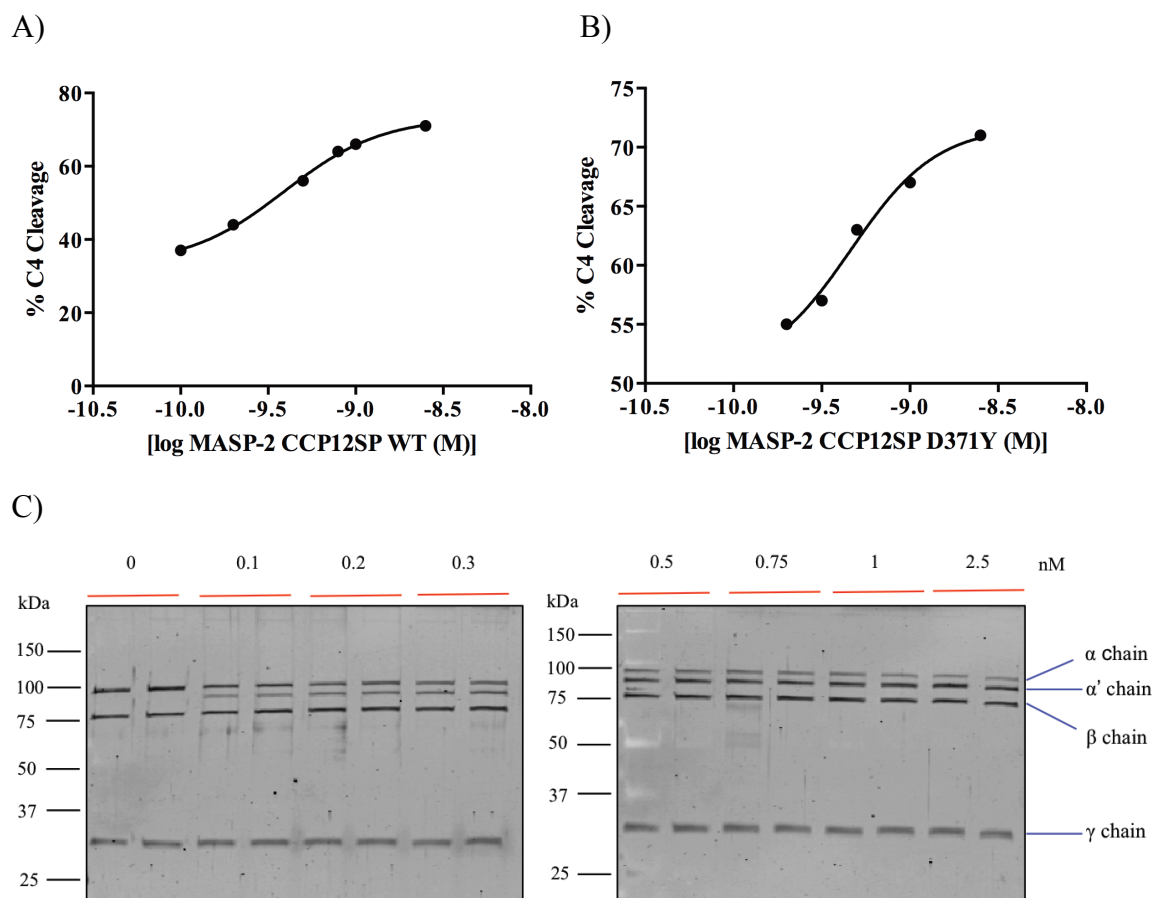
Figure 4.5: Determination of EC_{50} values for the cleavage of C4 by the MASP-2 mutant MASP-2 D371Y. A) EC_{50} response curve of MASP-2 CCP12SP Cys WT. B) EC_{50} reponse curve of MASP-2 CCP12SP D371Y. C) SDS-PAGE analysis depicting C4 cleavage by both MASP-2 CCP12SP Cys WT (Lanes 1, 3, 5, 7, 9, 11, 13 and 15) and MASP-2 CCP12SP Cys D371Y (Lanes 2, 4, 6, 8, 10, 12, 14 and 16). C4 was used at 25 nM, with both MASP-2 variants using concentrations from 0-2.5 nM. Reactions were ended at 10 min by adding reducing SDS-PAGE loading buffer.

4.5.2 C2 cleavage efficacy of the MASP-2 D371Y mutant

In an effort to pinpoint why the D371Y mutation of MASP-2 is linked to increased susceptibility to certain diseases, we also examined the cleavage efficacy of this mutation for MASP-2's other major substrate, C2. As was done with C4, investigation into the cleavage efficacy of the D371Y mutation for C2 was done by determining EC_{50} values. In the experiment, as MASP-2 has a K_M of ~ 5 μM for C2 (Ambrus et al., 2003, Rossi et al., 2005), 1 μM of C2 was used, with both MASP-2 variants in a range from 0-25 nM. From the results, it appears that the D371Y mutation of MASP-2 does not impact the cleavage efficacy of MASP-2 for C2 (Figure 4.6 and Table 4.4). Both wild-type and the mutation

recorded similar EC_{50} values that were not significantly different (Table 4.4). It therefore appears that this mutation does not decrease the cleavage efficacy of MASP-2 for C2.

Table 4.4: MASP-2 D371Y mutant C2 EC_{50} values

M2 form	C2 EC_{50} (nM)
M2 WT	2.72
M2 D371Y	3.64
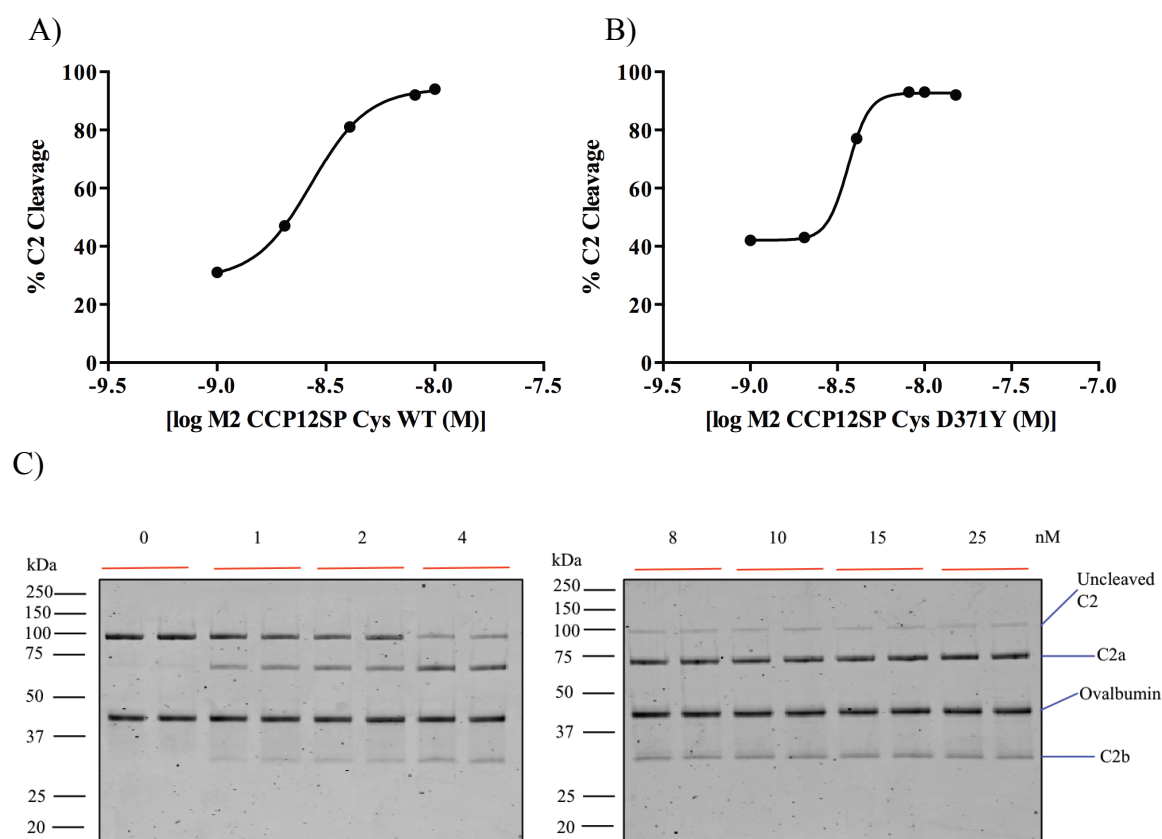
Figure 4.6: Determination of EC_{50} values for cleavage of C2 by the MASP-2 mutant MASP-2 D371Y. A) EC_{50} response curve of MASP-2 CCP12SP Cys WT. B) EC_{50} response curve of MASP-2 CCP12SP D371Y. C) SDS-PAGE analysis depicting C2 cleavage by both MASP-2 CCP12SP Cys WT (Lanes 1, 3, 5, 7, 9, 11, 13 and 15) and MASP-2 CCP12SP Cys D371Y (Lanes 2, 4, 6, 8, 10, 12, 14 and 16). C2 was used at 1 μM, with both MASP-2 variants using concentrations from 0-25 nM. The reaction was ended at 1 hr using reducing SDS-PAGE loading buffer.

4.6 Investigations into the time course of C2 and C4 cleavage by the MASP-2 D371Y mutant

4.6.1 Time course of C4 cleavage by the MASP-2 D371Y mutant

In addition to the determination of EC_{50} values, the time course of C4 cleavage by the MASP-2 D371Y mutant was also examined to verify the impact of the mutation upon efficient C4 cleavage. In the assays, a final concentration of 25 nM of C4 was used, with both MASP-2 variants used at a final concentration of concentration of 1 nM.

From the time course analysis, it is evident that the mutation does not affect C4 cleavage, with the cleavage time course for the D371Y mutant following that of wild-type MASP-2 quite closely (Figure 4.7). This correlates with the EC_{50} values determined, in which the D371Y mutant displayed no difference in cleavage efficiency compared to the wild-type MASP-2 (Table 4.3). These results reinforce that the D371Y mutation does not affect C4 cleavage efficacy, and so a reduction in C4 cleavage efficacy does not appear to be the reason this mutation has been linked to increased susceptibility to a number of diseases.

A)

B)
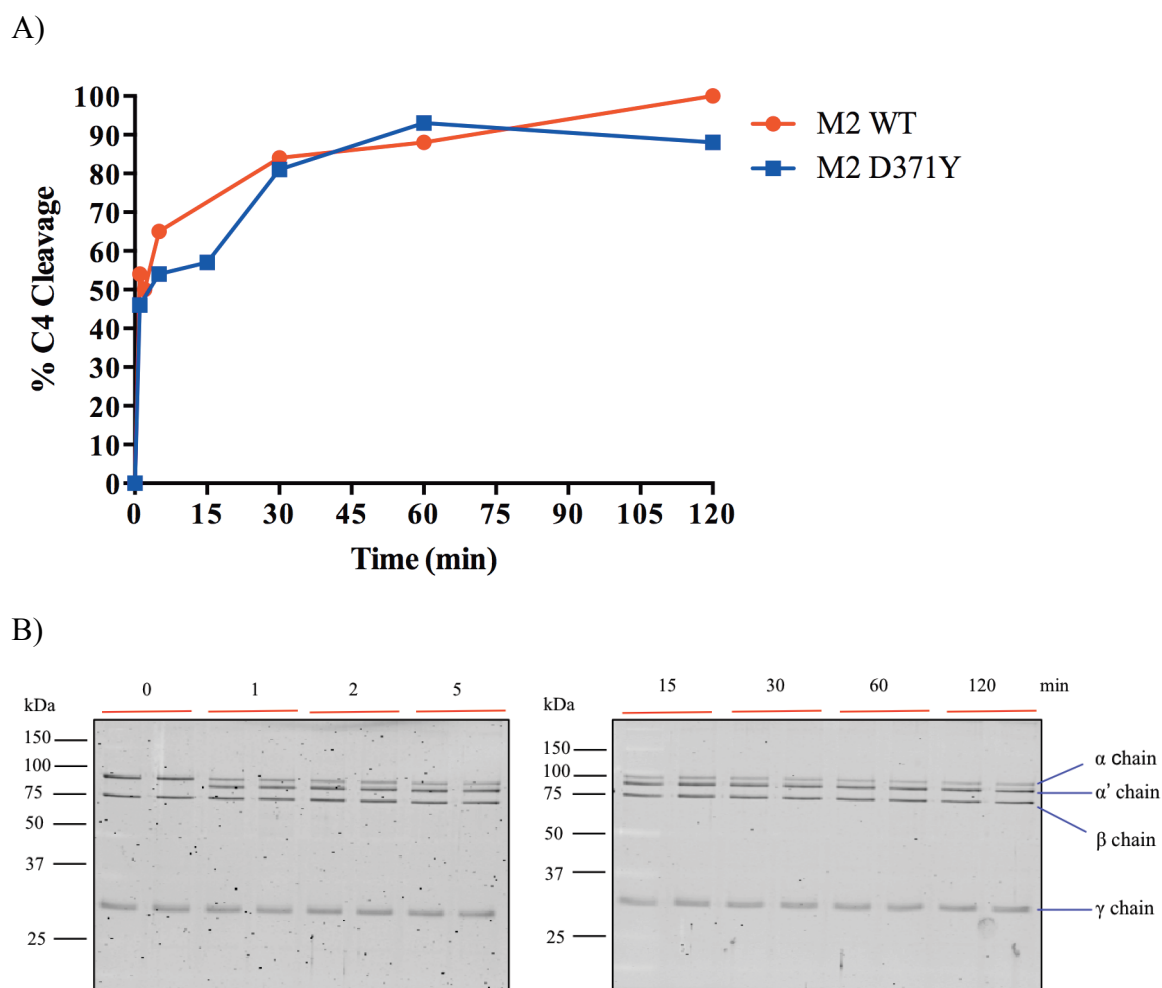
Figure 4.7: Time course for C4 cleavage by the MASP-2 mutant D371Y. A) Graphical depiction of the C4 cleavage time course for the MASP-2 CCP12SP Cys D371Y mutant. The α chain of C4 was analysed using densitometry, with the C4 γ chain used as a loading control. B) SDS-PAGE analysis for time course of C4 cleavage by MASP-2 CCP12SP Cys D371Y. Reactions were ended using reducing SDS loading buffer.

4.6.2 Time course of C2 cleavage by the MASP-2 D371Y mutant

As was done with C4, a time course analysis was performed to examine the efficiency of cleavage of C2 by the D371Y mutant. The time courses were carried out at 37°C using final concentrations of 1 μM of C2 and MASP-2 at 5 nM.

From analysis of the data, it appears that the D371Y mutation does not affect the cleavage of C2 by MASP-2. Both wild-type and the D371Y mutant displayed a similar time course of cleavage for C2, which, along with the EC_{50} values determined, indicates that this mutation does not impair the ability of MASP-2 to cleave C2 in an efficient manner (Figure 4.8 and Table 4.4). This suggests that impaired C2 cleavage is not the

cause of the link between the D371Y mutation and increased susceptibility to the development of certain diseases.

A)
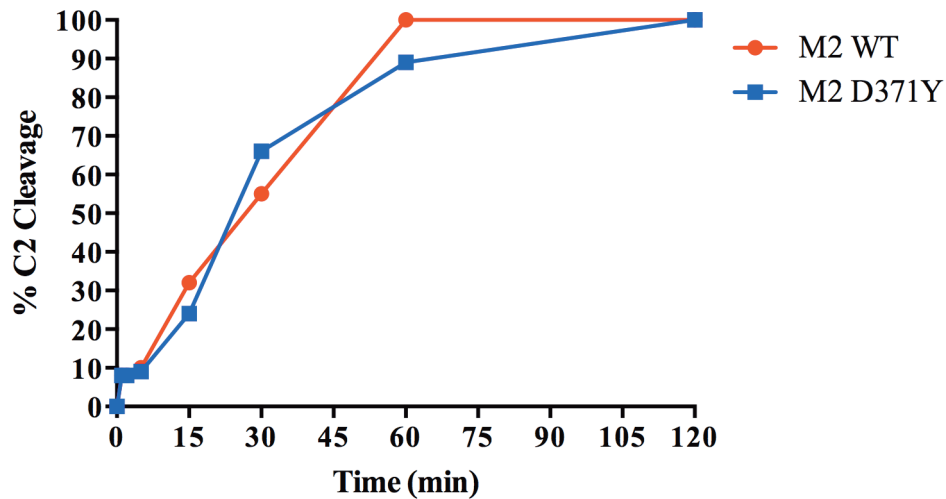
B)
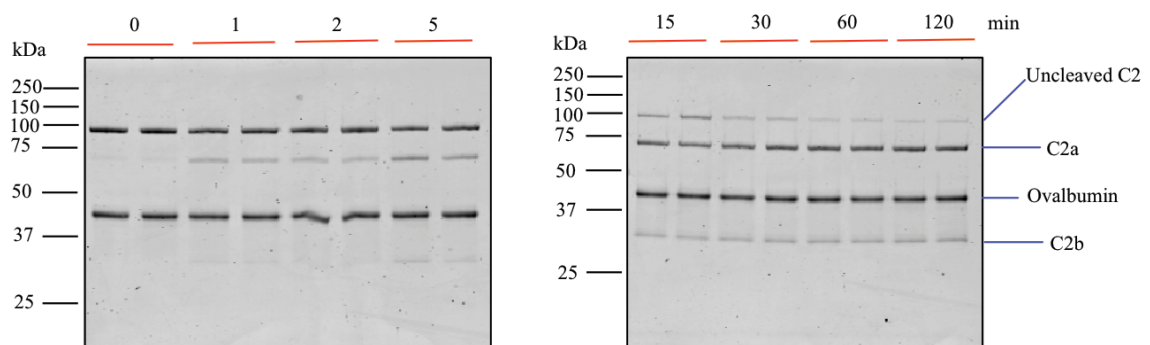
Figure 4.8: Time course for C2 cleavage by the MASP-2 mutant D371Y. A) Graphical depiction of the C2 cleavage time course for the MASP-2 CCP12SP Cys D371Y mutant. Time points of 0, 1, 2, 5, 15, 30, 60 and 120 min were selected. The disappearance of uncleaved C2 was analysed using densitometry, with ovalbumin used as a loading control. B) SDS-PAGE analysis for time course of C2 cleavage by MASP-2 CCP12SP Cys D371Y. Reactions were ended using reducing SDS loading buffer.

4.7 Functional analysis of the ability of the MASP-2 D371Y mutant to bind to C4 using Surface Plasmon Resonance (SPR)

4.7.1 Activation of MASP-2 CCP12SP Cys D371Y S618A

From the data discussed earlier in this chapter, it appears that the D371Y mutation does not affect the cleavage efficiency of MASP-2 for either of its substrates, C4 and C2. It was decided to examine the binding of MASP-2 D371Y to C4 through SPR to confirm that the mutation causes no differences in C4 binding.

As discussed in previous chapters, a catalytically inactive version of MASP-2 is required when examining C4 binding due to production of unwanted artifacts through C4 cleavage. Therefore, the catalytic serine of the active site of MASP-2 (S618A, or S195A in chymotrypsin numbering) was mutated to create the construct MASP-2 CCP12SP Cys D371Y S618A. Due to mutation of the catalytic serine, this construct was unable to autoactivate upon the QFF-Sepharose during purification and required manual activation. This was achieved by loading the protein onto a column lined with active wild-type MASP-2 CCP12SP and incubating it at 26°C overnight in a pH 7.0 buffer. The protein was eluted the next day with the same buffer, but at pH 6.0 instead of 7.0. When analysed using SDS-PAGE under reducing conditions, successful activation could be seen: the zymogen form, which exhibits a single band at ~ 44 kDa, was gone, while activated MASP-2 could be seen, where it migrated in two bands, one representing the SP domain at ~ 28 kDa and the CCP1-CCP2 domains at ~ 17 kDa (Figure 4.9).
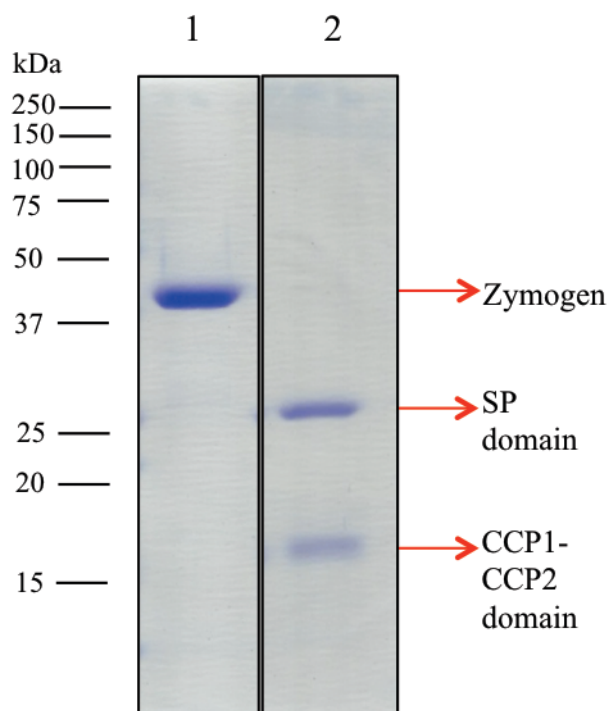
Figure 4.9: The activation of the MASP-2 D371Y mutant. Lane 1 shows the zymogen form of MASP-2 CCP12SP Cys D371Y S618A under reducing conditions, while Lane 2 shows the activated form of the enzyme. Samples were reduced before electrophoresis.

4.7.2 Analysis of the ability of MASP-2 CCP 12SP Cys D371Y S618A to bind to C4 using Surface Plasmon Resonance (SPR)

Under the newly deduced conditions described in Chapter 3, immobilisation of wild-type MASP-2 CCP12SP Cys S618A and the MASP-2 CCP12SP Cys D371Y S618A mutant to a CM5 chip was carried out through thiol coupling. This was successful, with an acceptable level of each MASP-2 mutant immobilising to the chip, as evidenced by the subsequent binding analysis. After immobilisation was completed, serial dilutions of C4 were performed from 0-500 nM. This was completed in single analyses done three times consecutively upon the Biacore X100 instrument.

4.7.2.1 Steady-state affinity and its application to the binding interaction between MASP-2 and C4

Using the data obtained, the affinity of the interaction between the MASP-2 variants and C4 was examined using the steady-state affinity model. This model utilises the equation $R_{eq} = K_A C R_{max}/K_A C + 1$, where R_{eq} is the equilibrium response level, C is the concentration of analyte, and K_A is the equilibrium association constant calculated by fitting a plot of R_{eq} against analyte concentration. This allowed us to obtain the dissociation constant value (K_D) for the binding of each MASP-2 variant to C4.

Activated wild-type MASP-2 obtained a K_D value of 82.6 nM (Figure 4.10 and Table 4.5). The D371Y mutant appeared to be unaffected, obtaining a K_D value of 70.7 nM (Figure 4.10 and Table 4.5). As the results between wild-type MASP-2 and the D371Y mutant are very similar, this suggests that the mutation does not affect the ability of MASP-2 to bind efficiently to C4.

Table 4.5: Steady-state K_D values for MASP-2 S618A and MASP-2 D371Y S618A.

M2 form	K_D (nM)
S618A n= 9	82.6 ± 6.5
D371Y S618A n = 3	70.7 ± 12.4

A)

B)
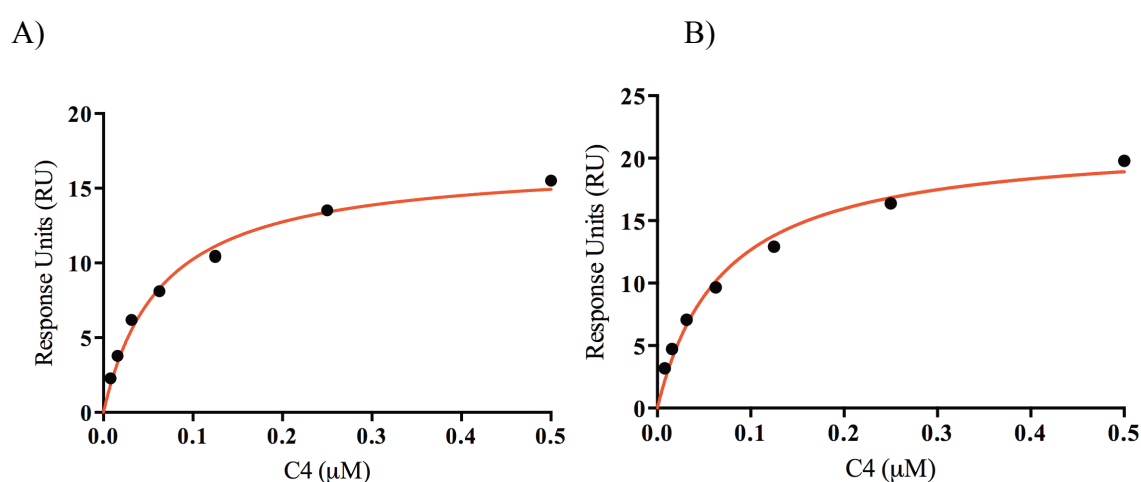
Figure 4.10: Analysis of binding of A) MASP-2 CCP12SP Cys S618A and B) MASP-2 CCP12SP Cys D371Y S618A to C4, using fitting to a steady-state equation. The binding of both mutants to C4 was examined over a concentration range of 0-500 nM C4.

4.7.2.2 A two-state binding model for the binding interaction between MASP-2 and C4

As done in Chapter 3, and in previous work (Perry, A., *et al*. 2013), a two-state binding model was used to fit the data in order to obtain the kinetic constants for C4 binding by wild-type MASP-2 and the MASP-2 D371Y mutant. In this model, the equation M2 + C4 ⇆ M2:C4 ⇆ M2*C4, where the initial complex (M2:C4) is converted to a higher affinity complex (M2*C4) due to conformational change, is used. Use of the two-state binding model allowed kinetic rate constants to be derived. The data was also fitted to a one-state binding model, but it obtained a very poor fit and so could not be used for analysis.

The data obtained from the two-state binding model, and the resulting kinetic constants, show that the results for each aspect of the binding interaction between MASP-2 and C4 are very similar in both wild-type MASP-2 and the MASP-2 D371Y mutant (Figure 4.11 and Table 4.6). This suggests that the MASP-2 D371Y mutation does not affect the binding interaction between MASP-2 and C4. This correlates with the C4 EC_{50} values determined and the C4 cleavage time course results, with the MASP-2 D371Y obtaining results very close to those obtained for wild-type MASP-2 (Figure 4.7 and Table 4.3).

Table 4.6: Two-State binding model and associated kinetic data for the binding of C4 by MASP-2

M2 form	k_{a1} $(M^{-1}.s^{-1})$	k_{d_1} (s^{-1})	K_1 $(M^{-1}.s^{-1})$	k_{a_2} (s^{-1})	k_{d_2} (s^{-1})	K_2 (s^{-1})	K_a $(M^{-1}.s^{-1})$
S618A n = 9	1.2×10^6 $\pm 1.8 \times 10^5$	0.2 ± 0.032	6.0×10^6	5.4×10^{-3} ± 0.001	3.2×10^{-2} ± 0.010	0.17	6.9×10^6
D371Y S618A n = 3	1.2×10^6 $\pm 6.0 \times 10^4$	0.24 ± 0.057	5.5×10^6	8.2×10^{-3} ± 0.005	4.8×10^{-2} ± 0.022	0.11	6.1×10^6

Figure 4.11: Binding of C4 to immobilised MASP-2 constructs. SPR curves for 0–500 nM C4 flowed over A) the immobilised activated form of MASP-2 CCP12SP Cys S618A without fit lines, as compared to B) which includes lines of fit for each concentration. SPR curves for 0–500 nM C4 flowed over C) the immobilised activated form of MASP-2 CCP12SP Cys D371Y S618A without fit lines, and D) which includes lines of fit for each concentration. The obtained responses were fitted to a two-state binding equation within the program BIAevaluation.

4.8 Investigations into the cleavage of the MASP-2 D371Y mutant by MASP-1 and MASP-2

With results indicating that the D371Y mutation did not lead to reduced efficiency in C2 or C4 cleavage by MASP-2, it was decided to investigate other facets of MASP-2 functionality that could be impacted by such a mutation. One such facet is that of MASP-2 activation. For many years, it was thought that the primary means of MASP-2 activation was through autoactivation, and thus it represented the minimum requirement for lectin

pathway activation. Further research indicates that this is not the complete story, with MASP-1 being found to be the main activator of MASP-2 (Degn et al., 2012, Heja et al., 2012b, Megyeri et al., 2013). Therefore, to examine the effects of the D371Y mutation on MASP-2 activation by MASP-1 and MASP-2, the catalytically inactive construct of the D371Y mutant was used (MASP-2 CCP12SP Cys D371Y S618A), along with the catalytically inactive wild-type MASP-2 construct (MASP-2 CCP12SP Cys S618A), and their activation by active wild-type MASP-1 or MASP-2 over 4 hours was then examined. In the time course, wild-type MASP-1 and MASP-2 were diluted to a final concentration of 200 nM in EC_{50} Assay Buffer, with 1 μg of zymogen wild-type MASP-2 and zymogen MASP-2 D371Y used in each reaction. Bovine Serum Albumin (BSA) was added to each reaction to act as a loading control during analysis of the results.

The time courses show the zymogen MASP-2 D371Y construct being cleaved in a very similar manner to zymogen wild-type MASP-2 by both MASP-1 and MASP-2. From the time course, it appears that the D371Y mutation does not impact the activation of MASP-2 by either MASP-1 or MASP-2 (Figures 4.12 and 4.13). This suggests that the link between increased susceptibility to particular diseases and the MASP-2 D371Y mutation is not due to impaired MASP-2 activation.

A)
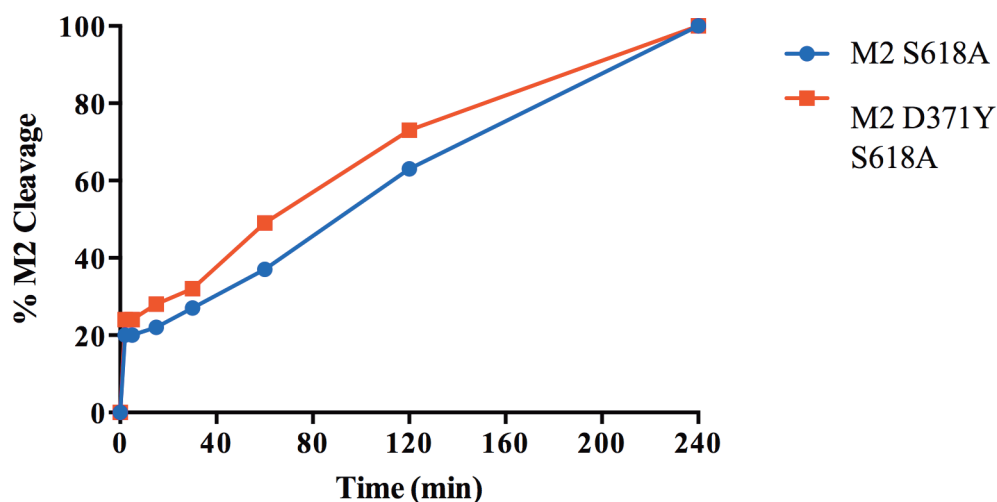
B)
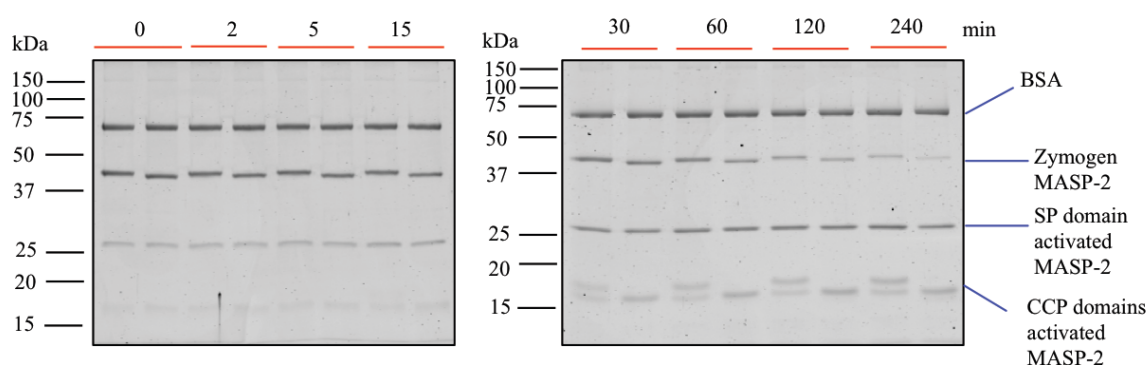
Figure 4.12: Activation of the MASP-2 D371Y S618A zymogen by MASP-2. A) Graph documenting the amount of cleavage of zymogen wild-type (CCP12SP Cys S618A), and D371Y MASP-2 (CCP12SP Cys D371Y S618A). Time points of 0, 2, 5, 15, 30, 60, 120 and 240 min were selected for the reaction to be ended using reducing SDS loading buffer. B) SDS-PAGE results for activation of zymogen wild-type MASP-2 and zymogen MASP-2 D371Y by MASP-2. Lanes 1, 3, 5, 7, 9, 11, 13 and 15 show the activation of zymogen wild-type MASP-2 and Lanes 2, 4, 6, 8, 10, 12, 14 and 16 show the activation of zymogen MASP-2 D371Y. The disappearance of the zymogen band was then analysed using densitometry, with BSA acting as a loading control.

A)

B)
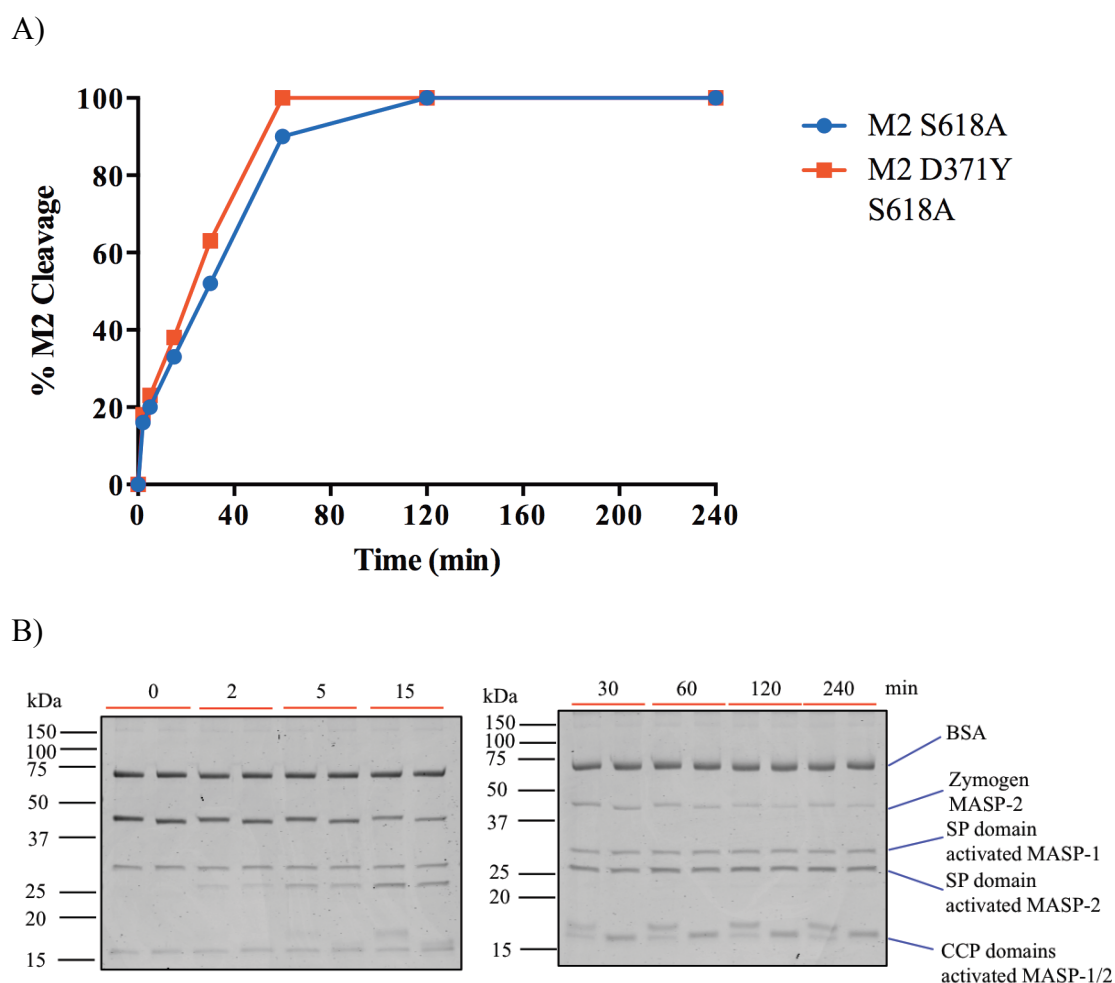
Figure 4.13: Activation of the MASP-2 D371Y S618A zymogen by MASP-1. A) Graph documenting the amount of cleavage of zymogen wild-type (CCP12SP Cys S618A), and D371Y MASP-2 (CCP12SP Cys D371Y S618A). Time points of 0, 2, 5, 15, 30, 60, 120 and 240 min were selected for the reaction to be ended using reducing SDS loading buffer. B) SDS-PAGE analysis for activation of zymogen wild-type MASP-2 and zymogen MASP-2 D371Y by MASP-1. Lanes 1, 3, 5, 7, 9, 11, 13 and 15 show the activation of zymogen wild-type MASP-2 and Lanes 2, 4, 6, 8, 10, 12, 14 and 16 show the activation of zymogen MASP-2 D371Y. The disappearance of the zymogen band was then analysed using densitometry, with BSA acting as a loading control.

4.9 Discussion

The aim of this study was to investigate the role of the MASP-2 mutant D371Y and to attempt to ascertain the potential reason for this mutation being linked to a number of diseases. The mutant refolded and purified in similar manner to wild-type MASP-2, and work with the peptide substrate C4 P4-P4' showed that the MASP-2 D371Y mutant

obtained similar $K_{0.5}$ and k_{cat} values to wild-type MASP-2. This provides an indication that the mutation does not have a deleterious effect on MASP-2 folding, as improper folding would likely have led to active site disruption. Full confirmation of the impact of the mutation on MASP-2 folding and structural stability could be ascertained through methods such as circular dichroism (CD) or differential scanning calorimetry (DSC), but the present work indicates that impacted folding is perhaps not the cause of the D371Y mutation's link to increased susceptibility to certain diseases.

As discussed earlier, it has been postulated that the mutation could potentially create modifications to the substrate specificity of MASP-2 (Tulio et al., 2011). The data obtained, however, demonstrates that the D371Y mutant did not affect either the C4 or C2 cleavage efficacy of MASP-2, as the EC_{50} values and cleavage time courses for each substrate indicated no difference between wild-type MASP-2 and MASP-2 D371Y. Work on the D371A mutant in Chapter 3 also showed that mutation of the 371 residue to alanine did not affect C4 cleavage efficacy, with the EC_{50} value of the mutant not being significantly different from that obtained by wild-type MASP-2. The results obtained suggest that a reduction in C2 and C4 cleavage efficacy is not the reason that leads to this mutation being linked to susceptibility to certain diseases. The results obtained through SPR also confirmed the EC_{50} values and cleavage time course results obtained, as no difference in binding to C4 was seen between wild-type MASP-2 and the MASP-2 D371Y mutant. These results are perhaps not unsurprising, as residue 371 is located on the periphery of the CCP domain binding exosite, nor does it appear to make any contacts with C4 according to crystal structures (Kidmose et al., 2012). It is also unsurprising that C2 cleavage is unaffected by the mutation, as past studies indicate that the CCP domains of MASP-2 do not play a role in the cleavage of C2, only the SP domain (Rossi et al., 1998, Ambrus et al., 2003, Duncan et al., 2012a).

Given that C2 and C4 cleavage were shown to be unaffected by the D371Y mutation, another potential area that could be deleteriously impacted by the mutation was the activation of the enzyme, either by MASP-1 or MASP-2. It was believed for some time that activation of MASP-2 was achieved through autoactivation alone, and that activation of MASP-2 was the minimum requirement for lectin pathway activation (Vorup-Jensen et al., 2000, Ambrus et al., 2003, Chen and Wallis, 2004). However, recent research has found that MASP-1 is in fact the primary activator of MASP-2 (Heja et al.,

2012b, Megyeri et al., 2013). To investigate this, we examined the activation of zymogen MASP-2 D371Y and zymogen wild-type MASP-2 by MASP-2 and MASP-1 through an activation time course. From the time course, it appears that the D371Y mutation does not impact activation of MASP-2 by either MASP-1 or MASP-2, as the mutant recorded similar levels of activation as the wild-type MASP-2. This indicates that the mutation is not affecting activation of MASP-2 by either MASP-1 or MASP-2, and so is unlikely to be the cause of this mutation's link to increased susceptibility to certain diseases. The SP domain and CCP domains of the zymogen MASP-2 D371Y appeared to run slightly differently to that of zymogen wild-type MASP-2 in the assay. DNA sequencing confirmed both constructs had correct sequencing, and when the constructs were activated overnight on a Hi-Trap NHS column lined with wild-type MASP-2, both ran in the same manner upon SDS-PAGE analysis as was seen in the assays. It is therefore unlikely that the construct was being cleaved at any other point other than the MASP-2 Arg-Ile activation cleavage point. To confirm that cleavage is occurring in the correct location, mass spectrometry and N-terminal sequencing could be carried out upon the CCP and SP domains of the constructs.

From the results collected, it appears that the MASP-2 D371Y mutation does not have a detrimental impact upon active site stability, binding and cleavage of either C4 or C2, nor activation of MASP-2 by either MASP-1 or MASP-2. The mutation may instead be exerting an influence on an interaction outside of the complement pathway. Research over the last few decades has shown that the complement cascade does not act in isolation. It is known to have links to many different aspects of the adaptive and innate immune system (i.e. Toll-Like Receptor pathways, T and B-cell differentiation and functioning), as well as links to the coagulation system, apoptotic pathways and more (Kolev et al., 2014). Therefore, the impacts of this mutation on MASP-2 function may be seen outside of the complement system.

Outside of complement, MASP-2 is known to play a role in the coagulation system. MASP-2 has been shown to be capable of activating prothrombin to form thrombin in a similar manner to factor Xa, with the thrombin then able to activate its two main protein substrates- fibrinogen and factor VIII, which lead to clot formation (Krarup, A., *et al.* 2007). It has also been shown that complexes of MASP-1 and MASP-2 with either L-ficolins or MBL are capable of generating clots when incubated with calcified

plasma or purified fibrinogen and Factor VIII (Gulla et al., 2010). It has been proposed that MASP-1 is capable of cleaving fibrinogen and factor VIII, and that cleavage of fibrinogen produces both fibirin and the formation of chemotactic fibrinopeptides, which attract neutrophils to the area of infection (Hajela et al., 2002, Krarup et al., 2008). Now that it is known that MASP-1 activates MASP-2, a cycle of amplification can be seen to increase immune cell recruitment and coagulation in the area of infection. MASP-1 activates MASP-2, which then is able to activate prothrombin to thrombin, which leads to more fibrinogen and Factor VIII cleavage, in addition to the fibrinogen and factor VIII cleavage by MASP-1. This leads to the formation of more chemotactic fibrinopeptides to attract neutrophils, as well as localised coagulation in the area of infection. This localised coagulation may lead to reduced infection spread. In mice, fibrinogen deficient mouse models have been shown to succumb to doses of *Listeria monocytogenes* that genetically matched control mice survive (Mullarky et al., 2005). Fibrin(ogen) was shown to limit growth of *L. monocytogenes* in infected hepatic tissue, and was shown to aid clearance of *Staphylococcus aureus* from the peritoneal cavity (Mullarky et al., 2005). There is potential that mutation of residue 371 interferes with MASP-2 binding and/or cleavage of prothrombin to thrombin, and that this may increase the risk of the infection spreading by reducing the amount of coagulation occurring at the site of infection, as well as reducing fibrinopeptide recruitment of other immune cells, such as neutrophils. This would lead to an increased susceptibility to infection, such as seen with Hepatitis C, HTLV-1 infection and development of clinically significant infection after orthotopic liver transplantation (de Rooij et al., 2010, Tulio et al., 2011, Coelho et al., 2013).

Another important aspect of MASP-2 cleavage of prothrombin to thrombin is that thrombin has itself been found to cleave complement components C3 and C5 into active fragments (Huber-Lang et al., 2006). As well as their important contributions to the complement cascade, C3 and C5 have been found to have further roles in establishing an adaptive immune response. Two products of C3 and C5 cleavage, C3a and C5a, have been shown to induce and/or amplify complement mediated receptor effects by the receptors C3aR and C5aR1 respectively, which are expressed by Antigen-Presenting Cells (APCs), such as dendritic cells and macrophages (Kolev et al., 2014). APCs play an important role in determining optimal T-cell activation and lineage development. Activation of the C3aR and C5aR1 receptors through C3a and C5a has been shown to induce or supress IL-12 release, with IL-12 being required for the formation of a T Helper 1 (T_H1) response, and

not for a T Helper 2 (T$_H$2) response (Strainic et al., 2008, Strainic et al., 2013, Van der Touw et al., 2013). T$_H$1 responses help in the clearance of intracellular pathogens. Whether IL-12 production is suppressed or induced appears to depend on the disease model, the route of delivery of the antigen to be opsonized and the maturation status of the APC (Droiun et al., 2002, Hawslich et al., 2004, Kawamoto et al., 2004, Hawslich et al., 2005). Therefore, if the D371Y mutation affected the ability of MASP-2 to bind and/or cleave prothrombin into thrombin, the ability to launch an appropriate adaptive immune response against the pathogen could be compromised, thus leading to an increased susceptibility to disease.

From the above discussion, it can be seen that if the D371Y mutation alters MASP-2 binding and/or cleavage of prothrombin, it could potentially lead to a reduced immune response to infection, or lead to an inappropriate adaptive immune response, thus increasing susceptibility to infection and reducing the ability of the immune system to clear it. However, it is worth reiterating that the results from this chapter show that the MASP-2 D371Y mutant is able to bind and cleave C2 and C4 in a manner similar to that of wild-type MASP-2. Therefore, when confronted with an invading pathogen, the complement pathway should function in a normal manner. If the complement pathway and the other aspects of innate immunity are unable to clear the infection, an adaptive immune response will be required to do so. However, if the adaptive immune response is compromised, such as could happen if the MASP-2 D371Y mutant has a negative impact on MASP-2 binding and/or cleavage of prothrombin to thrombin, thus reducing thrombin cleavage of C3 and C5, which in turn then reduces IL-12 expression stimulated by the C3aR and C5aR1 receptors, the infectious pathogen could remain uncleared. This would give the pathogen a greater chance to increase in number and spread. This potentially could lead to increased levels of inflammation in the body, as various aspects of innate immunity, such as the complement pathway, would continue to be triggered through the presence of the pathogen. Increased levels of inflammation have been shown to contribute to the development of cardiovascular and cerebrovascular diseases (Carter, 2005, Libby et al., 2009). Indeed, inflammation plays an important role in both the development and progression of RHD and CCC (Beltrame et al., 2014, Cunha-Neto and Chevillard, 2014.). In addition, continual complement activation could lead to complement-induced damage to the host. Over the years there has been increasing evidence supporting a link between the lectin pathway, in particular MBL, and the development of RHD due to damage

caused by complement activation (Schafranksi et al., 2004, Messias Reason et al., 2006, Beltrame et al., 2014). Therefore, if the MASP-2 D371Y mutant compromises the adaptive immune response by being unable to bind and/or cleave prothrombin, the increased levels of inflammation and damage caused by complement activation by the uncleared pathogen may increase the risk of complications, such as the development of RHD and CCC.

In conclusion, this study found that despite being linked to increased susceptibility to certain infectious diseases, the MASP-2 D371Y mutation does not impact the ability of MASP-2 to bind and cleave C2 and C4 in an efficient manner, nor does it impact activation of MASP-2 by MASP-1 or MASP-2. It therefore appears that if the mutation has an impact on MASP-2, it will be on the role of MASP-2 outside of the complement system, with the binding and/or cleavage of prothrombin perhaps the most likely candidate.

Chapter 5

'Investigation into the role of the MASP-2 SP domain binding exosite in the kinetic mechanism of interaction between MASP-2 and its substrate C4'

5.1 Introduction

As discussed in previous chapters, for many years, it was thought that a binding exosite for C4 existed on the CCP domains of MASP-2. However, it was thought unlikely that there was any C4 binding exosites located on the SP domain of MASP-2. Studies done at the time indicated there was no C4 binding exosite on the SP domain of MASP-2, with blocking of the active site by the synthetic peptide inhibitor EGRck appearing to remove the ability of the MASP-2 SP domain construct to bind to C4 (Duncan et al., 2012a). In the studies performed by Rossi *et al*. (2005), domain swapping between C1s and MASP-2 appeared to show that the CCP domains of MASP-2 were the most likely to house a C4 binding exosite, not the SP domain (Rossi et al., 2005).

However, the potential for there to be a C4 binding exosite on the SP domain of C4 was reinvigorated by the discovery of a C4 binding exosite on the SP domain of C1s (Duncan et al., 2012b). The work done suggests that the residues of this exosite interact with a string of sulfated tyrosines on C4, as anti-sulfotyrosine antibodies showed strongly inhibited binding to the C4 sulfated tyrosine residues in the presence of C1s (Duncan et al., 2012b). Following this, the release of the structure of MASP-2 and C4 in complex a few months later structurally demonstrated that, in addition to a CCP domain binding exosite for C4, MASP-2 also contained another potential C4 binding exosite, located on the SP domain of MASP-2 (Figure 5.1) (Kidmose et al., 2012). In this structure, the residue K503 was shown to be interacting with the C4 sulfated tyrosine residue 1417 (Figure 5.1). Residues K450, R578 and R583 of MASP-2 were all found to interact with residue D1419 of C4. Although the structure does not show these residues directly interacting with the sulfated tyrosines of C4 (residues 1417, 1420 and 1422), they potentially do interact with them in different complex confirmations other than that shown in the structure. This in particular applies to residue 1422- this sulfated tyrosine residue was not shown in the structure, and so its interactions with MASP-2 are as of yet unknown.
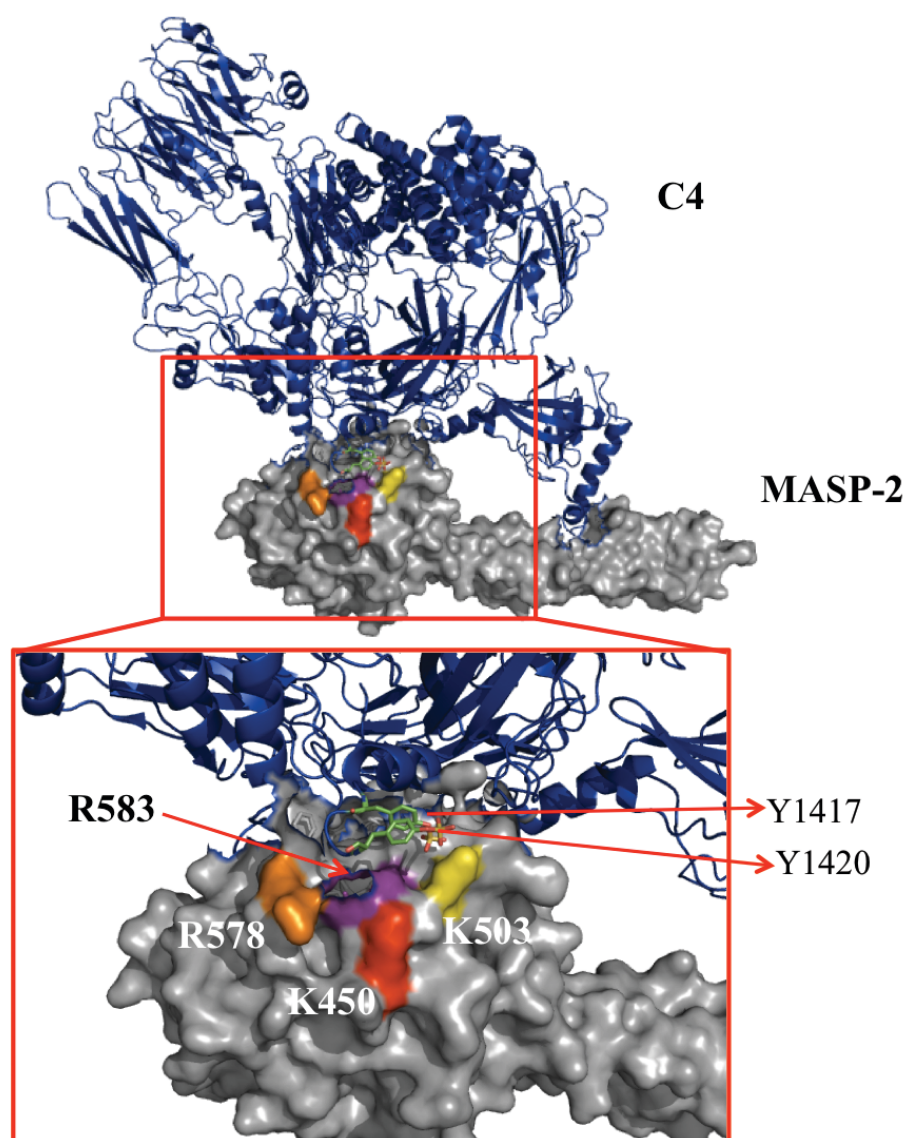
Figure 5.1: The potential SP domain binding exosite of MASP-2. This exosite consists of the MASP-2 residues K450 (red), K503 (yellow), R578 (orange) and R583 (purple). The sulfated tyrosine residues of C4, of which Y1417 and Y1420 are visible in the structure, are thought to interact with the exosite, and are depicted as green sticks. The MASP-2 molecule is in grey, while C4 is blue. Image generated using PDB file 4FXG (DOI: 10.2210/pdb4fxg/pdb).

In the paper, Kidmose *et al.* (2012) identified K450, K503, R578 and R583 as potential components of an SP domain binding exosite for C4 on MASP-2, but no work was carried out to determine if this was the case (Kidmose et al., 2012). Therefore, the aims of this study were to determine if these four residues do in fact comprise an SP binding exosite for C4, and to characterise the contribution of each residue to the kinetic mechanism of the interaction between this potential MASP-2 SP domain binding exosite and C4. In order to do this, a number of neutral charge mutants of the four residues were

produced and subjected to a series of kinetic tests to determine and measure any potential effect the mutation may have upon the binding and cleavage of C4 by MASP-2. Following this, the ability of selected mutants of the SP domain binding exosite to bind C4 were examined using Surface Plasmon Resonance (SPR).

5.2 Materials and Methods

Please refer to Chapter 2 for the protocols relevant to the experiments carried out in this chapter.

5.3 Selection of MASP-2 SP domain exosite mutations

To examine the potential SP domain exosite highlighted in the MASP-2/C4 complex structure, four residues were selected for mutation- K450, K503, R578 and R583 (Figure 5.2). These residues were implicated by Kidmose *et al.* (2012) as although only the K503 residue was shown to interact with one of the sulfated tyrosine residues of C4 (Y1417), it appears K450, R578 and R583 could also potentially interact with the other sulfated tyrosines (Y1420 and Y1422) in other conformational states between MASP-2 and C4. Therefore, all were selected to undergo glutamine-scanning mutagenesis.

In addition to the above mutants, based upon data gathered for the single mutants and work with the CCP domain exosite, a double mutant (MASP-2 CCP12SP Cys R578Q R583Q), and a triple mutant (MASP-2 CCP12SP Cys K503Q R578Q R583Q) were produced (Table 5.1). In order to observe the effect of impacting both exosites simultaneously on MASP-2 binding and cleavage of C4, a quadruple mutant, where the double mutants from the CCP and SP exosites were mutated simultaneously was also created (MASP-2 CCP12SP Cys E333Q D365N R578Q R583Q) (Table 5.1).

Table 5.1: Table of MASP-2 SP domain exosite mutants to be examined

SP domain exosite mutants
K450Q
K503Q
R578Q
R583Q
R578Q R583Q
K503Q R578Q R583Q
E333Q D365N R578Q R583Q
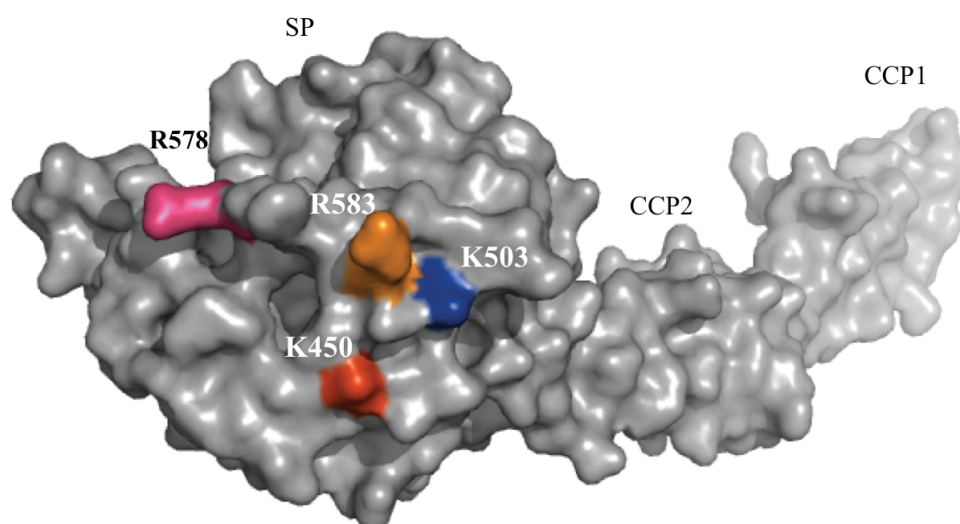
Figure 5.2: MASP-2 SP domain exosite mutant locations. Residue K450 is in red, K503 in blue, R578 in magenta and R583 in orange. The CCP1 domain is in teal, the CCP2 domain in pink and the SP domain in yellow. Image generated using PDB file 1ZJK (DOI: 10.2210/pdb1zjk/pdb).

5.4 Production and characterisation of MASP-2 SP domain exosite mutants

As discussed in Chapter 3, all mutants were created on a MASP-2 construct featuring an additional free cysteine residue on the N-terminus of the protein. All mutants that were selected for examination through SPR also had an additional construct produced, where the catalytic serine (S618, or S195 in chymotrypsin numbering) was mutated to an alanine (S618A). The protease was extracted from the inclusion bodies, denatured, refolded, dialysed and purified under similar conditions to those described previously (Ambrus et al., 2003, Duncan et al., 2012b). The amount of enzyme recovered for the various mutations ranged from 0.1-0.6 mg/ml per litre of *E. coli* culture. Each of the mutants purified in a similar manner to the wild type MASP-2 CCP12SP construct, being eluted in the same peaks when purified using an anion-exchange Q-Sepharose column and a Superdex 75 16:60 gel filtration column.

SDS-PAGE analysis confirmed that all the mutants purified to homogeneity. All of the active mutants were able to autoactivate during purification upon the Q-Sepharose column, which was confirmed upon SDS-PAGE gel analysis. Under reducing conditions, activated MASP-2 runs as two fragments: the SP domain at ~28 kDa and the CCP domains at ~17 kDa (Figure 5.3). This indicates that cleavage of the Arg-Ile bond of the protease was complete. Zymogen MASP-2 runs as a single fragment in reducing conditions at ~ 44 kDa. Each mutant was incubated with a molar excess of the serpin, C1-INH, to confirm the active concentration of each mutant. All mutants reacted with C1-INH at a 1:1 ratio of protease: serpin, confirming that the proteases were fully active.
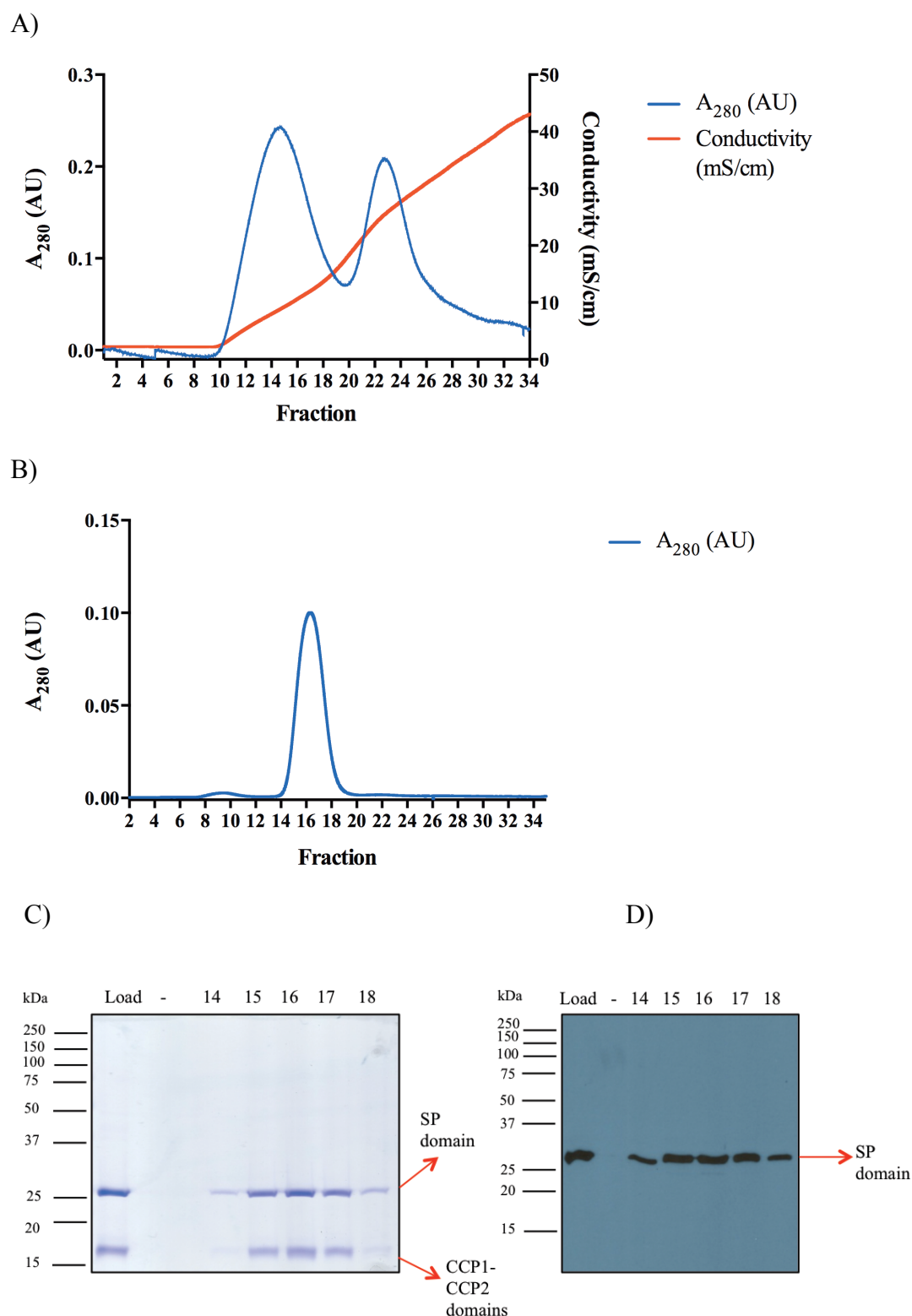
Figure 5.3: Purification of MASP-2 CCP12SP Cys E333Q D365N R578Q R583Q. A) The purification profile of the quadruple MASP-2 mutant from anion-exchange chromatography on QFF-Sepharose:. MASP-2 was eluted in the second peak. B) The gel filtration chromatography profile of the quadruple MASP-2 CCP12SP mutant C) SDS-PAGE analysis of quadruple MASP-2 mutant after gel filtration chromatography, with a corresponding Western blot using a peptide antibody directed against the SP domain of MASP-2 (D). The antibody used on the Western blot is targeted to the SP domain of MASP-2. Samples were reduced prior to SDS-PAGE analysis.

5.5 Testing the active site integrity of MASP-2 SP domain exosite mutants

When mutating residues in MASP-2, particularly in the SP domain, there is always the potential of destabilising the active site, which would affect the ability of MASP-2 to cleave C4. To ensure that any results generated were due to the mutations created, and not due to instability of the active site, each MASP-2 mutant was assayed for cleavage of the C4 peptide substrate C4 P4-P4' [2Abz-GLQRALEI-Lys(Dnp)-NH$_2$]. This peptide mimics the cleavage site on C4 for MASP-2. For the assays, a final concentration of 10 nM of each MASP-2 mutant was used against varying concentrations of C4 P4-P4' peptide, ranging from 0-100 µM. From the results, it appears that the mutations do not change the active site of MASP-2, as the $K_{0.5}$ values of all mutants were similar to that obtained for the wild-type MASP-2 enzyme (Table 5.2). The k_{cat} values obtained for wild-type MASP-2 and each mutant were also quite similar, and were within the range of k_{cat} values found for MASP-2 with this peptide in previous experiments (Table 5.2) (Duncan et al., 2012a). It therefore appears that any changes in C4 binding and cleavage exhibited by the mutants reflect the effect of the mutation upon C4 binding and cleavage and are not caused by changes to active site integrity.

Table 5.2: Comparison of the kinetics of cleavage of the synthetic peptide C4 P4-P4' by SP domain exosite mutants

M2 form	$K_{0.5}$ (µM)	k_{cat} (s^{-1})	$k_{cat}/K_{0.5}$ (M^{-1}·s^{-1})
WT	9.08 ± 0.7	0.35	3.8 x 10^4
K450Q	13.4 ± 1.5	0.53	3.9 x 10^4
K503Q	8.8 ± 0.7	0.31	3.5 x 10^4
R578Q	10.3 ± 1.4	0.38	3.7 x 10^4
R583Q	8.3 ± 0.8	0.39	4.7 x 10^4
R578Q R583Q	15.8 ± 1.0	0.33	2.1 x 10^4
K503Q 578Q R583Q	13.5 ± 1.2	0.34	2.5 x 10^4
E333Q D365N R578Q R583Q	10.1 ± 0.5	0.27	2.7 x 10^4

5.6 Investigation into the C4 cleavage efficiency of the MASP-2 SP domain exosite mutants

As discussed in Chapter 3, the protocol required to allow the determination of EC_{50} values in examining C4 cleavage efficacy needed some adjustments due to the differing kinetic parameters of the interaction between MASP-2 and C4, as compared to C1s and C4. Initially, EC_{50} values were determined using 100 nM C4, as was done with the CCP domain exosite mutants. The results showed that the single mutants K450Q and K503Q recording EC_{50} values that were not significantly different from wild-type MASP-2, indicating that these mutations were not affecting the ability of MASP-2 to bind and cleave C4 efficiently (Table 5.3). However, the single mutants R578Q and R583Q showed some EC_{50} values that were significantly different from wild-type MASP-2, and some that were not (Table 5.3). This was unlike in Chapter 3, where mutants consistently displayed EC_{50} values significantly different or similar to that of wild-type MASP-2.

This gave rise to concerns that even the reduction of C4 concentration to 100 nM was not enough for us to be examining first-order kinetics in the assay, and that this meant that the protocol was not sensitive enough at this concentration of C4. However, the concentration of C4 could not be lowered any further if Coomassie blue staining was to be used, due to the limits of sensitivity for this stain. In order to rectify this, Sypro Ruby stain was used instead. Due to the high sensitivity of the Sypro Ruby stain, this allowed us to reduce the amount of C4 to a final concentration of 25 nM, which is well below the 58 nM K_M value of MASP-2 for C4 (Duncan et al., 2012a).

Table 5.3: MASP-2 SP domain exosite mutant C4 EC_{50} values using 100 nM C4

M2 form	Mutant analysis 1 (nM)	WT analysis 1 (nM)	Mutant analysis 2 (nM)	WT analysis 2 (nM)	Mutant analysis 3 (nM)	WT analysis 3 (nM)
K450Q	0.18	0.23	0.38	0.47	-	-
K503Q	0.30	0.50	0.30	0.49	-	-
R578Q	*0.64*	*0.31*	0.29	0.89	0.66	0.60
R583Q	*0.57*	*0.26*	*0.58*	*0.21*	0.88	0.44

Mutants with significant alterations in EC_{50} value are bolded and italicised.

Table 5.4: MASP-2 SP domain exosite mutant C4 EC_{50} values using 25 nM C4

M2 form	Mutant analysis 1 (nM)	WT analysis 1 (nM)	Mutant analysis 2 (nM)	WT analysis 2 (nM)	Mutant analysis 3 (nM)	WT analysis 3 (nM)
K450Q	0.24	0.21	0.21	0.45		
K503Q	0.57	0.56	0.68	0.45		
R578Q	*0.82*	*0.26*	*1.44*	*0.65*		
R583Q	*0.74*	*0.39*	*0.84*	*0.34*		
R578Q R583Q	*11.7*	*0.41*	*9.3*	*0.68*	*8.4*	*0.65*
K503Q R578Q R583Q	*19.63*	*0.21*	*17.90*	*0.63*		
E333Q D365N R578Q R583Q	*412.80*	*0.20*	*390.70*	*0.57*	*649.40*	*0.45*

Mutants with significant alterations in EC_{50} value are bolded and italicised.

Using 25 nM C4, both the R583Q and R578Q mutants displayed consistently impaired cleavage, with an increase in EC_{50} values of ~2 to 3-fold for the R578Q mutant and 1.9-2.5-fold increases in EC_{50} values for the R583Q mutant (Table 5.4). The K450Q and K503Q mutants still displayed no significant differences in EC_{50} value from wild-type MASP-2 (Table 5.4). In light of this information, the MASP-2 SP domain exosite double mutant (MASP-2 CCP12SP Cys R578Q R583Q) was created. This double mutant shows greatly impaired C4 cleavage efficiency, with a ~ 13-28-fold increase in EC_{50} value over that of wild-type MASP-2 (Table 5.4).

Given that the K503 residue is known to interact with the sulfated tyrosine residue 1417 of C4 (Kidmose et al., 2012), it was surprising that mutation of this residue caused no effect on C4 cleavage efficacy. A triple mutant (MASP-2 CCP12SP Cys K503Q R578Q R583Q) was therefore created to investigate if this held true when this residue was mutated in addition to the two residues already shown to impact C4 cleavage efficiency. From the EC_{50} values obtained, mutation of the K503 residue caused the EC_{50} value to increase by less than 2-fold over the EC_{50} value obtained by the double mutant, so it appears that this residue does not play a significant role in ensuring efficient C4 cleavage (Table 5.4).

Using the information gathered from the EC_{50} values on the CCP and SP domain exosites, a quadruple mutant was created by combining the double mutants of the CCP and SP domain exosites (MASP-2 CCP12SP Cys E333Q D365N R578Q R583Q). Creating this mutant allowed us to investigate how impacting the CCP and SP domain exosites simultaneously affected the C4 cleavage efficacy of MASP-2. The assays showed that simultaneously impacting both exosites indeed had a deleterious effect on the ability of MASP-2 to cleave C4, with the quadruple mutant showing an increase in EC_{50} values of between 680 to 2000-fold compared to that of wild-type MASP-2 (Figure 5.4 and Table 5.4). This information suggests that the effects of the exosites upon C4 cleavage by MASP-2 are cumulative- while removal of one exosite leads to moderately affected C4 cleavage efficiency, removal of both leads to a severe reduction in C4 cleavage.
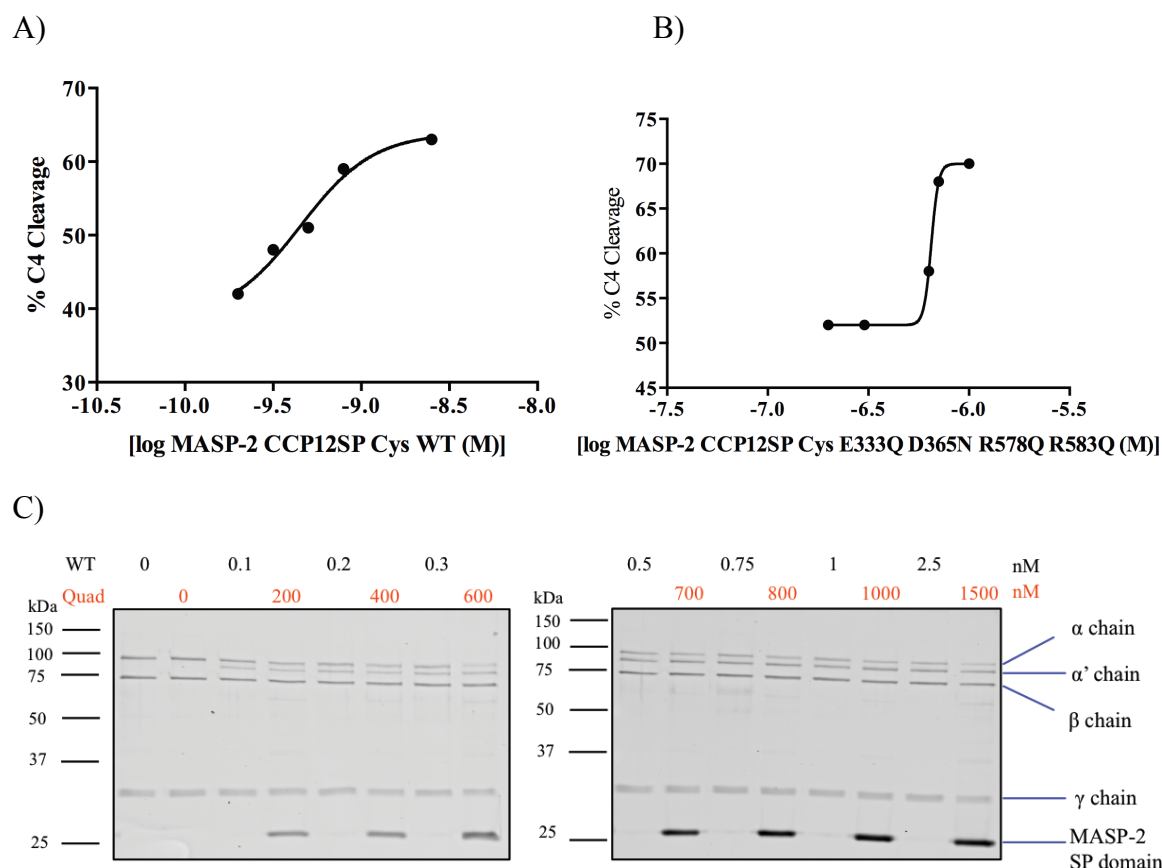
Figure 5.4: Determination of EC_{50} values for cleavage of C4 by the MASP-2 quadruple mutant MASP-2 CCP12SP Cys E333Q D365N R578Q R583Q. A) EC_{50} response curve of MASP-2 CCP12SP Cys WT. B) EC_{50} response curve of MASP-2 CCP12SP E333Q D365N R578Q R583Q. C) SDS-PAGE analysis depicting C4 cleavage by both MASP-2 CCP12SP Cys WT and the MASP-2 quadruple mutant (Quad – concentrations values in red). C4 was used at 25 nM, with wild-type MASP-2 concentrations from 0-2.5 nM (in black), and the MASP-2 quadruple mutant using a concentration range of 0-1500 nM (in red). The reaction was ended at 30 min with reducing SDS-PAGE loading buffer.

5.7 Investigations into the time course of C4 cleavage by MASP-2 SP domain exosite mutants

From the data obtained from the EC_{50} values, further investigations were carried out into how each of the SP domain exosite mutations affected the ability of MASP-2 to cleave C4 over a period of 2 h.
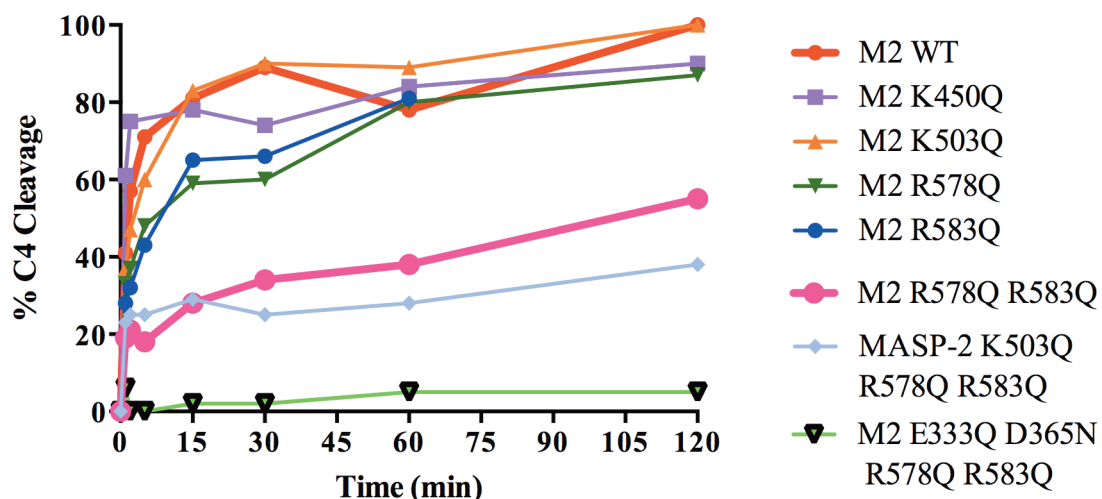
Figure 5.5: C4 cleavage time course for MASP-2 SP domain exosite mutants. Timepoints of 0, 1, 2, 5, 15, 30, 60 and 120 min were selected. The α chain of C4 was analysed using densitometry, with the C4 γ chain used as a loading control.

Much like the CCP domain exosite mutants discussed in Chapter 3, the SP domain exosite domain mutants showed time courses for C4 cleavage that correlated well with the EC_{50} values obtained. Displaying unaffected EC_{50} values, the K450Q and K503Q single mutations showed little impact upon C4 cleavage during the time course, recording results similar to that of wild-type MASP-2 (Figure 5.5). The R578Q and R583Q single mutants, both of which revealed reduced EC_{50} values compared to wild-type MASP-2, showed altered C4 cleavage during the time courses, only reaching similar levels of cleavage as the wild-type after an hour (Figure 5.5). The SP domain exosite double mutant MASP-2 R578Q R583Q showed significantly impacted C4 cleavage, reaching only ~ 55% cleavage of C4 in 2 h (Figure 5.5). Compared to the double mutant, the SP domain exosite triple mutant MASP-2 K503Q R578Q R583Q recorded a slightly more impacted time course of C4 cleavage, reaching ~ 40% cleavage in 2 h (Figure 5.5). The quadruple mutant MASP-2 E333Q D365N R578Q R583Q, where both the CCP and SP domain exosites were impacted, showed severely reduced C4 cleavage over the time course, barely reaching 10% cleavage even after 2 h (Figures 5.5 and 5.6). This correlates with the EC_{50} values obtained, as the quadruple mutant obtained EC_{50} values over 600-fold greater than those achieved by wild-type MASP-2.
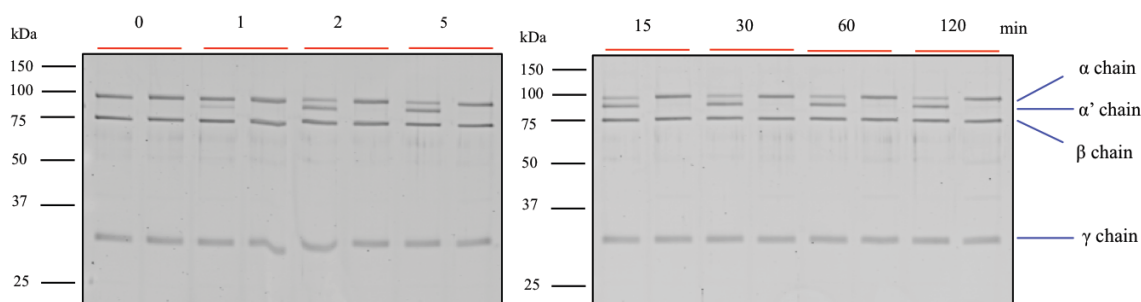
Figure 5.6: Time course for C4 cleavage by the MASP-2 quadruple mutant E333Q D365N R578Q R583Q. Time points of 0, 1, 2, 5, 15, 30, 60 and 120 min were selected, with each reaction ended using reducing SDS loading buffer. The α chain of C4 was analysed using densitometry, with the C4 γ chain used as a loading control.

5.8 Analysis of the contribution of the MASP-2 SP domain exosite to C4 binding using Surface Plasmon Resonance (SPR)

5.8.1 Selection of MASP-2 mutants to undergo SPR and their activation

In Chapter 3, the double CCP domain exosite mutant MASP-2 CCP12SP Cys E333Q D365N was selected to undergo further examination using SPR. For further study of the SP domain exosite's contribution to C4 binding, the double mutant MASP-2 CCP12SP Cys R578Q R583Q was selected for examination using SPR. In addition, the quadruple mutant (MASP-2 CCP12SP Cys E333Q D365N R578Q R583Q) was also selected to be examined using SPR to allow us to study how impacting both exosites simultaneously would affect the ability of MASP-2 to bind C4. As per previous protocol (see Chapter 3), catalytically inactive constructs of each mutant were made through mutation of the catalytic serine (MASP-2 CCP12SP Cys R578Q R583Q S618A and MASP-2 CCP12SP Cys E333Q D365N R578Q R583Q S618A).

Due to the mutation of the catalytic serine, the MASP-2 constructs could not autoactivate. Therefore, all MASP-2 constructs used in SPR studies required manual activation. Each variant was placed onto a column lined with active wild-type MASP-2 CCP12SP, and incubated at 26°C overnight in a pH 7.0 buffer. They were eluted the next day with the same buffer, but at pH 6.0. When analysed using SDS-PAGE under reducing conditions, the activated MASP-2 migrated in two bands under reducing conditions (Figure 5.7). The SP domain migrates as a band at ~28 kDa, while the CCP1-CCP2 domains form a band at ~17 kDa (Figure 5.7). This indicated that cleavage at the Arg/Ile

134

bond of the protease had occurred. Zymogen MASP-2 exhibits a single ~44 kDa band under reducing conditions (Figure 5.7).
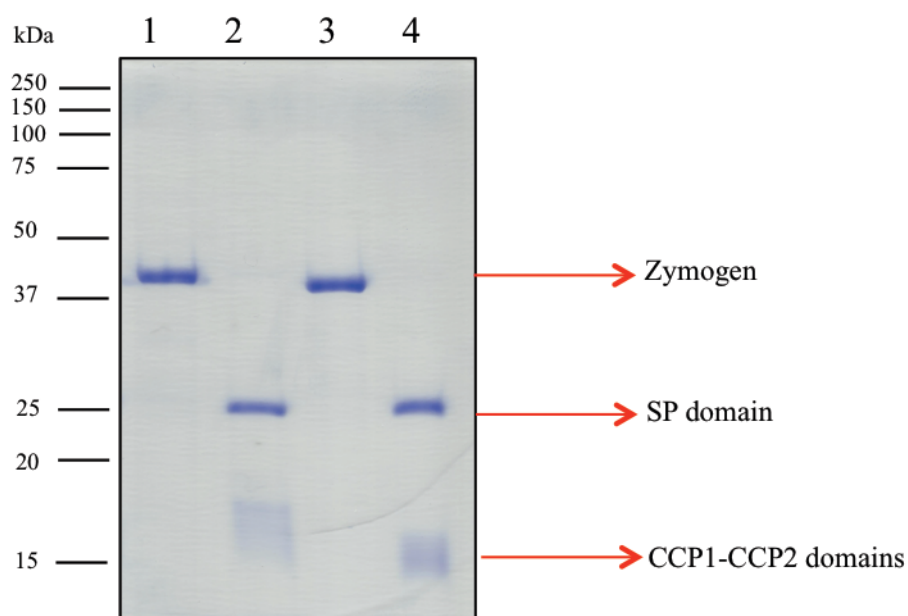
Figure 5.7: The activation of the MASP-2 variants used in SPR. Lane 1 shows the zymogen form of the double SP domain exosite mutant MASP-2 CCP12SP Cys R578Q R583Q S618A, while Lane 2 shows the activated form of the enzyme. Lane 3 shows the zymogen form of the quadruple mutant MASP-2 CCP12SP Cys E333Q D365N R578Q R583Q S618A, while Lane 4 shows its activated form. All samples were reduced prior to electrophoresis.

5.8.2 Analysis of the ability of selected MASP-2 SP domain exosite mutants to bind C4 using Surface Plasmon Resonance (SPR)

5.8.2.1 Steady-state affinity and its application to the binding interaction between MASP-2 and C4

As done in Chapter 3 with the MASP-2 CCP domain exosite, and in previous work completed in the laboratory (Perry et al., 2013), the data gathered allowed the affinity of the interaction to be examined using the steady-state affinity model, using the equation $R_{eq} = K_A C R_{max}/K_A C+1$, where R_{eq} is the equilibrium response level, C is the concentration of analyte, and K_A is the equilibrium association constant calculated by fitting a plot of R_{eq} against analyte concentration (Figure 5.8 and Table 5.5). This allowed us to obtain the dissociation constant value (K_D) for the binding of each MASP-2 variant to C4.

Activated wild-type MASP-2 yielded a K_D value of 82.6 nM (Table 5.5). The SP domain exosite double mutant was severely affected, with a K_D of 518 nM, showing a ~6-

fold increase in K_D value over that obtained by wild-type MASP-2 (Table 5.5). This is an increase slightly less than that caused by the CCP domain exosite double mutant, which caused a 10-fold increase in K_D. Interestingly, the quadruple mutant was shown to be unable to bind C4 (Table 5.5). These results indicate that the SP domain exosite of MASP-2 is crucial in promoting efficient binding to C4, just as the CCP domain exosite was found to be in Chapter 3. It also appears that these exosites influence C4 binding by MASP-2 in a cumulative manner, as impacting both exosites simultaneously abolished MASP-2 binding to C4. This impact on C4 binding would contribute to the steep reduction in C4 cleavage efficacy recorded by the quadruple mutant in the EC_{50} assays and C4 cleavage time course analysis.

Table 5.5: Steady-state K_D values for MASP-2 R578Q R583Q and MASP-2 E333Q D365N R578Q R583Q

M2 form	K_D (nM)
S618A n = 9	82.6 ± 6.5
SP exosite n = 10	517 ± 36.2
Quadruple mutant n = 3	*nb*

nb= no binding

136

A)

B)
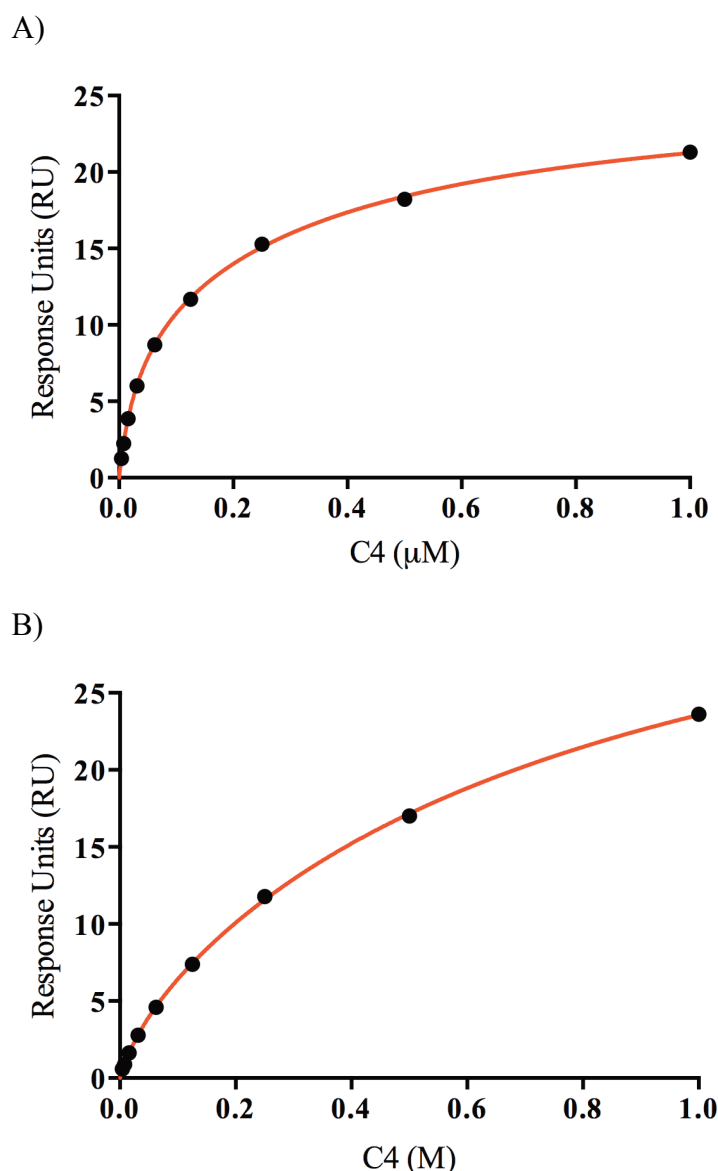
Figure 5.8: Analysis of binding of A) MASP-2 CCP12SP Cys S618A and b) MASP-2 CCP12SP Cys R578Q R583Q S618A to C4 using fitting to a steady-state equation. The binding of both mutants to C4 was examined over a concentration range of 0-1 μM C4.

5.8.2.2 A two-state binding model and its application to the binding interaction between MASP-2 and C4

As done in Chapter 3, and in previous work in the laboratory (Perry, A., *et al.* 2013), a two-state binding model was used to fit the data in order to obtain the kinetic constants for C4 binding by MASP-2 (Figure 5.9 and Table 5.6). In this model, the equation M2 + C4 ⇆ M2:C4 ⇆ M2*C4, where the initial complex (M2:C4) is converted to a higher affinity complex (M2*C4) due to conformational change, is used. Use of the

two-state binding model allowed kinetic rate constants to be derived. The data was also fitted to a one-state binding model, but it obtained a very poor fit. The overall association rate constant (K_1) for the first step of the reaction and the overall association rate constant for the entire reaction (K_a), were both approximately 5-fold lower for the SP domain exosite mutant compared to the results obtained for wild-type MASP-2 (Table 5.6). This indicates that the SP domain exosite plays a moderately important role in the association between MASP-2 and C4 compared to the CCP domain exosite, which recorded a 10-fold lower K_1 value and a 6-fold lower K_a value (Table 5.6). Mutations to the SP domain exosite decreased the conformational change constant (K_2) value ten-fold (Table 5.6), indicating that the SP domain exosite plays a major role in the conformational change required to achieve a high affinity complex between MASP-2 and C4.

Table 5.6: Two-state binding model and associated kinetic data for the binding of C4 by MASP-2

M2 form	k_{a1} $(M^{-1}.s^{-1})$	k_{d_1} (s^{-1})	K_1 $(M^{-1}.s^{-1})$	k_{a_2} (s^{-1})	k_{d_2} (s^{-1})	K_2 (s^{-1})	K_a $(M^{-1}.s^{-1})$
S618A	1.2×10^6	0.2	6.0×10^6	5.4×10^{-3}	3.2×10^{-2}	0.17	6.9×10^6
n = 9	$\pm 1.8 \times 10^5$	± 0.032		± 0.001	± 0.010		
SP exosite	6.6×10^5	0.56	1.2×10^6	2.1×10^{-4}	0.066	0.015	1.2×10^6
n = 10	$\pm 9.7 \times 10^4$	± 0.033		$\pm 5.3 \times 10^{-5}$	± 0.052		
Quadruple Mutant n = 3	*nd*	*nd*	*nd*	*nd*	*nd*	*nd*	*nd*

nd= not determined
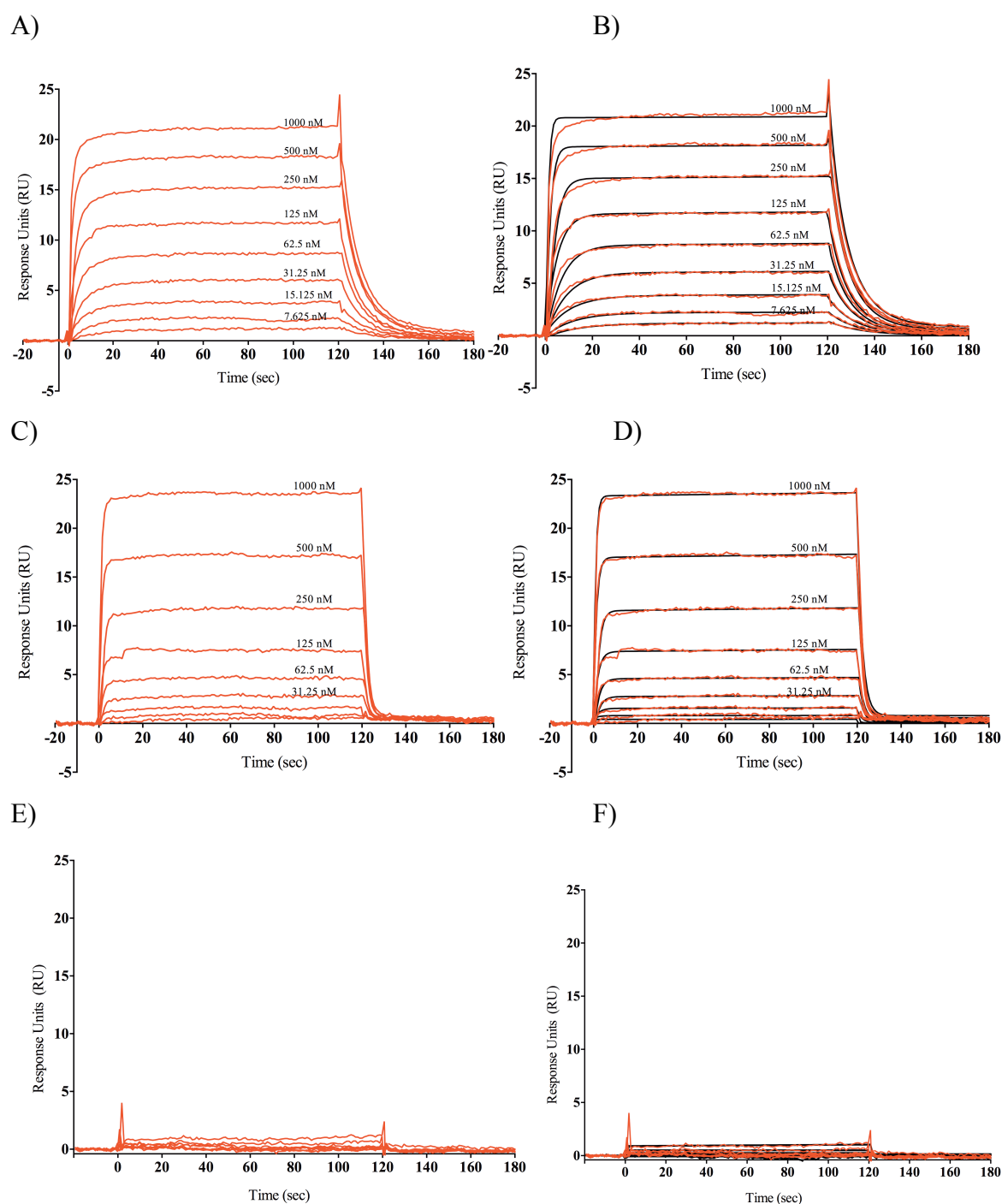
Figure 5.9: Binding of C4 to immobilised MASP-2 constructs. SPR curves for 0–1 μM C4 flowed over A) the immobilised activated form of MASP-2 CCP12SP Cys S618A without fit lines, as compared to B), which includes lines of fit for each concentration. SPR curves for 0–1 μM C4 flowed over C) the immobilised activated form of MASP-2 CCP12SP Cys R578Q R583Q double mutant without fit lines, and D) which includes lines of fit for each concentration. SPR curves for 0–1 μM C4 flowed over E) the immobilised activated form of MASP-2 CCP12SP Cys E333Q D365N R578Q R583Q quadruple mutant without fit lines, and F) which includes lines of fit for each concentration. The obtained responses were fitted to a two-state binding equation within the program BIAevaluation.

5.9 Discussion

For many years, the existence of a C4 binding exosite located upon the CCP domains of MASP-2 was thought to be highly probable. When the structure of MASP-2 and C4 in complex was released, it revealed not only the location of this CCP domain exosite, but also showed a potential exosite on the SP domain. This came as a surprise, as earlier work had suggested that the likelihood of an exosite being found on the SP domain was low (Duncan et al., 2012a). While some kinetic work was completed to confirm that the CCP domain exosite contributed to C4 binding, none was completed upon the potential SP domain exosite being shown. Therefore, the aim of this project was to confirm that this was indeed a binding exosite for C4, and to kinetically quantify the contribution of the exosite to the mechanism of interaction between MASP-2 and C4.

Active site stability testing using the synthetic peptide substrate C4 P4-P4' confirmed that none of the mutations led to active site instability, as the mutants displayed similar $K_{0.5}$ and k_{cat} values to that of the wild-type MASP-2.

Determination of EC_{50} values showed that of the four residues earmarked as making up the MASP-2 SP domain exosite, only two appeared to make significant contributions to the exosite (residues R578 and R583). The K450Q and K503Q mutations showed no significant increase in EC_{50} value compared to wild-type MASP-2. This was especially surprising for the K503Q mutation, as this residue was shown in the structure of MASP-2 in complex with C4 to be interacting with the sulfated tyrosine residue Y1417. However, results with the triple SP domain mutant created (MASP-2 K503Q R578Q R583Q) confirmed that this residue appears not to play a large role in the functioning of this exosite, as in EC_{50} assays the triple SP domain mutant recorded EC_{50} values 2-fold higher or less than those achieved by the double SP domain mutant MASP-2 R578Q R583Q. Structural observations appear to support these results. Upon binding C4, the MASP-2 residues R578 and R583 undergo large alterations in their structural positioning (5.4 and 7.8 angstrom alterations in position respectively), while residues K450 and K503 do not (Figure 5.10). Thus, there appears to be a structural explanation for the EC_{50} values obtained using the single mutants.
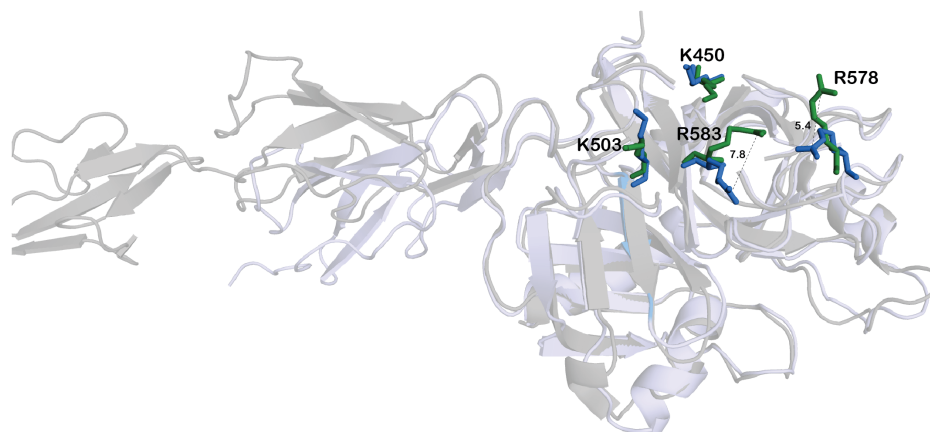
Figure 5.10: Structural changes of MASP-2 SP domain residues upon binding C4. The positioning of MASP-2 residues when activated is shown in blue, and their position upon C4 binding is shown in green. The distances between the R583 and R578 residues in the absence and presence of C4 are indicated in angstroms. Image created using PDB files 1Q3X (DOI: 10.2210/pdb1q3x/pdb) and 4FXG (DOI: 10.2210/pdb4fxg/pdb).

Much as seen with the CCP domain exosite mutants in Chapter 3, the effects of mutations appeared to be cumulative. The R578Q and R583Q single mutants created a ~2-fold increase in EC_{50} value, while the double mutant R578Q R583Q showed an increase in EC_{50} value over 20-fold higher than that of wild-type MASP-2. The most severe effects however occurred when both exosites were impacted simultaneously with the quadruple mutant. The EC_{50} values obtained by the quadruple mutant were over 600-fold higher than those obtained by wild-type MASP-2. It suggests that the exosites also work in a cumulative manner to ensure efficient binding and cleaving of C4- impacting one exosite leads to moderate decreases in C4 cleavage efficacy, while the loss of both exosites leads to a severe reduction in C4 cleavage efficacy.

The time courses for cleavage of C4 also appeared to reflect the results seen in the EC_{50} values obtained. The unaffected K450Q and K503Q single mutants recorded time courses very similar to that of wild-type MASP-2. The two affected single mutants, R578Q and R583Q, both recorded time courses showing a reduced rate of C4 cleavage over the first hour of the time course, only reaching a similar level of cleavage to wild-type MASP-2 by the second hour. Unsurprisingly, given the EC_{50} results, the double mutant MASP-2 R578Q R583Q showed a quite strong reduction in C4 cleavage in the time course, only reaching ~ 55% cleavage by the second hour. The quadruple mutant confirmed its reduced C4 cleavage efficacy, barely reaching 10% cleavage by the second

hour, thus giving further credence to the theory that the exosites of MASP-2 act in a cumulative manner to ensure efficient cleavage of C4 by MASP-2.

Investigations into how the SP domain exosite double mutant and the quadruple mutant affected MASP-2 binding to C4 provided some very interesting results. The data obtained revealed that the double SP domain exosite mutant R578Q R583Q exhibited an impacted steady-state affinity, with a 6-fold increase in K_D value over that of wild-type MASP-2. This increase in K_D value demonstrates the importance of the SP domain exosite in promoting a high affinity interaction between MASP-2 and C4. The quadruple mutant MASP-2 E333Q D365N R578Q R583Q exhibited no binding to C4, and so a K_D could not be determined. This lack of binding provides an explanation for the severe reduction in C4 cleavage efficacy shown by the quadruple mutant in the EC_{50} assays and C4 cleavage time courses: as MASP-2 is severely hindered in its ability to bind C4 with both exosites impacted, it therefore cannot cleave C4 in an efficient manner.

As was done to the CCP domain exosite mutants in Chapter 3, a two-state binding model was used, exemplifying the equation M2 + C4 $\leftrightarrows$ M2:C4 $\leftrightarrows$ M2*C4, where the initial complex (M2:C4) is converted to a higher affinity complex (M2*C4) due to conformational change. Use of this model then allowed us to obtain kinetic constants from the data. The overall association rate constant (K_1) for the first step of the reaction and the overall association rate constant for the entire reaction (K_a), were both approximately 5-fold lower for the SP domain exosite mutant compared to the results obtained for wild-type MASP-2. This indicates that the SP domain exosite plays a more moderate role in the association between MASP-2 and C4 compared to the CCP domain exosite, where the double mutant MASP-2 E333Q D365N displayed a 10-fold reduction in K_1 value, and a 6-fold reduction in K_a value, suggesting that the CCP domain exosite exerts the greatest influence on C4 binding in the initial interaction between MASP-2 and C4.

The kinetic constants derived from the data gathered suggest that, as the SP domain exosite double mutant records a 10-fold decrease in K_2 value compared to wild-type MASP-2, the SP domain exosite makes its largest contribution to C4 binding in the second phase of the interaction between MASP-2 and C4. In this phase, a conformational change is likely to occur in either or both molecules in the reaction. An explanation for these results most likely lies in structural changes undergone by MASP-2 upon C4 binding. In the structure of MASP-2 in complex with C4, one of the major conformational

changes seen in MASP-2 when in complex with C4 was a rotation of 24-29° by the SP domain relative to the CCP2 domain (Kidmose et al., 2012). This provides a structural explanation as to why the SP domain exosite appears to make its largest contribution to C4 binding in the second phase of the interaction between MASP-2 and C4, as compared to the CCP domain exosite, which makes its largest contribution in the initial phase of the interaction.

In conclusion, the results indicate that the potential MASP-2 SP domain exosite shown in the MASP-2/C4 complex structure is in fact a functional exosite. The crucial nature of this exosite in allowing MASP-2 to bind and cleave C4 in an efficient manner is shown, and, in addition, the results show that the CCP and SP domain exosites work in a cumulative manner to promote efficient binding and cleavage of C4 by MASP-2.

Chapter 6

'Investigations into the regulation of MASP-2 activity by heparin and polyphosphate'

6.1 Introduction

Complement system activity plays an important role in innate immunity. However, like all biological systems and pathways, it relies upon a number of control measures to ensure that its activity is tightly regulated to occur only in appropriate situations so as to prevent self-damage. An important figure in complement system control is the serpin C1-INH. As discussed earlier, C1-INH is responsible for controlling the activity of a number of key proteases in both the classical and lectin pathways (C1s, C1r, MASP-1 and MASP-2) (Arlaud et al., 1979, Matsushita et al., 2000). People suffering from Hereditary Angioedema (HAE) have been found to either have a deficiency of C1-INH due to autosomal dominant mutations in the C1-INH gene, or to possess mutations in the C1-INH gene that lead to the production of dysfunctional C1-INH (Donaldson and Evans, 1963, Kaplan, 2010.). With over 150 mutations in the C1-INH gene having been found in HAE patients, those with the disorder suffer from spontaneous C4 cleavage, leading to low serum levels of C4, as well as recurrent tissue swelling due to the unimpeded bradykinin formation thanks to a lack of control over kallikrein, factor XI and factor XII, which also have their activity modulated by C1-INH (Ruddy et al., 1967, Kaplan, 2010, Kaplan and Ghebrehiwet, 2010). This swelling can be fatal if it occurs in the airways (Li et al., 2015).

The activity of C1-INH towards its target proteases is modified by highly charged polyanionic molecules. The structure of C1-INH shows an area of high positive charge on the 'top' end of the C1-INH molecule (Figure 6.1) (Beinrohr et al., 2007).
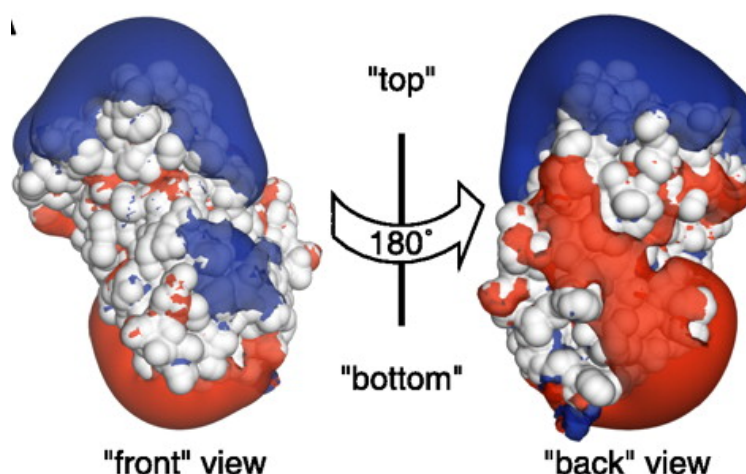
Figure 6.1: The charge pattern of the contact surfaces of C1-INH. C1-INH has been shown to display a uniform positive charge (shown in blue) on the "top" of the molecule, while the 'bottom' displays a negative charge (shown in red). The white depicts a neutral charge. Image from Beinrohr et al., 2007.

In addition, this region of positive charge overlaps with the area where the protease contacts C1-INH to form the initial recognition (Michaelis) complex (Johnson et al., 2006, Beinrohr et al., 2007). This led to the formation of the 'sandwich theory' to explain why polyanions quite often potentiate C1-INH activity (Beinrohr et al., 2007). It is believed that the polyanions are attracted to and bind to this patch of high positive charge underneath the RCL of C1-INH. By doing so, they neutralize the charge of this patch, or even change the charge of the patch into a negative one. This alteration in charge on the surface of C1-INH causes it be more attractive to its protease targets, which often have highly positively charged patches surrounding their active site, such as seen with C1s (Gaboriaud et al., 2000, Beinrohr et al., 2007, Perry et al., 2013). Therefore, a 'sandwich' is made, with the polyanionic molecules in between the serpin and its protease target.

One naturally occurring example of a polyanion that influences C1-INH activity is that of the glycosaminoglycan (GAG), heparin (Figure 6.2). Heparin is a naturally occurring highly polyanionic and polydisperse linear polysaccharide involved in the clotting cascade, where it acts as an anticoagulant (Yu et al., 2005). Previous work has shown that heparin interacts with numerous complement components (Raepple et al., 1976, Sahu and Pangburn, 1993, Yu et al., 2005). In the complement system, it has been shown to have potentiating effect upon the function of C1-INH, accelerating its inhibition of C1s and C1r (Sim et al., 1980, Nilsson and Wiman, 1983, Murray-Rust et al., 2009).

Although much less study has been done, it has also been shown to accelerate C1-INH activity against MASP-1 and MASP-2 (Parej et al., 2013). However, the level of potentiation offered by heparin to C1-INH against MASP-1 and MASP-2 appears to be less than that seen with C1s, with the second order association rate constant (K_a) of the MASP-2/C1-INH reaction showing a moderate acceleration (about 10-fold) with the addition of heparin (1.3 x 10^6 M^{-1} s^{-1} as compared to 1.6 x 10^5 M^{-1} s^{-1}) (Nilsson and Wiman, 1983, Murray-Rust et al., 2009, Parej et al., 2013). It also appears to be influenced by whether the initial lectin complex consists of MBL or H-Ficolin, as Parej *et al*. (2013) found that heparin potentiated C1-INH activity less in the MBL-dependent pathway than in the H-Ficolin dependent pathway when measuring C3 and C4 deposition (Parej et al., 2013). In the MBL-dependent pathway, heparin reduced the IC_{50} rate for C4 deposition from 56 nM to 31 nM, while in the H-Ficolin dependent pathway, it decreased from 220 nM to 48 nM (Parej et al., 2013).
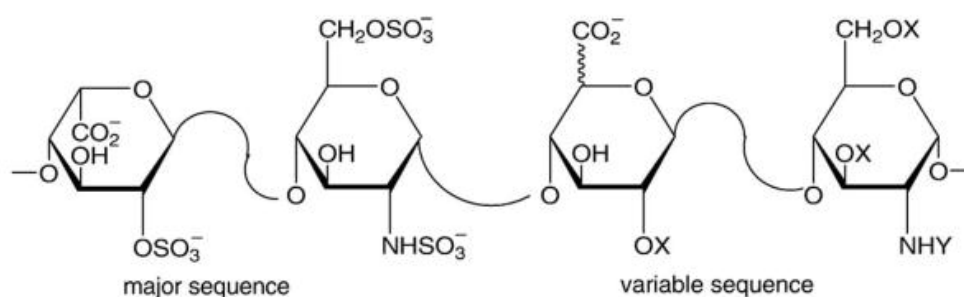
Figure 6.2: Structure of heparin. Heparin is a polydisperse, highly anionic, linear polysaccharide molecule. Heavily sulfated, heparin is mostly an intracellular polysaccharide, and is stored in granules of mast cells. The figure shows the major and variable disaccharide sequences, where X=SO_3^- or H, and Y=SO_3^-, $COCH_3$ or H. Taken from Yu et al., 2005.

Use of polyanions to potentiate C1-INH activity against complement components is an idea that has been floated for some time as a treatment for certain HAE sufferers, and, given the more recent link between MASP-2 activity and damage during events of myocardial, gastrointestinal and ischemia reperfusion injury, as well as the link to ischemia-related necrotic myocardial injury, it also poses a potential method for reducing complement activity during these events (Murray-Rust et al., 2009, Schwaeble et al.,

2011, Zhang et al., 2013). However, potentiation of C1-INH activity by other non-physiological GAGs, such as dextran sulfate, has been shown to be far greater than that produced by heparin (Wuillemin et al., 1997, Murray-Rust et al., 2009). These synthetic molecules may produce unwanted side effects, such as the charged nature of the dextran-sulfate molecule DXS5k, a candidate for the pharmacological manipulation of C1-INH activity against the complement system, potentially leading to thrombocytopenia (Murray-Rust et al., 2009). Therefore, there is great interest in finding another naturally occurring polyanion that is able to potentiate C1-INH activity more strongly than heparin is capable of. The greater cofactor activity of non-physiological cofactors (i.e. dextran sulfate) suggest that a better, more physiologically relevant cofactor could potentially be found within the body.

Recently, another polyanion involved in the coagulation cascade has been found to influence complement activity. Inorganic polyphosphate (polyP) is a linear polymer of orthophosphate, linked by high energy phosphoanhydride bonds (Figure 6.3). At physiological pH, each unit possesses a monovalent negative charge, leading to a highly charged anionic polymer (Morrissey et al., 2012).
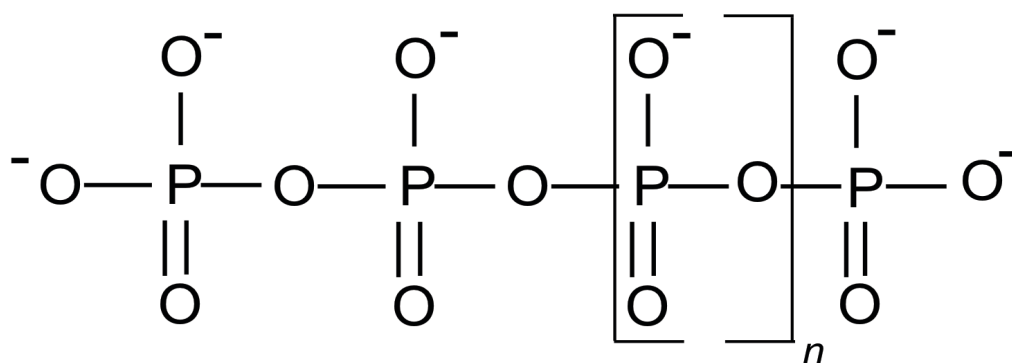
Figure 6.3: Structure of polyphosphate. Polyphosphate is a linear, highly anionic molecule that comes in a range of lengths. The brackets indicate a polyphosphate unit. Polyphosphate produced by platelets is around 60-100 units long, while microbes are capable of producing polyphosphate of many thousands of units. Adapted from Morrissey et al., 2012.

PolyP is a common polymer, and is found in all mammalian cells and in lower organisms (Wat et al., 2014). In mammalian cells polyP has been found to be localized in

lysosomes, dense granules in platelets, mitochondria and nuclei (Pisoni and Lindley, 1992, Kornberg, 1995, Ruiz et al., 2004). The length of the polymer differs depending on variables such as cell type and organism, but in human platelets the range is ~60-100 units, and in platelets it is found at a concentration of ~1-3 μM. PolyP has been found to play a role in a number of biological processes, including angiogenesis, apoptosis, cell proliferation, osteoblast function, bone mineralization, energy metabolism and tumour metastasis (Leyhausen et al., 1998, Schroder et al., 2000, Wang et al., 2003, Kawazoe et al., 2004, Hernandez-Ruiz et al., 2006, Han et al., 2007, Tamnenkoski et al., 2008, Galasso and Zollo, 2009, Pavlov et al., 2010).

PolyP has been found to be prothrombotic and proinflammatory, and acts at many different points in the coagulation cascade to achieve these outcomes. Different length polyP molecules appear to influence different sections of the coagulation cascade (Smith et al., 2010). Although acting at a number of points in the coagulation cascade, longer length polyP molecules (~1000-2000 units), often contained in microbes or even expressed upon their capsule in some instances, appear to exert their largest influence on initiating blood clotting via the contact pathway (Noegel and Gotschlich, 1983, Kornberg et al., 1999, Smith et al., 2006, Smith et al., 2010). Platelet length polyP polymers (~ 60-100 units) have been shown to accelerate factor Xa and thrombin activation of factor V to Va, and, due to the role of factor Va as an essential cofactor in promoting prothrombin activation, this leads to a burst of thrombin production during plasma clotting reactions (Smith et al., 2006). It also led to the anticoagulant function of Tissue Factor Pathway Inhibitor (TFPI) being abrogated (Smith et al., 2006). In addition, it was also found that platelet length polyP potently accelerates factor XI autoactivation and activation by thrombin (Choi et al., 2011). Platelet length polyP has also been shown to strengthen fibrin clot formation. When Smith *et al.* (2008) mixed fibrinogen with polyP and plasma concentrations of Ca^{2+}, and then added thrombin, the resulting fibrin clots were more turbid, had fibrils with higher mass/length ratios, were more resistant to elastic stretching, and were more resistant to fibrinolysis than were clots formed under identical conditions, but without polyP (Smith and Morrissey, 2008). Given the influence of polyP in the control of the coagulation system, the question was raised whether polyP could also mediate an effect upon the functioning of the complement system, which is evolutionarily related to the coagulation system. Wat *et al.* (2014) found that polyP is capable of affecting the terminal complement pathway by destabilizing the C5b and C6 molecules

(Wat et al., 2014). The C5b and C6 molecules displayed a concentration dependent alteration in thermal stability when incubated with increasing amounts of polyP, while the C5 and C7 complement components did not (Wat et al., 2014). PolyP was also shown to suppress Terminal Pathway complement-mediated lysis of red blood cells by reducing the binding and integration of the C5b-C7 and C5b-C8 complement complexes into the cell membrane, which leads to reduced formation of the MAC and subsequently a reduced rate of lysis (Wat et al., 2014).

At this point in time, no work has been done to investigate if polyP has any effect upon complement components outside of the terminal pathway. In recent years MASP-2 activity has been linked to contributing to damage caused by myocardial and gastrointestinal ischemia/reperfusion injury, where MASP-2 deficient mice showed smaller infarct volumes (Schwaeble et al., 2011). MASP-2 has also been linked to ischemia-related necrotic myocardial injury (Zhang et al., 2013). Therapeutic targeting of the classical and lectin pathways using recombinant human C1-INH has also been shown to confer protection from ischemia/reperfusion induced renal damage, where it reduced complement deposition, recruitment of inflammatory cells and tubulointerstitial damage (Castellano et al., 2010). Therefore, the ability to control MASP-2 activity could potentially prove useful in the prevention of injury caused during these events. Although heparin has been shown to potentiate C1-INH activity against C1s, and to a lesser degree MASP-2, it is not as effective in doing so as other non-endogenous polyanions, such as dextran sulfate (Murray-Rust et al., 2009). It is hoped that polyP may represent a more potent naturally occurring polyanion, which could represent a potential new therapeutic molecule for inhibiting MASP-2 activity through enhancing C1-INH activity. Therefore, the focus of this study was to investigate if heparin and polyP are indeed capable of binding MASP-2, and what effects each polyanion exerts upon the regulation of MASP-2 activity by C1-INH.

6.2 Materials and Methods

6.2.1 Investigation of polyphosphate binding to MASP-2 through Electromobility Shift
    Assays (EMSA)

Binding of the polyphosphate (>1000 units) molecule to MASP-2 was examined by
the running of TBE (Tris, Borate and EDTA) gels. Polyphosphate was diluted in MilliQ
water to range of final concentrations from 0-200 µM, and wild-type MASP-2 and the
CCP and SP domain exosite mutants being examined were diluted to a concentration of
2.27 µM in 20 mM HEPES, pH 7.4. Polyphosphate and MASP-2 were incubated together
at room temperature for 10 min before 6 x DNA loading dye (New England BioLabs,
Ipswich, MA, USA) was added to end the reaction. The samples were centrifuged at room
temperature for 1 min at 13,000 x g before being loaded onto 10% TBE gels. Samples
were electrophoresed at 12 mA for 5 h and then stained using either 0.2 µm filtered
Coomassie blue R-250 for 1 h or 0.2 µm filtered toluidine blue-O stain [0.05% (w/v)
toluidine blue-O, 25% (v/v) methanol, 5% (v/v) glycerol] for 10 min, which visualises
highly negatively charged molecules, such as polyphosphate. Gels stained in Coomassie
blue R-250 were then destained using a solution of 40% (v/v) methanol and 10% (v/v)
acetic acid, while gels stained in toluidine blue-O were destained in a solution of 25%
(v/v) methanol and 5% (v/v) glycerol.

6.2.2 Effect of polyphosphate upon the interaction between C1-INH and MASP-2

Polyphosphate (70-120 units) was diluted in MilliQ water to produce a range of
concentrations that would allow final concentrations of 0-100 µM during the experiment.
A 2 µM stock of wild-type MASP-2 and the CCP and SP domain exosite mutants being
examined were made in 1 x Hank's Buffered Saline Solution (HBSS) (Life Technologies,
Mulgrave, Victoria, Australia), to allow for a final concentration of 500 nM during the
experiment. C1-INH was also diluted in 1x HBSS to make a 2 µM stock to allow a final
concentration of 500 nM, ensuring a 1:1 ratio between MASP-2 and C1-INH.
Each component of the experiment was added in a sequential order. At room temperature,
polyphosphate and C1-INH were added first and second, with MASP-2 being added last.
After the addition of MASP-2, the reaction was incubated for 1 h at 37°C, after which
reducing SDS loading buffer was added to end the reaction. Samples were then incubated

at 95°C for 5 min, centrifuged at 13,000 x g for 1 min and loaded onto 10% SDS-PAGE gels and electrophoresed. After electrophoresis, gels were stained with 0.2 μm filtered Coomassie blue R-250 for 1 h, and destained.

Activity levels were also examined through activity assays using the coumarin substrate LGR (Z-LGR-AMC) (GL Biochem, Shanghai, China). As in the SDS-PAGE protocol, polyphosphate (70-120 units) was diluted in MilliQ water to produce a range of concentrations that would allow final concentrations of 0-100 μM during the experiment. A 200 nM stock of each MASP-2 variant was made in 1 x HBSS to allow for a final concentration of 50 nM during the experiment. C1-INH was also diluted in 1x HBSS to make a 200 nM stock to allow a final concentration of 50 nM, ensuring a 1:1 ratio between MASP-2 and C1-INH.

Each component of the experiment was added in a sequential order. At room temperature, polyphosphate and C1-INH were added first and second, with MASP-2 being added last. After the addition of MASP-2, the reaction was incubated for 1 h at 37°C. After the incubation, a final concentration of 50 μM LGR substrate was added to the reaction, and the activity of the reaction was measured in duplicate on a BMG FLUOstar Omega fluorescent plate reader (BMG LabTech, Offenburg, Germany), using an excitation wavelength of 360 nm, an emission wavelength of 460 nm and a gain of 700. The raw data was then visualized using GraphPad Prism Version 6.0.

6.2.3 Analytical heparin-Sepharose chromatography

Wild-type MASP-2 and the CCP and SP domain exosite mutants being examined were subjected to gel filtration chromatography in 20 mM Tris, 70 mM NaCl, pH 7.4 using a Superdex 75 16/60 column (GE Healthcare, Uppsala, Sweden), and the fractions analysed using a 12.5% SDS-PAGE gel. The relevant fractions were then concentrated down to 1 mL. A Hi-Trap Heparin HP 1 mL column (GE Healthcare, Uppsala, Sweden) was equilibrated in 6 column volumes of Buffer A (20 mM Tris, 70 mM NaCl, pH 7.4), and the protein injected onto the column. The protein was then eluted from the column through a linear NaCl gradient using Buffer B (20 mM Tris, 1 M NaCl, pH 7.4) over 17 mL at 1 mL/ min. The A_{280} (AU) and conductivity (mS/cm) were then plotted using GraphPad Prism Version 6.0.

6.2.4 Effect of heparin upon the interaction between C1-INH and MASP-2

Heterogenous heparin (Heparin sodium salt derived from porcine intestinal mucosa Grade I-A (Sigma-Aldrich, St. Louis, MO, USA) was diluted in MilliQ water to produce a range of concentrations that would allow final concentrations of 0-50 μg/ mL during the experiment. A 2 μM stock of wild-type MASP-2 and the CCP and SP domain exosite mutants being examined were made in 1 x HBSS to allow for a final concentration of 500 nM during the experiment. C1-INH was also diluted in 1x HBSS to make a 2 μM stock to allow a final concentration of 500 nM, ensuring a 1:1 ratio between MASP-2 and C1-INH.

Each component of the experiment was added in a sequential order. At room temperature, heparin and C1-INH were added first and second, with MASP-2 being added last. After the addition of MASP-2, the reaction was incubated for 1 h at 37°C, after which reducing SDS loading buffer was added to end the reaction. Samples were then incubated at 95°C for 5 min, centrifuged at 13,000 x g for 1 min and then loaded onto 10% SDS-PAGE gels and electrophoresed. After electrophoresis, gels were stained with 0.2 μm filtered Coomassie blue R-250 for 1 h, and then destained.

Activity levels were also examined through activity assays using the coumarin substrate LGR (Z-LGR-AMC) (GL Biochem, Shanghai, China). As in the SDS-PAGE protocol, heparin was diluted in MilliQ water to produce a range of concentrations that would allow final concentrations of 0-50 μg/ mL during the experiment. A 200 nM stock of wild-type MASP-2 and the CCP and SP domain exosite mutants being examined were made in 1 x HBSS to allow for a final concentration of 50 nM during the experiment. C1-INH was also diluted in 1x HBSS to make a 200 nM stock to allow a final concentration of 50 nM, ensuring a 1:1 ratio between MASP-2 and C1-INH. Each component of the experiment was added in a sequential order. At room temperature, heparin and C1-INH were added first and second, with MASP-2 being added last. After the addition of MASP-2, the reaction was incubated for 1 h at 37°C. After the incubation, a final concentration of 50 μM LGR substrate was added to the reaction, and the activity of the reaction was measured in duplicate on a BMG FLUOstar Omega fluorescent plate reader (BMG LabTech, Offenburg, Germany), using an excitation wavelength of 360 nm, an emission wavelength of 460 nm and a gain of 700. The raw data was then visualized using GraphPad Prism Version 6.0.

6.3 Binding of wild-type MASP-2 and selected MASP-2 CCP and SP domain exosite mutants to heparin

Heparin has been shown to bind to a number of complement components over the last few decades. At this point in time, complement components C1, C1q, C2, C3, C4, C4bp, C5, C6, C7, C8, C9, C1-INH, Factor I, Factor H, Factor B, Factor P, Vitronectin and C1s have all been shown to bind heparin (Sahu and Pangburn, 1993, Yu et al., 2005. Murray-Rust et al., 2009). However, data depicting heparin binding to components of the lectin pathway, such as MASP-2 and MASP-1, has yet to be published. We therefore investigated the ability of wild-type MASP-2 to bind to heparin using analytical heparin affinity chromatography. In Chapters 3 and 5, it was clearly illustrated that MASP-2 has two exosites (the CCP and SP domain exosites) that contribute to efficient binding and cleavage of C4. Duncan *et al.* (unpublished data) showed that mutation of the SP domain exosite of C1s abrogates the ability of C1s to bind heparin, which led to the question of whether the CCP and SP domain exosites of MASP-2 also contribute to the binding of heparin by MASP-2. We therefore examined the ability of the MASP-2 CCP domain exosite double mutant E333Q D365N, the SP domain exosite double mutant R578Q R583Q and the quadruple mutant E333Q D365N R578Q R583Q to bind to heparin, to observe if these exosites also plays a role in heparin binding.

From the heparin affinity chromatography results, it appears that MASP-2 is indeed capable of binding heparin, with wild-type MASP-2 and all the mutants investigated binding to the heparin-lined column (Figure 6.4). Interestingly, the results indicate that the MASP-2 SP domain exosite also plays a role in the binding of heparin. Both the MASP-2 SP domain exosite double mutant and the quadruple mutant exhibit altered binding to the heparin column compared to wild-type MASP-2 and the CCP domain exosite double mutant, eluting off the column at a lower salt concentration (Figure 4). This indicates these mutants containing mutations of the SP domain exosite have a lowered affinity for heparin compared to wild-type MASP-2 and the double CCP domain exosite mutant. However, the heparin affinity chromatography shows that mutation of the SP domain exosite residues R578 and R583 simultaneously does not appear to completely abrogate MASP-2 binding to heparin. These mutants, although exhibiting a lowered affinity for heparin, are still capable of binding to the heparin-lined column. This indicates

that while the heparin-binding site of MASP-2 does include the SP domain exosite residues R578 and R583, they constitute only part of it. Potentially, residues K450 and K503 may also contribute to the binding of heparin by MASP-2, as well as residues outside the SP domain exosite.

The CCP domain does not appear to play a role in heparin binding, as the CCP domain exosite double mutant E333Q D365N displayed a similar elution profile to wild-type MASP-2 (Figure 6.4). Wild-type MASP-2 and the double CCP domain exosite mutant both exhibited the elution of a smaller peak that eluted earlier than the main larger peak (Figure 6.4). It was theorized that this peak consisted of zymogen MASP-2, and further heparin affinity chromatography confirmed this, with zymogen MASP-2 found to elute at the same location as the smaller peak seen in the profiles of wild-type MASP-2 and the double CCP domain exosite mutant (Figure 6.4).

Therefore, from the results of the heparin affinity chromatography, it can be seen that MASP-2 is capable of binding to heparin, and that the SP domain exosite constitutes part of the heparin-binding site on MASP-2, while the CCP domain exosite does not contribute to heparin binding by MASP-2.
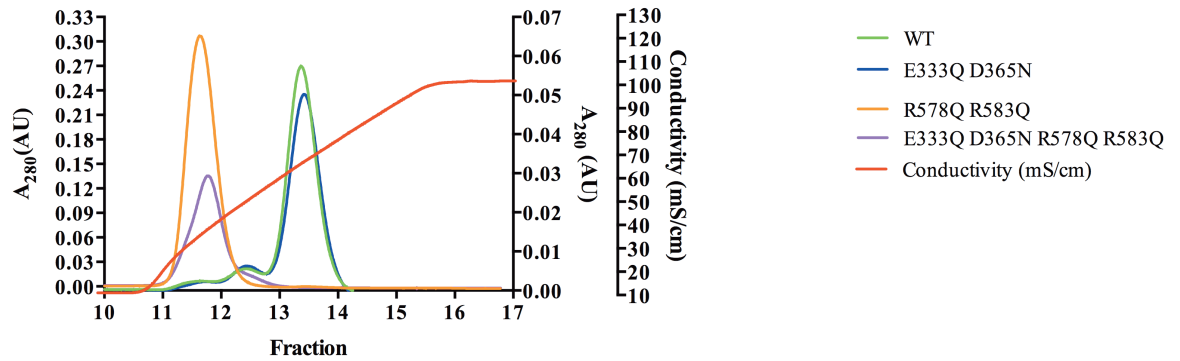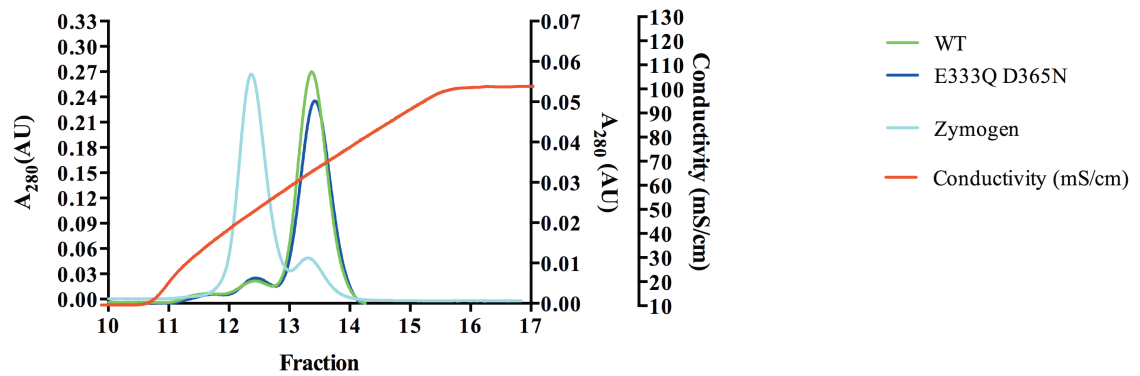
Figure 6.4: Analysis of heparin binding by wild-type MASP-2 and selected mutants using heparin affinity chromatography. A) Wild-type MASP-2 is depicted in green, the double CCP domain exosite mutant E333Q D365N in dark blue, the double SP domain exosite mutant R578Q R583Q in orange, and the quadruple mutant E333Q D365N R578Q R583Q in purple. B) Identification of the small peak from the wild-type and E333Q D365N mutant. Wild-type MASP-2 is depicted in green, the double CCP domain exosite mutant E333Q D365N in dark blue and zymogen MASP-2 in cyan.

6.4 Effects of heparin on inhibition of wild-type MASP-2 activity by the serpin, C1 inhibitor

Previous work has shown that heparin (and other polyanions) possesses the ability to potentiate C1-INH activity, and that this leads to a decrease in C1 and C1s activity (Caughman et al., 1982, Nilsson and Wiman, 1983, Wuillemin et al., 1997, Murray-Rust et al., 2009). Heparin has also been shown to promote MASP-1 inhibition by the serpin antithrombin, accelerating the reaction 30-fold (Presanis et al., 2004, Dobo et al., 2009). As MASP-2 is a known target of C1-INH (Matsushita et al., 2000, Kerr et al., 2008), we therefore investigated the effect of heparin upon inhibition of MASP-2 activity by C1-INH.

In order to better understand the effect of heparin on C1-INH activity against MASP-2, we examined a range of heparin concentrations from 0 to 50 μg/mL to observe the effect of increasing heparin concentration on C1-INH activity against MASP-2. A 1:1 ratio of MASP-2 to C1-INH (final concentration of 500 nM wild-type MASP-2 to 500 nM C1-INH) was used, with selected heparin concentrations between 0 to 50 μg/mL being used.

Interestingly, heparin appeared to reduce C1-INH activity, as the amount of final MASP-2/C1-INH complex reduces with increasing heparin concentration, almost completely disappearing by around 0.39 μg/mL of heparin (Figure 6.5). In addition, increasing heparin concentration increases the amount of intermediary MASP-2/C1-INH complex seen (where the MASP-2/C1-INH complex is at an intermediary stage in the pathway to the formation of the final inactive complex), along with the level of free C1-INH and MASP-2 molecules (Figure 6.5). These factors all point to heparin reducing the ability of C1-INH to inhibit MASP-2 activity.

Heparin (µg/mL)

Heparin (µg/mL)
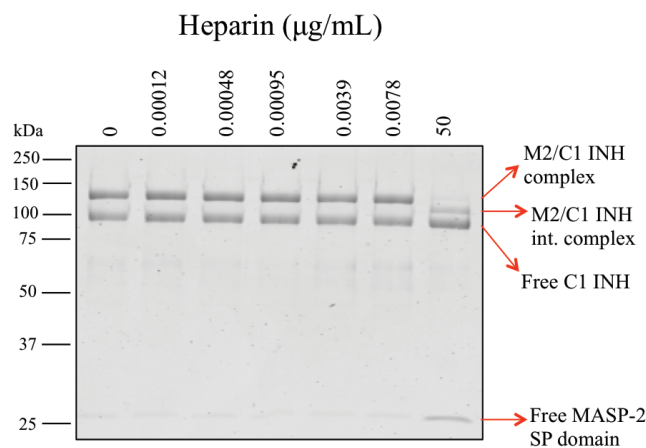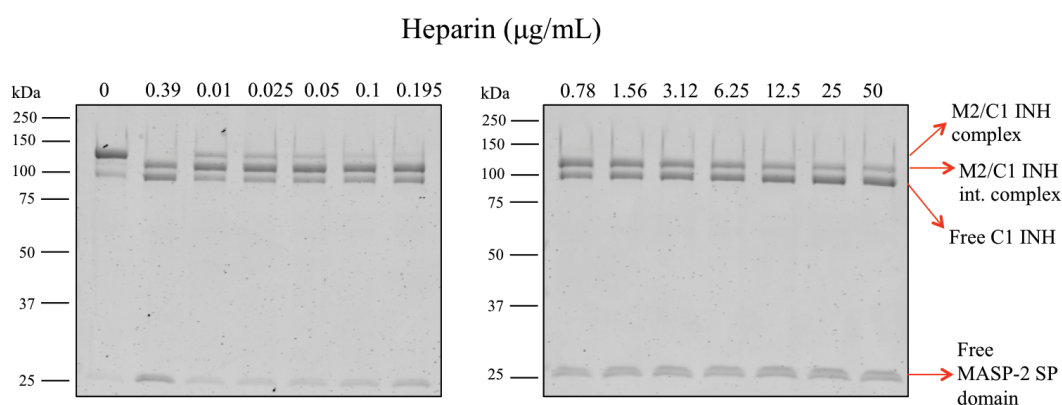
Figure 6.5: The effect of heparin addition on C1-INH activity against wild-type MASP-2. A) The effects of lower concentrations of heparin on C1-INH activity against wild-type MASP-2, and B) The effects of higher concentrations of heparin on C1-INH activity against wild-type MASP-2. MASP-2 and C1-INH were incubated together in a 1:1 ratio, with increasing concentrations of heparin added to examine its effects upon C1-INH activity against MASP-2. The reaction was incubated at 37°C for 1 h, and then ended with reducing SDS loading buffer. The samples were then electrophoresed on 10% SDS-PAGE gels, and stained using Coomassie blue R-250.

In addition to SDS-PAGE analysis, the level of inhibition of MASP-2 activity by C1-INH with or without heparin was also examined through peptide substrate assays. In the assay, MASP-2 and C1-INH were both used at a final concentration of 50 nM to

achieve a 1:1 ratio, and heparin was added in a concentration range from 0- 50 μg/mL. After incubation, a final concentration of 50 μM of the peptide substrate LGR was added to the components and a fluorescence plate reader used to test for any residual activity of the MASP-2 mutants.

Readings taken from the plate-reader were in agreement with the results seen in SDS-PAGE analysis. Without heparin, the activity of wild-type MASP-2 was completely inhibited by C1-INH at a 1:1 ratio, as no cleavage of the LGR peptide was detected by the plate reader (Figure 6.6). In SDS-PAGE analysis, concentrations of heparin ranging from 0 to 0.0078 μg/mL appeared to have no effect upon inhibition of MASP-2 activity by C1-INH (Figure 6.5). This was also seen on the plate reader, with enzyme-inhibitor mixtures incubated in heparin concentrations in this range showing no cleavage of the LGR peptide (Figure 6.6). From a heparin concentration of 0.012 μg/mL, cleavage of the LGR peptide was detected, and these cleavage levels increased with rising heparin concentration (Figure 6.6).

It therefore appears that heparin is not potentiating C1-INH activity against MASP-2, but instead is reducing it, with increasing heparin concentrations leading to reduced inhibitory activity against MASP-2.
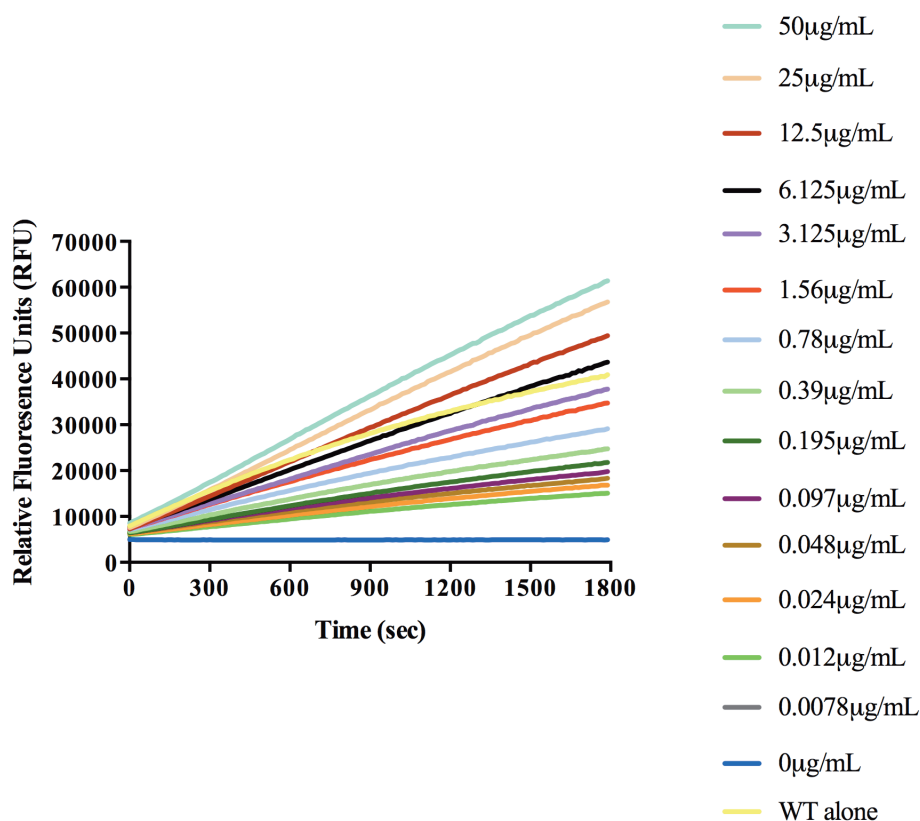
Figure 6.6: The effect of heparin addition on C1-INH activity against wild-type MASP-2 using a fluorescence plate reader. Using a fluorescence plate reader to read cleavage of the LGR peptide, the effect of heparin on inhibition of the activity of 500 nM wild-type MASP-2 by 500 nM C1-INH was examined. Alone = no C1-INH/heparin added.

6.5 Effects of heparin on the inhibition of activity of selected MASP-2 CCP and SP domain exosite mutants by the serpin, C1 inhibitor

In Section 6.3 of this chapter, we have determined that MASP-2 is capable of binding heparin, and that the MASP-2 SP domain exosite appears to be a part of the heparin-binding site on MASP-2. Work with wild-type MASP-2 shows that increasing concentrations of heparin interfere with the inhibition of MASP-2 activity by C1-INH. Given that the MASP-2 SP domain exosite double mutant (MASP-2 R578Q R583Q) and the quadruple mutant (MASP-2 E333Q D365N R578Q R583Q) showed altered binding properties in heparin affinity chromatography, it was decided to examine if these mutants also showed altered inhibition levels by C1-INH with increasing heparin concentrations. In addition to these mutants, the MASP-2 CCP domain exosite double mutant (MASP-2

E333Q D365N) was also examined, with the expectation that it would behave in a similar manner to wild-type MASP-2 based upon the results of heparin affinity chromatography.

The protocol followed was as completed in Section 6.4 with wild-type MASP-2, except that instead of a range of heparin concentrations, each mutant was examined using 0 and 50 µg/mL heparin.
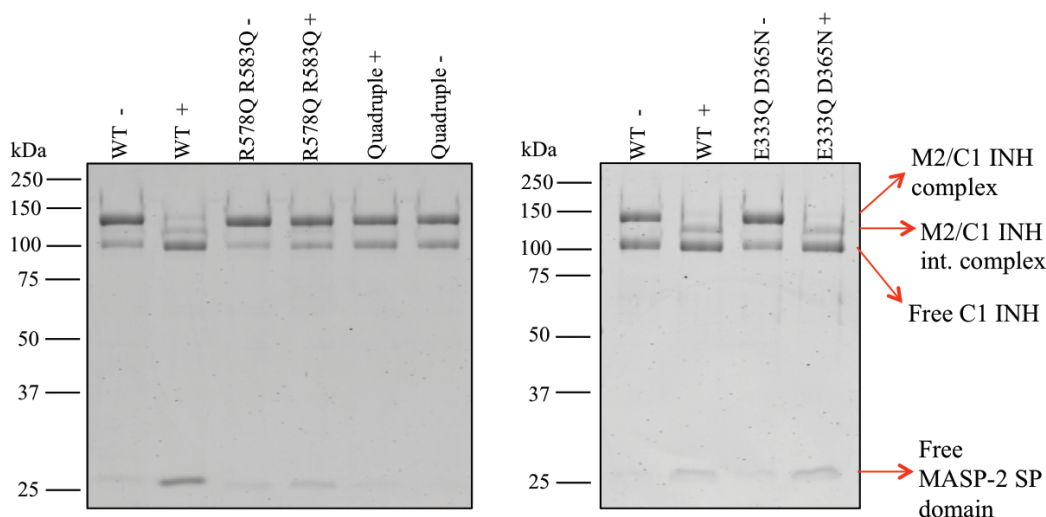
Figure 6.7: The effect of heparin addition on C1-INH activity against MASP-2 mutants. Selected MASP-2 CCP and SP domain exosite mutants and C1-INH were incubated together in a 1:1 ratio, with 0 or 50 µg/mL of heparin added to examine its effects upon C1-INH activity against the mutants. The reaction was incubated at 37°C for 1h, and then ended with reducing SDS loading buffer. Samples were then electrophoresed on 10% SDS-PAGE gels and stained using Coomassie blue R-250. + = 50 µg/mL heparin added, - = no heparin added.

The MASP-2 CCP domain exosite double mutant E333Q D365N was shown in heparin binding chromatography to exhibit a similar binding profile to wild-type MASP-2. It was therefore unsurprising that it exhibited similar results to wild-type MASP-2 when heparin was added to the interaction between MASP-2 and C1-INH, with heparin causing a reduction in the formation of MASP-2/C1-INH complex, suggesting reduced C1-INH activity against the mutant (Figure 6.7).

The MASP-2 SP domain exosite double mutant R578Q R583Q and the quadruple mutant E333Q D365N R578Q R583Q displayed altered binding properties in heparin affinity chromatography, with both eluting at a lower salt concentration that wild-type MASP-2. The addition of heparin to the interaction between C1-INH and these two mutants appears to have very little effect. SDS-PAGE analysis suggests that the inhibitory

activity of C1-INH against these MASP-2 mutants appears to be very similar whether heparin is or is not present, with similar amounts of MASP-2/C1-INH complex being formed (Figure 6.7). Both mutants appeared to show a very slight increase in free C1-INH and MASP-2 when heparin was added, indicating that the inhibitory activity of C1-INH against these mutants might be slightly reduced with addition of heparin. However, this reduction in inhibitory activity looks to be very small, and is certainly much smaller than the results seen with wild-type MASP-2 and the CCP domain exosite double mutant E333Q D365N (Figure 6.7).

In addition to SDS-PAGE analysis, the level of inhibition of the activity of selected MASP-2 mutants by C1-INH with or without heparin was also examined through peptide substrate assays. Following the protocol for Section 6.4, MASP-2 and C1-INH were both used at a final concentration of 50 nM to achieve a 1:1 ratio, and heparin was added at a concentration of either 0 or 50 μg/mL. After incubation, a final concentration of 50 μM of the peptide substrate LGR was added to the components and a fluorescence plate reader used to test for any residual activity of the MASP-2 mutants.

Readings taken from the plate-reader were reflected in the results seen in SDS-PAGE analysis. Without heparin, the activity of wild-type MASP-2 and all mutants was completely inhibited by C1-INH at a 1:1 ratio, as no cleavage of the LGR peptide was detected by the plate reader (Figure 6.8). When 50 μg/mL of heparin was added, both wild-type MASP-2 and the CCP domain exosite double mutant E333Q D365N showed clear cleavage of the peptide, indicating a reduced level of C1-INH activity was present (Figure 6.8). The SP domain exosite double mutant R578Q R583Q and quadruple mutant E333Q D365N R578Q R583Q both showed some cleavage of the peptide, however, the levels of cleavage were extremely low, indicating that had any reduction in C1-INH activity against MASP-2 occurred, it was not of a substantial scale (Figure 6.8).

These results appear to confirm that the MASP-2 SP domain exosite, and not the CCP domain exosite, is in fact a part of the MASP-2 heparin-binding site, as mutation of this exosite reduces the effects of heparin upon the interaction between C1-INH and MASP-2 quite severely.

Figure 6.8: The effect of heparin addition on C1-INH activity against MASP-2 mutants using a fluorescence plate reader. Using a fluorescence plate reader to read cleavage of the LGR peptide, the effect of heparin on inhibition of the activity of selected MASP-2 mutants (500 nM) by C1-INH (500 nM) was examined. The MASP-2 mutants examined were A) MASP-2 E333Q D365N, B) MASP-2 R578Q R583Q and C) MASP-2 E333Q D365N R578Q R583Q.
 -   = no heparin, + = 50 µg/mL heparin added, alone = no C1-INH/heparin added.

6.6 Binding of wild-type MASP-2 to long chain polyphosphate

PolyP has been found to bind directly to certain complement components, while not binding to others (Wat et al., 2014). We therefore examined if long chain polyP (>1000 units) was able to bind to MASP-2 using EMSA analysis. A concentration range of 0-50 μM polyP was used against a set final concentration of 1 μM of wild-type MASP-2.
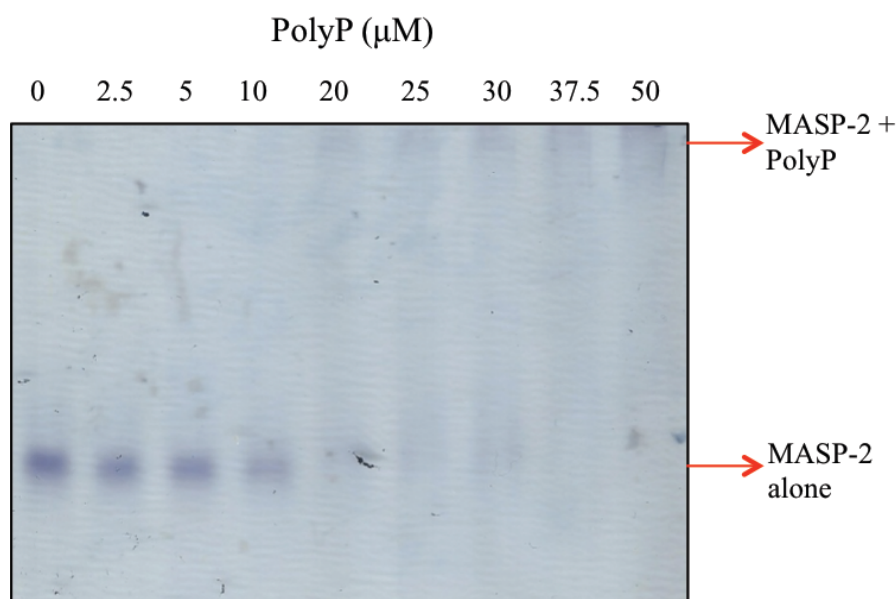
Figure 6.9: Binding of polyP to wild-type MASP-2 using EMSA analysis. A set concentration of 2 μM of wild-type MASP-2 was incubated with varying concentrations of polyP for 10 min, following which the samples were electrophoresed on 10% TBE gels and stained using Coomassie blue R-250.

From the results, it appears that polyP does bind to MASP-2. From 0-5 μM of polyP, the band depicting MASP-2 alone is very strong and quite uniform, with no shift shown (Figure 6.9). The intensity of the MASP-2 alone band decreases sharply at 10 μM of polyP, indicating that MASP-2 is binding to polyP in significant proportions, although little band shift can be visualized at this concentration (Figure 6.9). From 20 μM of polyP we can clearly see band shifting occurring as more MASP-2 binds PolyP, with the amount of MASP-2 alone decreasing and band shift increasing until it appears to have completely shifted by ~ 37.5 μM of polyP (Figure 6.9). This indicates that polyP does indeed bind to MASP-2, as the binding of polyP to MASP-2 changes the surface charge of MASP-2,

causing the protein to electrophorese in an altered manner, leading to a change in band position.

6.7 Binding of selected MASP-2 CCP and SP domain exosite mutants to long chain polyphosphate

In Sections 6.3 and 6.5, it was shown that the SP domain exosite of MASP-2 plays a role in the binding of heparin by MASP-2. This led to the question of whether the SP domain exosite also contributes to the binding of polyP by MASP-2. We therefore examined if long chain polyP (>1000 units) was able to bind to selected MASP-2 CCP and SP domain exosite mutants using EMSA analysis. From the CCP domain exosite, the single E333Q and D365N mutants, as well as the double E333Q D365N mutant were examined. For the SP domain exosite, the two single mutants found to contribute most to the exosite (R578Q and R583Q) were examined, as well as the double R578Q R583Q mutant. In addition, the quadruple mutant E333Q D365N R578Q R583Q was also tested.
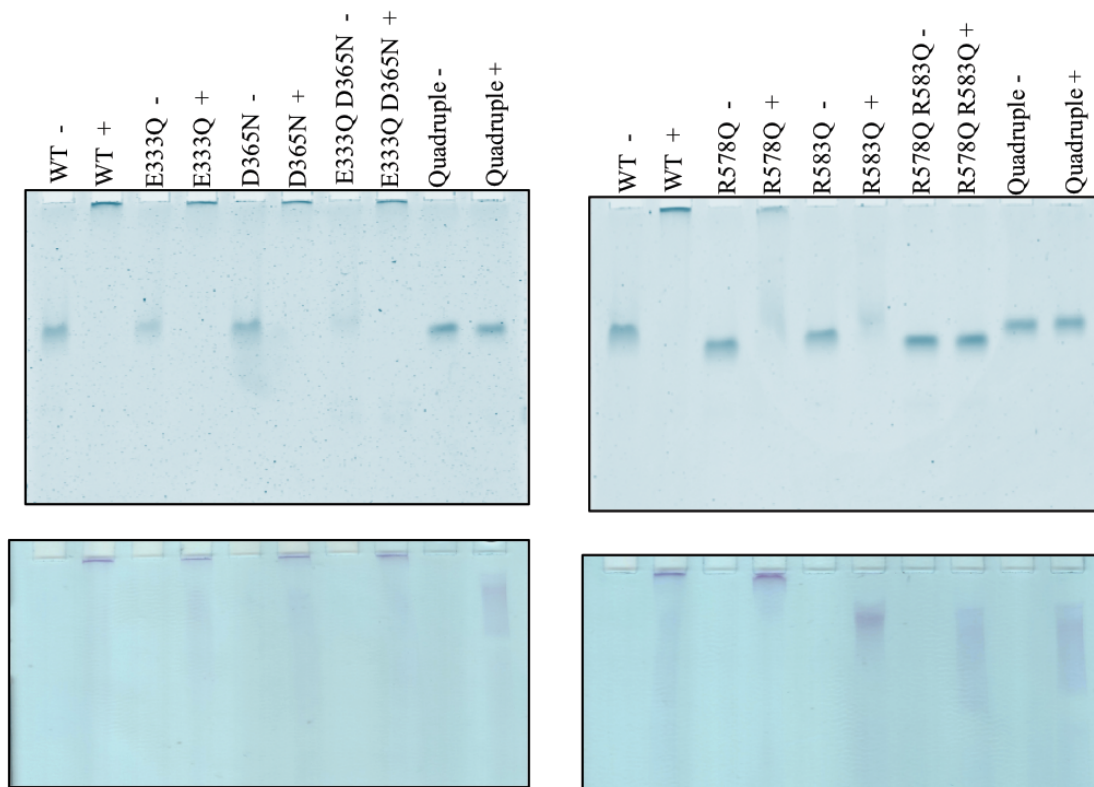
Figure 6.10: The binding of polyP to selected MASP-2 CCP and SP domain exosite mutants using EMSA analysis. A set concentration of 2 μM of each selected MASP-2 mutant was incubated with either 0 or 100 μM polyP for 10 min, following which the samples were electrophoresed on 10% TBE gels, and stained using Coomassie blue R-250 (top gels) or toluidine blue-O (bottom gels). + = 100 μM polyP added, - = no polyP added.

The gels show an interesting series of results. As seen with heparin binding, it appears that the MASP-2 CCP domain exosite plays no role in MASP-2 binding of polyP, as all CCP domain exosite mutants, whether single or double mutants, display a band shift like that of wild-type MASP-2 when incubated with 100 μM of polyP (Figure 6.10). The toluidine blue-O stain, which is capable of staining polyP due to its strong polyanionic charge, confirms that polyP is bound to these MASP-2 mutants, as it stains the same band as Coomassie blue (Figure 6.10). It therefore appears that the CCP domain exosite is not involved in the binding of polyP.

A very different story of interaction is told for the mutants of the MASP-2 SP domain exosite. Using Coomassie blue staining, the R578Q single mutant shows a band shift on the gel when 100 μM polyP is added, but it is not a complete band shift as seen with wild-type MASP-2 or any of the CCP domain exosite mutants (Figure 6.10). This

indicates that the binding of polyP to MASP-2 is somewhat impaired by this mutation, as some of the MASP-2 is able to bind it, while a portion is not. The toluidine blue-O staining confirms that polyP has indeed bound to the portion of the R578Q mutant that shifted, as it stains the shifted band (Figure 6.10). Using Coomassie blue staining, the R583Q single mutation also shows a partial band shift on the gel when 100 μM polyP is added (Figure 6.10). However, toluidine blue-O staining indicates that the binding between this MASP-2 mutant and polyP may be different, as the distance travelled by the shifted band was further than that seen with wild-type MASP-2 or any of the other mutants (Figure 6.10). The SP domain exosite double mutant R578Q R583Q showed no band shift on the gel with the addition of 100 μM polyP, indicating that this mutant is unable to bind polyP (Figure 6.10). Unsurprisingly, given that it contains the SP domain exosite double mutation, the quadruple mutant E333Q D365N R578Q R583Q also showed no band shift on the gel with the addition of 100 μM polyP, suggesting that it is also unable to bind polyP (Figure 6.10). The toludine blue-O staining pattern supports the results for these mutants, as only free polyP appears to have been stained (Figure 6.10). These results indicate that residues R578 and R583 are key residues in the binding of polyP by MASP-2.

The behavior of the MASP-2 SP domain exosite double mutant and the quadruple mutant with polyP could occur for two reasons. One is that the mutations cause MASP-2 to be completely incapable of binding polyP. The second is that the mutations lead to an impacted ability of MASP-2 to bind polyP, and that binding may only be seen at higher concentrations of polyP. In order to investigate which of these options applied to the affected mutants, each was incubated with a concentration range of polyP ranging from 0 to 200 μM. The results showed both mutants displaying no band shift on the gel, even when incubated with 200 μM polyP, indicating that the more likely of the two scenarios is that these mutants are incapable of binding polyP (Figure 6.11).

A)   B)
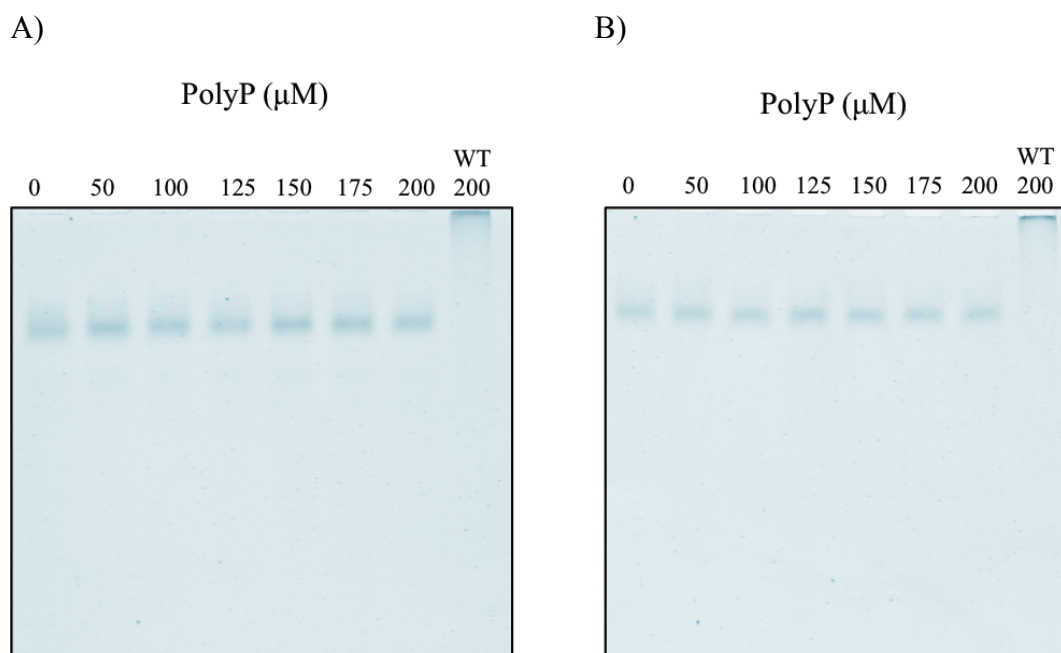
Figure 6.11: Binding of increased concentrations of polyP to A) the MASP-2 double mutant R578Q R583Q and B) the quadruple MASP-2 mutant E333Q D365N R578Q R583Q using EMSA analysis. A set concentration of 2 µM of each MASP-2 mutant was incubated with varying concentrations of polyP from 0-200 µM for 10 min, following which the samples were electrophoresed on 10% TBE gels, and stained using Coomassie blue R-250.

From the EMSA analysis, the results indicate that the SP domain exosite of MASP-2 is involved in the binding of polyP by MASP-2, while the CCP domain exosite is not. The results also suggest that the R578 and R583 residues of the SP domain exosite are the key residues involved in the binding of polyP by MASP-2, as simultaneous mutation of these residues rendered MASP-2 unable to bind polyP.

6.8 Effects of platelet-length polyphosphate molecules on the inhibition of wild-type MASP-2 activity by the serpin, C1 inhibitor

As discussed earlier, the endogenous polyanion heparin is known for its potentiation of C1-INH activity (Wuillemin, et al., 1997, Murray-Rust et al., 2009). However, it is not as potent at this as other non-endogenous polyanionic molecules, such as dextran sulfate. It is hoped that polyP may represent an endogenous molecule with a more potent ability to enhance C1-INH activity, and thus inhibit MASP-2 activity.

In order to better understand the effect of polyP on C1-INH activity against MASP-2, we utilized platelet-length (~70 units) polyP, and examined a range of concentrations to observe the effect of increasing polyP concentration on inhibition of MASP-2 by the serpin. A concentration range of 0-100 μM polyP was used against a 1:1 ratio of MASP-2 to C1-INH (final concentration of 500 nM wild-type MASP-2 to 500 nM C1-INH), and after incubation samples were analysed using SDS-PAGE.

PolyP (μM)
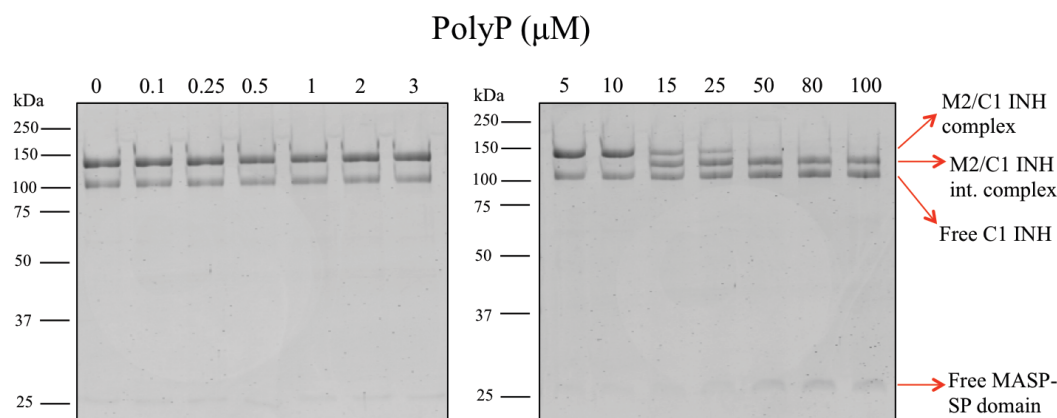
Figure 6.12: The effect of polyP addition to C1-INH activity against wild-type MASP-2. MASP-2 and C1-INH were incubated together in a 1:1 ratio, with increasing concentrations of polyP added (concentrations shown above each lane in the figure) to examine its effects upon C1-INH activity against MASP-2. The reaction was incubated at 37°C for 1 h, and then ended with reducing SDS loading buffer. Samples were then electrophoresed using 10% SDS-PAGE gels and stained using Coomassie blue R-250.

From the results, it appears that polyP is not having an effect on C1-INH activity against MASP-2 until a concentration between 10-15 μM is reached (Figure 6.12). At this concentration, polyP appears to be reducing C1-INH activity, as the amount of final MASP-2/C1-INH complex reduces with increasing polyP concentration, and the amount of intermediary MASP-2/C1-INH complex increases (Figure 6.12). In addition, the amount of free C1-INH and MASP-2 also rises with increasing polyP concentration (Figure 6.12).

In addition to SDS-PAGE analysis, the level of inhibition of MASP-2 activity by C1-INH with or without polyP was also examined through peptide substrate assays. In the assay, MASP-2 and C1-INH were both used at a final concentration of 50 nM to achieve a 1:1 ratio, and polyP was added at either a 0 or 100 μM concentration. After incubation, a final concentration of 50 μM of the peptide substrate LGR was added to the samples and a fluorescence plate reader used to test for any residual MASP-2 activity.
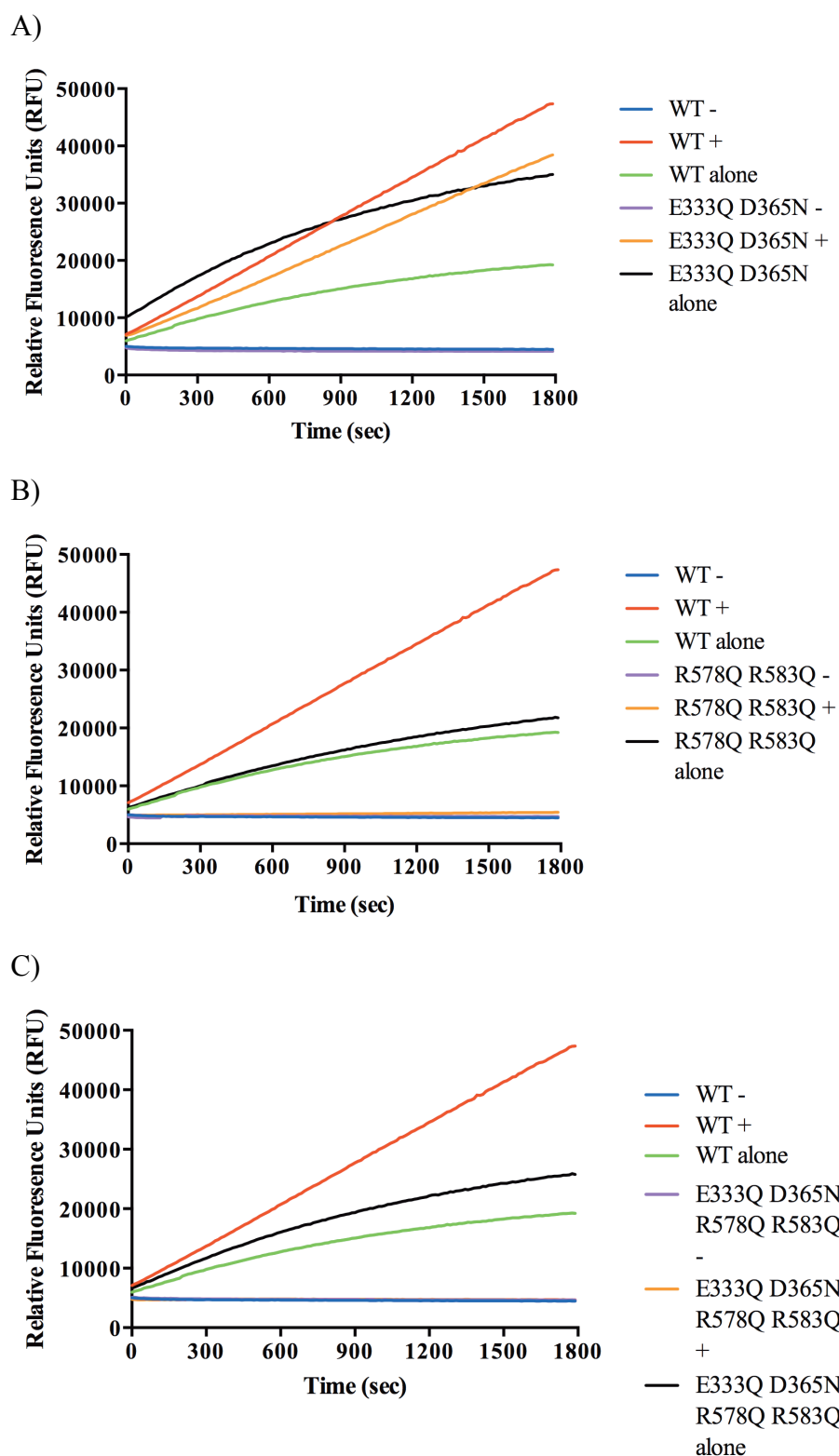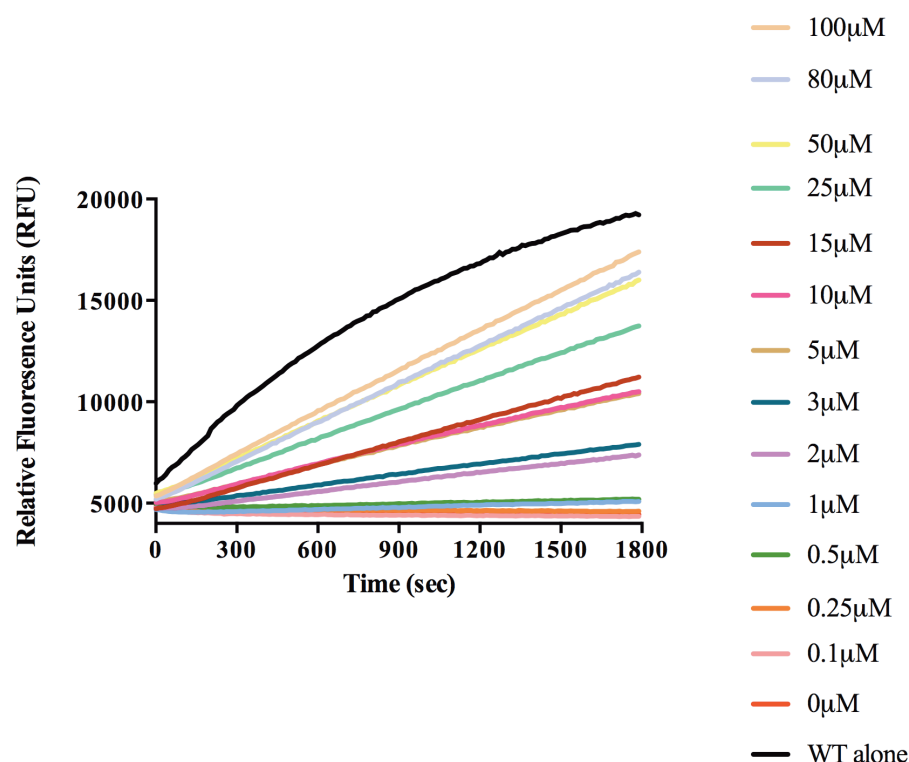
Figure 6.13: The effect of polyP addition on C1-INH activity against wild-type MASP-2 using a fluorescence plate reader. Using a fluorescence plate reader to read cleavage of the LGR peptide, the effect of polyP on inhibition of the activity of 500 nM wild-type MASP-2 by 500 nM C1-INH was examined. Alone = no C1-INH or polyP added.

The plate reader was able to detect residual MASP-2 activity from a concentration of 0.5 μM polyP, although this level of activity was very low until a concentration of 3 μM polyP was reached (Figure 6.13). The level of MASP-2 activity continued to rise with increasing polyP concentration, almost reaching the activity level of uninhibited MASP-2 at a polyP concentration of 100 μM (Figure 6.13). This indicates that polyP is indeed reducing the effectiveness of inhibition of MASP-2 by C1-INH. It was surprising, however, to see residual MASP-2 activity as early as 0.5 μM polyP, as SDS-PAGE analysis appeared to show no reduction in inhibition of MASP-2 activity by C1-INH until a polyP concentration between 10-15 μM was reached.

Therefore, it appears that polyP interferes with inhibition of MASP-2 activity by C1-INH, and that the level of interference increases as the concentration of polyP becomes higher.

6.9 Effects of platelet-length polyphosphate molecules on the inhibition of activity of selected MASP-2 CCP and SP domain exosite mutants by the serpin, C1 inhibitor

From the work completed in Section 6.8, it appears that increasing concentrations of platelet-size polyP (~70 units) reduces inhibition of wild-type MASP-2 activity by C1-INH. Given that the MASP-2 SP domain exosite double mutant (MASP-2 R578Q R583Q) and the quadruple mutant (MASP-2 E333Q D365N R578Q R583Q) were shown to be unable to bind polyP in the EMSA analyses completed, it was decided to examine if these mutants showed altered inhibition levels by C1-INH with increasing platelet-size polyP concentrations. In addition, the MASP-2 CCP domain exosite double mutant (MASP-2 E333Q D365N) was also examined, with the expectation that it would behave in a similar manner to wild-type MASP-2 based upon the results of the EMSA analyses.

The protocol followed was as completed in Section 6.5 with wild-type MASP-2, except that instead of a range of polyP concentrations, each mutant was examined using 0 and 100 μM polyP.
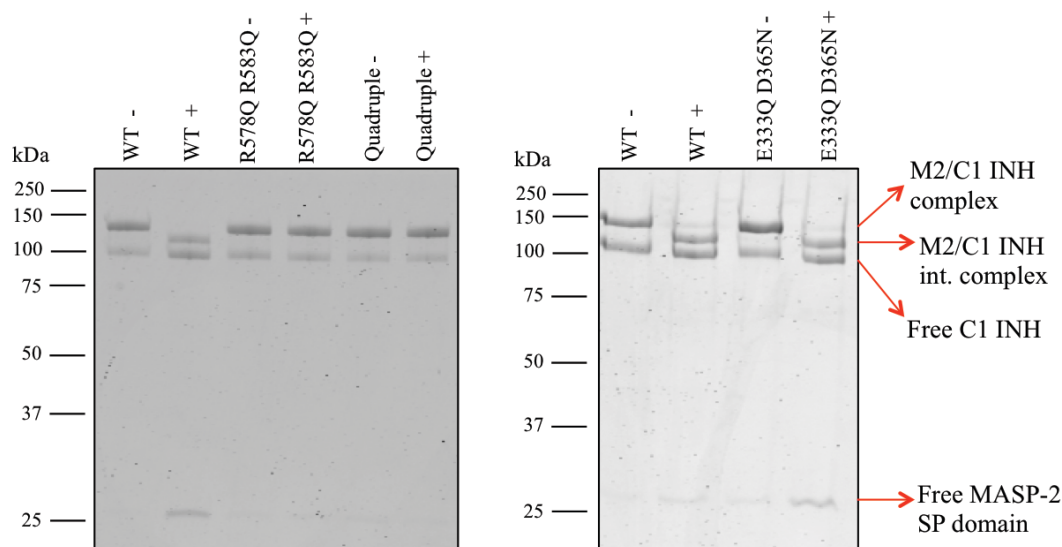
Figure 6.14: The effect of polyP addition on C1-INH activity against MASP-2 mutants. Selected MASP-2 CCP and SP domain exosite mutants and C1-INH were incubated together in a 1:1 ratio, with 0 or 100 μM polyP added to examine its effects upon C1-INH activity against the mutants. The reaction was incubated at 37°C for 1 h, and then ended with reducing SDS loading buffer and analysed using 10% SDS-PAGE. + = 100 μM polyP added, - = no polyP added.

With the EMSA results showing that it was capable of binding polyP, the MASP-2 CCP domain exosite double mutant E333Q D365N behaved in a very similar manner to wild-type MASP-2 (Figure 6.14). The results showed C1-INH exhibiting a reduced amount of complex formation against the mutant when 100 μM polyP was added, with increased levels of free C1-INH and MASP-2 being displayed, in addition to increased levels of intermediary MASP-2/C1-INH complex (Figure 6.14). These results suggest that C1-INH exhibits a reduced level of inhibitory activity against the mutant in the presence of polyP.

The MASP-2 SP domain exosite double mutant R578Q R583Q and the quadruple mutant E333Q D365N R578Q R583Q both showed no alteration in the levels of complex formed with C1-INH, even with the addition of 100 μM polyP (Figure 6.14). These results indicate that the presence of polyP does not affect C1-INH activity against these mutants. These findings correlate with the results of EMSA analyses, as both these mutants showed no binding of polyP, even at concentrations of 200 μM.

In addition to SDS-PAGE analysis, the level of inhibition of MASP-2 activity by C1-INH with or without polyP was also examined through peptide substrate assays. Following the protocol utilised in Section 6.5, MASP-2 and C1-INH were both used at a

final concentration of 50 nM to achieve a 1:1 ratio, and polyP was added at either a 0 or 100 μM concentration. After incubation, 50 μM of the peptide substrate LGR was added to the components and a fluorescence plate reader used to test for any residual activity of the MASP-2 mutants.

Readings taken from the plate-reader were in agreement with the results seen in the SDS-PAGE analysis (Figures 6.14 and 6.15). Without polyP, the activity of wild-type MASP-2 and all the mutants was completely inhibited by C1-INH at a 1:1 ratio, as no cleavage of the LGR peptide was detected by the plate reader (Figure 6.15). When 100 μM polyP was added, it led to a reduction in C1-INH activity against wild-type MASP-2 and the MASP-2 CCP domain exosite double mutant E333Q D365N, with cleavage of the LGR peptide being seen (Figure 6.15). However, addition of 100 μM polyP was shown not to reduce inhibition of the MASP-2 SP domain exosite double mutant R578Q R583Q and the quadruple mutant E333Q D365N R578Q R583Q by C1-INH, as no cleavage of the LGR peptide was detected (Figure 6.15).

From these results, it appears that polyP binding does reduce MASP-2 inhibition by C1-INH, as the two MASP-2 mutants containing SP domain mutations that are unable to bind polyP showed no alteration in inhibition of activity by C1-INH, while the MASP-2 CCP domain exosite mutant, which is capable of binding polyP, showed a reduction in inhibition of activity by C1-INH.
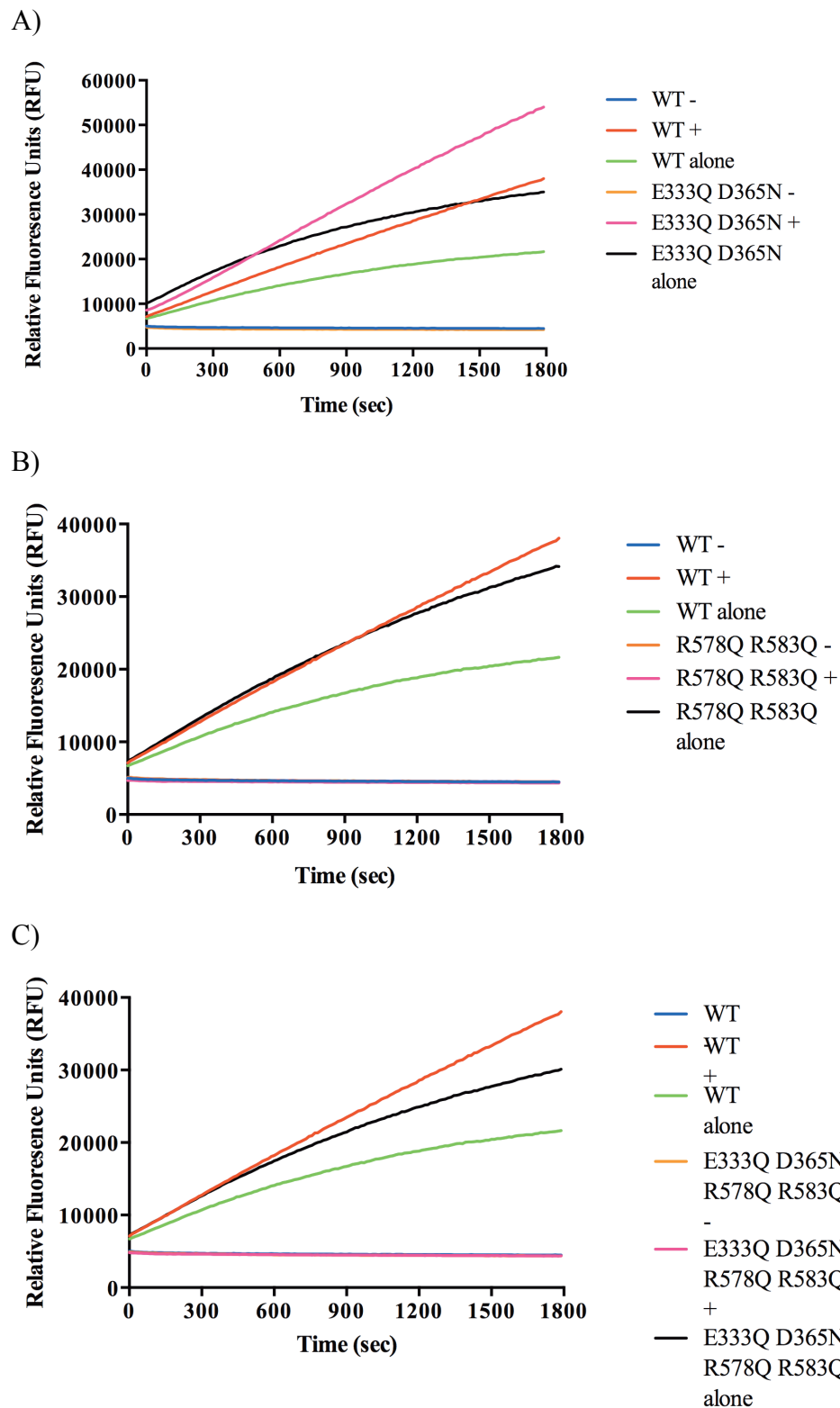
Figure 6.15: The effect of polyP addition on C1-INH activity against MASP-2 mutants using a fluorescence plate reader. Using a fluorescence plate reader to read cleavage of the LGR peptide, the effect of polyP on inhibition of the activity of selected MASP-2 mutants by C1-INH was examined. The MASP-2 mutants examined were A) MASP-2 E333Q D365N, B) MASP-2 R578Q R583Q and C) MASP-2 E333Q D365N R578Q R583Q. – = no polyP added, + = 100 µM polyP added, alone = no C1-INH or polyP added.

6.10 Effects of phosphate molecules on the inhibition of activity of selected MASP-2 CCP and SP domain exosite mutants by the serpin, C1 inhibitor.

In order to ensure that it was polyP molecules, not simple phosphate groups, leading to changes in inhibition of MASP-2 activity by C1-INH, the interaction between C1-INH and wild-type MASP-2, as well as the selected CCP and SP domain exosite mutants, was tested in the presence of 200 μM sodium phosphate. A similar protocol was used as in Sections 6.5 and 6.6 above, but with 200 μM sodium phosphate instead of polyP.

The results of SDS-PAGE analysis (Figure 6.16) and the peptide substrate assays performed on the fluorescence plate reader (not shown) indicated that the inhibitory activity of C1-INH against wild-type MASP-2 and the CCP and SP domain exosite mutants was not altered by the presence of phosphate. In SDS-PAGE analysis, C1-INH formed complexes with wild-type MASP-2 at similar levels in the presence of phosphate, and showed similar behaviour with the MASP-2 mutants. In peptide substrate assays, C1-INH activity against MASP-2 appeared to be unaffected by phosphate, as no MASP-2 activity was seen in the presence of phosphate for either wild-type MASP-2 or the MASP-2 mutants. These results show that it is the polyP molecules responsible for the changes in C1-INH activity against MASP-2 seen in previous experiments.
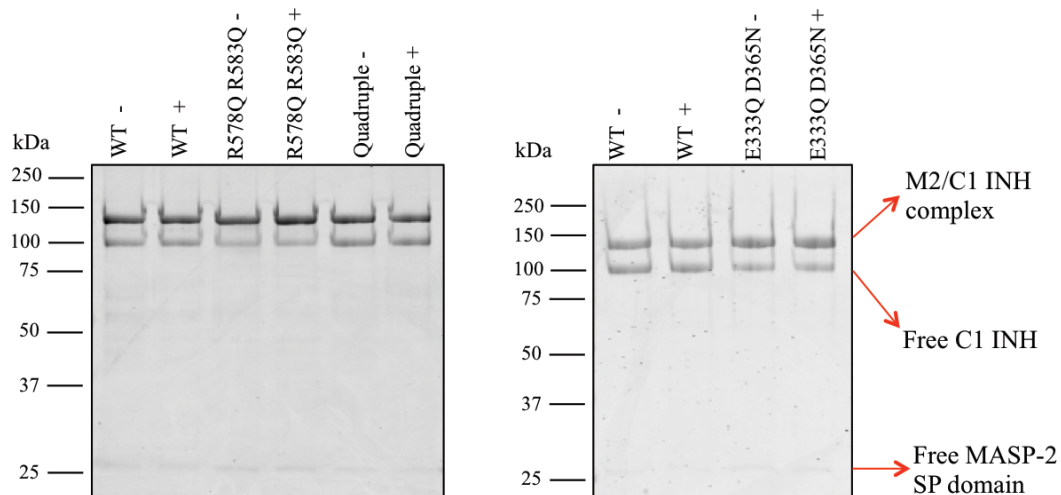
Figure 6.16: The effect of phosphate addition on C1-INH activity against MASP-2. Wild-type MASP-2, selected MASP-2 CCP and SP domain exosite mutants and C1-INH were incubated together in a 1:1 ratio, with 0 or 200 μM sodium phosphate added to examine its effects upon C1-INH activity against the mutants. The reaction was incubated at 37°C for 1 h, and then ended with reducing SDS loading buffer. It was then electrophoresed on 10% SDS-PAGE gels and stained using Coomassie blue R-250. + = 200 μM sodium phosphate added, - = no sodium phosphate added.

6.11 Discussion

The involvement of C1-INH in the complement system has been known for quite some time now. Initially, the focus was on C1-INH activity within the classical pathway, as it was not only recognized as an inhibitor of C1s and C1r, but also for its role in the disorder, HAE (Pensky et al., 1961, Landerman et al., 1962, Donaldson and Evans, 1963). However, its role in the lectin pathway has taken much longer to elucidate, with C1-INH only being recognized as an inhibitor of MASP-2 since more recently (Matsushita et al., 2000, Petersen et al., 2000). In fact, C1-INH has been found to exhibit a more rapid rate of inhibition against MASP-2 than C1s, with the first order rate of association between MASP-2 ad C1-INH being 50-fold faster than that between C1s and C1-INH (Kerr et al., 2008). Given that MASP-2 activity has been linked to causing damage during a number of inflammatory events, such as during myocardial and gastrointestinal ischemia/reperfusion injury, manipulation of C1-INH activity to regulate MASP-2 activity represents a potential treatment angle in the case of such events (Schwaeble et al., 2011).

C1-INH activity is modulated by a number of different polyanions, both endogenous and synthetic (Wuillemin et al., 1997. Murray-Rust et al., 2009). Of the endogenous polyanions found to alter C1-INH activity, heparin has so far been identified

as the most potent. Heparin has been shown to potentiate C1-INH activity against C1s, where it led to a reduced amount of peptide cleavage (Murray-Rust et al., 2009). Its effects on C1-INH activity against MASP-2 are much less understood, but it appears that the effects of heparin potentiation on C1-INH activity against MASP-2 are much lower (Parej et al., 2013). Another naturally occurring polyanion, polyphosphate (polyP), has recently been identified as influencing complement pathway activity by binding to complement components C5b and C6, and so represents another potential polyanion that could modulate C1-INH activity (Wat et al., 2014). At this point in time, no literature has been published to confirm the interaction between MASP-2 and polyP. The aim of this study was to determine if heparin and polyP were capable of binding to MASP-2, and to characterize the effects of each polyanion upon C1-INH activity against MASP-2.

From the EMSA analyses and heparin-affinity chromatography, we were able to discern that MASP-2 is indeed capable of binding polyP and heparin. In addition to this, through the use of the MASP-2 CCP and SP domain exosites, we were also able to discern approximately where the binding site for each polyanion on MASP-2 is located. Both polyP and heparin appear to utilize the SP domain exosite of MASP-2 for binding. The MASP-2 SP domain exosite seems to form part of the polyP binding site, as in the EMSA analyses simultaneous mutation of the residues R578 and R583 eliminates polyP binding to MASP-2, even at high polyP concentrations. This indicates that these residues play a dominant role in the binding of polyP by MASP-2. However, in heparin binding, the same mutation causes MASP-2 to be eluted from the heparin column at a lower salt concentration, but did not abrogate binding completely. This indicates that while the SP domain exosite residues R578 and R583 play a role in heparin binding, and do form part of the heparin-binding site, they make a lesser contribution to heparin binding than to polyP binding. It is possible that other SP domain exosite residues, K450 and K503, also contribute to the heparin-binding site of MASP-2. The MASP-2 CCP domain exosite appears to not play a role in either heparin or polyP binding, as none of the CCP domain exosite single mutants or the double CCP domain exosite mutant displayed altered binding of either polyanion when compared to wild-type MASP-2. This echoes the finding of the heparin-binding site on factor XIa, in which a group of positively charged residues on the 170 loop of the trypsin-like catalytic domain contribute to forming a heparin-binding site (Yang et al., 2009). In addition, Duncan *et al.* (unpublished results) found that mutation of the SP domain exosite caused C1s to be unable to bind to the column during heparin-

affinity chromatography, which indicates that the SP domain exosite was a major contributor to the heparin-binding site. If all four residues of the SP domain exosite were mutated simultaneously, it is likely that MASP-2 would be rendered unable to bind heparin, such was seen with C1s (Duncan et al., unpublished). The results from the EMSA analyses add weight to the 'sandwich' interaction theory proposed by Beinrohr *et al.* (2007), as the positively charged SP domain exosite of MASP-2 would be attracted to the negatively charged environment caused by heparin or polyP binding to C1-INH.

Past research has shown that heparin, among other polyanions, is capable of binding to C1s, and that within the complement system it potentiates C1-INH activity against C1s (Nilsson and Wiman, 1983, Wuillemin et al., 1997. Murray-Rust et al., 2009), as well as C1r to a lesser degree (Sim et al., 1980). As discussed earlier, initial work has suggested that heparin also modestly enhances C1-INH activity against MASP-2 (Parej et al., 2013). Given the effects of polyP on components of the terminal complement pathway, it was hypothesized that polyP would also enhance C1-INH activity against MASP-2 (Wat et al., 2014). However, in this study, the effects of polyP and heparin on C1-INH activity against MASP-2 do not appear to agree with this hypothesis. Increasing polyP and heparin concentrations led to a reduced level of C1-INH activity against MASP-2, with more intermediary MASP-2/C1-INH complex being seen in SDS-PAGE analysis, as well as increased levels of free C1-INH and MASP-2. Peptide substrate assays confirmed SDS-PAGE results, with an increase in peptide substrate cleavage being seen with increasing heparin and polyP concentrations, indicating incomplete C1-INH inhibition of MASP-2. The gels and peptide substrate assays also helped to confirm the role of the SP domain exosite in heparin and polyP binding. The SP domain exosite double mutant and the quadruple mutant, both of which were shown to be unable to bind polyP, showed no reduction in inhibitory activity by C1-INH against MASP-2 in either SDS-PAGE analysis or peptide substrate assays when 100 μM polyP was added to the reaction. Addition of 50 μg/mL heparin led to a very slight reduction in C1-INH activity against the MASP-2 SP domain exosite double mutant and the quadruple mutant, on both the gels and in the peptide substrate assays. However, this reduction in C1-INH activity against MASP-2 was very small, especially when compared to the reductions seen with wild-type MASP-2.

The explanation for the differences in the results seen in this study, and those achieved by Parej *et al.* (2013) is unlikely to be the size of heparin molecules used.

Evidence appears to suggest that the 'sandwich' mechanism of interaction characterizes the interaction between C1-INH, its target proteases and heparin, as Rossi *et al.* (2010) found that 10 saccharide unit heparin was enough to reach 50% potentiation of C1 inhibitor activity (Rossi et al., 2010). This is much smaller than would be required for another mode of interaction utilised by heparin to enhance serpin activity, the bridging mechanism (Beinrohr et al., 2007, Rossi et al., 2010). In this mechanism, the polyanion must be of a certain length to successfully enhance serpin activity, as it acts as a 'bridge' between the serpin and its protease substrate to speed the formation of the Michaelis complex and stabilize it (Beinrohr et al., 2007). A classic example of this interaction can be seen with the serpin antithrombin and how heparin enhances activity against its target protease, thrombin (Pike et al., 2005, Olson et al., 2010). Therefore, it is unlikely that the size of the heparin and polyP molecules used contributed to the differences in results seen in this study and by Parej *et al*. (Parej et al., 2013). One potential heparin characteristic that could contribute to the discrepancies seen between the results of this study and those by Parej *et al.* (2013) may lie in the source of heparin utilised. Parej *et al.* (2013) used heparin from bovine intestinal mucosa to perform their experiments, while in this study heparin from porcine intestinal muscosa was used (Parej et al., 2013). Heparin is a highly variable molecule, and its characteristics have been seen to vary even between closely connected tissues. For instance, the composition of heparin from porcine intestinal mucosa has been shown to possess less contamination from heparan sulfate that heparin obtained from the entire intestine (Linhardt and Gunay, 1999). Therefore, there could be variations between the heparin obtained from porcine and bovine intestinal mucosas that contribute to the differences in results obtained in this study and by Parej *et al*. (2013), such as with the level of sulfation. Murray-Rust *et al.* (2009) showed that reduced heparin sulfation levels lead to reduced binding to C1s, so this may potentially also occur with MASP-2 and C1-INH (Murray-Rust et al., 2009). Experiments comparing the effects of different sulfation levels on the interaction between heparin, C1-INH and MASP-2, such as done by Murray-Rust *et al.* (2009) would determine if heparin sulfation levels do in fact influence heparin binding to C1-INH and MASP-2, and what effects this may have on heparin potentiation of C1-INH against MASP-2.

Another potential explanation for these results may be the surface charge of the SP domain of MASP-2. Beinrohr *et al.* (2007) examined the effects of heparin on C1-INH activity against some of its other substrates, and saw that the more negative the surface

charge of the area surrounding the active site of the protease, the less potent the effects of heparin upon C1-INH activity (Beinrohr et al., 2007). Factor XIa has a very positively charged surface surrounding the active site, and heparin has a much more potent effect upon C1-INH activity against it (Wuillemin et al., 1996, Mauron et al., 1998). Factor XIIa on the other hand, has a very negatively charged contact surface, and heparin actually leads to a ~ 2-4 fold reduction in C1-INH activity against it (Wuillemin et al., 1996). Despite the presence of the positively charged SP domain exosite, MASP-2 is more neutral to negatively charged in the area surrounding its active site, (more so than C1s), and so theoretically would be attracted to the positively charged region under the RCL of C1-INH without the use of heparin. Heparin and polyP indeed could interfere with the interaction by altering the charge of this region to a negative one, thus causing repulsion between MASP-2 and C1-INH. This would explain the reduction in C1-INH activity against MASP-2 with the addition of heparin and polyP seen in this study. Further work in examining the influence of polyP and heparin on the kinetics of the interaction between MASP-2 and C1-INH, such as the effect on the rate of protease inhibition, would provide valuable information in characterizing the contributions of each polyanion to the interaction to determine if this was indeed the case.

Heparin and polyP were shown to bind to MASP-2 in this study. This raises the question of whether this binding affects the cleavage rate of MASP-2, and whether their binding to MASP-2 could potentially lead to cleaving of the RCL of C1-INH by MASP-2 in a suboptimal position, thus leading to reduced formation of the final C1-INH/MASP-2 inhibitory complex. The potential ability of heparin and polyP to enhance the cleavage rate of MASP-2 could be examined through activity assays, as well as through examining their effects on the S.I. of C1-INH for MASP-2. This would allow us to discern with more specificity the effects of heparin and polyP binding on the cleavage rate of MASP-2.

This study has demonstrated that the polyanions heparin and polyP are capable of binding to MASP-2, and that the SP domain exosite contributes to the binding sites of both heparin and polyP on MASP-2. These polyanions were seen to reduce the level of C1-INH activity against MASP-2, rather than enhance it, potentially due to the surface charge surrounding the active site of MASP-2. Further work is required to properly characterize the influence of heparin and polyP on C1-INH activity against MASP-2 if they are to be considered for use in a clinical setting.

Chapter 7

'General Discussion and Future Directions'

The complement system is of ancient origin, with the various genes encoding common complement system domain motifs, such as the CUB, EGF, CCP and SP domain motifs that make up MASP-2, being found in the cnidarian genome (Kimura et al., 2009). In the history of complement research, the lectin complement pathway is a relative newcomer, with activation of the pathway first being observed in MBL-dependent activation of C4 in 1987 (Ikeda et al., 1987). The research that has consequently followed this discovery has allowed a solid understanding of lectin pathway function to be garnered, especially on the serine proteases, MASP-1 and MASP-2. However, despite a steady increase in the understanding of the function of MASP-2 in the lectin complement pathway, structural and kinetic characterisation of the interaction between MASP-2 and its substrates C2 and C4 has proven somewhat more elusive.

As discussed previously, for a number of years, it was hypothesized that MASP-2 contained a binding exosite for C4, with research strongly suggesting that it would be located on the CCP domains (Rossi et al., 2001, Ambrus et al., 2003, Harmat et al., 2004, Rossi et al., 2005). In an early attempt to better understand the interaction of MASP-2 and C4, Harmat *et al.* (2004) produced a proposed model of interaction between MASP-2 and the C4d domain of C4 using the crystal structures of MASP-2 and C4 that had been solved at the time. In this model, the MASP-2 CCP2 domain residues E378, R376, E376 and E398 were thought to interact with C4 (Harmat et al., 2004). The location of this CCP domain exosite was elucidated in 2012, with Kidmose *et al.* (2012) releasing the structure of MASP-2 in complex with C4 (Kidmose et al., 2012). The exosite was found to span across the C-terminal region of the CCP1 domain, the linker region between the CCP domains, and across to the N-terminal of the CCP2 domain, and was found to consist of residues E333, P340, D365 and P368. In addition, a potential SP domain exosite, flagged as consisting of MASP-2 residues K450, K503, R578 and R583, was seen within the structure of the complex. While the structure clearly illustrated the location of the two MASP-2 exosites, limited kinetic work was completed only on the CCP domain exosite. The present study sought to further clarify and quantify the kinetic mechanism of interaction between MASP-2 and C4 through examination of these exosites.

The CCP domain exosite showed a clear contribution to efficient C4 cleavage. Mutation of residues E333 and D365 to create charge neutralized and charge reversal single mutants caused an increase in EC_{50} value of ~ 2.5-8 fold, with the charge reversal

mutations causing the largest increase in EC_{50} value. Given that residues E333 and D365 have been shown to interact with positively charged residues on C4 (such as E333 interacting with the C4 residue R1724), the large increases in EC_{50} value seen with the charge reversal mutations were likely due to charge repulsion, caused by inserting a similarly charged amino acid, such as arginine, at these locations on MASP-2. Mutation of both residues simultaneously in the form of the E333Q D365N double mutant led to even greater increases in EC_{50} value, showing ~ 6-17 fold increases in EC_{50} value. This suggests that the impact of each residue contributing to the exosite is cumulative, with each additional mutation further eroding the ability of the exosite to ensure efficient cleavage of C4 by MASP-2. The time courses for C4 cleavage echoed these results, with the double mutant E333Q D365N only reaching 55% cleavage in 2 h compared to the two single mutants E333Q and D365N, which, despite displaying a slower cleavage rate over the time course, still managed to achieve over 90% C4 cleavage by 2 h. These results concur with the results of C4b deposition assays performed by Kidmose *et al.* (2012) on mutants of the CCP domain exosite, with the MASP-2 E333R D365R double mutant exhibiting a much larger reduction in C4b deposition than the two single mutants (Kidmose et al., 2012). When the ability of the double mutant MASP-2 E333Q D365N to bind C4 was examined using SPR, a 7-fold increase in the K_D value was seen, indicating a reduced affinity between MASP-2 and C4. In analyses according to a two-state binding model, a 10-fold reduction in K_1 and a 6-fold reduction in the overall association rate constant for the entire reaction, K_a, is seen. This suggests that the CCP domain exosite is playing a key role in the first association event between enzyme and substrate. Therefore, the CCP domain exosite appears to act like an initial hotspot to promote the correct orientation between C4 and MASP-2 during the first contact event between the enzyme and substrate. Without it, MASP-2 appears to experience greater difficulty in orientating itself correctly with C4, which leads to a reduction in cleavage efficiency.

The revelation of a potential SP domain exosite on MASP-2 for C4 was an unexpected finding. Of the four residues highlighted by Kidmose *et al.* (2012) as potentially forming the exosite (K450, K503, R578 and R583), only R578 and R583 were found to contribute significantly to C4 binding and cleavage. This was a surprise, as these residues are not shown to directly interact with the sulfated tyrosines of C4 in the MASP-2/C4 complex structure, while residue K503 is shown to be interacting with the sulfated tyrosine residue 1417. This suggests that there may be other conformations that MASP-2

and C4 can exist in, which is given more weight by the fact that the area of C4 containing the sulfated tyrosines is not complete within the structure (only two of the three sulfated tyrosines are visible), indicating a flexibility within this region. It would be of great interest for further work to be done on these single residue mutations to more fully assess their sulfated tyrosine binding capabilities, such as was done by Duncan *et al.* (2012b) in their examination of the C1s SP domain binding exosite (Duncan et al., 2012b).

With a results pattern echoing those seen with the CCP domain exosite, the single mutations R578Q and R583Q recorded increases in EC_{50} value of ~ 2 to 3-fold, while the double mutant MASP-2 R578Q R583Q showed a ~ 13-28-fold increase in EC_{50} value over that of wild-type MASP-2. The time courses for C4 cleavage reflected these results, with the double mutant R578Q R583Q only reaching ~ 55% cleavage in 2 h compared to the two single mutants R578Q and R583Q, which, despite a slower cleavage rate, still managed to achieve over 80% C4 cleavage by 2 h. Analysis of C4 binding by the double mutant R578Q R583Q using SPR yielded some very different results to the double CCP domain exosite mutant. Like the CCP domain exosite mutant, the double mutant R578Q R583Q experienced an increase in K_D value of 6-fold. This signals that the loss of the SP domain exosite led to a reduced affinity between MASP-2 and C4. In analyses using a two-state binding model, the overall association rate constant (K_1) for the first step of the reaction and the overall association rate constant for the entire reaction (K_a) were mildly altered, indicating that the SP domain exosite plays only a moderately important role in the initial association between MASP-2 and C4. However, the conformational change constant (K_2) value decreased ten-fold for the R578Q R583Q mutant, indicating that the SP domain exosite plays a major role in the conformational change required to achieve a high affinity complex between MASP-2 and C4. Therefore, it appears that after MASP-2 binds C4, mainly using the CCP domain exosite, it then utilises the SP domain exosite to correctly orientate the SP domain to ensure the best possible conformation for optimal C4 cleavage by the active site.

The double mutants allowed us to examine how MASP-2 binding and cleavage of C4 was affected by the loss of each exosite, with the data showing that while the loss of each exosite has a negative impact on efficient C4 binding and cleavage by MASP-2, the enzyme is still able to overcome the loss of the exosite and retain some functionality. The creation of the quadruple mutant MASP-2 E333Q D365N R578Q R583Q allowed us to

examine MASP-2 binding and cleavage of C4 when both exosites were impacted simultaneously. The results clearly show that while MASP-2 may be able to compensate to a degree with the loss of a single exosite, the loss of both exosites simultaneously proves harder to overcome. The quadruple mutant showed severely reduced C4 cleavage, barely reaching 10% cleavage during the cleavage time course and recording EC_{50} values that were over 600-fold higher than those recorded by wild-type MASP-2. When the C4 binding abilities of the quadruple mutant were examined using SPR, it was found that the mutant was unable to bind C4. These results show the effects of exosite loss for MASP-2 are cumulative in nature- while the loss of one exosite may lead to moderately reduced efficiency in C4 binding and cleavage, loss of both exosites leads to far more severe effects.

From the studies, it is clear that these two exosites on MASP-2 play an important role in C4 binding and cleavage. Perhaps then the most logical question to be considered next is the role of these exosites in the binding and cleavage of MASP-2's other complement pathway substrate, C2. Thus far, the roles of these exosites in C2 binding and cleavage by MASP-2 are as yet unknown. Preliminary experimental findings suggest that the SP domain binding exosite is also important in ensuring efficient C2 binding and cleavage by MASP-2 (unpublished results from host laboratory). This is not unsurprising, as previous findings have shown that C2 binding and cleavage requires only the SP domain of MASP-2 (Ambrus et al., 2003, Rossi et al., 2005, Duncan et al., 2012). Based on this, one would therefore hypothesise that while the SP domain exosite will play an important role in efficient C2 binding and cleavage, the CCP domain exosite will not.

In addition to considering the effects of the MASP-2 exosites on C2 binding and cleavage, the effects of these exosites upon MASP-2 binding and cleavage of its coagulation cascade substrate, prothrombin, should also be considered (Krarup et al., 2007). At this point in time, no structure of MASP-2 and prothrombin in complex has been produced, and little is known about the kinetics and mechanism of the interaction. It is therefore an open book as to if and how each MASP-2 exosite affects the binding and cleavage of prothrombin by MASP-2. Most of the techniques used to study C4 binding and cleavage by MASP-2 in this study have the versatility to be refined for use in studying prothrombin binding and cleavage by MASP-2.

The characterization of the kinetic interaction of the MASP-2 CCP and SP domain exosites and C4 also provides valuable insight for potential therapeutic use. As discussed earlier, MASP-2 has been highlighted as a contributor to physiological damage in certain inflammatory conditions, such as myocardial and gastrointestinal ischemia/reperfusion injury, where MASP-2 deficient mice showed smaller infarct volumes (Schwaeble et al., 2011). MASP-2 has also been linked to ischemia-related necrotic myocardial injury (Zhang et al., 2013). Understanding the role that each exosite plays in the kinetic interaction between MASP-2 and C4 allows for the potential development of therapeutics such as small-molecule inhibitors and antibodies to regulate MASP-2 activity through these exosites. Temporary downregulation of MASP-2 activity during inflammatory events could serve to reduce the physiological damage MASP-2 has been shown to contribute to, which would lead to a better outcome for patients. Regulation of MASP-2 activity through its exosites provides a more targeted avenue of disease prevention and/or treatment than another form of MASP-2 activity regulation- the manipulation of C1 inhibitor activity. C1-INH is a serpin with a number of roles both within the complement pathway and outside it, such as the coagulation, fibrinolysis and contact pathways (Walford and Zuraw, 2014). Therefore, manipulation of C1-INH activity has a very real potential to disrupt multiple biological pathways in the body, which leads to an increased risk of unwanted side effects.

MASP-2 has a number of naturally occurring polymorphisms that occur in differing frequencies throughout the human population. Some, such as the D120G and R439H mutations, have been better characterized, and so the effects of the mutation on MASP-2 functionality are better understood (Thiel et al., 2007, Thiel et al., 2009). Characterisation of these naturally occurring MASP-2 polymorphisms provides an opportunity for a deeper understanding of MASP-2 and its interactions and functioning. The polymorphisms often expose locations on the enzyme that are critical for interaction with other complement components, such as the D120G and P126L mutations leading to MASP-2 being unable to bind MBL (Thiel et al., 2007. Thiel et al., 2009). They also uncover sites on the enzyme critical for MASP-2 functioning, such as the R439H mutation preventing MASP-2 from being able to activate (Thiel et al., 2009). It is therefore a worthwhile endeavor to characterize the various naturally occurring polymorphisms found in MASP-2, as it may present more targets for fine therapeutic targeting of MASP-2. In addition, it is also feasible, given the small number of polymorphisms in MASP-2 that naturally occur.

Of the naturally occurring MASP-2 polymorphisms, the D371Y mutation of the CCP2 domain has been linked to an increased susceptibility to certain infectious diseases and infectious disease complications. It has not as yet been characterized on a functional basis. Therefore, an aim of this study was to make the first attempt to characterize the functionality of this mutant in a number of areas critical for MASP-2 activity. This study shows that the mutation most likely does not affect the ability of MASP-2 to fold correctly, nor does it affect active site stability, as similar yields of the enzyme were obtained after refolding compared to wild-type MASP-2 and the mutant exhibited similar kinetics compared to wild type enzyme in cleaving the C4 P4-P4' peptide substrate. The mutation also caused no difference in activation of MASP-2 either by MASP-1 or MASP-2. Its cleavage of C2 and C4 was also not significantly different to that of wild-type MASP-2. It therefore appears that the D371Y mutation does not affect the ability of MASP-2 to fulfill its role in the complement system. If this mutation has an impact on MASP-2 activity, it is more likely to occur in a role performed by MASP-2 outside of the complement system. At this point in time, MASP-2 has also been shown to bind and cleave prothrombin to thrombin (of the coagulation system), which cleaves complement components C3 and C5 to produce C3a and C5a. The latter peptides bind to the receptors C3aR and C5aR1, respectively, and influence the expression of IL-12 by Antigen Presenting Cells (APC) (Krarup et al., 2007, Kolev et al., 2014). This potentially could alter the direction of the adaptive immune response, which, if not optimal, may lead to increased infection risk and reduced pathogen clearance abilities. This study therefore demonstrated that the effects of MASP-2 polymorphisms may not always directly affect its ability to function in the complement system, but instead may have a ripple effect in other biological pathways to which MASP-2 has links.

Control of complement pathway activity is a complex and finely tuned activity. The serpin C1-INH plays a critical role in the control of both the classical and lectin pathways, as it acts as an inhibitor for the proteases C1r, C1s, MASP-1 and MASP-2 (Arlaud et al., 1979, Matsushita et al., 2000), as well as inhibiting enzymes in other pathways, such as factor XIIa and kallikrein of the contact pathway (Schapira et al.,1982, Pixley et al., 1985). The binding of small polyanionic molecules to C1-INH has been shown to influence its activity. The best-known physiological example of this is the polyanionic glycosaminoglycan (GAG), heparin. A molecule normally associated with the coagulation pathway, heparin has been shown to potentiate C1-INH activity against a number of

complement system proteases, such as C1s and C1r (Sim et al., 1980, Murray-Rust et al., 2009). Although little work examining the effects of heparin on C1-INH inhibition of MASP-1 and MASP-2 activity has been done, the work published appears to indicate that heparin also potentiates C1-INH activity against MASP-1 and MASP-2 (Parej et al., 2013).

Use of polyanions to potentiate C1-INH activity against complement components is an idea that has been floated for some time as a treatment for certain Hereditary Angioedema (HAE) sufferers, and, given the more recent link between MASP-2 activity and damaging during events of myocardial and gastrointestinal ischemia reperfusion injury, as well as the link to ischemia-related necrotic myocardial injury, it also poses a potential method for reducing complement activity during these events (Murray-Rust et al., 2009, Schwaeble et al., 2011, Zhang, M et al., 2013). However, potentiation of C1-INH activity by other non-physiological GAGs, such as dextran sulfate, has been shown to be far greater than that produced by heparin (Wuillemin et al., 1997, Murray-Rust et al., 2009). These synthetic molecules may produce unwanted side effects, such as the charged nature of the dextran-sulfate molecule DXS5k, a candidate for the pharmacological manipulation of C1-INH activity against the complement system, potentially leading to thrombocytopenia (Murray-Rust et al., 2009). The finding that the polyanionic molecule, polyphosphate (polyP), is able to control complement pathway activity by directly binding to complement components C5b and C6 has revealed the presence of a new endogenous polyanion that can exert control over complement system activity (Wat et al., 2014). It is hoped that polyP may represent a more potent naturally occurring molecule for pharmacological manipulation of C1-INH activity. This study aimed to lay some of the initial groundwork in determining if polyP represents a molecule with the potential of altering MASP-2 activity through binding and potentiation of C1-INH activity against MASP-2.

This study found that MASP-2 is able to bind polyP, and that the SP domain, in particular the region containing the exosite, appears to house the polyP-binding site, as the SP domain exosite double mutant MASP-2 R578Q R583Q and the quadruple mutant MASP-2 E333Q D365N R578Q R583Q were shown to be unable to bind polyP in EMSA analyses. In addition, MASP-2 was also shown to bind heparin through the use of heparin affinity chromatography. Although heparin has been shown to bind to a number of complement components, its binding to MASP-2 at this point has not yet been shown.

Interestingly, the SP domain exosite was also shown to comprise at least a part of the heparin-binding site on MASP-2. However, it appears to contribute less to the heparin binding site than to polyP binding site, as despite displaying altered elution profiles to wild-type MASP-2, the SP domain exosite double mutant and the quadruple mutant were still able to bind heparin. Further studies into the binding of polyP to other complement components from all three pathways would be extremely interesting information. At this point in time, Wat *et al.* have shown that polyP is active in the final steps of complement pathway activity, as it is capable of binding to and destabilizing molecules C5b and C6, leading to reduced MAC binding to and lysing of the target cell. They showed this targeting is very specific, as polyP was shown not to bind C5 or C7 (Wat et al., 2014). In this study, we have shown that polyP is also capable of binding MASP-2. This signals that polyP may also be capable of binding complement molecules at earlier stages of the complement pathways. Another potential polyP target is C1s, as it also contains an SP domain exosite (Duncan et al., 2012b). Given that the SP domain exosite of MASP-2 has been shown to form part of the polyP binding site, it is a reasonable assumption that the SP domain exosite of C1s may also play a similar role in polyP binding. Whether polyP is capable of binding other serine proteases of the complement system, such as MASP-1, MASP-3 and C1r, cannot yet be predicted, as at this point in time there is no knowledge of the existence of exosites upon these proteases. Further work examining the binding of polyP to various complement components is required to determine whether polyP exerts a wide influence in the complement system through its binding to components, or if its sphere of influence is more specialized.

Contrary to expectations, both polyanions displayed an inhibitory effect against C1-INH. When inhibition of wild-type MASP-2 activity by C1-INH was examined, it was found that C1-INH activity against MASP-2 decreased as the concentration of polyP and heparin increased. The CCP domain exosite double mutant exhibited similar behavior to wild-type MASP-2, indicating that the CCP domain exosite is not involved in heparin or polyP binding. However, the behaviour of the SP domain exosite double mutant or the quadruple mutant in the presence of heparin and polyP was vastly different. When polyP was added, no change in C1-INH activity could be detected either on SDS-PAGE gels or in peptide substrate assays. There was a very slight reduction in C1-INH activity against MASP-2 when higher concentrations of heparin were added, as some free MASP-2 could be seen on the SDS-PAGE gels, and a very small amount of activity was seen in peptide

substrate assays carried out using a fluorescence plate reader, which indicates that MASP-2 was not fully inhibited by C1-INH. The results confirm that the SP domain exosite is involved in both the binding of heparin and polyP to MASP-2, while the CCP domain exosite is not. It will be interesting to see if these results are confirmed when examining the effects of heparin and polyP on inhibition of MASP-2 C2 and C4 cleavage by C1-INH.

As discussed earlier, the negatively charged nature of the area surrounding the active site of MASP-2 may be the reason why heparin and polyP are not potentiating C1-INH activity against MASP-2. The binding of these polyanions to the contact surface of C1-INH would lead to repulsion between C1-INH and MASP-2, as the contact surfaces of both molecules would be of a similar charge thanks to the binding of polyanions. These results indicate that more work is required to properly characterize the effects of heparin and polyP upon C1-INH activity against MASP-2. In particular, the effect of polyP size on the interactions needs to examined closely. Research done so far seems to indicate that polyP size is an important factor in determining the effect it has on an interaction in the coagulation system. For example, platelet-sized polyP (70-120 unit) is more adept at the acceleration of blood clotting (i.e. by promoting factor V activation) than in instigating it (i.e. poor triggering of the contact pathway of clotting) (Morrissey et al., 2012). Hence, an understanding of the effects of different sized polyP molecules on an interaction is paramount. PolyP molecule size also appears to be important to its suppression of complement activity. PolyP molecules under 30 units had a much less potent suppressive effect on terminal pathway activity, whereas polyP molecules of 40-60 units and over 1000 units were both shown to suppress terminal pathway activity at a similar level. Therefore, a solid understanding of the properties of polyP size in different pathways is an important requirement to be fulfilled before it can be at all considered for clinical use. As heparin potentiation of C1-INH has been shown to vary depending on whether MASP-2 was in an MBL or H-ficolin complex, this characterisation of polyP needs to cover a broad range of potential biological situations so that we can more fully understand its behavior in different biological circumstances (Parej et al., 2013). Once we have a greater understanding of the characteristics of polyP and how they contribute to its interactions with C1-INH and MASP-2, will we be able to determine if it is a suitable molecule for therapeutic manipulation of MASP-2 activity through C1-INH.

Overall, the work completed in this study demonstrates the importance of the CCP and SP domain exosites of MASP-2 in ensuring efficient binding and cleavage of C4 by MASP-2. It also showed that polyP is able to bind MASP-2, and reduces C1-INH activity against MASP-2, thus demonstrating another layer of control in the lectin complement pathway. From this, a deeper understanding of the kinetic mechanism of interaction between MASP-2 and C4, as well as a broadened understanding of the control of MASP-2 activity has been reached, and represents important information for future studies of the role of MASP-2 in disease, as well as for drug design in potential future therapeutics.

'References'

AMBRUS, G., GAL, P., KOJIMA, M., SZILAGYI, K., BALCZER, J., ANTAL, J., GRAF, L., LAICH, A., MOFFATT, B. E., SCHWAEBLE, W., SIM, R. B. & ZAVODSZKY, P. 2003. Natural substrates and inhibitors of mannan-binding lectin-associated serine protease-1 and -2: a study on recombinant catalytic fragments. *J Immunol,* 170**,** 1374-82.

ARIKI, S., TAKAHARA, S., SHIBATA, T., FUKUOKA, T., OZAKI, A., ENDO, Y., FUJITA, T., KOSHIBA, T. & KAWABATA, S. 2008. Factor C acts as a lipopolysaccharide-responsive C3 convertase in horseshoe crab complement activation. *J Immunol,* 181**,** 7994-8001.

ARLAUD, G. J., REBOUL, A., SIM, R. B. & COLOMB, M. G. 1979. Interaction of C1-inhibitor with the C1r and C1s subcomponents in human C1. *Biochim Biophys Acta,* 576**,** 151-62.

ARLAUD, G. J. & COLOMB, M. G. 1987. Modelling of C1, the first component of human complement: towards a consensus? *Mol Immunol,* 24**,** 317.

ARLAUD, G. J., GABORIAUD, C., THIELENS, N. M., ROSSI, V., BERSCH, B., HERNANDEZ, J. F. & FONTECILLA-CAMPS, J. C. 2001. Structural biology of C1: dissection of a complex molecular machinery. *Immunol Rev,* 180**,** 136-45.

ASGARI, E., FARRAR, C. A., LYNCH, N., ALI, Y. M., ROSCHER, S., STOVER, C., ZHOU, W., SCHWAEBLE, W. J. & SACKS, S. H. 2014. Mannan-binding lectin-associated serine protease 2 is critical for the development of renal ischemia reperfusion injury and mediates tissue injury in the absence of complement C4. *FASEB J.*

ATKINSON, J. P. & FRANK, M. M. 2006. Bypassing complement: evolutionary lessons and future implications. *J Clin Invest,* 116**,** 1215-8.

BALLY, I., ROSSI, V., THIELENS, N. M., GABORIAUD, C. & ARLAUD, G. J. 2005. Functional role of the linker between the complement control protein modules of complement protease C1s. *J Immunol,* 175**,** 4536-42.

BEINROHR, L., HARMAT, V., DOBO, J., LORINCZ, Z., GAL, P. & ZAVODSZKY, P. 2007. C1 inhibitor serpin domain structure reveals the likely mechanism of heparin potentiation and conformational disease. *J Biol Chem,* 282**,** 21100-9.

BELT, K. T., YU, C. Y., CARROLL, M. C. & PORTER, R. R. 1985. Polymorphism of human complement component C4. *Immunogenetics,* 21**,** 173-80.

BELTRAME, M. H., CATARINO, S. J., GOELDNER, I., BOLDT, A. B. & DE MESSIAS-REASON, I. J. 2014. The lectin pathway of complement and rheumatic heart disease. *Front Pediatr,* 2**,** 148.

BENTLEY, D. R. 1986. Primary structure of human complement component C2. Homology to two unrelated protein families. *Biochem J,* 239**,** 339-45.

BLANCHONG, C. A., CHUNG, E. K., RUPERT, K. L., YANG, Y., YANG, Z., ZHOU, B., MOULDS, J. M. & YU, C. Y. 2001. Genetic, structural and functional diversities of human complement components C4A and C4B and their mouse homologues, Slp and C4. *Int Immunopharmacol,* 1**,** 365-92.

BOCK, S. C., SKRIVER, K., NIELSEN, E., THOGERSEN, H. C., WIMAN, B., DONALDSON, V. H., EDDY, R. L., MARRINAN, J., RADZIEJEWSKA, E., HUBER, R. & ET AL. 1986. Human C1 inhibitor: primary structure, cDNA cloning, and chromosomal localization. *Biochemistry,* 25**,** 4292-301.

BODE, W. & HUBER, R. 1978. Crystal structure analysis and refinement of two variants of trigonal trypsinogen: trigonal trypsin and PEG (polyethylene glycol) trypsinogen and their comparison with orthorhombic trypsin and trigonal trypsinogen. *FEBS Lett,* 90**,** 265-9.

BOLDT, A. B., LUZ, P. R. & MESSIAS-REASON, I. J. 2011. MASP2 haplotypes are associated with high risk of cardiomyopathy in chronic Chagas disease. *Clin Immunol,* 140**,** 63-70.

BOLDT, A. B., GOELDNER, I., STAHLKE, E. R., THIEL, S., JENSENIUS, J. C. & DE MESSIAS-REASON, I. J. 2013. Leprosy association with low MASP-2 levels generated by MASP2 haplotypes and polymorphisms flanking MAp19 exon 5. *PLoS One,* 8**,** e69054.

BORK, P. & BECKMANN, G. 1993. The CUB domain. A widespread module in developmentally regulated proteins. *J Mol Biol,* 231**,** 539-45.

BOS, I. G., LUBBERS, Y. T., ROEM, D., ABRAHAMS, J. P., HACK, C. E. & ELDERING, E. 2003. The functional integrity of the serpin domain of C1-inhibitor depends on the unique N-terminal domain, as revealed by a pathological mutant. *J Biol Chem,* 278**,** 29463-70.

BUDAYOVA-SPANO, M., GRABARSE, W., THIELENS, N. M., HILLEN, H., LACROIX, M., SCHMIDT, M., FONTECILLA-CAMPS, J. C., ARLAUD, G. J. & GABORIAUD, C. 2002. Monomeric structures of the zymogen and active catalytic domain of complement protease c1r: further insights into the c1 activation mechanism. *Structure,* 10**,** 1509-19.

BUSBY, T. F. & INGHAM, K. C. 1990. NH2-terminal calcium-binding domain of human complement C1s- mediates the interaction of C1r- with C1q. *Biochemistry,* 29**,** 4613-8.

CAMPBELL, R. D., DODDS, A. W. & PORTER, R. R. 1980. The binding of human complement component C4 to antibody-antigen aggregates. *Biochem J,* 189**,** 67-80.

CARROLL, M. C. 2004. The complement system in B cell regulation. *Mol Immunol,* 41**,** 141-6.

CARTER, A. M. 2005. Inflammation, thrombosis and acute coronary syndromes. *Diab Vasc Dis Res,* 2**,** 113-21.

CASTELLANO, G., MELCHIORRE, R., LOVERRE, A., DITONNO, P., MONTINARO, V., ROSSINI, M., DIVELLA, C., BATTAGLIA, M., LUCARELLI, G., ANNUNZIATA, G., PALAZZO, S., SELVAGGI, F. P., STAFFIERI, F., CROVACE, A., DAHA, M. R., MANNESSE, M., VAN WETERING, S., PAOLO SCHENA, F. & GRANDALIANO, G. 2010. Therapeutic targeting of classical and lectin pathways of complement protects from ischemia-reperfusion-induced renal damage. *Am J Pathol,* 176**,** 1648-59.

CATARINO, S. J., BOLDT, A. B., BELTRAME, M. H., NISIHARA, R. M., SCHAFRANSKI, M. D. & DE MESSIAS-REASON, I. J. 2014. Association of MASP2 polymorphisms and protein levels with rheumatic fever and rheumatic heart disease. *Hum Immunol,* 75**,** 1197-202.

CAUGHMAN, G.B., BOACKLE, R.J. & VESELY, J., 1982. A postulated mechanism for heparin's potentiation of C1 inhibitor function. *Mol Immunol,* 19, 287-295.

CEDZYNSKI, M., SZEMRAJ, J., SWIERZKO, A. S., BAK-ROMANISZYN, L., BANASIK, M., ZEMAN, K. & KILPATRICK, D. C. 2004. Mannan-binding lectin insufficiency in children with recurrent infections of the respiratory system. *Clin Exp Immunol,* 136**,** 304-11.

CHEN, C. B. & WALLIS, R. 2004. Two mechanisms for mannose-binding protein modulation of the activity of its associated serine proteases. *J Biol Chem,* 279**,** 26058-65.

CHOI, S. H., SMITH, S. A. & MORRISSEY, J. H. 2011. Polyphosphate is a cofactor for the activation of factor XI by thrombin. *Blood,* 118**,** 6963-70.

CLARK, A., WEYMANN, A., HARTMAN, E., TURMELLE, Y., CARROLL, M., THURMAN, J. M., HOLERS, V. M., HOURCADE, D. E. & RUDNICK, D. A. 2008. Evidence for non-traditional activation of complement factor C3 during murine liver regeneration. *Mol Immunol,* 45**,** 3125-32.

COELHO, A. V., BRANDAO, L. A., GUIMARAES, R. L., LOUREIRO, P., DE LIMA FILHO, J. L., DE ALENCAR, L. C., CROVELLA, S. & SEGAT, L. 2013. Mannose binding lectin and mannose binding lectin-associated serine protease-2 genes polymorphisms in human T-lymphotropic virus infection. *J Med Virol,* 85**,** 1829-35.

CORTESIO, C. L. & JIANG, W. 2006. Mannan-binding lectin-associated serine protease 3 cleaves synthetic peptides and insulin-like growth factor-binding protein 5. *Arch Biochem Biophys,* 449**,** 164-70.

COUTINHO, M., AULAK, K. S. & DAVIS, A. E., 3RD 1994. Functional analysis of the serpin domain of C1 inhibitor. *J Immunol,* 153**,** 3648-54.

CUNHA-NETO, E. & CHEVILLARD, C. 2014. Chagas disease cardiomyopathy: immunopathology and genetics. *Mediators Inflamm,* 2014**,** 683230.

DAHL, M. R., THIEL, S., MATSUSHITA, M., FUJITA, T., WILLIS, A. C., CHRISTENSEN, T., VORUP-JENSEN, T. & JENSENIUS, J. C. 2001. MASP-3 and its association with distinct complexes of the mannan-binding lectin complement activation pathway. *Immunity,* 15**,** 127-35.

DEGN, S. E., HANSEN, A. G., STEFFENSEN, R., JACOBSEN, C., JENSENIUS, J. C. & THIEL, S. 2009. MAp44, a human protein associated with pattern recognition molecules of the complement system and regulating the lectin pathway of complement activation. *J Immunol,* 183**,** 7371-8.

DEGN, S. E., JENSEN, L., GAL, P., DOBO, J., HOLMVAD, S. H., JENSENIUS, J. C. & THIEL, S. 2010. Biological variations of MASP-3 and MAp44, two splice products of the MASP1 gene involved in regulation of the complement system. *J Immunol Methods,* 361**,** 37-50.

DEGN, S. E., JENSEN, L., HANSEN, A. G., DUMAN, D., TEKIN, M., JENSENIUS, J. C. & THIEL, S. 2012. Mannan-binding lectin-associated serine protease (MASP)-1 is crucial for lectin pathway activation in human serum, whereas neither MASP-1 nor MASP-3 is required for alternative pathway function. *J Immunol,* 189**,** 3957-69.

DEGN, S. E., JENSEN, L., OLSZOWSKI, T., JENSENIUS, J. C. & THIEL, S. 2013. Co-complexes of MASP-1 and MASP-2 associated with the soluble pattern-recognition molecules drive lectin pathway activation in a manner inhibitable by MAp44. *J Immunol,* 191**,** 1334-45.

DE ROOIJ, B. J., VAN HOEK, B., TEN HOVE, W. R., ROOS, A., BOUWMAN, L. H., SCHAAPHERDER, A. F., PORTE, R. J., DAHA, M. R., VAN DER REIJDEN, J. J., COENRAAD, M. J., RINGERS, J., BARANSKI, A. G., HEPKEMA, B. G., HOMMES, D. W. & VERSPAGET, H. W. 2010. Lectin complement pathway gene profile of donor and recipient determine the risk of bacterial infections after orthotopic liver transplantation. *Hepatology,* 52**,** 1100-10.

DOBO, J., HARMAT, V., BEINROHR, L., SEBESTYEN, E., ZAVODSZKY, P. & GAL, P. 2009. MASP-1, a promiscuous complement protease: structure of its catalytic region reveals the basis of its broad specificity. *J Immunol,* 183**,** 1207-14.

DODDS, A. W. 2002. Which came first, the lectin/classical pathway or the alternative pathway of complement? *Immunobiology,* 205**,** 340-54.

DODDS, A. W., REN, X. D., WILLIS, A. C. & LAW, S. K. 1996. The reaction mechanism of the internal thioester in the human complement component C4. *Nature,* 379**,** 177-9.

DONALDSON, V. H. & EVANS, R. R. 1963. A Biochemical Abnormality in Herediatry Angioneurotic Edema: Absence of Serum Inhibitor of C' 1-Esterase. *Am J Med,* 35**,** 37-44.

DROUIN, S. M., CORRY, D. B., HOLLMAN, T. J., KILDSGAARD, J. & WETSEL, R. A. 2002. Absence of the complement anaphylatoxin C3a receptor suppresses Th2 effector functions in a murine model of pulmonary allergy. *J Immunol,* 169**,** 5926-33.

DUNCAN, R. C., WIJEYEWICKREMA, L. C. & PIKE, R. N. 2008. The initiating proteases of the complement system: controlling the cleavage. *Biochimie,* 90**,** 387-95.

DUNCAN, R. C., BERGSTROM, F., COETZER, T. H., BLOM, A. M., WIJEYEWICKREMA, L. C. & PIKE, R. N. 2012a. Multiple domains of MASP-2, an initiating complement protease, are required for interaction with its substrate C4. *Mol Immunol,* 49**,** 593-600.

DUNCAN, R. C., MOHLIN, F., TALESKI, D., COETZER, T. H., HUNTINGTON, J. A., PAYNE, R. J., BLOM, A. M., PIKE, R. N. & WIJEYEWICKREMA, L. C. 2012b. Identification of a catalytic exosite for complement component C4 on the serine protease domain of C1s. *J Immunol,* 189**,** 2365-73.

FEINBERG, H., UITDEHAAG, J. C., DAVIES, J. M., WALLIS, R., DRICKAMER, K. & WEIS, W. I. 2003. Crystal structure of the CUB1-EGF-CUB2 region of mannose-binding protein associated serine protease-2. *EMBO J,* 22**,** 2348-59.

FREDSLUND, F., JENNER, L., HUSTED, L. B., NYBORG, J., ANDERSEN, G. R. & SOTTRUP-JENSEN, L. 2006. The structure of bovine complement component 3 reveals the basis for thioester function. *J Mol Biol,* 361**,** 115-27.

FREDSLUND, F., LAURSEN, N. S., ROVERSI, P., JENNER, L., OLIVEIRA, C. L., PEDERSEN, J. S., NUNN, M. A., LEA, S. M., DISCIPIO, R., SOTTRUP-JENSEN, L. & ANDERSEN, G. R. 2008. Structure of and influence of a tick complement inhibitor on human complement component 5. *Nat Immunol,* 9**,** 753-60.

FUJITA, T., MATSUSHITA, M. & ENDO, Y. 2004. The lectin-complement pathway--its role in innate immunity and evolution. *Immunol Rev,* 198**,** 185-202.

GABORIAUD, C., ROSSI, V., BALLY, I., ARLAUD, G. J. & FONTECILLA-CAMPS, J. C. 2000. Crystal structure of the catalytic domain of human complement c1s: a serine protease with a handle. *EMBO J,* 19**,** 1755-65.

GABORIAUD, C., THIELENS, N. M., GREGORY, L. A., ROSSI, V., FONTECILLA-CAMPS, J. C. & ARLAUD, G. J. 2004. Structure and activation of the C1 complex of complement: unraveling the puzzle. *Trends Immunol,* 25**,** 368-73.

GAL, P., HARMAT, V., KOCSIS, A., BIAN, T., BARNA, L., AMBRUS, G., VEGH, B., BALCZER, J., SIM, R. B., NARAY-SZABO, G. & ZAVODSZKY, P. 2005. A true autoactivating enzyme. Structural insight into mannose-binding lectin-associated serine protease-2 activations. *J Biol Chem,* 280**,** 33435-44.

GAL, P., BARNA, L., KOCSIS, A. & ZAVODSZKY, P. 2007. Serine proteases of the classical and lectin pathways: similarities and differences. *Immunobiology,* 212**,** 267-77.

GAL, P., DOBO, J., ZAVODSZKY, P. & SIM, R. B. 2009. Early complement proteases: C1r, C1s and MASPs. A structural insight into activation and functions. *Mol Immunol,* 46**,** 2745-52.

GALASSO, A. & ZOLLO, M. 2009. The Nm23-H1-h-Prune complex in cellular physiology: a 'tip of the iceberg' protein network perspective. *Mol Cell Biochem,* 329**,** 149-59.

GOELDNER, I., SKARE, T., BOLDT, A. B., NASS, F. R., MESSIAS-REASON, I. J. & UTIYAMA, S. R. 2014. Association of MASP-2 levels and MASP2 gene polymorphisms with rheumatoid arthritis in patients and their relatives. *PLoS One,* 9**,** e90979.

GOZZO, A. J., NUNES, V. A., NADER, H. B., DIETRICH, C. P., CARMONA, A. K., SAMPAIO, M. U., SAMPAIO, C. A. & ARAUJO, M. S. 2003. Glycosaminoglycans affect the interaction of human plasma kallikrein with plasminogen, factor XII and inhibitors. *Braz J Med Biol Res,* 36**,** 1055-9.

GREGORY, L. A., THIELENS, N. M., ARLAUD, G. J., FONTECILLA-CAMPS, J. C. & GABORIAUD, C. 2003. X-ray structure of the Ca2+-binding interaction domain of C1s. Insights into the assembly of the C1 complex of complement. *J Biol Chem,* 278**,** 32157-64.

GREGORY, L. A., THIELENS, N. M., MATSUSHITA, M., SORENSEN, R., ARLAUD, G. J., FONTECILLA-CAMPS, J. C. & GABORIAUD, C. 2004. The X-ray structure of human mannan-binding lectin-associated protein 19 (MAp19) and its interaction site with mannan-binding lectin and L-ficolin. *J Biol Chem,* 279**,** 29391-7.

GULLA, K. C., GUPTA, K., KRARUP, A., GAL, P., SCHWAEBLE, W. J., SIM, R. B., O'CONNOR, C. D. & HAJELA, K. 2010. Activation of mannan-binding lectin-associated serine proteases leads to generation of a fibrin clot. *Immunology,* 129**,** 482-95.

HAJELA, K., KOJIMA, M., AMBRUS, G., WONG, K. H., MOFFATT, B. E., FERLUGA, J., HAJELA, S., GAL, P. & SIM, R. B. 2002. The biological functions of MBL-associated serine proteases (MASPs). *Immunobiology,* 205**,** 467-75.

HALILI, M. A., RUIZ-GOMEZ, G., LE, G. T., ABBENANTE, G. & FAIRLIE, D. P. 2009. Complement component C2, inhibiting a latent serine protease in the classical pathway of complement activation. *Biochemistry,* 48**,** 8466-72.

HAN, K. Y., HONG, B. S., YOON, Y. J., YOON, C. M., KIM, Y. K., KWON, Y. G. & GHO, Y. S. 2007. Polyphosphate blocks tumour metastasis via anti-angiogenic activity. *Biochem J,* 406**,** 49-55.

HARBOE, M., GARRED, P., KARLSTROM, E., LINDSTAD, J. K., STAHL, G. L. & MOLLNES, T. E. 2009. The down-stream effects of mannan-induced lectin complement pathway activation depend quantitatively on alternative pathway amplification. *Mol Immunol,* 47**,** 373-80.

HARMAT, V., GAL, P., KARDOS, J., SZILAGYI, K., AMBRUS, G., VEGH, B., NARAY-SZABO, G. & ZAVODSZKY, P. 2004. The structure of MBL-associated serine protease-2 reveals that identical substrate specificities of C1s and MASP-2 are realized through different sets of enzyme-substrate interactions. *J Mol Biol,* 342**,** 1533-46.

HAWLISCH, H., WILLS-KARP, M., KARP, C. L. & KOHL, J. 2004. The anaphylatoxins bridge innate and adaptive immune responses in allergic asthma. *Mol Immunol,* 41**,** 123-31.

HAWLISCH, H., BELKAID, Y., BAELDER, R., HILDEMAN, D., GERARD, C. & KOHL, J. 2005. C5a negatively regulates toll-like receptor 4-induced immune responses. *Immunity,* 22**,** 415-26.

HEJA, D., HARMAT, V., FODOR, K., WILMANNS, M., DOBO, J., KEKESI, K. A., ZAVODSZKY, P., GAL, P. & PAL, G. 2012a. Monospecific inhibitors show that both mannan-binding lectin-associated serine protease-1 (MASP-1) and -2 Are essential for lectin pathway activation and reveal structural plasticity of MASP-2. *J Biol Chem,* 287**,** 20290-300.

HEJA, D., KOCSIS, A., DOBO, J., SZILAGYI, K., SZASZ, R., ZAVODSZKY, P., PAL, G. & GAL, P. 2012b. Revised mechanism of complement lectin-pathway activation revealing the role of serine protease MASP-1 as the exclusive activator of MASP-2. *Proc Natl Acad Sci U S A,* 109**,** 10498-503.

HERNANDEZ-RUIZ, L., GONZALEZ-GARCIA, I., CASTRO, C., BRIEVA, J. A. & RUIZ, F. A. 2006. Inorganic polyphosphate and specific induction of apoptosis in human plasma cells. *Haematologica,* 91**,** 1180-6.

HOLERS, V. M. & THURMAN, J. M. 2004. The alternative pathway of complement in disease: opportunities for therapeutic targeting. *Mol Immunol,* 41**,** 147-52.

HORVATH, A., BERNADINE, G.C LU, PIKE, R & BOTTOMLEY, S. 2011. Methods to measure the kinetics of protease inhibitors by serpins. *Methods Enzymol*, 501, 223-35.

HUBER-LANG, M., SARMA, J. V., ZETOUNE, F. S., RITTIRSCH, D., NEFF, T. A., MCGUIRE, S. R., LAMBRIS, J. D., WARNER, R. L., FLIERL, M. A., HOESEL, L. M., GEBHARD, F., YOUNGER, J. G., DROUIN, S. M., WETSEL, R. A. & WARD, P. A. 2006. Generation of C5a in the absence of C3: a new complement activation pathway. *Nat Med,* 12**,** 682-7.

IKEDA, K., SANNOH, T., KAWASAKI, N., KAWASAKI, T. & YAMASHINA, I. 1987. Serum lectin with known structure activates complement through the classical pathway. *J Biol Chem,* 262**,** 7451-4.

ISAAC, L., AIVAZIAN, D., TANIGUCHI-SIDLE, A., EBANKS, R. O., FARAH, C. S., FLORIDO, M. P., PANGBURN, M. K. & ISENMAN, D. E. 1998. Native conformations of human complement components C3 and C4 show different dependencies on thioester formation. *Biochem J,* 329 (Pt 3)**,** 705-12.

IWAKI, D., KANNO, K., TAKAHASHI, M., ENDO, Y., LYNCH, N. J., SCHWAEBLE, W. J., MATSUSHITA, M., OKABE, M. & FUJITA, T. 2006. Small mannose-binding lectin-associated protein plays a regulatory role in the lectin complement pathway. *J Immunol,* 177**,** 8626-32.

IWAKI, D., KANNO, K., TAKAHASHI, M., ENDO, Y., MATSUSHITA, M. & FUJITA, T. 2011. The role of mannose-binding lectin-associated serine protease-3 in activation of the alternative complement pathway. *J Immunol,* 187**,** 3751-8.

JANSSEN, B. J., HUIZINGA, E. G., RAAIJMAKERS, H. C., ROOS, A., DAHA, M. R., NILSSON-EKDAHL, K., NILSSON, B. & GROS, P. 2005. Structures of complement component C3 provide insights into the function and evolution of immunity. *Nature,* 437**,** 505-11.

JANSSEN, B. J., CHRISTODOULIDOU, A., MCCARTHY, A., LAMBRIS, J. D. & GROS, P. 2006. Structure of C3b reveals conformational changes that underlie complement activity. *Nature,* 444**,** 213-6.

JOHNSON, D. J., LI, W., ADAMS, T. E. & HUNTINGTON, J. A. 2006. Antithrombin-S195A factor Xa-heparin structure reveals the allosteric mechanism of antithrombin activation. *EMBO J,* 25**,** 2029-37.

KAPLAN, A. P. 2010. Enzymatic pathways in the pathogenesis of hereditary angioedema: the role of C1 inhibitor therapy. *J Allergy Clin Immunol,* 126**,** 918-25.

KAPLAN, A. & GHEBREHIWET, B. 2010. The plasma bradykinin-forming pathways and its interrelationships with complement. *Mol Immunol,* 47, 2161-9.

KAWAMOTO, S., YALCINDAG, A., LAOUINI, D., BRODEUR, S., BRYCE, P., LU, B., HUMBLES, A. A., OETTGEN, H., GERARD, C. & GEHA, R. S. 2004. The anaphylatoxin C3a downregulates the Th2 response to epicutaneously introduced antigen. *J Clin Invest,* 114**,** 399-407.

KAWAZOE, Y., SHIBA, T., NAKAMURA, R., MIZUNO, A., TSUTSUMI, K., UEMATSU, T., YAMAOKA, M., SHINDOH, M. & KOHGO, T. 2004. Induction of calcification in MC3T3-E1 cells by inorganic polyphosphate. *J Dent Res,* 83**,** 613-8.

KENESI, E., KATONA, G. & SZILAGYI, L. 2003. Structural and evolutionary consequences of unpaired cysteines in trypsinogen. *Biochem Biophys Res Commun,* 309**,** 749-54.

KERR, M. A. 1980. The human complement system: assembly of the classical pathway C3 convertase. *Biochem J,* 189**,** 173-81.

KERR, F. K., THOMAS, A. R., WIJEYEWICKREMA, L. C., WHISSTOCK, J. C., BOYD, S. E., KAISERMAN, D., MATTHEWS, A. Y., BIRD, P. I., THIELENS, N. M., ROSSI, V. & PIKE, R. N. 2008. Elucidation of the substrate specificity of the MASP-2 protease of the lectin complement pathway and identification of the enzyme as a major physiological target of the serpin, C1-inhibitor. *Mol Immunol,* 45**,** 670-7.

KIDMOSE, R. T., LAURSEN, N. S., DOBO, J., KJAER, T. R., SIROTKINA, S., YATIME, L., SOTTRUP-JENSEN, L., THIEL, S., GAL, P. & ANDERSEN, G. R. 2012. Structural basis for activation of the complement system by component C4 cleavage. *Proc Natl Acad Sci U S A,* 109**,** 15425-30.

KIMURA, A., SAKAGUCHI, E. & NONAKA, M. 2009. Multi-component complement system of Cnidaria: C3, Bf, and MASP genes expressed in the endodermal tissues of a sea anemone, Nematostella vectensis. *Immunobiology,* 214**,** 165-78.

KIRKITADZE, M. D. & BARLOW, P. N. 2001. Structure and flexibility of the multiple domain proteins that regulate complement activation. *Immunol Rev,* 180**,** 146-61.

KISHORE, U. & REID, K. B. 2000. C1q: structure, function, and receptors. *Immunopharmacology,* 49**,** 159-70.

KOLEV, M., LE FRIEC, G. & KEMPER, C. 2014. Complement--tapping into new sites and effector systems. *Nat Rev Immunol,* 14**,** 811-20.

KORNBERG, A. 1995. Inorganic polyphosphate: toward making a forgotten polymer unforgettable. *J Bacteriol,* 177**,** 491-6.

KORNBERG, A., RAO, N. N. & AULT-RICHE, D. 1999. Inorganic polyphosphate: a molecule of many functions. *Annu Rev Biochem,* 68**,** 89-125.

KRARUP, A., WALLIS, R., PRESANIS, J. S., GAL, P. & SIM, R. B. 2007. Simultaneous activation of complement and coagulation by MBL-associated serine protease 2. *PLoS One,* 2**,** e623.

KRARUP, A., GULLA, K. C., GAL, P., HAJELA, K. & SIM, R. B. 2008. The action of MBL-associated serine protease 1 (MASP1) on factor XIII and fibrinogen. *Biochim Biophys Acta,* 1784**,** 1294-300.

KRISHNAN, V., XU, Y., MACON, K., VOLANAKIS, J. E. & NARAYANA, S. V. 2009. The structure of C2b, a fragment of complement component C2 produced during C3 convertase formation. *Acta Crystallogr D Biol Crystallogr,* 65**,** 266-74.

KRYCH-GOLDBERG, M. & ATKINSON, J. P. 2001. Structure-function relationships of complement receptor type 1. *Immunol Rev,* 180**,** 112-22.

LANDERMAN, N. S., WEBSTER, M. E., BECKER, E. L. & RATCLIFFE, H. E. 1962. Hereditary angioneurotic edema. II. Deficiency of inhibitor for serum globulin permeability factor and/or plasma kallikrein. *J Allergy,* 33**,** 330-41.

LAW, S. K., DODDS, A. W. & PORTER, R. R. 1984. A comparison of the properties of two classes, C4A and C4B, of the human complement component C4. *EMBO J,* 3**,** 1819-23.

LAW, S. K. & DODDS, A. W. 1997. The internal thioester and the covalent binding properties of the complement proteins C3 and C4. *Protein Sci,* 6**,** 263-74.

LEYHAUSEN, G., LORENZ, B., ZHU, H., GEURTSEN, W., BOHNENSACK, R., MULLER, W. E. & SCHRODER, H. C. 1998. Inorganic polyphosphate in human osteoblast-like cells. *J Bone Miner Res,* 13**,** 803-12.

LI, H. H., MOLDOVAN, D., BERNSTEIN, J. A., RESHEF, A., POREBSKI, G., STOBIECKI, M., BAKER, J., LEVY, R., RELAN, A. & RIEDL, M. 2015. Recombinant Human-C1 Inhibitor is Effective and Safe for Repeat Hereditary Angioedema Attacks. *J Allergy Clin Immunol Pract.*

LIBBY, P., RIDKER, P. M., HANSSON, G. K. & LEDUCQ TRANSATLANTIC NETWORK ON, A. 2009. Inflammation in atherosclerosis: from pathophysiology to practice. *J Am Coll Cardiol,* 54**,** 2129-38.

LINHARDT, R. J. & GUNAY, N. S. 1999. Production and chemical processing of low molecular weight heparins. *Semin Thromb Hemost,* 25 Suppl 3**,** 5-16.

LISZEWSKI, M. K., POST, T. W. & ATKINSON, J. P. 1991. Membrane cofactor protein (MCP or CD46): newest member of the regulators of complement activation gene cluster. *Annu Rev Immunol,* 9**,** 431-55.

LISZEWSKI, M.K. & ATKINSON, J. P. 2015. Complement regulators in human disease: lessons from modern genetics. *J Intern Med,* 277**,** 294-305.

LIU, D., CAI, S., GU, X., SCAFIDI, J., WU, X. & DAVIS, A. E., 3RD. 2003. C1 inhibitor prevents endotoxin shock via a direct interaction with lipopolysaccharide. *J Immunol,* 171**,** 2594-601.

LIU, D., ZHANG, D., SCAFIDI, J., WU, X., CRAMER, C. C. & DAVIS, A. E., 3RD. 2005. C1 inhibitor prevents Gram-negative bacterial lipopolysaccharide-induced vascular permeability. *Blood,* 105**,** 2350-5.

MATSUSHITA, M. 1996. The lectin pathway of the complement system. *Microbiol Immunol,* 40**,** 887-93.

MATSUSHITA, M., THIEL, S., JENSENIUS, J. C., TERAI, I. & FUJITA, T. 2000. Proteolytic activities of two types of mannose-binding lectin-associated serine protease. *J Immunol,* 165**,** 2637-42.

MAURON, T., LAMMLE, B. & WUILLEMIN, W. A. 1998. Influence of low molecular weight heparin and low molecular weight dextran sulfate on the inhibition of coagulation factor XIa by serpins. *Thromb Haemost,* 80**,** 82-6.

MAYILYAN, K. R., PRESANIS, J. S., ARNOLD, J. N. & SIM, R. B. 2006. Discrete MBL-MASP complexes show wide inter-individual variability in concentration: data from UK vs Armenian populations. *Int J Immunopathol Pharmacol,* 19**,** 567-80.

MEGYERI, M., HARMAT, V., MAJOR, B., VEGH, A., BALCZER, J., HEJA, D., SZILAGYI, K., DATZ, D., PAL, G., ZAVODSZKY, P., GAL, P. & DOBO, J. 2013. Quantitative characterization of the activation steps of mannan-binding lectin (MBL)-associated serine proteases (MASPs) points to the central role of MASP-1 in the initiation of the complement lectin pathway. *J Biol Chem,* 288**,** 8922-34.

MESSIAS REASON, I. J., SCHAFRANSKI, M. D., JENSENIUS, J. C. & STEFFENSEN, R. 2006. The association between mannose-binding lectin gene polymorphism and rheumatic heart disease. *Hum Immunol,* 67**,** 991-8.

MILDER, F. J., RAAIJMAKERS, H. C., VANDEPUTTE, M. D., SCHOUTEN, A., HUIZINGA, E. G., ROMIJN, R. A., HEMRIKA, W., ROOS, A., DAHA, M. R. & GROS, P. 2006. Structure of complement component C2A: implications for convertase formation and substrate binding. *Structure,* 14**,** 1587-97.

MORRISSEY, J. H., CHOI, S. H. & SMITH, S. A. 2012. Polyphosphate: an ancient molecule that links platelets, coagulation, and inflammation. *Blood,* 119**,** 5972-9.

MULLARKY, I. K., SZABA, F. M., BERGGREN, K. N., PARENT, M. A., KUMMER, L. W., CHEN, W., JOHNSON, L. L. & SMILEY, S. T. 2005. Infection-stimulated fibrin deposition controls hemorrhage and limits hepatic bacterial growth during listeriosis. *Infect Immun,* 73**,** 3888-95.

MULLER-EBERHARD, H. J. 1988. Molecular organization and function of the complement system. *Annu Rev Biochem,* 57**,** 321-47.

MURRAY-RUST, T. A., KERR, F. K., THOMAS, A. R., WU, T., YONGQING, T., ONG, P. C., QUINSEY, N. S., WHISSTOCK, J. C., WAGENAAR-BOS, I. C., FREEMAN, C. & PIKE, R. N. 2009. Modulation of the proteolytic activity of the complement protease C1s by polyanions: implications for polyanion-mediated acceleration of interaction between C1s and SERPING1. *Biochem J,* 422**,** 295-303.

NAITO, A. T., SUMIDA, T., NOMURA, S., LIU, M. L., HIGO, T., NAKAGAWA, A., OKADA, K., SAKAI, T., HASHIMOTO, A., HARA, Y., SHIMIZU, I., ZHU, W., TOKO, H., KATADA, A., AKAZAWA, H., OKA, T., LEE, J. K., MINAMINO, T., NAGAI, T., WALSH, K., KIKUCHI, A., MATSUMOTO, M., BOTTO, M., SHIOJIMA, I. & KOMURO, I. 2012. Complement C1q activates canonical Wnt signaling and promotes aging-related phenotypes. *Cell,* 149**,** 1298-313.

NILSSON, T. & WIMAN, B. 1983. Kinetics of the reaction between human C1-esterase inhibitor and C1r or C1s. *Eur J Biochem,* 129**,** 663-7.

NOEGEL, A. & GOTSCHLICH, E. C. 1983. Isolation of a high molecular weight polyphosphate from Neisseria gonorrhoeae. *J Exp Med,* 157**,** 2049-60.

O'BRIEN, G., QUINSEY, N. S., WHISSTOCK, J. C. & PIKE, R. N. 2003. Importance of the prime subsites of the C1s protease of the classical complement pathway for recognition of substrates. *Biochemistry,* 42**,** 14939-45.

OLESEN, H. V., JENSENIUS, J. C., STEFFENSEN, R., THIEL, S. & SCHIOTZ, P. O. 2006. The mannan-binding lectin pathway and lung disease in cystic fibrosis--disfunction of mannan-binding lectin-associated serine protease 2 (MASP-2) may be a major modifier. *Clin Immunol,* 121**,** 324-31.

OLSON, S. T., RICHARD, B., IZAGUIRRE, G., SCHEDIN-WEISS, S. & GETTINS, P. G. 2010. Molecular mechanisms of antithrombin-heparin regulation of blood clotting proteinases. A paradigm for understanding proteinase regulation by serpin family protein proteinase inhibitors. *Biochimie,* 92**,** 1587-96.

PAREJ, K., DOBO, J., ZAVODSZKY, P. & GAL, P. 2013. The control of the complement lectin pathway activation revisited: both C1-inhibitor and antithrombin are likely physiological inhibitors, while alpha2-macroglobulin is not. *Mol Immunol,* 54**,** 415-22.

PAVLOV, E., ASCHAR-SOBBI, R., CAMPANELLA, M., TURNER, R. J., GOMEZ-GARCIA, M. R. & ABRAMOV, A. Y. 2010. Inorganic polyphosphate and energy metabolism in mammalian cells. *J Biol Chem,* 285**,** 9420-8.

PAVLOV, V. I., SKJOEDT, M. O., SIOW TAN, Y., ROSBJERG, A., GARRED, P. & STAHL, G. L. 2012. Endogenous and natural complement inhibitor attenuates myocardial injury and arterial thrombogenesis. *Circulation,* 126**,** 2227-35.

PENSKY, J., LEVY, L. R. & LEPOW, I. H. 1961. Partial purification of a serum inhibitor of C'1-esterase. *J Biol Chem,* 236**,** 1674-9.

PERONA, J. J. & CRAIK, C. S. 1997. Evolutionary divergence of substrate specificity within the chymotrypsin-like serine protease fold. *J Biol Chem,* 272**,** 29987-90.

PERRY, A. J., WIJEYEWICKREMA, L. C., WILMANN, P. G., GUNZBURG, M. J., D'ANDREA, L., IRVING, J. A., PANG, S. S., DUNCAN, R. C., WILCE, J. A., WHISSTOCK, J. C. & PIKE, R. N. 2013. A molecular switch governs the interaction between the human complement protease C1s and its substrate, complement C4. *J Biol Chem,* 288**,** 15821-9.

PETERSEN, S. V., THIEL, S., JENSEN, L., VORUP-JENSEN, T., KOCH, C. & JENSENIUS, J. C. 2000. Control of the classical and the MBL pathway of complement activation. *Mol Immunol,* 37**,** 803-11.

PIKE, R. N., BUCKLE, A. M., LE BONNIEC, B. F. & CHURCH, F. C. 2005. Control of the coagulation system by serpins. Getting by with a little help from glycosaminoglycans. *FEBS J,* 272**,** 4842-51.

PISONI, R. L. & LINDLEY, E. R. 1992. Incorporation of [32P]orthophosphate into long chains of inorganic polyphosphate within lysosomes of human fibroblasts. *J Biol Chem,* 267**,** 3626-31.

PIXLEY, R. A., SCHAPIRA, M. & COLMAN, R. W. 1985. The regulation of human factor XIIa by plasma proteinase inhibitors. *J Biol Chem,* 260**,** 1723-9.

PRESANIS, J. S., HAJELA, K., AMBRUS, G., GAL, P. & SIM, R. B. 2004. Differential substrate and inhibitor profiles for human MASP-1 and MASP-2. *Mol Immunol,* 40**,** 921-9.

RAEPPLE, E., HILL, H. U. & LOOS, M. 1976. Mode of interaction of different polyanions with the first (C1, C1), the second (C2) and the fourth (C4) component of complement--I. Effect on fluid phase C1 and on C1 bound to EA or to EAC4. *Immunochemistry,* 13**,** 251-5.

REILLY, B. D. 2006. Structural comparison of human C4A3 and C4B1 after proteolytic activation by C1s. *Mol Immunol,* 43**,** 800-11.

ROORYCK, C., DIAZ-FONT, A., OSBORN, D. P., CHABCHOUB, E., HERNANDEZ-HERNANDEZ, V., SHAMSELDIN, H., KENNY, J., WATERS, A., JENKINS, D., KAISSI, A. A., LEAL, G. F., DALLAPICCOLA, B., CARNEVALE, F., BITNER-GLINDZICZ, M., LEES, M., HENNEKAM, R., STANIER, P., BURNS, A. J., PEETERS, H., ALKURAYA, F. S. & BEALES, P. L. 2011. Mutations in lectin complement pathway genes COLEC11 and MASP1 cause 3MC syndrome. *Nat Genet,* 43**,** 197-203.

ROSSI, V., BALLY, I., THIELENS, N. M., ESSER, A. F. & ARLAUD, G. J. 1998. Baculovirus-mediated expression of truncated modular fragments from the catalytic region of human complement serine protease C1s. Evidence for the involvement of both complement control protein modules in the recognition of the C4 protein substrate. *J Biol Chem,* 273**,** 1232-9.

ROSSI, V., CSEH, S., BALLY, I., THIELENS, N. M., JENSENIUS, J. C. & ARLAUD, G. J. 2001. Substrate specificities of recombinant mannan-binding lectin-associated serine proteases-1 and -2. *J Biol Chem,* 276**,** 40880-7.

ROSSI, V., TEILLET, F., THIELENS, N. M., BALLY, I. & ARLAUD, G. J. 2005. Functional characterization of complement proteases C1s/mannan-binding lectin-associated serine protease-2 (MASP-2) chimeras reveals the higher C4 recognition efficacy of the MASP-2 complement control protein modules. *J Biol Chem,* 280**,** 41811-8.

ROSSI, V., BALLY, I., ANCELET, S., XU, Y., FREMEAUX-BACCHI, V., VIVES, R. R., SADIR, R., THIELENS, N. & ARLAUD, G. J. 2010. Functional characterization of the recombinant human C1 inhibitor serpin domain: insights into heparin binding. *J Immunol,* 184**,** 4982-9.

RUDDY, S., GIGLI, I., SHEFFER, A.L. & AUSTEN, K.F. 1967. The laboratory diagnosis of hereditary angioedema. *Excerpta Medico International Congress Series, 162*, 351–359.

RUIZ, F. A., LEA, C. R., OLDFIELD, E. & DOCAMPO, R. 2004. Human platelet dense granules contain polyphosphate and are similar to acidocalcisomes of bacteria and unicellular eukaryotes. *J Biol Chem,* 279**,** 44250-7.

SAHU, A. & PANGBURN, M. K. 1993. Identification of multiple sites of interaction between heparin and the complement system. *Mol Immunol,* 30**,** 679-84.

SCHAFER, D. P., LEHRMAN, E. K., KAUTZMAN, A. G., KOYAMA, R., MARDINLY, A. R., YAMASAKI, R., RANSOHOFF, R. M., GREENBERG, M. E., BARRES, B. A. & STEVENS, B. 2012. Microglia sculpt postnatal neural circuits in an activity and complement-dependent manner. *Neuron,* 74**,** 691-705.

SCHAFRANSKI, M. D., STIER, A., NISIHARA, R. & MESSIAS-REASON, I. J. 2004. Significantly increased levels of mannose-binding lectin (MBL) in rheumatic heart disease: a beneficial role for MBL deficiency. *Clin Exp Immunol,* 138**,** 521-5.

SCHAPIRA, M., SCOTT, C. F. & COLMAN, R. W. 1982. Contribution of plasma protease inhibitors to the inactivation of kallikrein in plasma. *J Clin Invest,* 69**,** 462-8.

SCHRODER, H. C., KURZ, L., MULLER, W. E. & LORENZ, B. 2000. Polyphosphate in bone. *Biochemistry (Mosc),* 65**,** 296-303.

SCHWAEBLE, W. J., LYNCH, N. J., CLARK, J. E., MARBER, M., SAMANI, N. J., ALI, Y. M., DUDLER, T., PARENT, B., LHOTTA, K., WALLIS, R., FARRAR, C. A., SACKS, S., LEE, H., ZHANG, M., IWAKI, D., TAKAHASHI, M., FUJITA, T., TEDFORD, C. E. & STOVER, C. M. 2011. Targeting of mannan-binding lectin-associated serine protease-2 confers protection from myocardial and gastrointestinal ischemia/reperfusion injury. *Proc Natl Acad Sci U S A,* 108**,** 7523-8.

SELANDER, B., MARTENSSON, U., WEINTRAUB, A., HOLMSTROM, E., MATSUSHITA, M., THIEL, S., JENSENIUS, J. C., TRUEDSSON, L. & SJOHOLM, A. G. 2006. Mannan-binding lectin activates C3 and the alternative complement pathway without involvement of C2. *J Clin Invest,* 116**,** 1425-34.

SEPP, A., DODDS, A. W., ANDERSON, M. J., CAMPBELL, R. D., WILLIS, A. C. & LAW, S. K. 1993. Covalent binding properties of the human complement protein C4 and hydrolysis rate of the internal thioester upon activation. *Protein Sci,* 2**,** 706-16.

SIM, R. B., REBOUL, A., ARLAUD, G. J., VILLIERS, C. L. & COLOMB, M. G. 1979. Interaction of 125I-labelled complement subcomponents C-1r and C-1s with protease inhibitors in plasma. *FEBS Lett,* 97**,** 111-5.

SIM, R. B., ARLAUD, G. J. & COLOMB, M. G. 1980. Kinetics of reaction of human C1-inhibitor with the human complement system proteases C1r and C1s. *Biochim Biophys Acta,* 612**,** 433-49.

SIM, R. B. & TSIFTSOGLOU, S. A. 2004. Proteases of the complement system. *Biochem Soc Trans,* 32**,** 21-7.

SIRMACI, A., WALSH, T., AKAY, H., SPILIOPOULOS, M., SAKALAR, Y. B., HASANEFENDIOGLU-BAYRAK, A., DUMAN, D., FAROOQ, A., KING, M. C. & TEKIN, M. 2010. MASP1 mutations in patients with facial, umbilical, coccygeal, and auditory findings of Carnevale, Malpuech, OSA, and Michels syndromes. *Am J Hum Genet,* 87**,** 679-86.

SKJOEDT, M. O., HUMMELSHOJ, T., PALARASAH, Y., HONORE, C., KOCH, C., SKJODT, K. & GARRED, P. 2010. A novel mannose-binding lectin/ficolin-associated protein is highly expressed in heart and skeletal muscle tissues and inhibits complement activation. *J Biol Chem,* 285**,** 8234-43.

SMITH, S. A., MUTCH, N. J., BASKAR, D., ROHLOFF, P., DOCAMPO, R. & MORRISSEY, J. H. 2006. Polyphosphate modulates blood coagulation and fibrinolysis. *Proc Natl Acad Sci U S A,* 103**,** 903-8.

SMITH, S. A. & MORRISSEY, J. H. 2008. Polyphosphate enhances fibrin clot structure. *Blood,* 112**,** 2810-6.

SMITH, S. A., CHOI, S. H., DAVIS-HARRISON, R., HUYCK, J., BOETTCHER, J., RIENSTRA, C. M. & MORRISSEY, J. H. 2010. Polyphosphate exerts differential effects on blood clotting, depending on polymer size. *Blood,* 116**,** 4353-9.

SORENSEN, R., THIEL, S. & JENSENIUS, J. C. 2005. Mannan-binding-lectin-associated serine proteases, characteristics and disease associations. *Springer Semin Immunopathol,* 27**,** 299-319.

SOTTRUP-JENSEN, L., STEPANIK, T. M., KRISTENSEN, T., LONBLAD, P. B., JONES, C. M., WIERZBICKI, D. M., MAGNUSSON, S., DOMDEY, H., WETSEL, R. A., LUNDWALL, A. & ET AL. 1985. Common evolutionary origin of alpha 2-macroglobulin and complement components C3 and C4. *Proc Natl Acad Sci U S A,* 82**,** 9-13.

STENFLO, J., STENBERG, Y. & MURANYI, A. 2000. Calcium-binding EGF-like modules in coagulation proteinases: function of the calcium ion in module interactions. *Biochim Biophys Acta,* 1477**,** 51-63.

STENGAARD-PEDERSEN, K., THIEL, S., GADJEVA, M., MOLLER-KRISTENSEN, M., SORENSEN, R., JENSEN, L. T., SJOHOLM, A. G., FUGGER, L. & JENSENIUS, J. C. 2003. Inherited deficiency of mannan-binding lectin-associated serine protease 2. *N Engl J Med,* 349**,** 554-60.

STEPHAN, A. H., MADISON, D. V., MATEOS, J. M., FRASER, D. A., LOVELETT, E. A., COUTELLIER, L., KIM, L., TSAI, H. H., HUANG, E. J., ROWITCH, D. H., BERNS, D. S., TENNER, A. J., SHAMLOO, M. & BARRES, B. A. 2013. A dramatic increase of C1q protein in the CNS during normal aging. *J Neurosci,* 33**,** 13460-74.

STOVER, C. M., SCHWAEBLE, W. J., LYNCH, N. J., THIEL, S. & SPEICHER, M. R. 1999a. Assignment of the gene encoding mannan-binding lectin-associated serine protease 2 (MASP2) to human chromosome 1p36.3-->p36.2 by in situ hybridization and somatic cell hybrid analysis. *Cytogenet Cell Genet,* 84**,** 148-9.

STOVER, C. M., THIEL, S., THELEN, M., LYNCH, N. J., VORUP-JENSEN, T., JENSENIUS, J. C. & SCHWAEBLE, W. J. 1999b. Two constituents of the initiation complex of the mannan-binding lectin activation pathway of complement are encoded by a single structural gene. *J Immunol,* 162**,** 3481-90.

STRAINIC, M. G., LIU, J., HUANG, D., AN, F., LALLI, P. N., MUQIM, N., SHAPIRO, V. S., DUBYAK, G. R., HEEGER, P. S. & MEDOF, M. E. 2008. Locally produced complement fragments C5a and C3a provide both costimulatory and survival signals to naive CD4+ T cells. *Immunity,* 28**,** 425-35.

STRAINIC, M. G., SHEVACH, E. M., AN, F., LIN, F. & MEDOF, M. E. 2013. Absence of signaling into CD4(+) cells via C3aR and C5aR enables autoinductive TGF-beta1 signaling and induction of Foxp3(+) regulatory T cells. *Nat Immunol,* 14**,** 162-71.

STRANG, C. J., CHOLIN, S., SPRAGG, J., DAVIS, A. E., 3RD, SCHNEEBERGER, E. E., DONALDSON, V. H. & ROSEN, F. S. 1988. Angioedema induced by a peptide derived from complement component C2. *J Exp Med,* 168**,** 1685-98.

TAKAHASHI, M., ENDO, Y., FUJITA, T. & MATSUSHITA, M. 1999. A truncated form of mannose-binding lectin-associated serine protease (MASP)-2 expressed by alternative polyadenylation is a component of the lectin complement pathway. *Int Immunol,* 11**,** 859-63.

TAKAHASHI, M., ISHIDA, Y., IWAKI, D., KANNO, K., SUZUKI, T., ENDO, Y., HOMMA, Y. & FUJITA, T. 2010. Essential role of mannose-binding lectin-associated serine protease-1 in activation of the complement factor D. *J Exp Med,* 207**,** 29-37.

TAMMENKOSKI, M., KOIVULA, K., CUSANELLI, E., ZOLLO, M., STEEGBORN, C., BAYKOV, A. A. & LAHTI, R. 2008. Human metastasis regulator protein H-prune is a short-chain exopolyphosphatase. *Biochemistry,* 47**,** 9707-13.

TATEISHI, K., KANEMOTO, T., FUJITA, T. & MATSUSHITA, M. 2011. Characterization of the complex between mannose-binding lectin trimer and mannose-binding lectin-associated serine proteases. *Microbiol Immunol,* 55**,** 427-33.

TATEISHI, K. & MATSUSHITA, M. 2011. Activation of the alternative complement pathway by mannose-binding lectin via a C2-bypass pathway. *Microbiol Immunol,* 55**,** 817-21.

TEILLET, F., DUBLET, B., ANDRIEU, J. P., GABORIAUD, C., ARLAUD, G. J. & THIELENS, N. M. 2005. The two major oligomeric forms of human mannan-binding lectin: chemical characterization, carbohydrate-binding properties, and interaction with MBL-associated serine proteases. *J Immunol,* 174**,** 2870-7.

THIEL, S., STEFFENSEN, R., CHRISTENSEN, I. J., IP, W. K., LAU, Y. L., REASON, I. J., EIBERG, H., GADJEVA, M., RUSEVA, M. & JENSENIUS, J. C. 2007. Deficiency of mannan-binding lectin associated serine protease-2 due to missense polymorphisms. *Genes Immun,* 8**,** 154-63.

THIEL, S., KOLEV, M., DEGN, S., STEFFENSEN, R., HANSEN, A. G., RUSEVA, M. & JENSENIUS, J. C. 2009. Polymorphisms in mannan-binding lectin (MBL)-associated serine protease 2 affect stability, binding to MBL, and enzymatic activity. *J Immunol,* 182**,** 2939-47.

THIELENS, N. M., VILLIERS, C. L., VILLIERS, M. B. & COLOMB, M. G. 1984. Comparative study of the fluid-phase proteolytic cleavage of human complement subcomponents C4 and C2 by C1s and C1r2-C1s2. *FEBS Lett,* 165**,** 111-6.

THIELENS, N. M., CSEH, S., THIEL, S., VORUP-JENSEN, T., ROSSI, V., JENSENIUS, J. C. & ARLAUD, G. J. 2001. Interaction properties of human mannan-binding lectin (MBL)-associated serine proteases-1 and -2, MBL-associated protein 19, and MBL. *J Immunol,* 166**,** 5068-77.

TULIO, S., FAUCZ, F. R., WERNECK, R. I., OLANDOSKI, M., ALEXANDRE, R. B., BOLDT, A. B., PEDROSO, M. L. & DE MESSIAS-REASON, I. J. 2011. MASP2 gene polymorphism is associated with susceptibility to hepatitis C virus infection. *Hum Immunol,* 72**,** 912-5.

VAN DEN ELSEN, J. M., MARTIN, A., WONG, V., CLEMENZA, L., ROSE, D. R. & ISENMAN, D. E. 2002. X-ray crystal structure of the C4d fragment of human complement component C4. *J Mol Biol,* 322**,** 1103-15.

VAN DER TOUW, W., CRAVEDI, P., KWAN, W. H., PAZ-ARTAL, E., MERAD, M. & HEEGER, P. S. 2013. Cutting edge: Receptors for C3a and C5a modulate stability of alloantigen-reactive induced regulatory T cells. *J Immunol,* 190**,** 5921-5.

VILLIERS, C. L., ARLAUD, G. J. & COLOMB, M. G. 1985. Domain structure and associated functions of subcomponents C1r and C1s of the first component of human complement. *Proc Natl Acad Sci U S A,* 82**,** 4477-81.

VORUP-JENSEN, T., PETERSEN, S. V., HANSEN, A. G., POULSEN, K., SCHWAEBLE, W., SIM, R. B., REID, K. B., DAVIS, S. J., THIEL, S. & JENSENIUS, J. C. 2000. Distinct pathways of mannan-binding lectin (MBL)- and C1-complex autoactivation revealed by reconstitution of MBL with recombinant MBL-associated serine protease-2. *J Immunol,* 165**,** 2093-100.

WALFORD, H. H. & ZURAW, B. L. 2014. Current update on cellular and molecular mechanisms of hereditary angioedema. *Ann Allergy Asthma Immunol,* 112**,** 413-8.

WALLIS, R. & DODD, R. B. 2000. Interaction of mannose-binding protein with associated serine proteases: effects of naturally occurring mutations. *J Biol Chem,* 275**,** 30962-9.

WALLIS, R., DODDS, A. W., MITCHELL, D. A., SIM, R. B., REID, K. B. & SCHWAEBLE, W. J. 2007. Molecular interactions between MASP-2, C4, and C2 and their activation fragments leading to complement activation via the lectin pathway. *J Biol Chem,* 282**,** 7844-51.

WALLIS, R., MITCHELL, D. A., SCHMID, R., SCHWAEBLE, W. J. & KEEBLE, A. H. 2010. Paths reunited: Initiation of the classical and lectin pathways of complement activation. *Immunobiology,* 215**,** 1-11.

WANG, L., FRALEY, C. D., FARIDI, J., KORNBERG, A. & ROTH, R. A. 2003. Inorganic polyphosphate stimulates mammalian TOR, a kinase involved in the proliferation of mammary cancer cells. *Proc Natl Acad Sci U S A,* 100**,** 11249-54.

WANG, Y., YAN, J., SHI, Y., LI, P., LIU, C., MA, Q., YANG, R., WANG, X., ZHU, L., YANG, X. & CAO, C. 2009. Lack of association between polymorphisms of MASP2 and susceptibility to SARS coronavirus infection. *BMC Infect Dis,* 9**,** 51.

WAT, J. M., FOLEY, J. H., KRISINGER, M. J., OCARIZA, L. M., LEI, V., WASNEY, G. A., LAMEIGNERE, E., STRYNADKA, N. C., SMITH, S. A., MORRISSEY, J. H. & CONWAY, E. M. 2014. Polyphosphate suppresses complement via the terminal pathway. *Blood,* 123**,** 768-76.

WEIS, W. I., DRICKAMER, K. & HENDRICKSON, W. A. 1992. Structure of a C-type mannose-binding protein complexed with an oligosaccharide. *Nature,* 360**,** 127-34.

WEISS, V., FAUSER, C. & ENGEL, J. 1986. Functional model of subcomponent C1 of human complement. *J Mol Biol,* 189**,** 573-81.

WUILLEMIN, W. A., MINNEMA, M., MEIJERS, J. C., ROEM, D., EERENBERG, A. J., NUIJENS, J. H., TEN CATE, H. & HACK, C. E. 1995. Inactivation of factor XIa in human plasma assessed by measuring factor XIa-protease inhibitor complexes: major role for C1-inhibitor. *Blood,* 85**,** 1517-26.

WUILLEMIN, W. A., ELDERING, E., CITARELLA, F., DE RUIG, C. P., TEN CATE, H. & HACK, C. E. 1996. Modulation of contact system proteases by glycosaminoglycans. Selective enhancement of the inhibition of factor XIa. *J Biol Chem,* 271**,** 12913-8.

WUILLEMIN, W. A., TE VELTHUIS, H., LUBBERS, Y. T., DE RUIG, C. P., ELDERING, E. & HACK, C. E. 1997. Potentiation of C1 inhibitor by glycosaminoglycans: dextran sulfate species are effective inhibitors of in vitro complement activation in plasma. *J Immunol,* 159**,** 1953-60.

YANG, L., SUN, M. F., GAILANI, D. & REZAIE, A. R. 2009. Characterization of a heparin-binding site on the catalytic domain of factor XIa: mechanism of heparin acceleration of factor XIa inhibition by the serpins antithrombin and C1-inhibitor. *Biochemistry,* 48**,** 1517-24.

YANG, Y., LHOTTA, K., CHUNG, E. K., EDER, P., NEUMAIR, F. & YU, C. Y. 2004. Complete complement components C4A and C4B deficiencies in human kidney diseases and systemic lupus erythematosus. *J Immunol,* 173**,** 2803-14.

YONGQING, T., WILMANN, P. G., REEVE, S. B., COETZER, T. H., SMITH, A. I., WHISSTOCK, J. C., PIKE, R. N. & WIJEYEWICKREMA, L. C. 2013. The x-ray crystal structure of mannose-binding lectin-associated serine proteinase-3 reveals the structural basis for enzyme inactivity associated with the Carnevale, Mingarelli, Malpuech, and Michels (3MC) syndrome. *J Biol Chem,* 288**,** 22399-407.

YU, H., MUNOZ, E. M., EDENS, R. E. & LINHARDT, R. J. 2005. Kinetic studies on the interactions of heparin and complement proteins using surface plasmon resonance. *Biochim Biophys Acta,* 1726**,** 168-76.

ZHANG, M., HOU, Y. J., CAVUSOGLU, E., LEE, D. C., STEFFENSEN, R., YANG, L., BASHARI, D., VILLAMIL, J., MOUSSA, M., FERNAINE, G., JENSENIUS, J. C., MARMUR, J. D., KO, W. & SHEVDE, K. 2013. MASP-2 activation is involved in ischemia-related necrotic myocardial injury in humans. *Int J Cardiol,* 166**,** 499-504.

ZHU, Y., THANGAMANI, S., HO, B. & DING, J. L. 2005. The ancient origin of the complement system. *EMBO J,* 24**,** 382-94.

ZIPFEL, P. F. & SKERKA, C. 2009. Complement regulators and inhibitory proteins. *Nat Rev Immunol,* 9**,** 729-40.

'Appendices'

Table A.1: Primers for MASP-2 mutagenesis

Mutant	Forward Primer	Reverse Primer
Cys tag	atggctagcatgtgcactggttggaagatc	gatcttccaaccagtgcacatgctagccat
D370A	ctgtggccctcctgctgatctacccagtggc	gccactgggtagatcagcaggagggccacag
D371A	ctgtggccctcctgatgctctacccagtggc	gccactgggtagagcatcaggagggccacag
D371Y	ctgtggccctcctgattatctacccagtggc	gccactgggtagataatcaggagggccacag
E333Q	cgagactggctatcagcttctgcaaggtcac	gtgaccttgcagaagctgatagccagtctcg
D365N	gcgtgcagcattgttaactgtggccctcctgatc	gatcaggagggccacagttaacaatgctgcacgc
E333R	gcgagactggctatcggcttctgcaaggtcac	gtgaccttgcagaagccgatagccagtctcgc
D365R	gcgtgcagcattgttcgctgtggccctcctgat	atcaggagggccacagcgaacaatgctgcacgc
K450Q	ggagggcaacaagcaaaacctgg	ccaggttttgcttgttgccctcc
K503Q	gggcaccctgcaaagactatcacc	ggtgatagtctttgcagggtgccc
R578Q	ggattaacccaacaaggttttcttgc	gcaagaaaaccttgttgggttaatcc
R583Q	ggttttcttgctcaaaatctaatg	cattagattttgagcaagaaaacc
R578Q	ggattaacccaacaaggttttcttgctcaaaatctaatg	cattagattttgagcaagaaaaccttgttgggttaatcc
R583Q		

Paper: 'Investigation of the mechanism of interaction between Mannose-binding lectin-associated serine protease-2 and complement C4'

Molecular Immunology, in press, accepted June 11th, 2015

Investigation of the mechanism of interaction between Mannose-binding lectin-associated serine protease-2 and complement C4

Nicole Drentin[1], Paul Conroy[1], Menachem J. Gunzburg[1], Robert N. Pike[1,2#*], Lakshmi C. Wijeyewickrema[2#]

[1]Department of Biochemistry and Molecular Biology, Monash University, Melbourne, Victoria, 3800, Australia.
[2]Department of Biochemistry & Genetics, La Trobe Institute of Molecular Science, La Trobe University, Melbourne, Victoria, 3086, Australia.
[#]These authors contributed equally to the work

Running title: *MASP-2 binding of C4*

*To whom correspondence should be addressed: Robert N. Pike, Department of Biochemistry and Genetics, La Trobe University, Melbourne, Victoria, 3086, Australia,

Abbreviations

CCP, complement control protein domain; SP, serine protease domain; MASP, mannose-binding lectin-associated serine protease; AFU, arbitrary fluorescent units; Abz, ortho-aminobenzoate.

Abstract

The interaction between mannose-binding lectin [MBL]-associated serine protease-2 (MASP-2) and it first substrate, C4 is crucial to the lectin pathway of complement, which is vital for innate host immunity, but also involved in a number of inflammatory diseases. Recent data suggests that two areas outside of the active site of MASP-2 (so-called exosites) are crucial for efficient cleavage of C4: one at the junction of the two complement control protein (CCP) domains of the enzyme and the second on the serine protease (SP) domain. Here, we have further investigated the roles of each of these exosites in the binding and cleavage of C4. We have found that both exosites are required for high affinity binding and efficient cleavage of the substrate protein. Within the SP domain exosite, we have shown here that two arginine residues are most important for high affinity binding and efficient cleavage of C4. Finally, we show that the CCP domain exosite appears to play the major role in the initial interaction with C4, while the SP domain exosite plays the major role in a secondary conformational change between the two proteins required to form a high affinity complex. This data has provided new insights into the binding and cleavage of C4 by MASP-2, which may be useful in the design of molecules that modulate this important interaction required to activate the lectin pathway of complement.

1.1 Introduction

Mannose-binding lectin-associated serine protease-2 (MASP-2) is a key enzyme in the lectin pathway of the complement system. The enzyme is able to bind to a number of pattern recognition molecules, such as Mannose Binding Lectin (MBL), the ficolins and collectin-11 (Thiel et al., 2009) and is activated upon the binding of such molecules to their ligands. While MASP-2 is able to auto-activate, leading to suggestions that it represents the minimal requirement for lectin pathway activation (Gal et al., 2005, Vorup-Jensen et al., 2000), new evidence suggests that the associated protease, MASP-1, is primarily responsible for activation of MASP-2 (Degn et al., 2012; Heja et al., 2012). Activated MASP-2 cleaves the C4 and C2 complement components, thus giving rise to the C4b and C2a cleavage products that form the C3 convertase complex, which in turn leads to activation of the rest of the complement system and eventual formation of the membrane attack complex. While MASP-1 is likely to be partially responsible for cleavage of C2 (Heja et al., 2012), MASP-2 is solely responsible for cleavage of C4, thus making this enzyme-substrate interaction a key point in the activation of the lectin pathway of complement.

MASP-2 is a six domain protease, with the N-terminal CUB1-EGF-CUB2 segment playing a key role in binding to MBL or ficolins, while the C-terminal CCP1-CCP2-SP segment plays a key role in catalysis of substrate cleavage (Yongqing et al., 2012). Studies suggested that the CCP1 and CCP2 domains of MASP-2 were likely to house an exosite required for efficient cleavage of C4 (Ambrus et al., 2003; Harmat et al., 2004; Rossi et al., 2001; Rossi et al., 2005) and this was confirmed by the solution of the structure of a catalytically inactive form of MASP-2 CCP12SP in complex with C4, which showed that residues E333, P340, D365 and P368 of the CCP1 and CCP2 domains of MASP-2 were involved in binding to the C345C domain of C4 (Kidmose et al., 2012). The information from the structure was reinforced by biochemical studies. In the case of C1s, the classical pathway protease that also cleaves C4, an exosite consisting of 4 positively charged amino acids on the SP domain of the protease is critical for binding and cleavage of C4 (Duncan et al., 2012b; Perry et al., 2013). The MASP-2/C4 structure did indicate another binding exosite upon the SP domain of the enzyme that interacted with key tyrosine sulphate and negatively charged residues on the C4 protein. This exosite appeared to involve residues K450, K503, R578 and R583, but the role of each residue and the overall role of this exosite in C4 binding and cleavage was not further characterised. Here, we have further

explored the kinetic mechanism of the binding interaction between MASP-2 and C4 and the role of the CCP and SP exosites in the binding and cleavage of C4.

2.1 Materials and Methods

2.1.1 Production of the MASP-2 enzyme forms

Prior to the creation of the MASP-2 mutants, a cysteine residue was inserted at the N-terminal end of the wild-type MASP-2 CCP12SP protein, between the T7 promoter region and the beginning of the protein sequence. This wild-type MASP-2 construct with the added cysteine was then used as a template for mutagenesis for the investigation. Primers for each mutation were generated (Geneworks, Adelaide, Australia) and PCR-based mutagenesis was carried out as previously described (Duncan et al., 2012b). Upon confirmation of successful sequencing, the plasmids were inserted into the *Escherichia coli* strain BL21*DE3 PLysS and expressed as described previously (Duncan et al., 2012b). The protease was extracted from the inclusion bodies, denatured, refolded, dialysed and purified under similar conditions to those described previously (Duncan et al., 2012b). The amount of enzyme recovered for the various mutations ranged from 0.1-0.5 mg/ml per litre of *E. coli* culture. Each of the mutants eluted similarly from anion-exchange and gel filtration chromatography as the wild type MASP-2 CCP12SP construct.

SDS-PAGE analysis confirmed that all the mutants purified to homogeneity. The mutants containing all catalytic residues were able to autoactivate during anion exchange chromatography, which was confirmed upon SDS-PAGE gel analysis showing fragments of 28 and 17 kDa, indicative of activation of the enzyme from the 44 kDa zymogen form. Each mutant was titrated with the serpin, C1-inhibitor, to confirm the active concentration of each mutant: all mutants reacted with C1 Inhibitor at a 1:1 ratio of protease: serpin, confirming that the proteases were fully active.

2.1.2 Analysis of kinetics of cleavage of a C4 P4-P4' peptide substrate

Assays were carried out in fluorescence assay buffer [50 mM Tris, 150 mM NaCl, 0.2% (w/v) PEG, pH 7.4] at 37°C. Fluorescence quenched substrate C4 P4-P4' [2Abz-GLQRALEI-Lys(Dnp)-NH$_2$] (GL Biochem, Shanghai, China) was solubilised in 10% (v/v) N,N-dimethylformamide. A BMG Technologies FluoStar Galaxy fluorescent plate reader (BMG LabTech, Ortenberg, Germany) was used with an excitation wavelength of 320 nm and an emission wavelength of 420 nm. The MASP-2 mutants were used at a 10 nM final concentration, with the substrate concentration range extending from 0-100 μM. All

measurements were done in duplicate. To determine steady-state reaction constants, the data was analysed using non-linear regression in GraphPad Prism Version 5 (GraphPad Software, San Diego, USA) using the following equation: $Y = (V_{max} [S]^h)/(K_{0.5}^h + [S]^h)$.

2.1.3 Analysis of the cleavage of C4

MASP-2 enzymes were diluted to a concentration range 0-1500 nM in Assay Buffer (20 mM sodium phosphate, 150 mM NaCl, 5 mM EDTA, pH 7.4). C4 (Complement Technology Inc., Tyler, Texas, USA) was also diluted in the EC_{50} Assay Buffer to a final concentration of either 25 or 100 nM. The proteases and substrates were separately incubated for 5 min at 37°C before being added together in a 1:1 ratio to begin the cleavage reaction. For C4, the reaction proceeded for 10 min before being ended by adding 4x SDS-PAGE loading buffer to the reaction and electrophoresing the samples on 10% SDS-PAGE gels. Gels for analysis of the cleavage of 100 nM C4 were stained using Coomassie blue R-250, while those for analysis of the cleavage of 25 nM C4 samples were visualised using Sypro Ruby (Molecular Probes, Invitrogen). Densitometry analysis of SDS-PAGE gels was carried out on a Typhoon Trio and ImageQuant TL software's 1D Gel analysis option (GE Healthcare Life Sciences). The cleavage of the C4 α band was quantitated using the C4 γ band as a loading control. The data generated from the analysis was then entered into GraphPad Prism software and an EC_{50} value obtained using the non-linear regression equation: log (inhibitor) vs. response- variable slope equation $[Y = Ymin + (Ymax - Ymin)/(1 + 10^{((LogEC50-X)*h)})]$, where Ymin is the minimum Y value, Y max the maximum Y value and h is the Hill slope. The time course for cleavage of C4 by MASP-2 enzyme forms was determined in a similar manner to that described above using a final concentration of 1 nM of the enzyme, C4 at a final concentration of 25 or 100 nM and time points of 0, 1, 2, 5, 15, 30, 60 and 120 min.

2.1.4 Analysis of MASP-2 binding of C4 using Surface Plasmon Resonance (SPR)

Surface Plasmon Resonance Studies were carried out using Biacore T100 and X100 instruments (GE Healthcare). Activated and zymogen forms of MASP-2 were engineered to contain a free Cys residue close to the N-terminus. This allowed immobilisation on flow cells of a Biacore Series S CM5 sensor chip for use in the Biacore T100, or a CM5 sensor chip for use in the Biacore X100 by using the thiol coupling kit as outlined by the manufacturer (GE Healthcare Life Sciences). The protein was immobilized in 10 mM sodium acetate, pH 5. Parallel assays determined that this buffer did not affect subsequent activity of the enzyme, indicating that it did not have a detrimental effect on enzyme

stability. For the Biacore T100, triplicate runs of $0 - 1 \, \mu M$ C4 were performed, with the protein being injected at $30 \, \mu l/min$ for 2 min, with a 5 min dissociation period. On the Biacore X100, each run was performed individually three times in a row, with sample ranges of C4 from 0 to 500 or $1 \, \mu M$, depending upon the MASP-2 variant being examined. The data obtained was then examined using the BIAevaluation software (GE Healthcare Life Sciences) in two ways. Firstly, the affinity of the interaction was examined using the Steady-State Affinity model, using the equation $R_{eq} = K_A C R_{max}/K_A C + 1$, where R_{eq} is the equilibrium response level, C is the concentration of analyte, and K_A is the equilibrium association constant calculated by fitting a plot of R_{eq} against analyte concentration. Secondly, a two-state binding model was examined, interpreted using the reaction scheme, $M2 + C4 \leftrightarrows M2{:}C4 \leftrightarrows M2^*C4$, where the initial complex (M2:C4) is converted to a higher affinity complex (M2*C4) due to conformational change. The data obtained were then used to determine the rate constants for the first ($K_1 = k_{a1}/ k_{d1}$) and second steps ($K_2 = k_{a2}/k_{d2}$) of the interaction. Calculation of the K_1 and K_2 constants allowed the determination of the overall association rate constant [$K_a = K_1 (1 + K_2)$] for the interaction.

3.1 Results

3.1.1 Selection of MASP-2 CCP and SP binding exosite domain mutations

The structure of the MASP-2- C4 complex shows two potential binding exosites on MASP-2 for C4 (Kidmose et al., 2012): one at the junction of the CCP1 and CCP2 domains and the other on the SP domain, where it potentially contacts up to three sulfated tyrosine residues on C4. The role of each residue of the potential binding exosites was examined by mutating selected residues to assess their impact on the ability of MASP-2 to cleave C4. To examine the potential SP domain exosite highlighted in the MASP-2/C4 complex structure, four residues (K450, K503, R578 and R583) were selected for mutation to glutamine residues in order to examine the effects of the positive charges on interactions between MASP-2 and C4. These residues were selected due to their identification as part of the SP exosite of MASP-2 in recent work by Kidmose *et al.* (Kidmose et al., 2012). Residues E333 and D365 (identified in Kidmose *et al.,* 2012) were selected for mutation to allow further study of the CCP domain binding exosite. In addition to the above mutants, a quadruple mutant where both the CCP and SP exosites were mutated was created (M2 E333Q/D365N/R578Q/R583Q) to examine the effects of impairing both exosites simultaneously on the ability of MASP-2 to bind and cleave C4. It should be noted that all mutants were made on the background of a wild type molecule that had a Cys residue

added at the N-terminus of the molecule, which had no effect on the ability of the wild type molecule to bind and cleave peptide and protein substrates (data not shown). All mutants were tested for their ability to cleave the C4 P4-P4' peptide substrate [2Abz-GLQRALEI-Lys(Dnp)-NH$_2$] and all were shown to display kinetics of cleavage of the peptide substrate similar to the wild type enzyme (supplementary Table 1), indicating that their active sites were not altered by the mutations carried out.

3.1.2 Investigation into the C4 cleavage efficiency of the MASP-2 exosite mutants

The ability of each MASP-2 mutant to cleave C4 efficiently was investigated by determining the EC$_{50}$ value for C4 cleavage for each mutant. Two different concentrations of C4 were employed for the analysis in order to better detect differences from wild type enzyme for some mutants. The R583Q and R578Q MASP-2 mutants displayed impaired cleavage of C4, with the EC$_{50}$ values for the cleavage increased approximately 2-fold (Table 1). Surprisingly, the K450Q and K503Q mutants of MASP-2 did not significantly affect the cleavage of C4. In light of this information, the MASP-2 SP domain exosite double mutant (M2 R578Q/R583Q) was created. This double mutant showed greatly impaired C4 cleavage efficiency, with a 29-fold increase in EC$_{50}$ value over that of the wild type enzyme (Table 1). Given that the K503 residue was shown to interact with the sulfated tyrosine residue 1417 of C4 (Kidmose *et al.*, 2012), we were surprised that mutation of this residue caused no effect on C4 cleavage efficacy when mutated. A triple mutant (M2 K503Q/R578Q/R583Q) was therefore created to investigate if this held true when this residue was mutated in addition to the two residues shown to impact C4 cleavage. This mutant had an EC$_{50}$ value that was increased over the EC$_{50}$ value obtained for the double mutant, but the difference was less than two-fold, suggesting that K503 plays a minor role in C4 cleavage.

Mutation of the E333 and D365 residues impacted the ability of MASP-2 to cleave C4, with individual neutralization of the charge of these residues causing an approximately 2-fold increase in the EC$_{50}$ values obtained (Table 1). Mutation of both residues (M2 E333Q/D365N) yielded a 12-fold increase in the EC$_{50}$ value, indicating that these two residues were indeed pivotal to the function of the exosite located at the junction of the CCP domains.

The information gathered from the above assays led to the creation of a quadruple mutant combining the double mutants of the CCP and SP domain exosites (M2 E333Q/D365N/R578Q/R583Q) to investigate the effects of impairing both exosites. The

assays showed that removal of the exosites indeed had a strong deleterious impact on the ability of MASP-2 to cleave C4, with the quadruple mutant showing a 1600-fold increase in EC_{50} value compared to that of wild-type MASP-2. This information suggests that the effects of the exosites upon C4 cleavage by MASP-2 are cumulative: while removal of one exosite leads to moderately affected C4 cleavage rates, removal of both leads to severe reductions in C4 cleavage efficiency.

The mutants that showed impacted C4 cleavage efficiency were studied in terms of their ability to cleave C4 in a time-dependent manner compared to wild type MASP-2 (Fig. 1). The R578Q and R583Q single mutants, both of which had increased EC_{50} values compared to wild-type MASP-2, showed altered time courses for C4 cleavage, only reaching similar levels of cleavage to the wild-type after one hour. The K450Q and K503Q single mutations showed little impact upon C4 cleavage over the time course. The SP domain exosite double mutant showed significantly impacted C4 cleavage, reaching only 55% C4 cleavage in two hours. The SP domain exosite triple mutant was slightly more impacted, reaching only 40% cleavage in two hours. This correlates with the EC_{50} values obtained, as the triple mutant displayed an EC_{50} value that was increased less than 2-fold over the values obtained for the SP domain exosite double mutant. The MASP-2 E333Q and D365N mutants showed a reduced rate of catalysis, only reaching similar levels of cleavage to the wild type MASP-2 after one hour. The E333Q/D365N double mutant showed severely reduced cleavage rates and only managed to reach ~50% cleavage in two hours. These results correlated well with the results for cleavage efficiency, as the E333Q/D365N mutant showed a large reduction in C4 cleavage efficiency. The quadruple mutant, where both the CCP and SP exosites were impacted, showed severely reduced cleavage over the time course, barely reaching 10% cleavage even after two hours. This correlates with the 1600-fold greater EC_{50} value obtained for the quadruple mutant compared to the wild-type control.

3.1.3 Analysis of the binding interaction between MASP-2 and C4 using surface plasmon resonance (SPR) studies.

Based on the results from the C4 cleavage assays, the two double mutants for the CCP and SP domain exosites (M2 E333Q/D365N and M2 R578Q/R583Q, respectively), as well as the quadruple mutant (M2 E333Q/D365N/R578Q/R583Q) were selected to be examined using SPR to investigate how the mutations affected the ability of each mutant to bind C4. In addition, the zymogen form of wild-type MASP-2 was also examined to deduce if there

was a difference in binding between zymogen and activated MASP-2. All enzyme forms used for SPR studies contained an S618A mutation to render the enzyme inactive in order to prevent unwanted artifacts in the SPR system caused by enzyme cleavage events (Perry *et al.*, 2013). The MASP-2 S618A mutants were activated by overnight incubation with immobilized active wild-type MASP-2. All activated MASP-2 enzymes migrated as two bands, indicating that the enzymes had been fully activated.

The data obtained here showed that wild-type activated MASP-2 bound C4 efficiently under the conditions employed for surface plasmon resonance studies (Fig. 2), while the zymogen form of MASP-2 was not able to bind to C4 under the conditions employed here (data not shown). Fitting of data to a steady state analysis yielded a K_D value of 82.6 nM for the binding of the wild type activated enzyme to C4. The CCP and SP exosite double mutants showed approximately 6-7-fold increases in K_D values (608 and 518 nM, respectively). The quadruple mutant showed no binding to C4. These results indicate that both exosites of MASP-2 are important in allowing efficient binding to C4 and that removal of both severely impairs the ability of MASP-2 to bind C4.

A two-state binding model was then used to fit the data in order to obtain the kinetic constants for C4 binding by MASP-2 (Table 2). It should be noted that the data could not be fitted well to a one-state binding model. The overall association rate constant (K_1) for the first step of the reaction and the overall association rate constant for the entire reaction (K_a), were both approximately 5-fold lower for the SP exosite mutant, indicating that this exosite plays a moderately important role in the association between MASP-2 and C4. Mutations to the CCP domain exosite decreased K_1 ten-fold and also decreased the overall association constant by approximately six-fold, indicating that this exosite plays an important role in the first association event between enzyme and substrate. Conversely, mutations to the CCP domain exosite appeared to actually increase the conformational change constant (K_2) four-fold, while mutations to the SP domain exosite decreased the K_2 value ten-fold, indicating that the SP domain exosite plays a major role in the conformational change required to achieve a high affinity complex between MASP-2 and C4.

4.1 Discussion

It was strongly suspected for some time that there was a binding exosite for C4 located within the CCP domains of MASP-2 (Ambrus et al., 2003; Duncan et al., 2012a; Harmat et al., 2004; Rossi et al., 2001; Rossi et al., 2005). The more recent determination of the structure of MASP-2 in complex with C4 has precisely pinpointed the location of the exosite at the junction of the CCP domains of C4 (Kidmose et al., 2012) and the published study provided biochemical evidence that supported the crystallographic evidence in this area. The structure also revealed an additional potential exosite on the SP domain of MASP-2 contacting negatively charged residues of C4, but in this case no corroborating evidence of the role of the four positively charged residues proposed to constitute this exosite in binding C4 was provided. It has been shown that the C1s enzyme of the classical pathway of complement, which also binds and cleaves C4, has a similar exosite on its SP domain composed of four positively charged residues that have each been demonstrated to play a role in the cleavage of C4 (Duncan et al., 2012b). This exosite on C1s was shown to be vital for the binding of C4 and to be deformed in the zymogen form of the enzyme (Perry et al., 2013). It has been assumed that all four positively charged residues of the proposed SP exosite of MASP-2 are similarly important for binding and cleavage of C4, but this has not been demonstrated and the role of each exosite in the binding and cleavage of the substrate by MASP-2 has also not been elucidated. Understanding these aspects of the structure and function of MASP-2 were the aims of the present study.

The data obtained for the efficiency of cleavage of C4 by MASP-2 allowed initial investigation of the importance of each amino acid in the interaction between enzyme and substrate. This allowed the first determination of the importance each residue in the proposed SP exosite of MASP-2, yielding the somewhat surprising result that the K450 and K503 residues appeared to play, respectively, no role and a minor role in the interaction between the enzyme and the substrate. This was particularly surprising for the K503 residue as it was the only one that could be seen contacting a sulphated tyrosine (Y1417) in the MASP-2-C4 structure (Kidmose et al., 2012). However, the results obtained with the triple mutant created (M2 K503Q/R578Q/R583Q) confirmed this, with the additional mutation of the K503 residue only slightly decreasing the efficiency of cleavage of C4. It seems likely therefore that the predictions based upon the crystal structure of the MASP-2-C4 complex need to be amended somewhat given the situation that is occurring with the molecules in the non-crystalline state. This data indicates that the sulphotyrosine residues of C4 might have considerable conformational flexibility, with the conformation

captured in the crystal structure perhaps not perfectly mimicking the circumstances found in solution. Nevertheless, as would be predicted from the crystal structure, the R578Q and R583Q single mutants were both shown to cause impaired C4 cleavage, increasing the EC_{50} values obtained approximately two-fold. The combined double SP domain exosite mutant (M2 R578Q/R583Q) showed a high level of impairment in C4 cleavage, with a ~30-fold increase in EC_{50} value over the wild-type. This mutant was therefore chosen for further studies on the overall role of the SP exosite in binding interactions with C4. The data obtained with the two residues from the CCP domains of MASP-2 are highly consistent with results shown before (Kidmose et al., 2012). Single mutants of these residues had strong impacts upon C4 cleavage efficiency. However, the largest impact came from mutating both residues simultaneously to create a double mutant (M2 E333Q/D365N), which had an EC_{50} value that was ~20-fold increased over that seen for the wild type enzyme. This mutant was therefore selected for further analysis of the role of the CCP-based exosite in C4 binding. Finally, removing both the CCP and SP domain exosites (M2 E333Q/D365N/R578Q/R583Q) increased the EC_{50} value 1600-fold over wild type MASP-2. This illustrates that the removal of both exosites from the enzyme appears to have greater effects than might be predicted from the results obtained with the removal of each one individually.

Both the SP and CCP domain exosites appear to play major roles in the binding of C4, with steady state analysis indicating 6 to 7-fold increases in the K_D values for these mutants over the wild type MASP-2 S618A enzyme. The quadruple mutant, which combined the CCP and SP domain exosite double mutants, displayed no binding to C4 at all. It appears that the exosites assist MASP-2 in binding C4 in a cumulative manner- the removal of one exosite impairs binding of C4 moderately, but removal of both exosites severely inhibits it. The kinetic constants for the interaction between MASP-2 and C4 suggest that the CCP domain exosite plays a major role in the initial interaction between the molecules, with the SP domain exosite playing a supporting role in this regard. The situation is reversed in the second phase of the interaction involving a likely conformational change in one or both molecules: in this phase the SP domain exosite plays a more major role. There is almost no doubt that the initial interaction between the molecules would occur very similarly with an active version of MASP-2, thus the two exosites do both seem important for the initial interaction, but the CCP domain exosite does appear to play the major role in this regard. The next phase of the reaction with an active variant might involve conformational change in the enzyme to achieve cleavage, but this is not certain. The active enzyme would cleave

C4 to yield C4b, which, based upon the large conformational changes seen between C3 and C3b (Janssen et al., 2006), is likely to undergo a major conformational change upon the formation of the C4b product. Thus the data obtained for the second phase of the reaction is of more questionable relevance, but it does appear that the major rearrangements that occur would be with regard to the SP domain exosite of the enzyme. The structure of MASP-2 in complex with C4 (Kidmose et al., 2012) revealed that the major conformational change that occurred when the molecules complexed was a large rotation of the SP domain of MASP-2 relative to the CCP2 domain. Thus it is possible that the SP domain exosite plays a major role in this relative conformational rearrangement of the domains and that this is reflected in the effects on the constants for the second phase of the reaction seen here. It should be noted that a comparison of the positions of the sidechains of the four positively charged residues proposed by Kidmose et al. (2012) to make up the SP exosite in the activated state of MASP-2 alone (Harmat et al., 2004) versus in complex with C4 (Kidmose et al., 2012), reveals that the sidechains of R578 and R583 are markedly shifted in the presence of C4 (Fig. 3), while those of K450 and K503 are hardly changed, indicating that the residues identified to be important in this study do indeed undergo major changes in structural positioning when bound to C4. This indicates a molecular basis for the results that we have obtained in the current study.

Somewhat at odds with current published literature, zymogen MASP-2 did not bind to C4 under the conditions employed here for SPR analysis (Chen and Wallis, 2004; Gal et al., 2005; Wallis et al., 2007). This apparent discrepancy is most likely the result of the different conditions used here, especially the flow rates employed. All results do indicate that zymogen MASP-2 does bind C4 much more poorly than the activated form and our results certainly support this outcome. Comparison of the structures of wild type MASP-2 in the zymogen (Gal et al., 2005) and activated (Harmat et al., 2004) states reveals that the R578 residue is particularly changed in the two different states, with the R583 residue in slightly different positions (Fig. 3). The loop containing the R578 residue is markedly shifted in position between the zymogen and activated forms, resulting in the sidechain of this residue being moved 12 angstroms in the zymogen versus activated forms of the molecule. The sidechain of R578 is thus pointing away from the position found in the activated state, with the position found in the zymogen state being much less conducive to co-ordinated efforts with the R583 residue in particular. The conformational re-arrangement of this residue in particular is therefore likely to form the basis for the lack of binding of C4 displayed by the zymogen form of MASP-2 in our hands.

The work carried out here has clearly delineated the kinetic mechanism underlying the binding of C4 by MASP-2 for the first time. These data provide important insights into the mechanism of the interaction, suggesting that the CCP and SP-based exosites cooperate to achieve the high affinity binding of C4 required for efficient cleavage of the substrate.

5.1 Acknowledgements

6.1 References

Ambrus, G., Gal, P., Kojima, M., Szilagyi, K., Balczer, J., Antal, J., Graf, L., Laich, A., Moffatt, B. E., Schwaeble W., Sim, R. B., Zavodszky, P., 2003. Natural substrates and inhibitors of mannan-binding lectin-associated serine protease-1 and -2: a study on recombinant catalytic fragments. J. Immunol. 170, 1374-1382.

Chen, C. B., Wallis R., 2004. Two mechanisms for mannose-binding protein modulation of the activity of its associated serine proteases. J. Biol. Chem. 279, 26058-26065.

Degn, S. E., Jensen, L., Hansen, A. G., Duman, D., Tekin, M., Jensenius, J. C., Thiel, S., 2012. Mannan-binding lectin-associated serine protease (MASP)-1 is crucial for lectin pathway activation in human serum, whereas neither MASP-1 nor MASP-3 is required for alternative pathway function. J. Immunol. 189, 3957-3969.

Duncan, R. C., Bergstrom, F., Coetzer, T. H., Blom, A. M., Wijeyewickrema, L. C., Pike, R. N., 2012a. Multiple domains of MASP-2, an initiating complement protease, are required for interaction with its substrate C4. Mol. Immunol. 49, 593-600.

Duncan, R. C., Mohlin, F., Taleski, D., Coetzer, T. H., Huntington, J. A., Payne, R. J., Blom, A. M., Pike R. N., Wijeyewickrema, L. C., 2012b. Identification of a catalytic exosite for complement component C4 on the serine protease domain of C1s. J. Immunol. 189, 2365-2373.

Gal, P., Harmat, V., Kocsis, A., Bian, T., Barna, L., Ambrus, G., Vegh, B., Balczer, J., Sim, R. B., Naray-Szabo, G., Zavodszky, P., 2005. A true autoactivating enzyme. Structural insight into mannose-binding lectin-associated serine protease-2 activations. J. Biol. Chem. 280, 33435-33444.

Harmat, V., Gal, P., Kardos, J., Szilagyi, K., Ambrus, G., Vegh, B., Naray-Szabo, G., Zavodszky, P., 2004. The structure of MBL-associated serine protease-2 reveals that identical substrate specificities of C1s and MASP-2 are realized through different sets of enzyme-substrate interactions. J. Mol. Biol. 342, 1533-1546.

Heja, D., Kocsis, A., Dobo, J., Szilagyi, K., Szasz, R., Zavodszky, P., Pal, G., Gal, P., 2012. Revised mechanism of complement lectin-pathway activation revealing the role of serine protease MASP-1 as the exclusive activator of MASP-2. Proc. Natl. Acad. Sci U. S. A. 109, 10498-10503.

Janssen, B. J., Christodoulidou, A., McCarthy, A., Lambris, J. D., Gros, P., 2006. Structure of C3b reveals conformational changes that underlie complement activity. Nature 444, 213-216.

Kidmose, R. T., Laursen, N. S., Dobo, J., Kjaer, T. R., Sirotkina, S., Yatime, L., Sottrup-Jensen, L., Thiel, S., Gal, P., Andersen, G. R., 2012. Structural basis for activation of the complement system by component C4 cleavage. Proc. Natl. Acad. Sci. U. S. A. 109, 15425-15430.

Perry, A. J., Wijeyewickrema, L. C., Wilmann, P. G., Gunzburg, M. J., D'Andrea, L., Irving, J. A., Pang, S. S., Duncan, R. C., Wilce, J. A., Whisstock, J. C., Pike, R. N., 2013.

A molecular switch governs the interaction between the human complement protease C1s and its substrate, complement C4. J. Biol. Chem. 288, 15821-15829.

Rossi, V., Cseh, S., Bally, I., Thielens, N. M., Jensenius, J. C., Arlaud, G. J., 2001. Substrate specificities of recombinant mannan-binding lectin-associated serine proteases-1 and -2. J. Biol. Chem. 276, 40880-40887.

Rossi, V., Teillet, F., Thielens, N. M., Bally, I., Arlaud, G. J., 2005. Functional characterization of complement proteases C1s/mannan-binding lectin-associated serine protease-2 (MASP-2) chimeras reveals the higher C4 recognition efficacy of the MASP-2 complement control protein modules. J. Biol. Chem. 280, 41811-41818.

Thiel, S., Kolev, M., Degn, S., Steffensen, R., Hansen, A. G., Ruseva, M., Jensenius, J. C., 2009. Polymorphisms in mannan-binding lectin (MBL)-associated serine protease 2 affect stability, binding to MBL, and enzymatic activity. J. Immunol. 182, 2939-2947.

Vorup-Jensen, T., Petersen, S. V., Hansen, A. G., Poulsen, K., Schwaeble, W., Sim, R. B., Reid, K. B., Davis, S. J., Thiel, S., Jensenius, J. C., 2000. Distinct pathways of mannan-binding lectin (MBL)- and C1-complex autoactivation revealed by reconstitution of MBL with recombinant MBL-associated serine protease-2. J. Immunol. 165, 2093-2100.

Wallis, R., Dodds, A. W., Mitchell, D. A., Sim, R. B., Reid, K. B., Schwaeble, W. J., 2007. Molecular interactions between MASP-2, C4, and C2 and their activation fragments leading to complement activation via the lectin pathway. J. Biol. Chem. 282, 7844-7851.

Yongqing, T., Drentin, N., Duncan, R. C., Wijeyewickrema, L. C., Pike, R. N., 2012. Mannose-binding lectin serine proteases and associated proteins of the lectin pathway of complement: two genes, five proteins and many functions? Biochim. Biophys. Acta. 1824, 253-262.

Table 1: Efficiency of cleavage of C4 by MASP-2 mutants

MASP-2 mutant	EC_{50} (nM)*	EC_{50} (nM)[#]
Wild Type	0.3	0.4
R578Q	0.64	0.82
R583Q	0.58	0.74
K450Q	0.38	0.26
K503Q	0.3	0.57
R578Q/R583Q	*nd*	11.7[§]
K503Q/R578Q/R583Q	*nd*	17.9
E333Q	0.64	*nd*
D365N	0.63	*nd*
E333Q D365N	3.6	8.4[§]
E333Q/D365N/R578Q/R583Q	*nd*	649[§]

*EC50 values were determined after cleavage of 100 nM C4. All values are representative of analysis in duplicate, except where indicated (§), in which case triplicate measurements were undertaken.

[#]EC50 values were determined after cleavage of 25 nM C4. All values are representative of analysis in duplicate, except where indicated (§), in which case triplicate measurements were undertaken.

Table 2: Kinetic data for the binding of C4 by MASP-2

Enzyme form	k_{a1} $(M^{-1}.s^{-1})$	k_{d_1} (s^{-1})	K_1 $(M^{-1}.s^{-1})$	k_{a_2} (s^{-1})	k_{d_2} (s^{-1})	K_2 (s^{-1})	K_a $(M^{-1}.s^{-1})$	K_D* (nM)
S618A n = 9	1.2×10^6	0.2	6.0×10^6	5.4×10^{-3}	3.2×10^{-2}	0.17	6.9×10^6	82.6
CCP exosite n = 7	2.7×10^5	0.45	6.0×10^5	1.4×10^{-3}	1.9×10^{-3}	0.756	1.1×10^6	608
SP exosite n = 10	6.6×10^5	0.56	1.2×10^6	2.1×10^{-4}	6.6×10^{-2}	0.015	1.2×10^6	518

*Derived by regression analysis of plots of SPR response units at equilibrium versus C4 concentration fitted to a single-site binding equation.
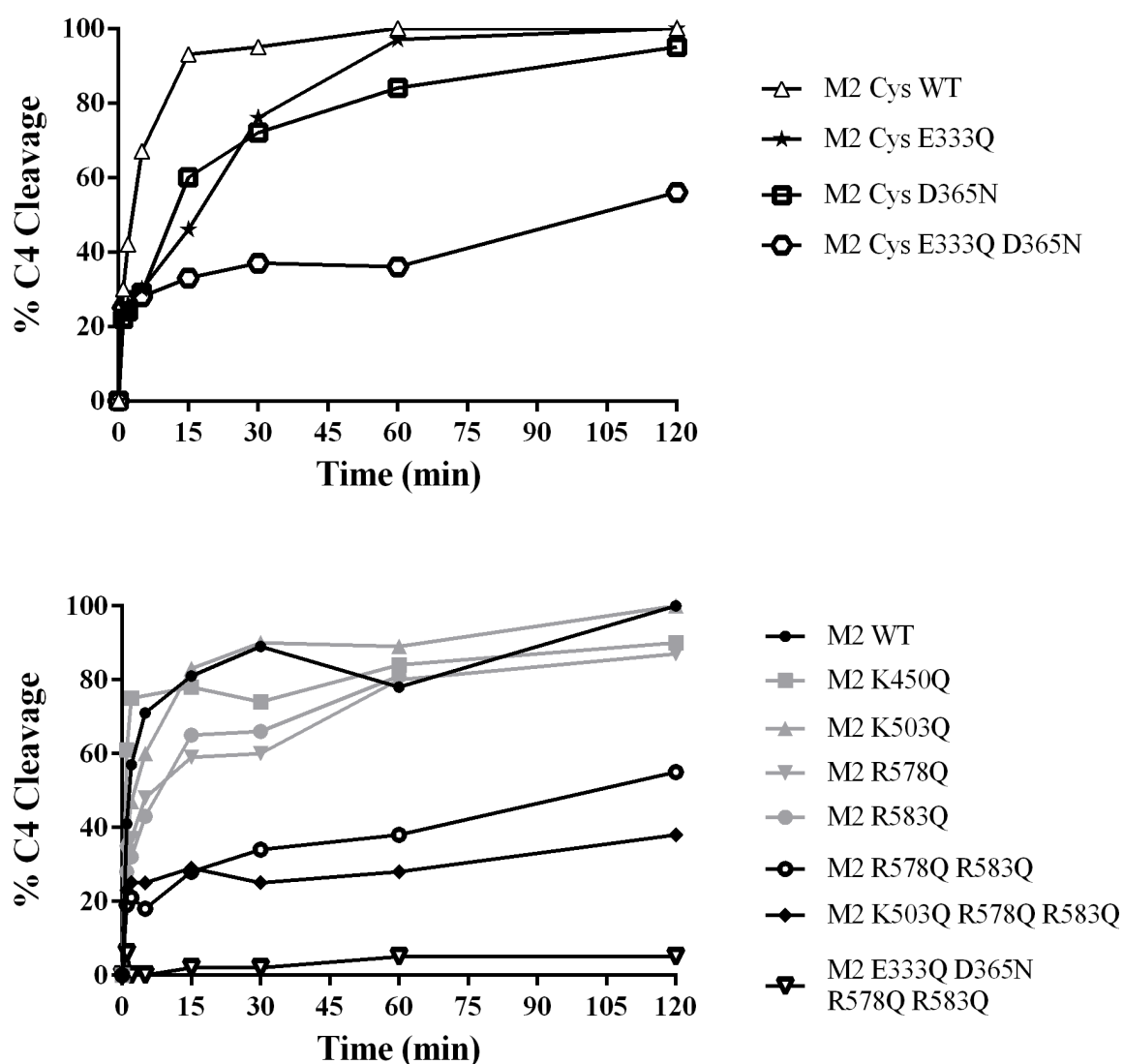
Figure 1

Figure 1: Time course analysis for cleavage of C4 by MASP-2 enzyme forms. Selected MASP-2 mutants were incubated with either 100 nM (upper panel) or 25 nM (lower panel) of C4 at 37°C over a series of time points up to 2 hours. In all experiments, the cleavage rate was determined through the disappearance of the α-chain using densitometry, with the γ-chain used as a loading control.
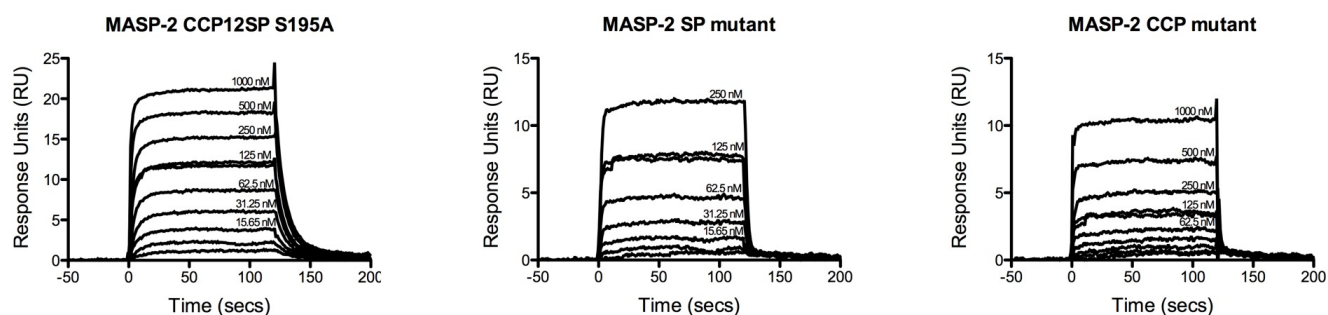
Figure 2

Figure 2: Binding of C4 to immobilised MASP-2. SPR curves for 0–1000 nM C4 flowed over the immobilised activated form of CCP1-CCP2-SP MASP-2 S618A (wild-type) [left hand side] compared to the MASP-2 R578Q/R583Q [centre] and MASP-2 E333Q/D365N double mutants. The obtained responses were fitted to a two-state binding equation within the program SCRUBBER.
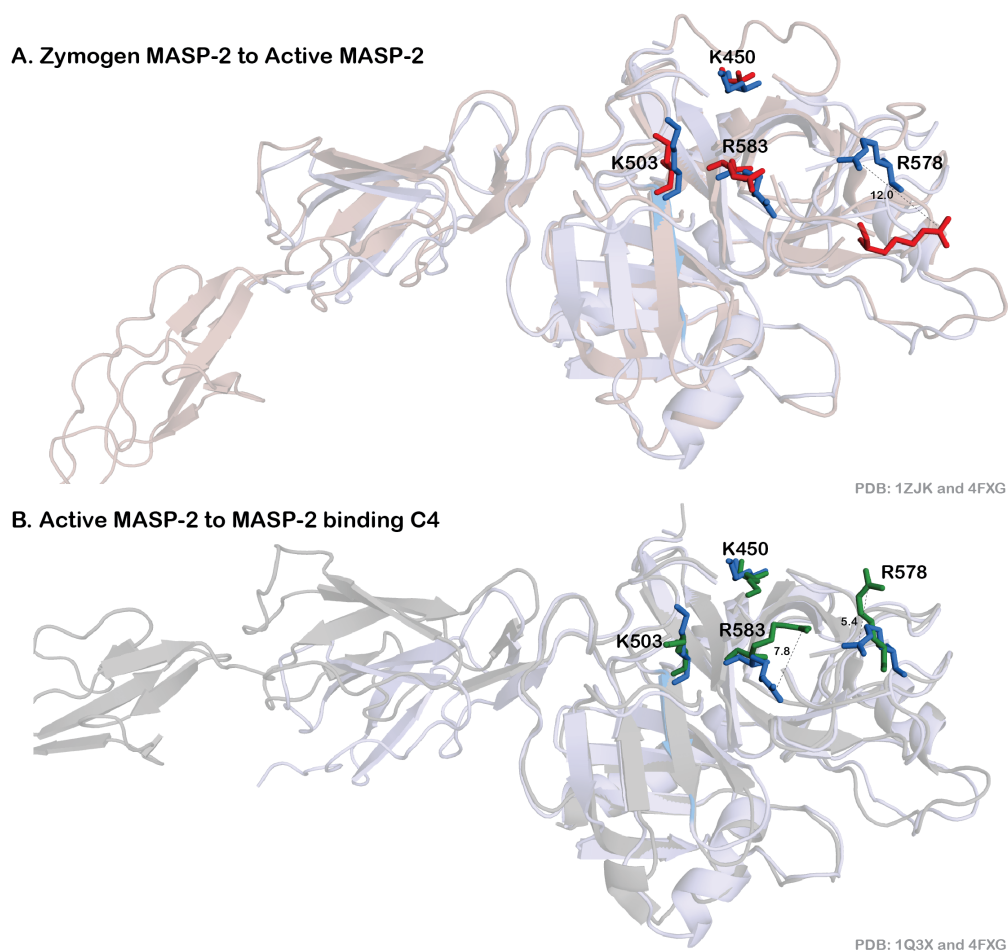
Figure 3

A. Zymogen MASP-2 to Active MASP-2

PDB: 1ZJK and 4FXG

B. Active MASP-2 to MASP-2 binding C4

PDB: 1Q3X and 4FXG

Figure 3: Structural comparison of SP exosite residues of MASP-2 in different states

A. Comparison of zymogen versus activated MASP-2. The structures of zymogen (PDB: 1ZJK [light orange ribbon]) and activated MASP-2 (PDB: 4FXG [light blue ribbon]) were overlaid. The positions of the four positively charged residues proposed to make up the SP exosite of MASP-2 are shown in ball-and-stick configuration (zymogen position in red, activated position in blue). The distance between the zymogen versus activated form of R578 (12.0 angstroms) is also indicated. B. Comparison between activated MASP-2 alone and in complex with C4. The structures of activated MASP-2 in the absence (PDB: 4FXG [light blue ribbon]) and presence of C4 (PDB: 1Q3X [dark brown ribbon]) were overlaid. The positions of the four positively charged residues proposed to make up the SP exosite of MASP-2 are shown in ball-and-stick configuration (activated MASP-2 alone in blue, in the presence of C4 in green). The distances between R583 and R578 sidechains in the absence and presence of C4 are indicated in angstroms.